致密QCD物质：状态方程与相变

陈列文

(上海交通大学 物理与天文学院，粒子与核物理研究所-INPAC)

- 致密QCD物质
- 致密QCD物质的状态方程:
  - 对称能：核物质和夸克物质的状态方程
  - 中子皮：Pb/Ca中子半径之谜
  - 引力波：对称能的高密行为
- 致密QCD物质的相变：
  - QCD相图：概述
  - 重离子碰撞：粒子产生的并合模型
  - 致密星：中子星、超新星、双星并合
- 总结和展望

“QCD与重离子碰撞物理”暑期学校，复旦大学，上海，2024年8月15-16日

目录

- 致密QCD物质
- 致密QCD物质的状态方程:
  - 对称能：核物质和夸克物质的状态方程
  - 中子皮：Pb/Ca中子半径之谜
  - 引力波：对称能的高密行为
- 致密QCD物质的相变：
  - QCD相图：概述
  - 重离子碰撞：粒子产生的并合模型
  - 致密星：中子星、超新星、双星并合
- 总结和展望

致密QCD物质

自然界中的致密QCD物质存在于何处?

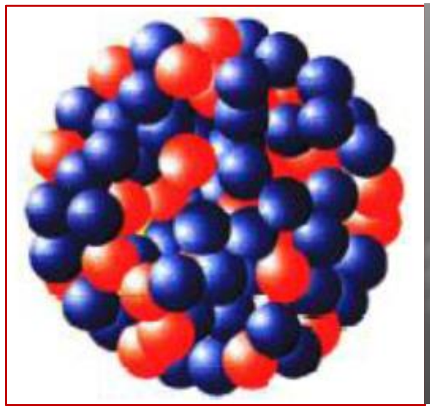
原子核

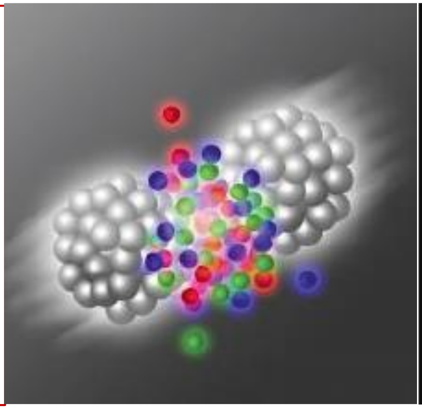
重离子碰撞

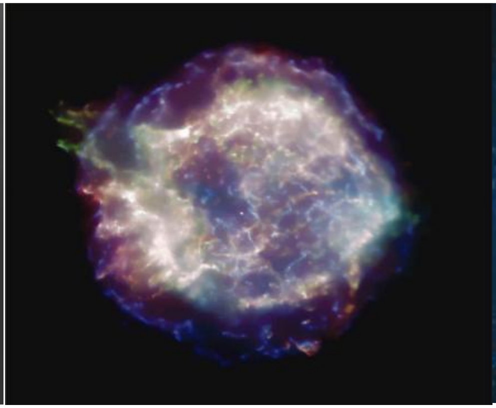
超新星

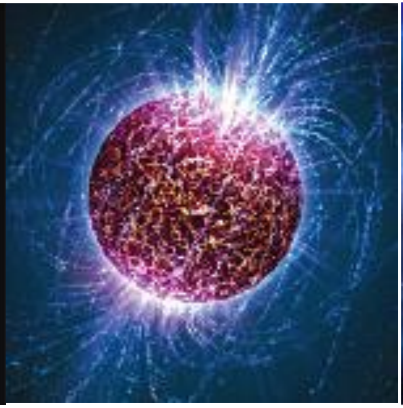
中子星


中子星并合

致密QCD物质

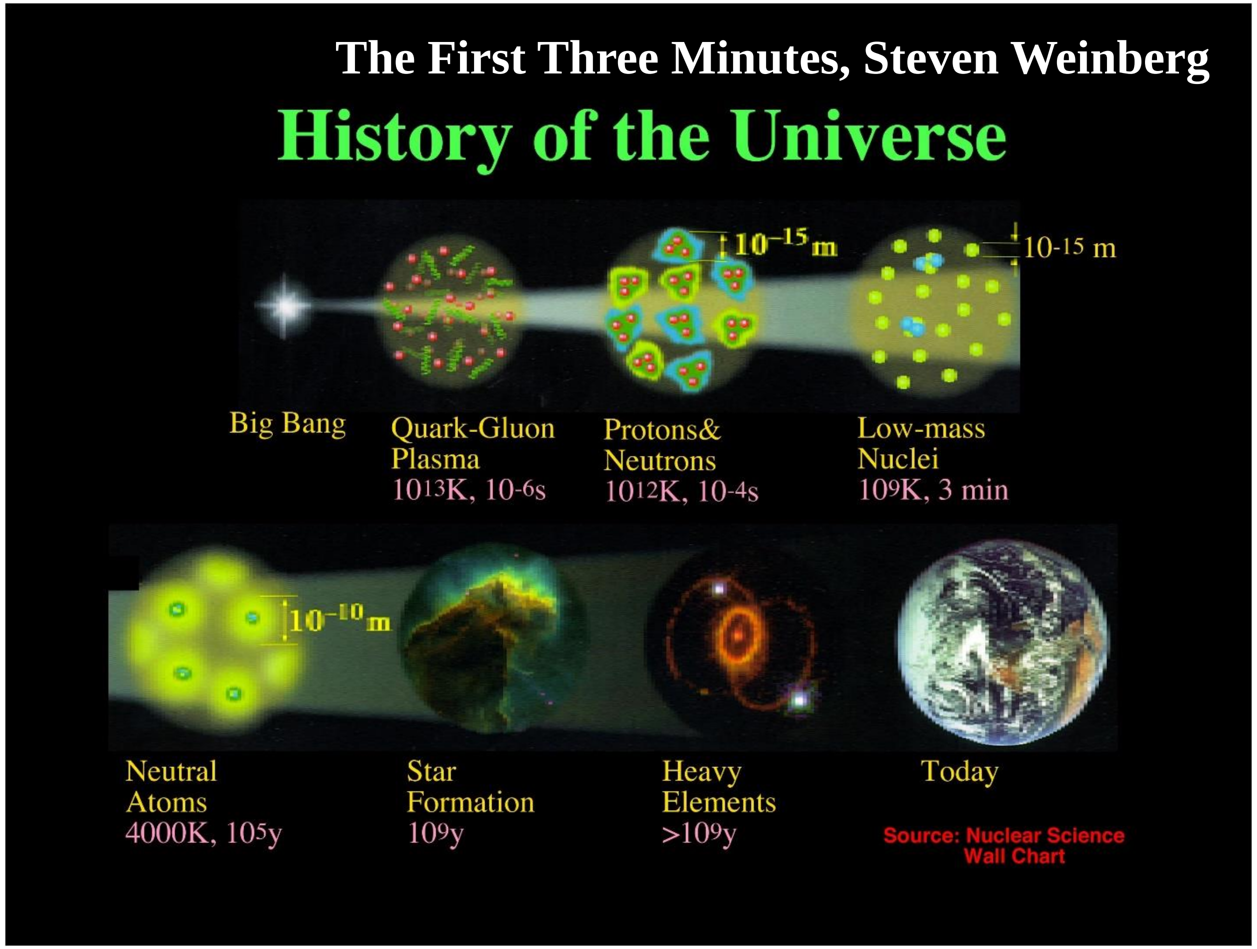

QCD物质-夸克胶子等离子体(QGP)-大量存在于宇宙大爆炸初期

原子核

- 原子核由质子和中子组成
- 核素: 给定中子数和质子数的原子核
- 元素: 给定质子数的原子核
- 同位素: 相同质子数但不同中子数的原子核
- 重离子：质量数大于4的离子，亦即比α粒子(^{4}He)重的离子

Mass number —— Charge number —— $^{12}_{6}C$

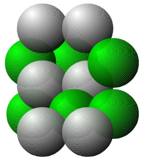

^1_1H ^2_1H ^3_1H

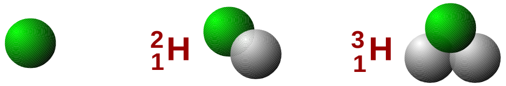

- 同位旋：
  - 就核力的性质而言，质子与中子可以看成同一种粒子(统称为核子)的两种不同状态，类比自旋的概念引入抽象的同位旋(isospin)空间(海森堡，1932年)
  - 核子的同位旋为$I=1/2$，$I_3=1/2$为质子，$I_3=-1/2$为中子，它们组成$I=1/2$的同位旋二重态
  - 对于强相互作用，同位旋是一个好量子数

W.K. Heisenberg
(1901 - 1976)

原子核的大小及密度分布

Contemporary picture –
APS DNP Nuclear Wall Chart:

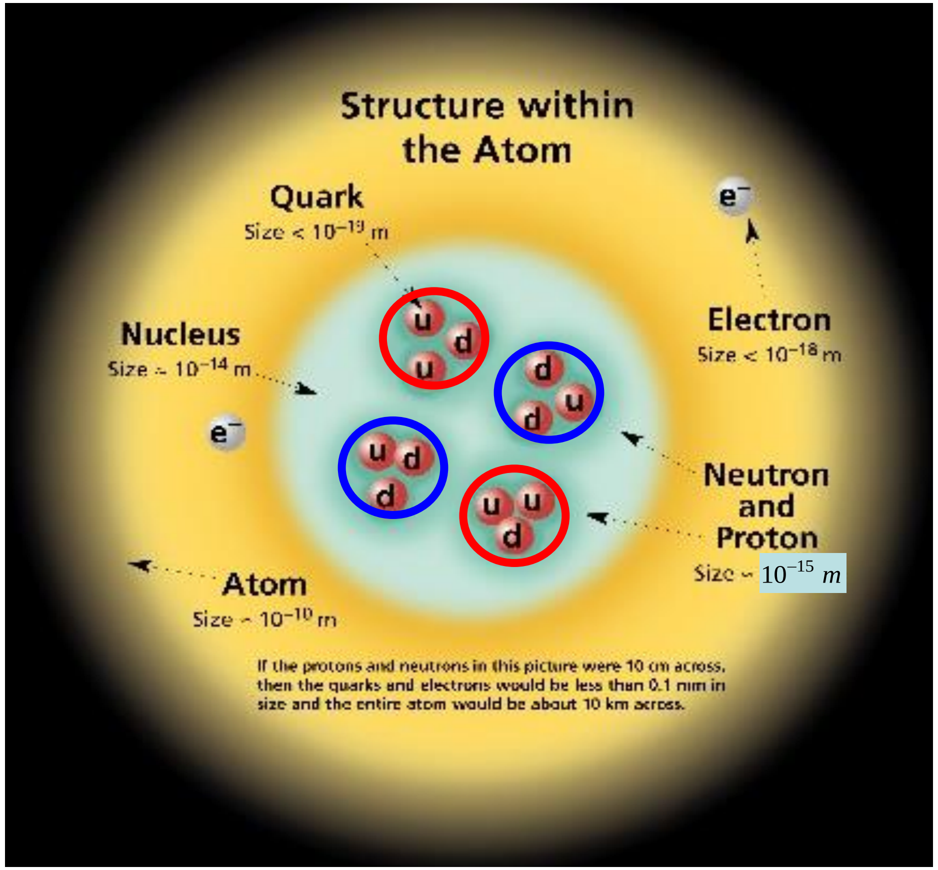

http://www.lbl.gov/abc/wallchart/index.html

Size of Nuclei

- Robert Hofstadter performs experiment at Stanford using a new linear accelerator for electrons in 1950s
- E = 100 -- 500 MeV
- $\lambda = h / p = 2.5$ fm
- The proton is not a point! (Deviation of elastic scattering rate from Rutherford Scattering prediction)
- Proton and nuclei have extended charge distributions
- Nobel prize in 1961

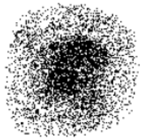

nucleus

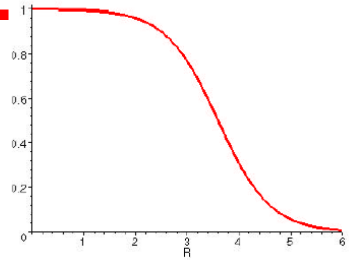

$$\rho(r) = \frac{\rho_0}{1+\exp[(r-R)/a]} \qquad R \approx 5.8 \text{ fm } (A=100)$$

$$R \approx r_0 A^{1/3} \qquad V = \frac{4}{3}\pi R^3 \propto A = \#\text{nucleons}$$

$$r_0 = 1.2 \times 10^{-15} \text{ m} = 1.2 \text{ fm}$$

$$a = 0.5 \text{ fm}$$

R. Hofstadter
(1915 - 1990)

原子核中心密度

(核物质饱和密度)

$\rho_0 \approx 0.16 \text{ nucleon/fm}^3$,

$\approx 2.7 \times 10^{14} \text{ g/cm}^3$,

水的密度: 1 g/cm^3

原子核内的物质是极端致密的！

重离子碰撞

“小爆炸”——产生极端高温高密物质新形态-夸克胶子等离子体(QGP)！

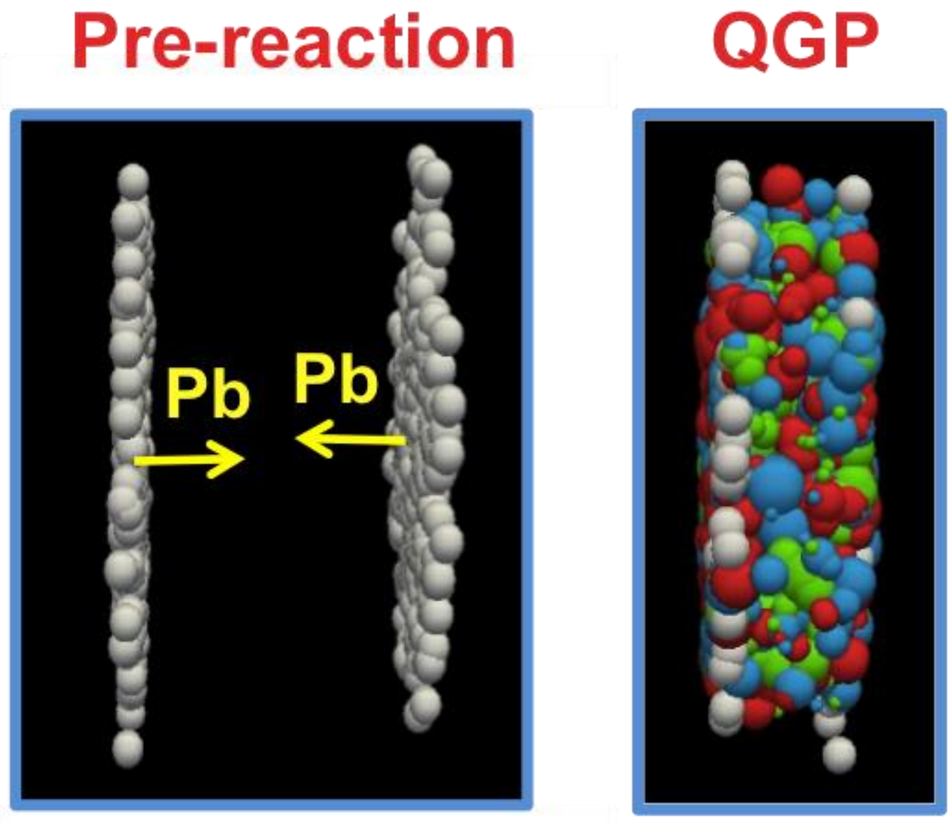

三维QCD相图

~ $4\rho_0$ ($30\rho_0$) with T~110 (500-110) MeV

For AuAu collisions at sqrt(s_NN) = 3.3 (39) GeV

Yu. B. Ivanov and A. A. Soldatov, PRC 101, 024915 (2020)

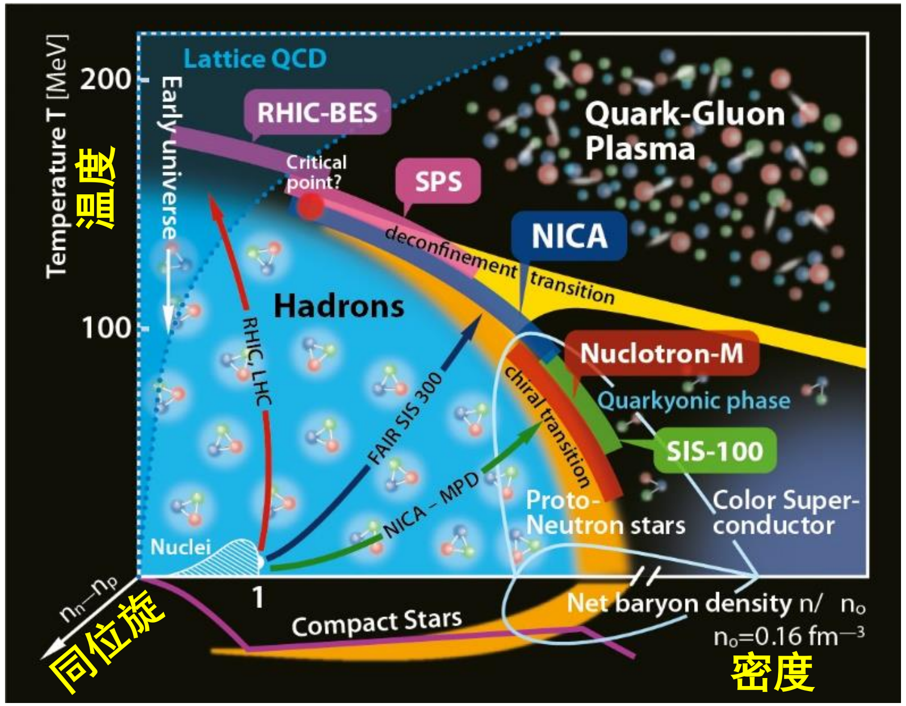

重离子碰撞能在地球上产生高温、高密、高同位旋(强磁场、强涡旋场？)的QCD物质！

恒星的演化

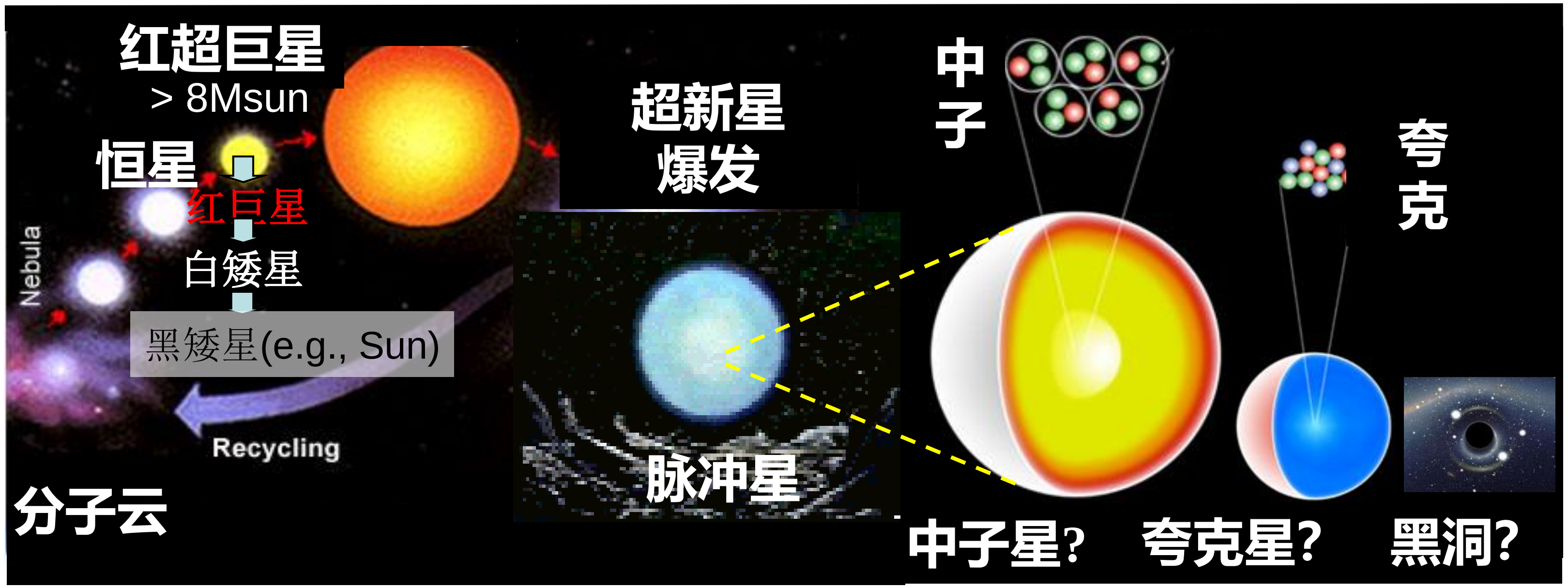

L.D. Landau
(1908 - 1968)

1932: Lev Landau – Neutron Stars

F. Zwicky
(1898 - 1974)

1934: Fritz Zwicky and Walter Baade – NS might be formed in supernova explosions

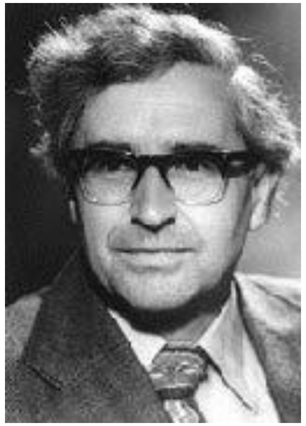

A. Hewish
(1924 - 2021)

S. J. Bell
(1943 -)

1967: A. Hewish, S. J. Bell, J. D. H. Pilkington, P. F. Scott, and R. A. Collins, "Observation of a rapidly pulsating radio source", Nature (London) 217, 709–713 (1968)

脉冲星

- The predicted rate of supernova explosions is about 1 to 3 per century in our galaxy
- The most studied early supernova (Crab) explosion was recorded in China in 1054 A.D.
- The most recent one was 1987A in LMC.
- Over 3000s pulsars (**FAST:~900**) have been identified, while about 10^8 are predicted to exist. Only about 10 of them can be associated with the approximately 220 known supernova remnants

The lighthouse model of pulsars (rotating neutron stars)

Antony Hewish: won The Nobel Prize for Physics in 1974

(The NoBell Nobel – 没有贝尔的诺贝尔! 第一次授予天文学家)

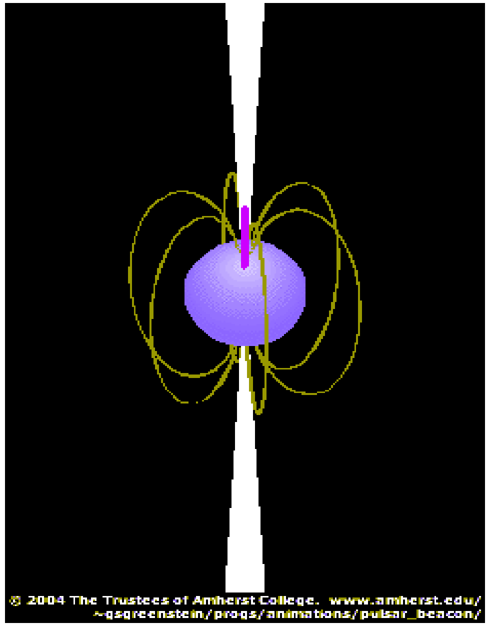

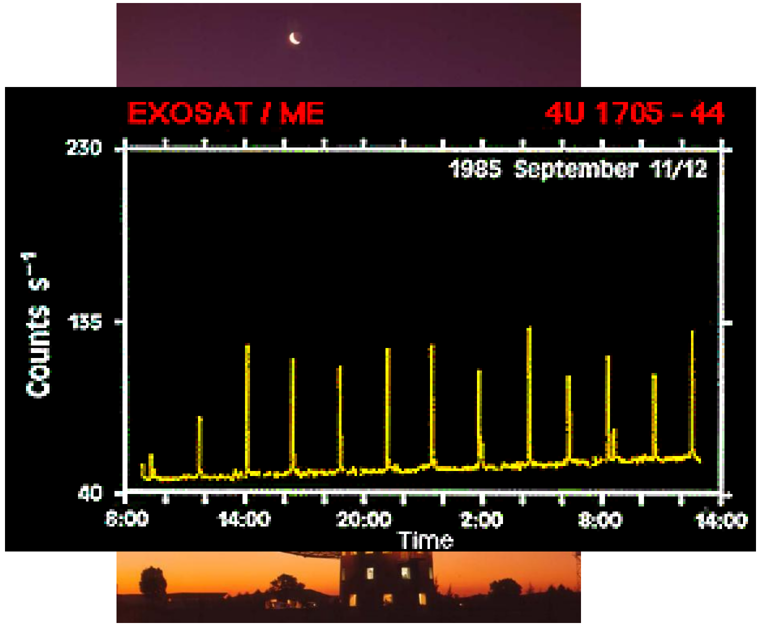

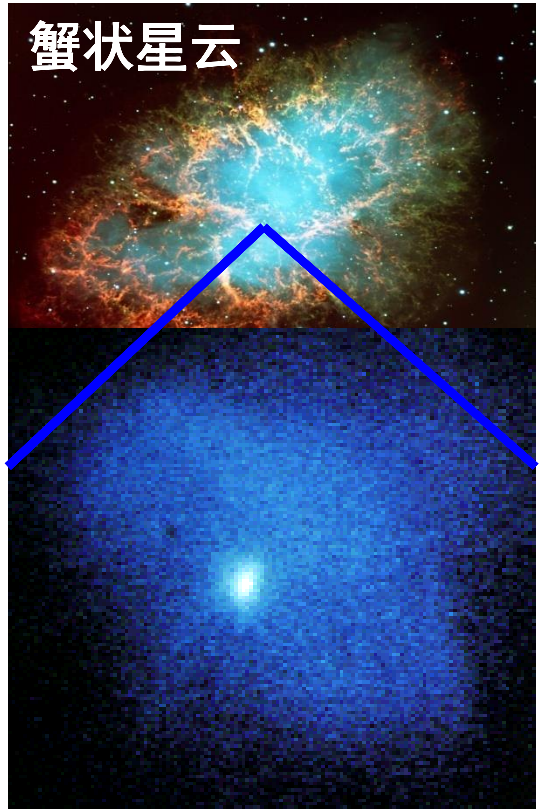

超新星

核塌缩型超新星(CCSN)

by Xu-Run Huang (黄旭润)

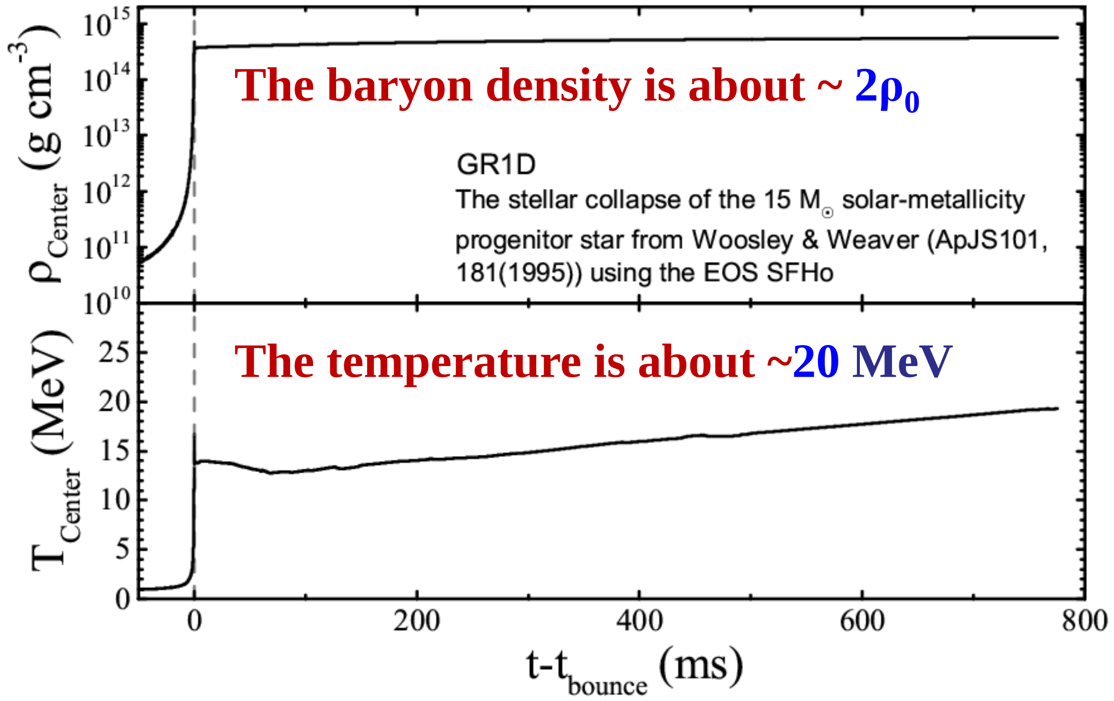

超新星

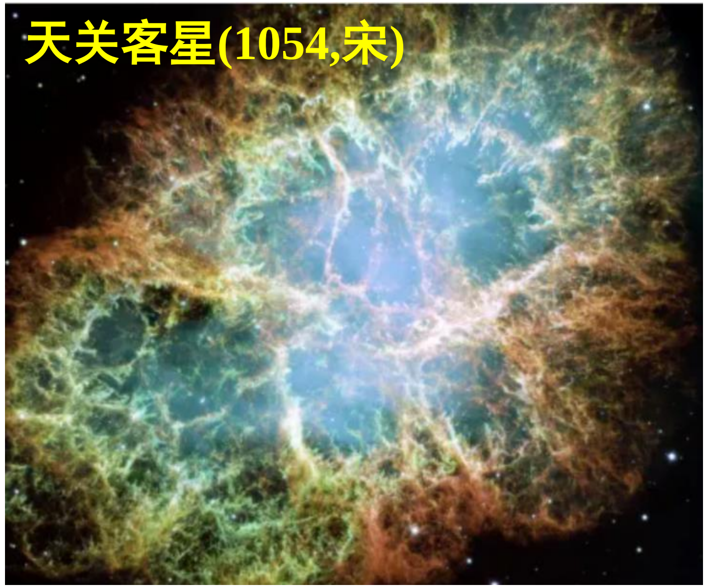

哈勃望远镜拍摄的蟹状星云
(NASA, ESA, J. Hester and A. Loll, Arizona State University)

中心密度: ~ $2\rho_0$
中心温度: ~ 20 MeV
(激波附近~50 MeV)
同位旋：高

核塌缩型超新星能产生高温、高密、高同位旋的致密QCD物质！

“中国超新星” – 蟹状星云的前身

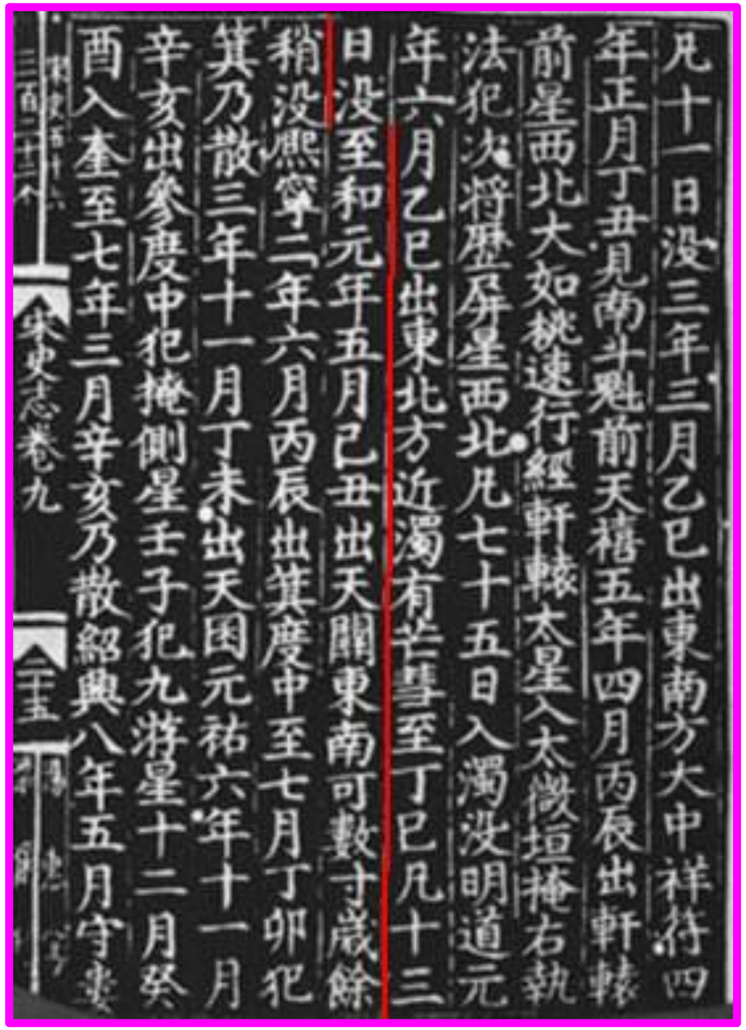
凡十一日沒三年三月乙巳出東南方大中祥符四
年正月丁丑見南斗魁前天禧五年四月丙辰出軒轅
前星西北大如桃速行經軒轅太星入太微垣掩右執
法犯次將歷屏星西北凡七十五日入濁沒明道元
年六月乙巳出東北方近濁有芒彗至丁巳凡十三
日沒至和元年五月己丑出天關東南可數寸歲餘
稍沒熙寧二年六月丙辰出箕度中至七月丁卯犯
箕乃散三年十一月丁未出天囷元祐六年十一月
辛亥出參度中犯掩側星壬子犯九游星十二月癸
酉入奎至七年三月辛亥乃散紹興八年五月守婁

1054年北宋仁宗“至和元年”，《宋史》记载：“至和元年五月己丑，出天关东南可数寸，岁余稍没。”

综合各种史料记载，这颗超新星爆发于1054年7月4日凌晨4点左右，最后消逝的日期是1056年4月6日，共可见643天。位置在金牛座ζ星（天关星）附近，在这个位置上，用望远镜就可以看到有一片蟹状星云M1。直到1969年，现代天文学通过光学、X射线及射电等多方面研究，最终确定蟹状星云的中心有一颗中子星，同时也无可置疑地表明它正是我国宋代人亲眼见到的那颗天关客星的遗迹，也是第一颗由现代天文观测所认证的古人曾有记载的超新星遗迹，更是我国古代天象观测在当代天文学研究中发挥独特作用的光辉范例。正因为此，1054超新星才被国际天文界称为“中国超新星”。需要说明的是，即便宋朝人看到的天关客星爆发也不是那颗恒星当时正在发生的事情，而是很久之前的历史事件，因为光信号从现场传到地球人这里需要很长时间，蟹状星云距离地球是6300光年，这也就是说，1054超新星真正爆发的年代距离宋人已经是6300年前，距今更是7200多年之前的事件了。

超新星

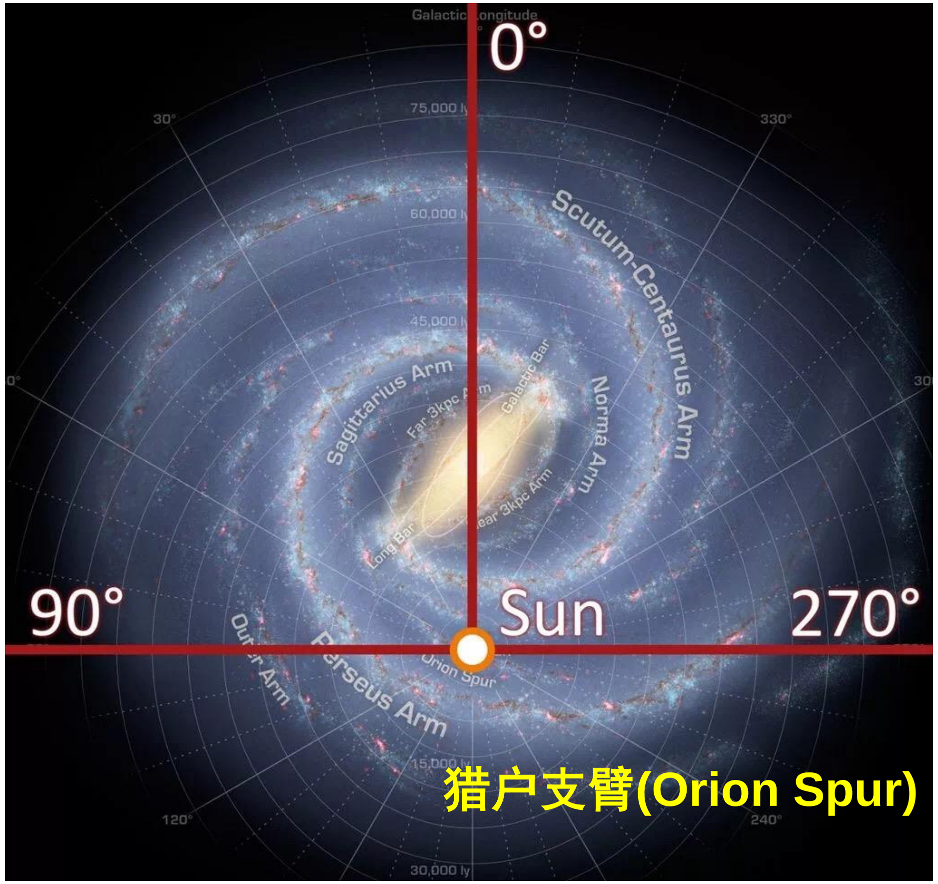

Diameter of the Milky Way Galaxy

~10^5 light-years ~ 30 kpc (kiloparsec)

L.-S. The et al., A&A 450, 1037–1050 (2006)

Table B.1. Recent galactic supernova record.

Name	Year	Distance (kpc)	l	b	Type	
Lupus (SN 1006)天狼座	1006	2.2	327.57	14.57	Ia	
Crab	1054	2.0	184.55	−5.79	II	CCSN
3C 58 (SN 1181)	1181	2.6	130.73	3.07	II	CCSN
Tycho	1572	2.4	120.09	1.42	Ia[a]	
Kepler	1604	4.2	4.53	6.82	Ib/II[b]	CCSN?
Cas A Cassiopeia A (仙后座)	1680	2.92	111.73	−2.13	Ib	CCSN

[a] Studies of X-ray emission from Tycho's shocked ejecta show the SNR was created by a type Ia SN (Hwang et al. 1998; Badenes et al. 2003, 2005).
[b] The uncertainty of Kepler's SN Type was reviewed by Blair (2005).

过去1000年历史文献记录到了6颗河内超新星爆发，其中大概4颗是核塌缩型超新星（CCSNe）

中子星

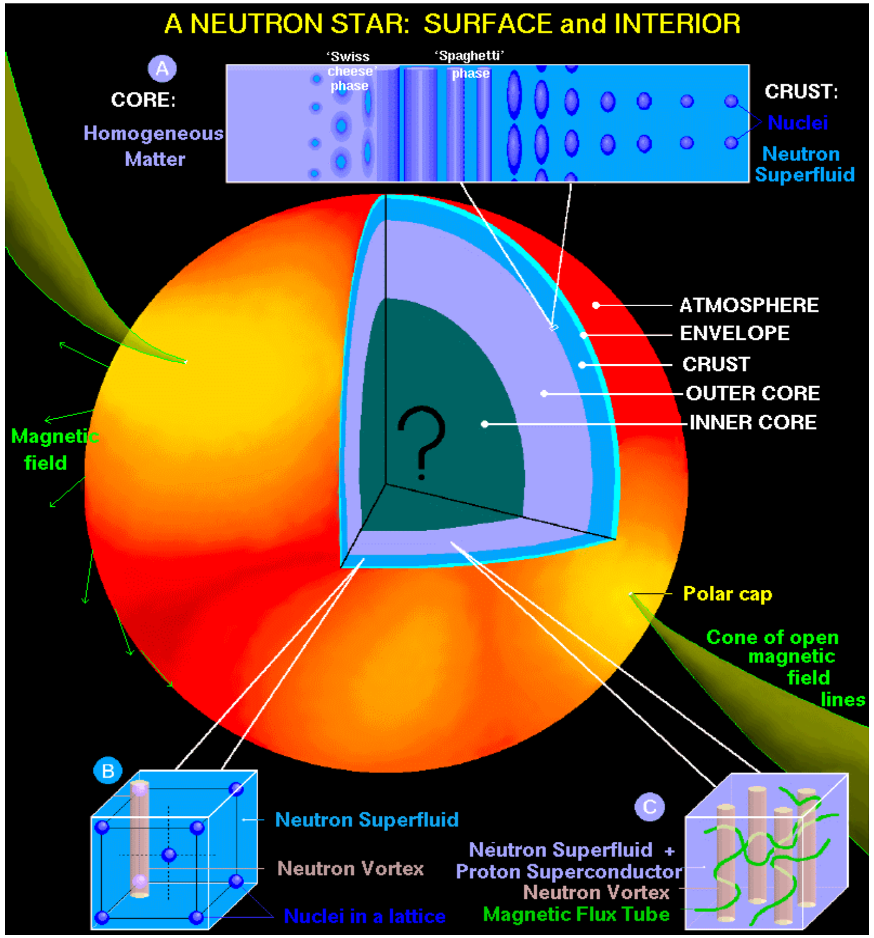

Lattimer/Prakash, Science 304, 536 (2004)

Neutron stars:
mass $\sim$ 1.4 $M_\odot$ ($M_\odot \sim 2 \times 10^{30}$kg),
radius $\approx$ 10 km,
$\rho_{NS} \simeq 6.7 \times 10^{14}$ g/cm^3

中心密度: $\sim 6\rho_0$
中心温度: ~ 0
同位旋：极端高

原子核内的物质是极端致密的！中子星内部的密度更加致密！

中子星

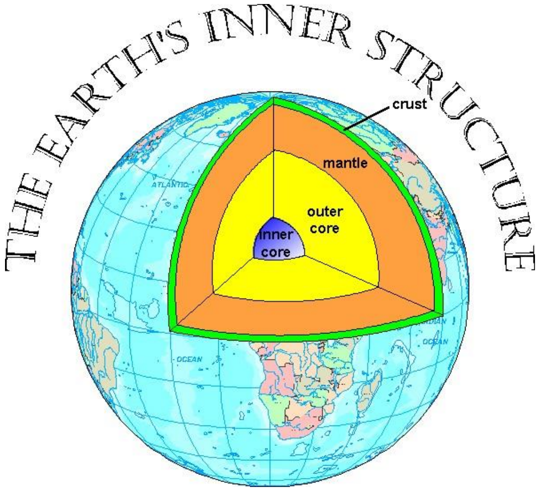

Earth:
$M_E \simeq 6 \times 10^{24}$kg,
$R_E \simeq 6.4 \times 10^3$km
Compactness M/R
$\simeq 5 \bullet 10^{-10}$ $(M_\odot/\text{km})$
$\rho_E \simeq 5.5$ g/cm^3

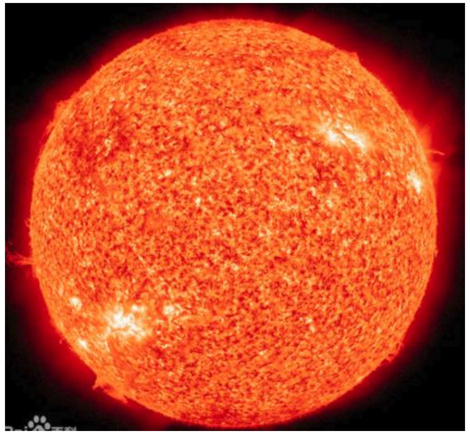

Sun:
$M_\odot \simeq 2 \times 10^{30}$kg,
$R_\odot \simeq 7 \times 10^5$km
Compactness M/R
$\simeq 1.4 \times 10^{-6}$ $(M_\odot/\text{km})$
$\rho_\odot \simeq 1.4$ g/cm^3

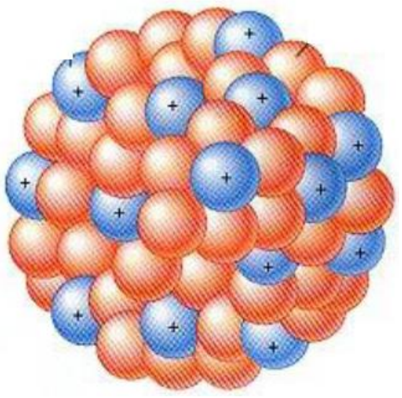

208Pb:
mass $\simeq 3 \times 10^{-25}$kg,
radius $\simeq 7 \times 10^{-18}$km
Compactness M/R
$\simeq 2 \times 10^{-38}$ $(M_\odot/\text{km})$
$\rho_{Pb} \simeq 2.1 \times 10^{14}$ g/cm^3

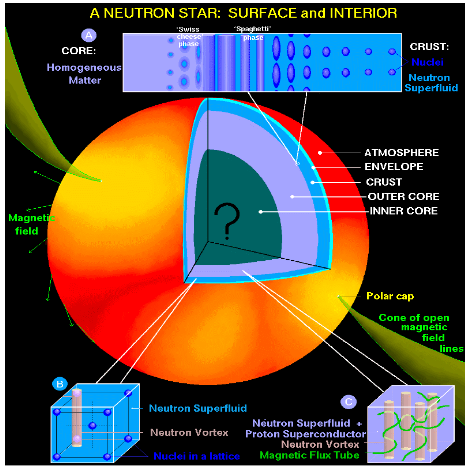

Neutron stars:
mass $\sim 1.4\ M_\odot$,
radius ≈ 10 km,
compactness M/R
$\simeq 0.14$ $(M_\odot/\text{km})$
$\rho_{NS} \simeq 6.7 \times 10^{14}$ g/cm^3

Lattimer/Prakash, Science 304, 536 (2004)

中子星

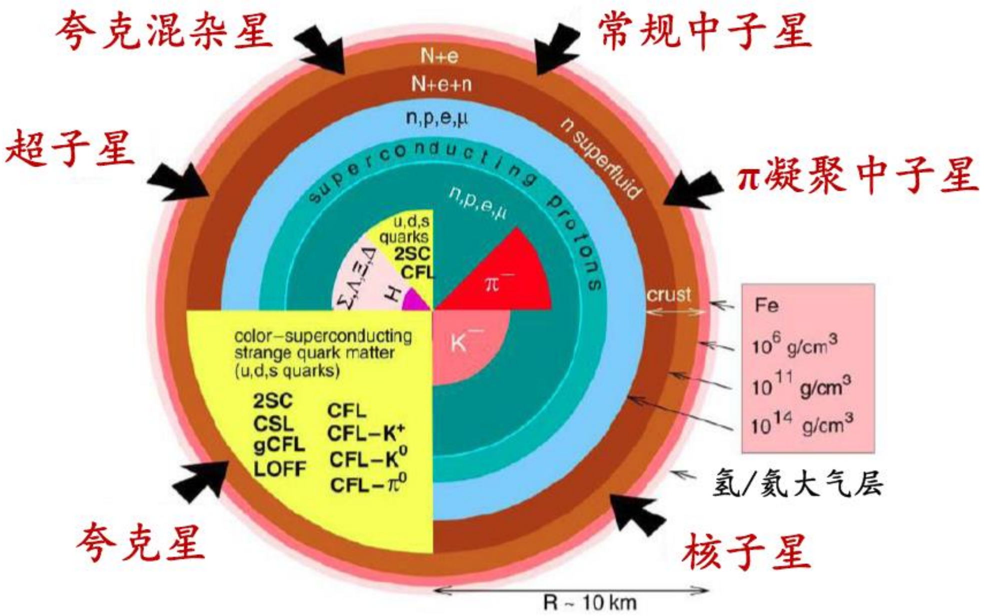

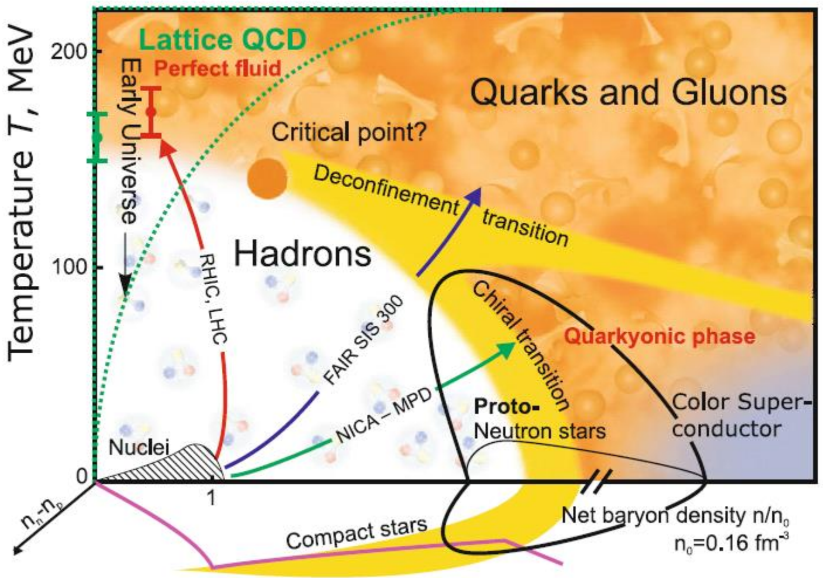

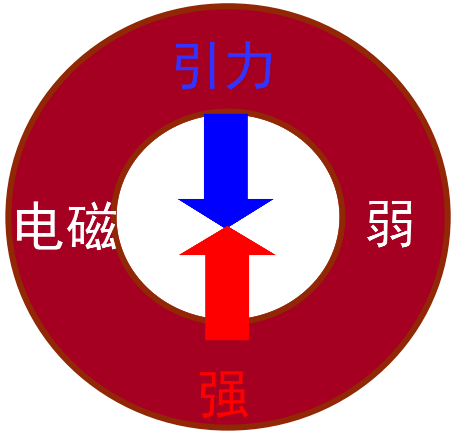

中子星-致密QCD物质（核物质）天然场所

致密星内部密度： $\sim 6\rho_0$

892 Am. J. Phys. 72 (7), July 2004

Neutron stars for undergraduates

Richard R. Silbar[a] and Sanjay Reddy[b]
Theoretical Division, Los Alamos National Laboratory, Los Alamos, New Mexico 87545

(Received 16 September 2003; accepted 13 February 2004)

INSTITUTE OF PHYSICS PUBLISHING EUROPEAN JOURNAL OF PHYSICS
Eur. J. Phys. 27 (2006) 577–610 doi:10.1088/0143-0807/27/3/012

Compact stars for undergraduates

Irina Sagert, Matthias Hempel, Carsten Greiner and Jürgen Schaffner-Bielich

双中子星并合

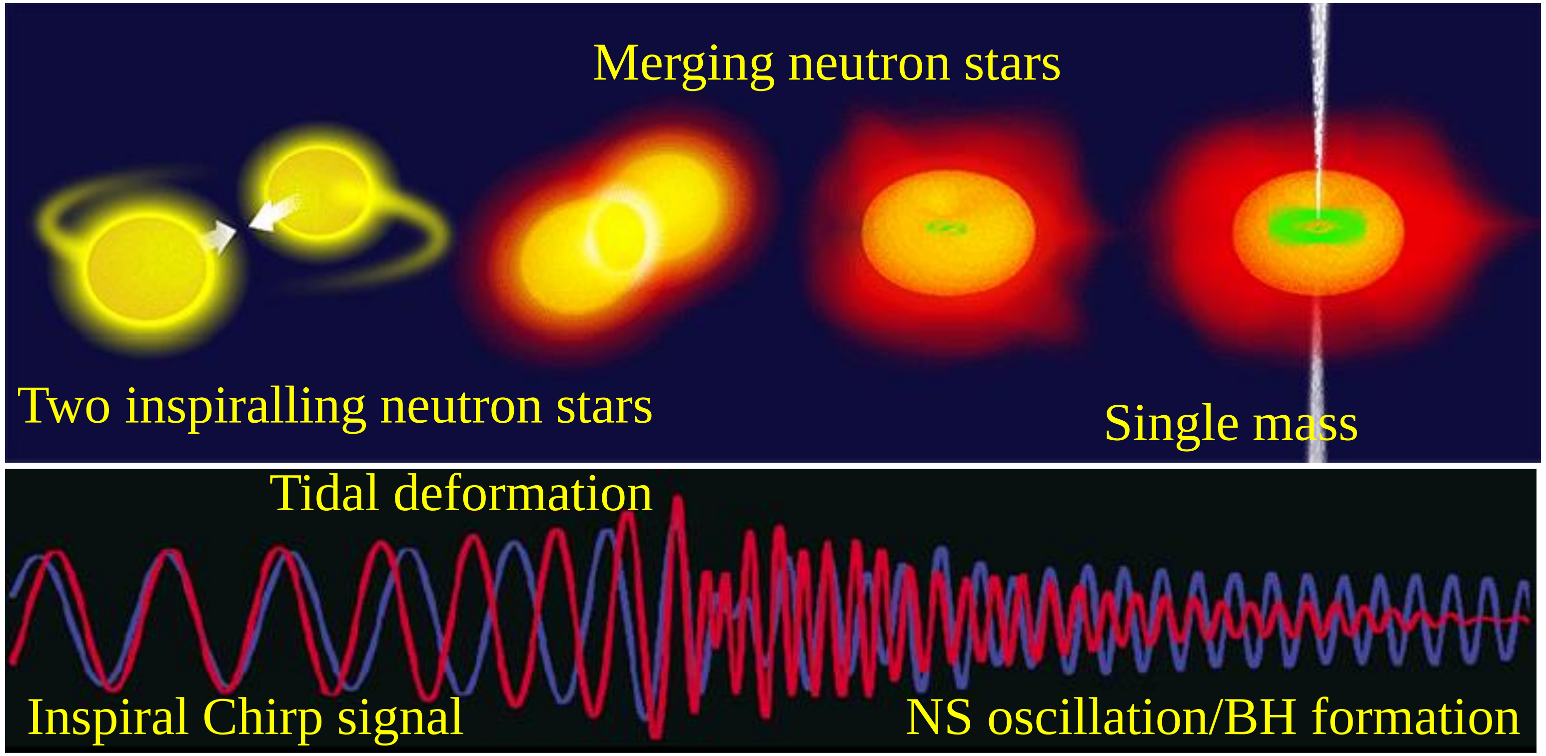

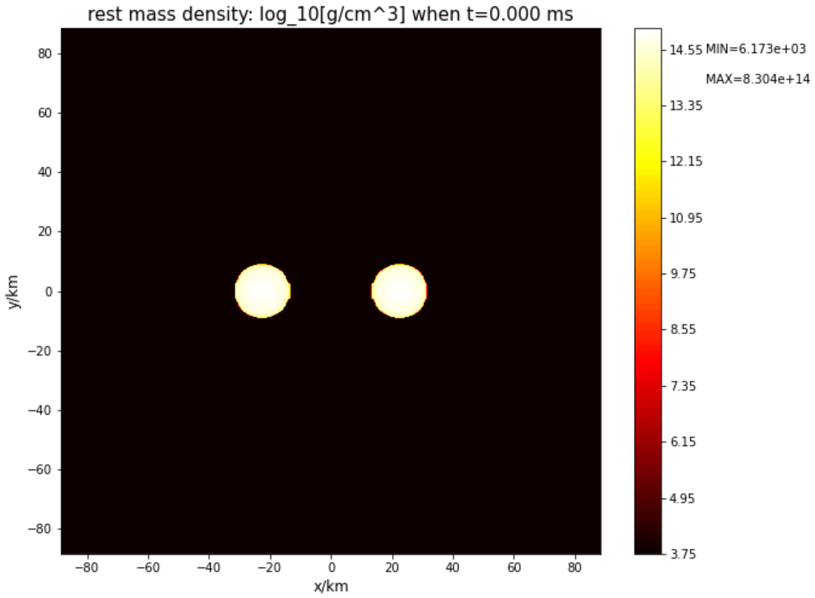

Matter density evolution of BNS mergers with equal mass 1.364M$_\odot$ (LS220 EOS) by Bai-Min Bai (白济民)

中子星并合过程中重子数密度能到达~15ρ_0 而温度能达到 ~50 MeV，但具有非常高的同位旋！

Refs: Elias R. Most et al., PRL122, 061101 (2019)， Andreas Bauswein et al., PRL122, 061102 (2019)

黑洞

黑洞的密度一定很大吗？

$$r = \frac{2GM}{c^2}$$

$$V = \frac{4}{3}\pi r^3$$

$$\rho = \frac{M}{V} = \frac{M}{\frac{4}{3}\pi r^3} = \frac{M}{\frac{4}{3}\pi\left(\frac{2GM}{c^2}\right)^3} = \frac{3c^6}{32\pi G^3 M^2}$$

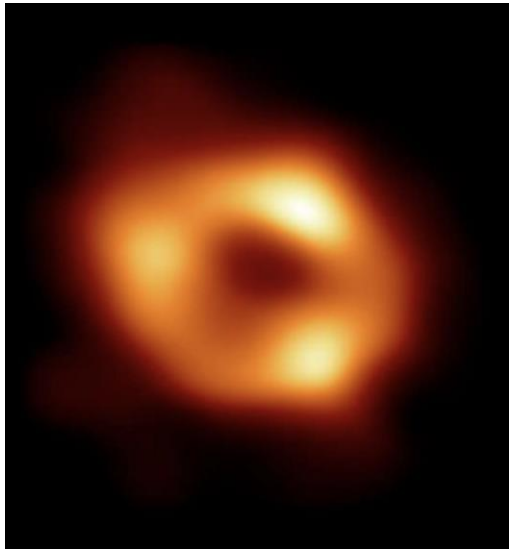

银心黑洞-人马座A*照片
by 事件视界望远镜(EHT), 2022.5.12

- **恒星级黑洞的平均密度 ~ 水的2000万亿倍**
- **430万倍$M_{\odot}$的银心超大质量黑洞—人马座A*(Sagittarius A* -Sgr A*) ~ 水的1000倍**
- **如果黑洞的质量达到太阳的1.36亿倍，其平均密度与水相当!**

目录

- 致密QCD物质
- 致密QCD物质的状态方程:
  - 对称能：核物质和夸克物质的状态方程
  - 中子皮：Pb/Ca中子半径之谜
  - 引力波：对称能的高密行为
- 致密QCD物质的相变：
  - QCD相图：概述
  - 重离子碰撞：粒子产生的并合模型
  - 致密星：中子星、超新星、双星并合
- 总结和展望

物质的状态方程

状态方程(EOS-Equation of State): **a relationship among several state variables**

van der Waals EOS: $$[p + a(\frac{n}{\mathrm{v}})^2](\mathrm{v} - nb) = nRT$$

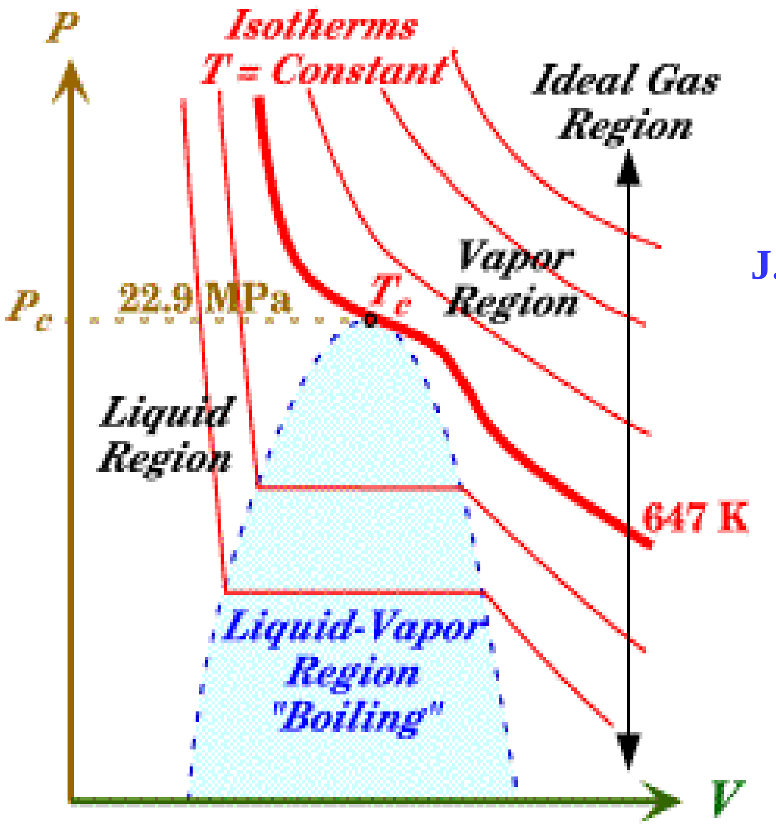

J.D. van der Waals
(1837 - 1923)

The Nobel Prize in Physics 1910 was awarded to Johannes Diderik van der Waals "*for his work on the equation of state for gases and liquids*".

- The EOS depends on the interactions and properties of the particles in the matter.
- It describes how the state of the matter changes under different conditions

SHANGHAI JIAO TONG UNIVERSITY 上海交通大學

核物质的状态方程及对称能

$$E(\rho,\delta)=E(\rho,0)+E_{\text{sym}}(\rho)\delta^2+O(\delta^4),\quad \delta=(\rho_n-\rho_p)/\rho$$

Symmetric Nuclear Matter (relatively well-determined)

Symmetry energy term (poorly known)

Isospin asymmetry

Incompressibility: $K_0=9\rho_0^2(\frac{d^2E}{d\rho^2})_{\rho_0}$

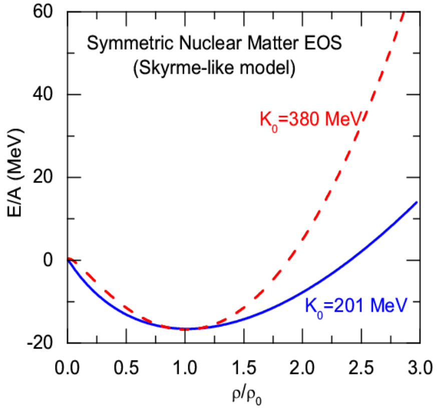

核物质对称能

$$\boxed{E_{\text{sym}}(\rho)\equiv\frac{1}{2}\frac{\partial^2E(\rho,\delta)}{\partial\delta^2}}$$

饱和密度：$\rho_0\approx0.16\ \text{fm}^{-3}$

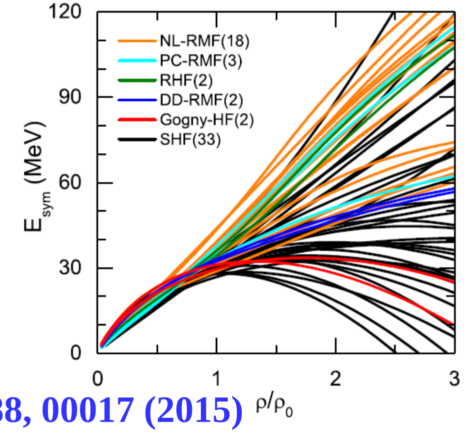

LWC, EPJ Web of Conf. 88, 00017 (2015)

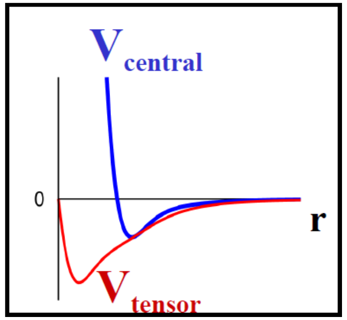

Nature of the nuclear force?

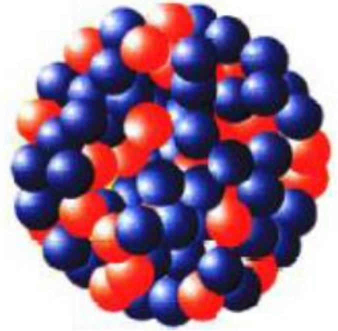

Structure and stability of nuclei?

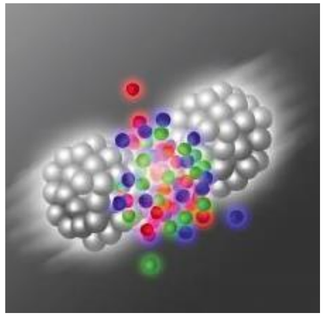

Dynamics of heavy ion collisions?

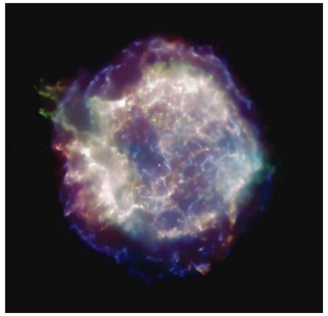

Mechanism of supernova explosion?

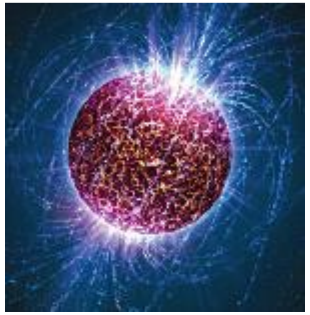

Nature of compact stars?

GW from binary NS merger?

有限核的对称能

$$\boxed{a_4(N-Z)^2/A}$$

$$\boxed{A(\text{核子数}) = N(\text{中子数}) + Z(\text{质子数})}$$

(Bethe-Weizsäcker mass formula, 1935)

泡利不相容原理

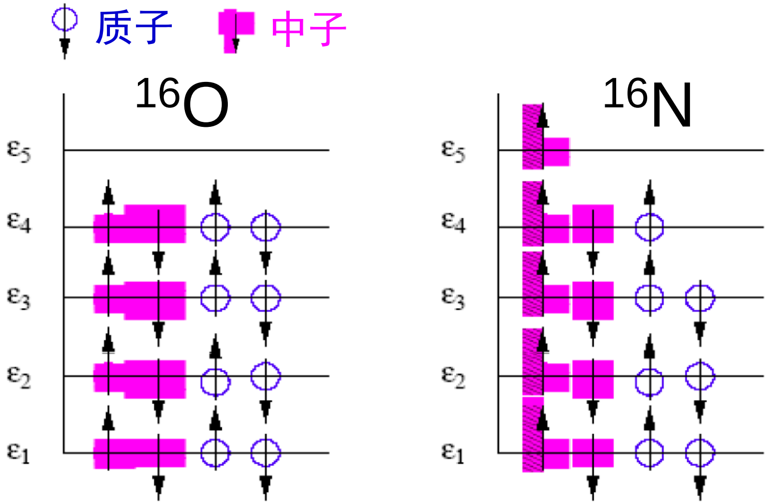

对称能：
使中子数和质子数
趋于对称

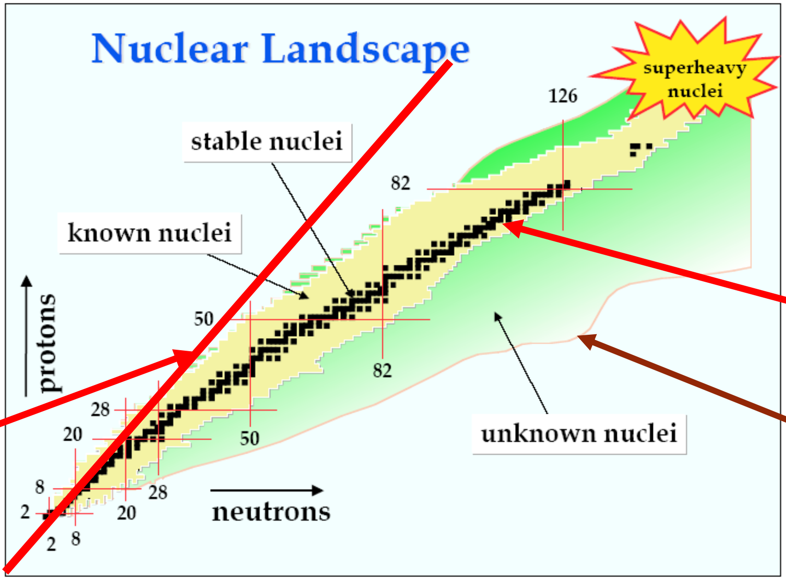

库仑能：
使中子数和质子数
偏离对称

N > Z

N = Z

Esym(2/3ρ_0) 与 中子滴线位置 存在强关联!

R. Wang (王睿) /LWC, PRC92, 031303(R) (2015)

原子核滴线和r过程路径的位置

Rui Wang(王睿) and LWC, PRC92, 031303(R) (2015)

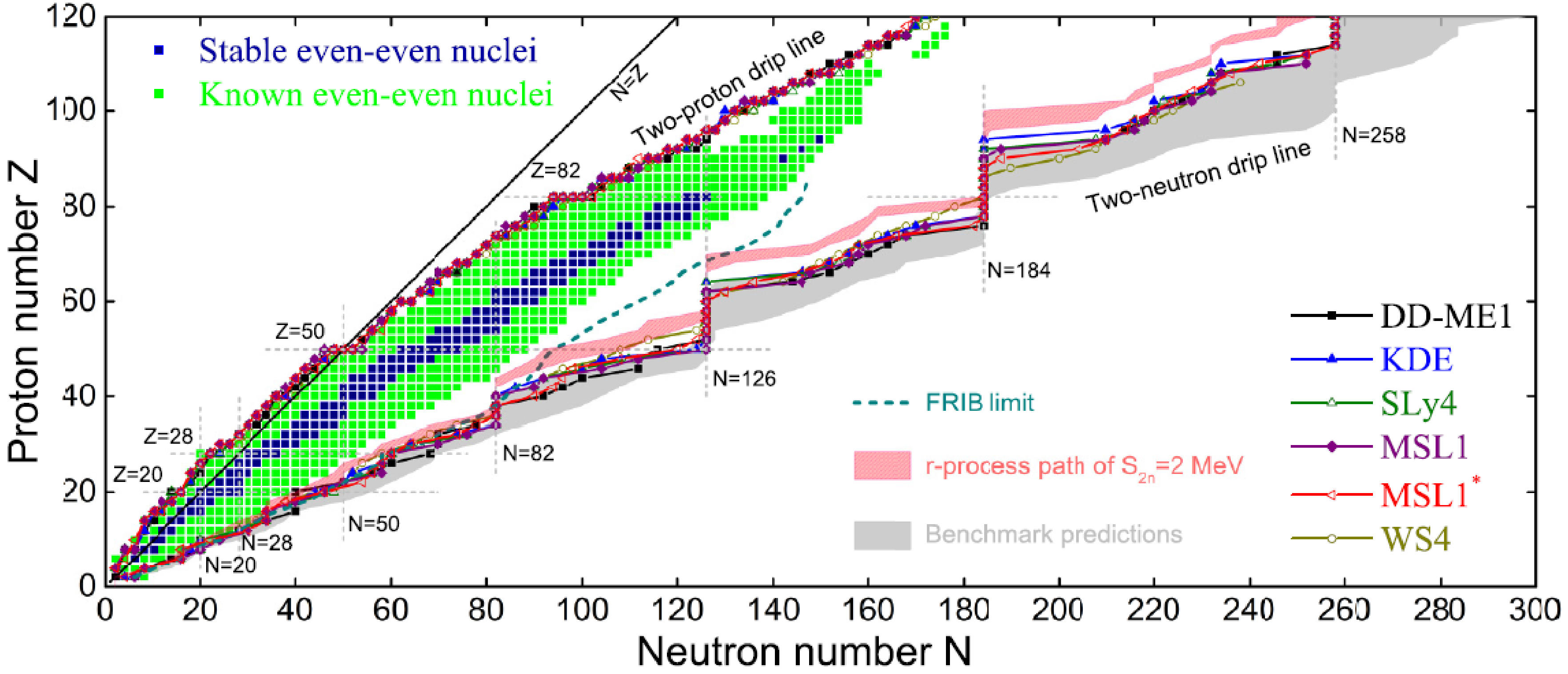

their even-even neighbors [22]. Accordingly, we estimate the total number of bound nuclei to be 6794, 6895, 7115, and 6659 for KDE, SLy4, MSL1, and MSL1*, respectively, leading to a precise estimate of 6866 ± 166 (only 3191 have been discovered experimentally [47]). Although the above

Note: The continuum and resonance states may also be important! (J. Meng et al., F.R. Xu et al., …)

Perhaps it makes more sense to talk about the r-process path!!!

上海交通大学 SHANGHAI JIAO TONG UNIVERSITY

为什么研究对称能？

Nuclear Physics
on the Earth

Astrophysics and Cosmology
in Heaven

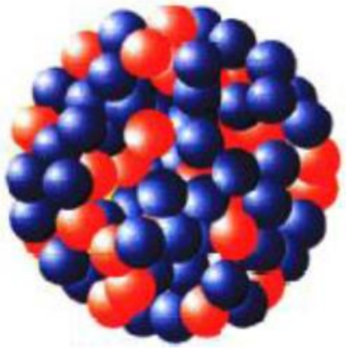

Symmetry Energy

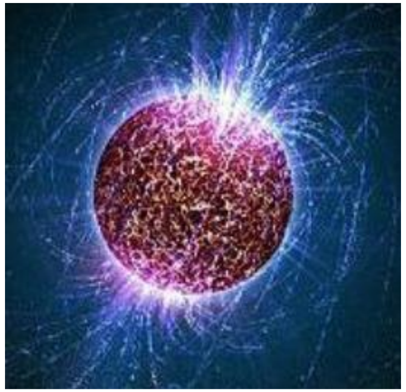

Physics at fm scale (~10 fm)

Size different by 18 orders !!!

Physics at km scale (~10 km)

对称能是回答两个以下重大科学问题的关键量
- 中子星和致密核物质的性质是什么?
- 宇宙中的元素是怎样产生的?

The Frontiers of Nuclear Science
A LONG RANGE PLAN
《美国核科学前沿长期规划》
The Nuclear Science Advisory Committee

- **确定对称能**已成为一些核物理大科学装置的重要物理目标，比如：**中国兰州CSR/惠州HIAF、日本RIBF/RIKEN、美国FRIB/MSU和德国FAIR/GSI**

为什么研究对称能？

本世纪11个最重要的物理问题（美国《发现》2002）

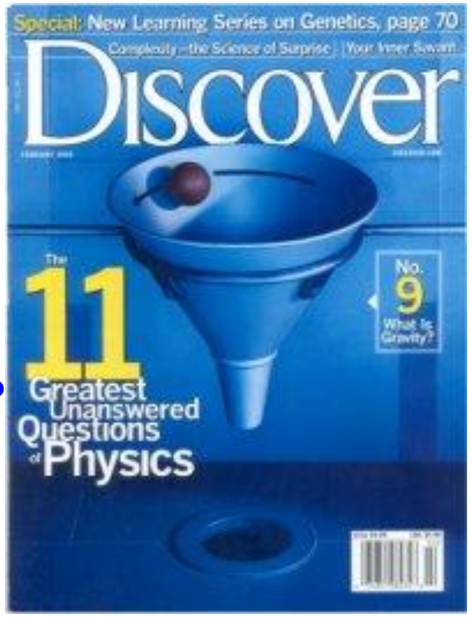

1. What is dark matter
2. What is dark energy
3. How were the heavy elements from iron to uranium made?
   从铁到铀等重元素是如何形成的？–高温、高密、高同位旋
4. Do neutrinos have mass?
5. Where do ultrahigh-energy particles come from?
6. Is a new theory of light and matter needed to explain what happens at very high energies and temperatures?
7. Are there new states of matter at ultrahigh temperatures and densities?
   极端高温、高密条件下会出现新物态吗？–高温、高密
8. Are protons unstable?
9. What is gravity?
10. Are there extra dimensions?
11. How did the universe begin?

QCD相图

V.E. Fortov, Extreme States of Matter – on Earth and in the Cosmos, Springer-Verlag, 2011

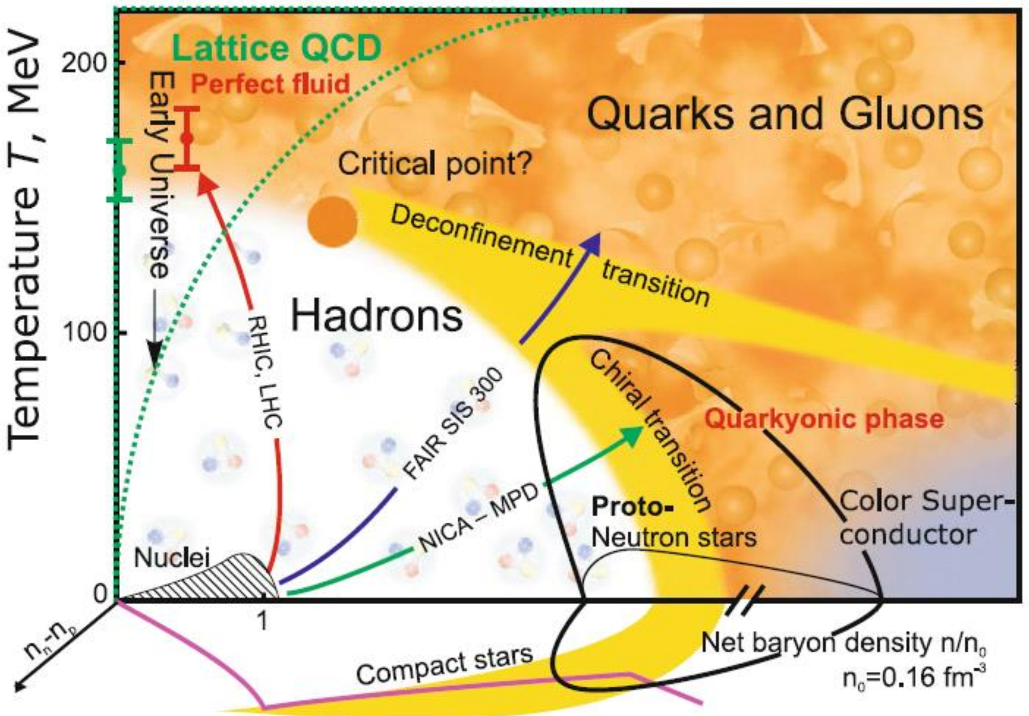

Holy Grail
of
Nuclear
Physics

Probing QCD phase diagram in
Nuclei and Heavy Ion Collisions
in terrestrial labs

and in NS Merger, SN, and NStar
in heaven?

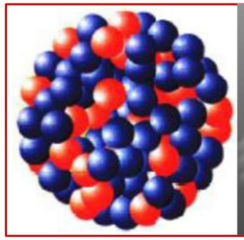
Nuclei

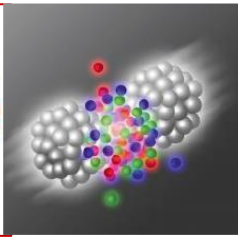
HIC

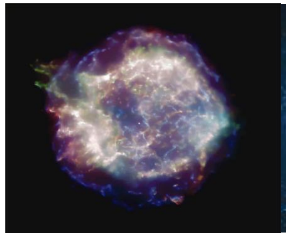
SN

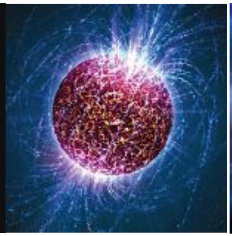
NStar


NS Merger

- Small baryon chemical potential:
  Smooth Crossover Transition
- Large baryon chemical potential:
  First-order Phase Transition
- QCD Critical Endpoint (CEP):
  where the first-order phase transition ends

NS Mergers/NStar/CCSNe:
Ideal and unique site to probe QCD phase diagram at
low T and high densities (and large isospin)!
Quark Matter Symmetry Energy?

M. Di Toro et al., NPA775 (2006); P.C. Chu (初鹏程)/LWC, ApJ780 (2014); LWC,《原子核物理评论》34, 20 (2017) [arXiv:1708.04433]

核物质对称能：多体理论方法

The nuclear matter EOS cannot be measured experimentally, its determination thus depends on theoretical approaches

●微观多体理论

Non-relativistic Brueckner-Bethe-Goldstone (BBG) Theory
Relativistic Dirac-Brueckner-Hartree-Fock (DBHF) approach
Self-Consistent Green's Function (SCGF) Theory
Variational Many-Body (VMB) approach
Green's Function Monte Carlo Calculation
V_{lowk} + Renormalization Group
Nuclear Lattice Approach
Chiral Perturbation Theory (ChPT)
QCD-based theory

优势:
- 无可调参数
- 外推性好

不足：
- 多体相互作用复杂，结果收敛慢
- 计算耗时，目前主要用于中低质量原子核及较低密度纯中子物质

● 密度泛函理论

Non-relativistic Hartree-Fock (Skyrme-Hartree-Fock)
Relativistic mean-field (RMF) theory

优势:
- 可描述整个周期表上的原子核
- 提供了描述原子核、重离子碰撞以及中子星的统一理论框架

不足：
- 参数是唯像的，结果具有较大的模型依赖

核物质对称能: 多体理论方法

L.W. Chen, Nucl. Phys. Rev. (原子核物理评论) 34, 20 (2017)
[arXiv:1708.04433]

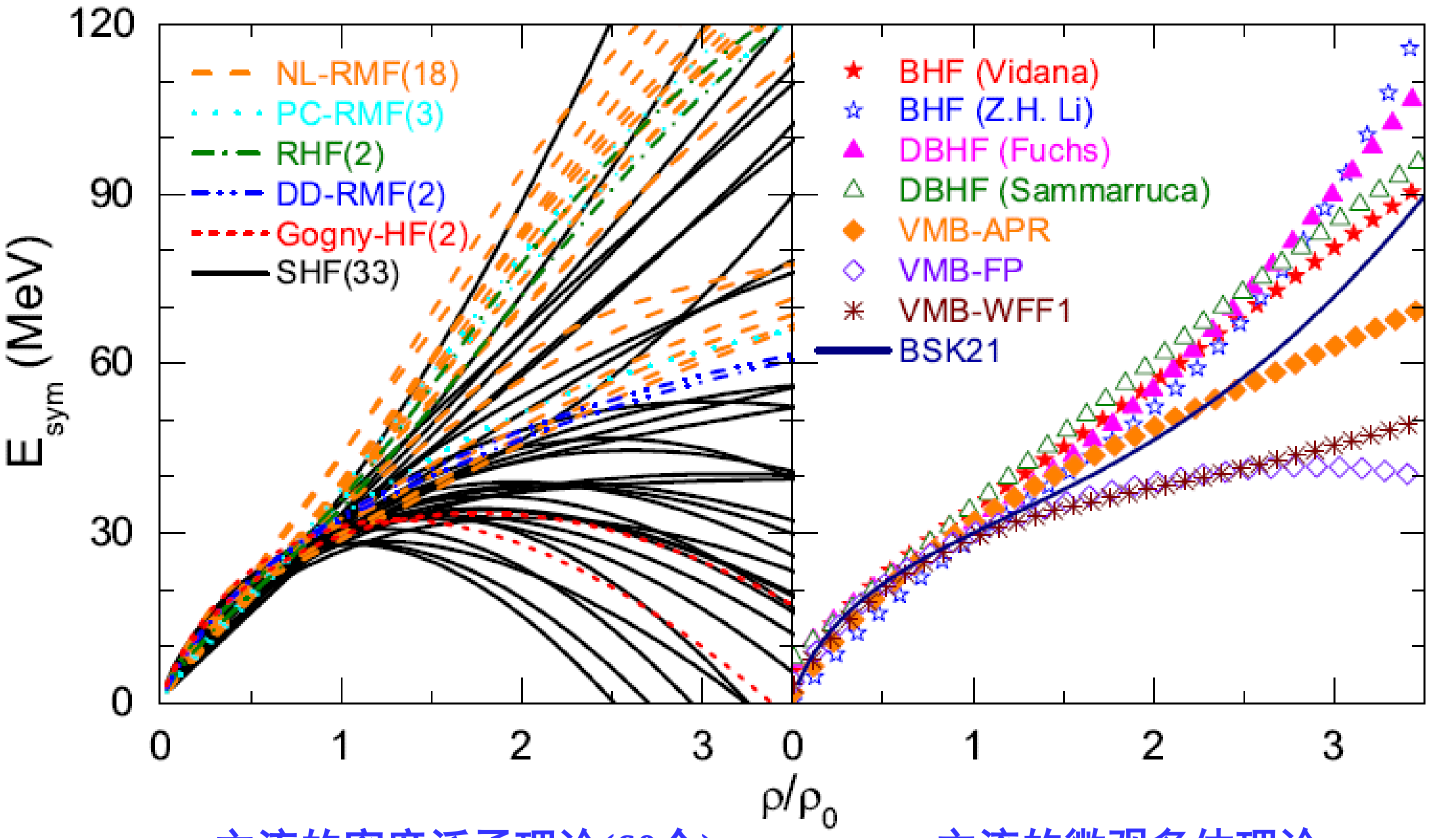

主流的密度泛函理论(60个)　　主流的微观多体理论

核物质对称能：多体理论方法

非相对论的能量密度泛函-extended Skyrme-Hartree-Fock(eSHF)模型

T.H.R Skyrme
(1922 - 1987)
Nucl. Phys. 9, 615 (1959)

$$
\begin{aligned}
v_{i,j} =\ & t_0(1+x_0P_\sigma)\delta(\boldsymbol{r}) \\
& + \frac{1}{2}t_1(1+x_1P_\sigma)[\boldsymbol{K}'^2\delta(\boldsymbol{r})+\delta(\boldsymbol{r})\boldsymbol{K}^2] \\
& + t_2(1+x_2P_\sigma)\boldsymbol{K}'\cdot\delta(\boldsymbol{r})\boldsymbol{K} \\
& + \frac{1}{6}t_3(1+x_3P_\sigma)n(\boldsymbol{R})^\alpha\delta(\boldsymbol{r}) \\
& + iW_0(\boldsymbol{\sigma}_i+\boldsymbol{\sigma}_j)\boldsymbol{K}'\cdot\delta(\boldsymbol{r})\boldsymbol{K} \\
& + \frac{1}{2}t_4(1+x_4P_\sigma)[\boldsymbol{K}'^2 n(\boldsymbol{R})^\beta\delta(\boldsymbol{r})+\delta(\boldsymbol{r})n(\boldsymbol{R})^\beta\boldsymbol{K}^2] \\
& + t_5(1+x_5P_\sigma)\boldsymbol{K}'\cdot n(\boldsymbol{R})^\gamma\delta(\boldsymbol{r})\boldsymbol{K}
\end{aligned}
$$

D. Vautherin and D. M. Brink, PRC5, 626 (1972);
D. Vautherin, PRC7, 296 (1973)

N. Chamel, S. Goriely, and J.M. Pearson, PRC80, 065804 (2009)

Z. Zhang(张振)/LWC, PRC94, 064326 (2016)

Momentum-dependence of many-body forces

LWC/Ko/Li/Xu, PRC82, 024321(2010)

13 Skyrme parameters: $\boxed{\alpha,\ t_0 \sim t_5,\ x_0 \sim x_5}$

$$
\mathcal{H} = \mathcal{K} + \mathcal{H}_0 + \mathcal{H}_3 + \mathcal{H}_{\rm eff} + \frac{G_S}{2}(\nabla\rho)^2 - \frac{G_V}{2}(\nabla\rho_1)^2 - \frac{G_{SV}}{2}\delta\nabla\rho\nabla\rho_1 + \mathcal{H}_{\rm Coul} + \mathcal{H}_{\rm SO} + \mathcal{H}_{\rm sg}, \quad (
$$

13 macroscopic nuclear properties:

$\boxed{n_0,\ E_0,\ K_0,\ J_0,\ E_{\rm sym},\ L,\ K_{\rm sym},\ m^*_{s,0},\ m^*_{v,0},\ G_S,\ G_V,\ G_{SV},\ G'_0}$

核物质对称能：多体理论方法

相对论协变的能量密度泛函-相对论平均场(RMF)模型

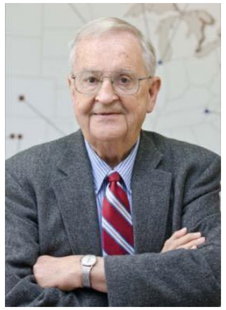

J.D. Walecka
(1932 -)

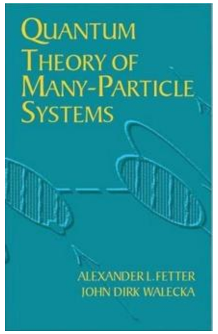

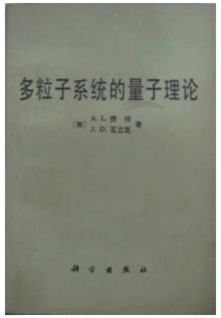

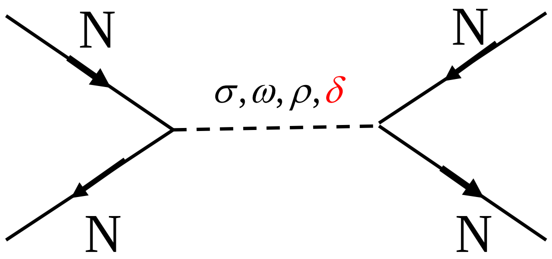

σ 介子：m_σ~500 MeV, $f_0(500)$，$I^G(J^{PC})=0^+(0^{++})$
ω 介子：m_ω = 783 MeV, $I^G(J^{PC})=0^-(1^{--})$
ρ 介子：m_ρ = 763 MeV, $I^G(J^{PC})=1^+(1^{--})$
δ 介子：m_δ = 980 MeV, $a_0(980)$，$I^G(J^{PC})=1^-(0^{++})$

$$
\begin{aligned}
\mathcal{L} = & \bar{\psi}(i\partial_\mu\gamma^\mu - m)\psi \\
& + g_\sigma\sigma\bar{\psi}\psi - g_\omega\omega_\mu\bar{\psi}\gamma^\mu\psi - g_\rho\vec{\rho}_\mu\bar{\psi}\gamma^\mu\vec{\tau}\psi + g_\delta\vec{\delta}\bar{\psi}\vec{\tau}\psi \\
& + \frac{1}{2}(\partial_\mu\sigma\partial^\mu\sigma - m_\sigma^2\sigma^2) - \frac{1}{3}b_\sigma m(g_\sigma\sigma)^3 - \frac{1}{4}c_\sigma(g_\sigma\sigma)^4 \\
& - \frac{1}{4}\omega_{\mu\nu}\omega^{\mu\nu} + \frac{1}{2}m_\omega^2\omega_\mu\omega^\mu + \frac{1}{4}c_\omega(g_\omega^2\omega_\mu\omega^\mu)^2 \\
& - \frac{1}{4}\rho_{\mu\nu}\rho^{\mu\nu} + \frac{1}{2}m_\rho^2\vec{\rho}_\mu\vec{\rho}^\mu + \frac{1}{2}\Lambda_V(g_\rho^2\vec{\rho}_\mu\vec{\rho}^\mu)(g_\omega^2\omega_\mu\omega^\mu) \\
& + \frac{1}{2}\left(\partial_\mu\vec{\delta}\partial^\mu\vec{\delta} - m_\delta^2\vec{\delta}^2\right) + \frac{1}{2}C_{\delta\sigma}(g_\sigma^2\sigma^2)\left(g_\delta^2\vec{\delta}^2\right)
\end{aligned}
$$

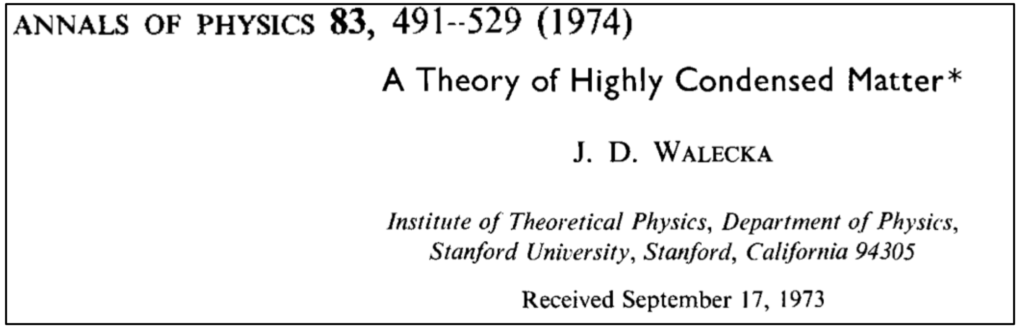
ANNALS OF PHYSICS 83, 491--529 (1974)

A Theory of Highly Condensed Matter*

J. D. WALECKA

Institute of Theoretical Physics, Department of Physics,
Stanford University, Stanford, California 94305

Received September 17, 1973

- ☐ 传统的RMF模型只包括σ、ω、ρ三种介子
- ☐ δ介子的重要性： Kubis/Kutschera, PLB(97)
  - ✓ 介子交换模型都包含了 δ 介子
  - ✓ δ 介子将引起中子和质子 Dirac 有效质量劈裂，与微观多体理论计算一致
  - ✓ 质量较大，主要影响同位旋相关的短程核力
  - ✓ 对高密同位旋非对称核物质以及中子星的性质起重要作用
  - ✓ 导致非对称核物质中质子和中子有效质量劈裂，从而影响重离子碰撞的同位旋效应以及中子星物质的输运性质
  - ✓ σ和δ耦合可以导致对称能高密行为变软

Fan Li (李帆), B.J. Cai(蔡宝军), Y. Zhou(周颖), W.Z. Jiang, and LWC, ApJ 929, 183 (2022)

核物质对称能: 多体理论方法

The nuclear energy density functional theory (e.g., SHF/RMF) is still the only realistic framework to simultaneously investigate the physics of heavy nuclei and neutron stars as well as heavy-ion collisions !!!

重离子碰撞: 微观输运模型

输运模型

Ni + Au, E/A = 45 MeV/A

Central collisions

Transport Models for HIC's at intermediate energies:

N-body approaches
CMD, QMD,IQMD,IDQMD,
ImQMD,ImIQMD,AMD,FMD

One-body approaches
BUU/IBUU, BNV, LV, IBL

Relativistic covariant approaches
RBUU,RVUU,RQMD…

Broad applications of transport models

in astrophyics, plasma physics, electron transport in semiconductor and nanostructures, particle and nuclear physics, nuclear stockpile stewardship

重离子碰撞: 微观输运模型

输运模型评估计划

Transport Model Evaluation Project (TMEP)

Transport 2014, Shanghai, Jan. 8-12, 2014.

重离子碰撞: 微观输运模型

输运模型评估计划

Transport Model Evaluation Project (TMEP)

PHYSICAL REVIEW C 93, 044609 (2016)

Understanding transport simulations of heavy-ion collisions at 100A and 400A MeV: Comparison of heavy-ion transport codes under controlled conditions

Jun Xu,[1,*] Lie-Wen Chen,[2,†] ManYee Betty Tsang,[3,‡] Hermann Wolter,[4,§] Ying-Xun Zhang,[5,∥] Joerg Aichelin,[6] Maria Colonna,[7] Dan Cozma,[8] Pawel Danielewicz,[3] Zhao-Qing Feng,[9] Arnaud Le Fèvre,[10] Theodoros Gaitanos,[11] Christoph Hartnack,[6] Kyungil Kim,[12] Youngman Kim,[12] Che-Ming Ko,[13] Bao-An Li,[14] Qing-Feng Li,[15] Zhu-Xia Li,[5] Paolo Napolitani,[16] Akira Ono,[17] Massimo Papa,[18] Taesoo Song,[19] Jun Su,[20] Jun-Long Tian,[21] Ning Wang,[22] Yong-Jia Wang,[15] Janus Weil,[19] Wen-Jie Xie,[23] Feng-Shou Zhang,[24] and Guo-Qiang Zhang[1]

TABLE I. The names, code authors and correspondents, and representative references of nine BUU-type and nine QMD-type models participating in the transport-code-comparison project. The intended beam-energy range for each code is given in GeV.

BUU type	Code correspondents	Energy range	Reference	QMD type	Code correspondents	Energy range	Reference
BLOB	P. Napolitani, M. Colonna	0.01–0.5	[19]	AMD	A. Ono	0.01–0.3	[28]
GIBUU-RMF	J. Weil	0.05–40	[20]	IQMD-BNU	J. Su, F. S. Zhang	0.05–2	[29]
GIBUU-Skyrme	J. Weil	0.05–40	[20]	IQMD	C. Hartnack, J. Aichelin	0.05–2	[30–32]
IBL	W. J. Xie, F. S. Zhang	0.05–2	[21]	CoMD	M. Papa	0.01–0.3	[33,34]
IBUU	J. Xu, L. W. Chen, B. A. Li	0.05–2	[11,22]	ImQMD-CIAE	Y. X. Zhang, Z. X. Li	0.02–0.4	[35]
pBUU	P. Danielewicz	0.01–12	[23,24]	IQMD-IMP	Z. Q. Feng	0.01–10	[36]
RBUU	K. Kim, Y. Kim, T. Gaitanos	0.05–2	[25]	IQMD-SINAP	G. Q. Zhang	0.05–2	[37]
RVUU	T. Song, G. Q. Li, C. M. Ko	0.05–2	[26]	TuQMD	D. Cozma	0.1–2	[38]
SMF	M. Colonna, P. Napolitani	0.01–0.5	[27]	UrQMD	Y. J. Wang, Q. F. Li	0.05–200	[39,40]

9 BUU-type codes and 9 QMD-type codes

重离子碰撞: 微观输运模型

输运模型评估计划

Transport Model Evaluation Project (TMEP)

PHYSICAL REVIEW C 93, 044609 (2016)

Understanding transport simulations of heavy-ion collisions at 100*A* and 400*A* MeV: Comparison of heavy-ion transport codes under controlled conditions

Jun Xu,[1,*] Lie-Wen Chen,[2,†] ManYee Betty Tsang,[3,‡] Hermann Wolter,[4,§] Ying-Xun Zhang,[5,∥] Joerg Aichelin,[6] ...

PHYSICAL REVIEW C 97, 034625 (2018)

Comparison of heavy-ion transport simulations: Collision integral in a box

Ying-Xun Zhang,[1,2,*] Yong-Jia Wang,[3,†] Maria Colonna,[4,‡] Pawel Danielewicz,[5,§] Akira Ono,[6,∥] Manyee Betty Tsang,[5,¶] ...

PHYSICAL REVIEW C 100, 044617 (2019)

Comparison of heavy-ion transport simulations: Collision integral with pions and Δ resonances in a box

Akira Ono,[1,*] Jun Xu,[2,3,†] Maria Colonna,[4] Pawel Danielewicz,[5] Che Ming Ko,[6] Manyee Betty Tsang,[5] Yong-Jia Wang,[7] ...

PHYSICAL REVIEW C 104, 024603 (2021)

Comparison of heavy-ion transport simulations: Mean-field dynamics in a box

Maria Colonna,[1,*] Ying-Xun Zhang,[2,3,†] Yong-Jia Wang,[4,‡] Dan Cozma,[5] Pawel Danielewicz,[6,§] Che Ming Ko,[7] Akira Ono,[8,∥] Manyee Betty Tsang,[6,¶] Rui Wang,[9,10] Hermann Wolter,[11,#] Jun Xu,[12,9,**] Zhen Zhang,[13] Lie-Wen Chen,[14] Hui-Gan Cheng,[15] Hannah Elfner,[16,17,18] Zhao-Qing Feng,[15] Myungkuk Kim,[19] Youngman Kim,[20] Sangyong Jeon,[21] Chang-Hwan Lee,[22] Bao-An Li,[23] Qing-Feng Li,[4,24] Zhu-Xia Li,[2] Swagata Mallik,[25] Dmytro Oliinychenko,[26,27] Jun Su,[13] Taesoo Song,[16,28] Agnieszka Sorensen,[29] and Feng-Shou Zhang[30,31]

Progress in Particle and Nuclear Physics 125 (2022) 103962

Contents lists available at ScienceDirect

Progress in Particle and Nuclear Physics

journal homepage: www.elsevier.com/locate/ppnp

Review

Transport model comparison studies of intermediate-energy heavy-ion collisions

Hermann Wolter [1,*], Maria Colonna [2], Dan Cozma [3], Pawel Danielewicz [4,5], Che Ming Ko [6], Rohit Kumar [4], Akira Ono [7], ManYee Betty Tsang [4,5], Jun Xu [8,9], Ying-Xun Zhang [10,11], Elena Bratkovskaya [12,13], Zhao-Qing Feng [14], Theodoros Gaitanos [15], Arnaud Le Fèvre [12], Natsumi Ikeno [16], Youngman Kim [17], Swagata Mallik [18], Paolo Napolitani [19], Dmytro Oliinychenko [20], Tatsuhiko Ogawa [21], Massimo Papa [2], Jun Su [22], Rui Wang [9,23], Yong-Jia Wang [24], Janus Weil [25], Feng-Shou Zhang [26,27], Guo-Qiang Zhang [9], Zhen Zhang [22], Joerg Aichelin [28], Wolfgang Cassing [25], Lie-Wen Chen [29], Hui-Gan Cheng [14], Hannah Elfner [12,13,20], K. Gallmeister [25], Christoph Hartnack [28], Shintaro Hashimoto [21], Sangyong Jeon [30], Kyungil Kim [17], Myungkuk Kim [31], Bao-An Li [32], Chang-Hwan Lee [33], Qing-Feng Li [24,34], Zhu-Xia Li [10], Ulrich Mosel [25], Yasushi Nara [35], Koji Niita [36], Akira Ohnishi [37], Tatsuhiko Sato [21], Taesoo Song [12], Agnieszka Sorensen [38,39], Ning Wang [11,40], Wen-Jie Xie [41], (TMEP collaboration)

重离子碰撞: 微观输运模型

Boltzmann-Uehling-Uhlenbeck(BUU)输运模型

Phase−space distributions $f(\vec{r},\vec{p},t)$ satisfy the Boltzmann equation

$$\frac{\partial f(\vec{r},\vec{p},t)}{\partial t} + \vec{\nabla}_p \varepsilon \cdot \vec{\nabla}_r f - \vec{\nabla}_r \varepsilon \cdot \vec{\nabla}_p f = I_c(f, \sigma_{NN})$$

- Solve the Boltzmann equation using test particle method
- Isospin-dependent initialization
- Isospin- (momentum-) dependent mean field potential

$$\boxed{V = V_0 + \frac{1}{2}(1-\tau_z)V_C + V_{sym}}$$

EOS

- Isospin-dependent N-N cross sections

  a. Experimental free space N-N cross section σ_{exp}

  b. In-medium N-N cross section from the Dirac-Brueckner approach based on Bonn A potential $\sigma_{in\text{-}medium}$

  c. Mean-field consistent cross section due to m*
- Isospin-dependent Pauli Blocking

重离子碰撞: 微观输运模型-LBUU

上海交通大学 SHANGHAI JIAO TONG UNIVERSITY

(1) 格点Hamiltonian方法

Ground state LHV Calculations

The rms radius, fraction of bound nucleons, binding energy of ground state evolution

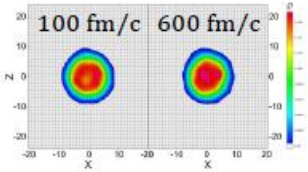

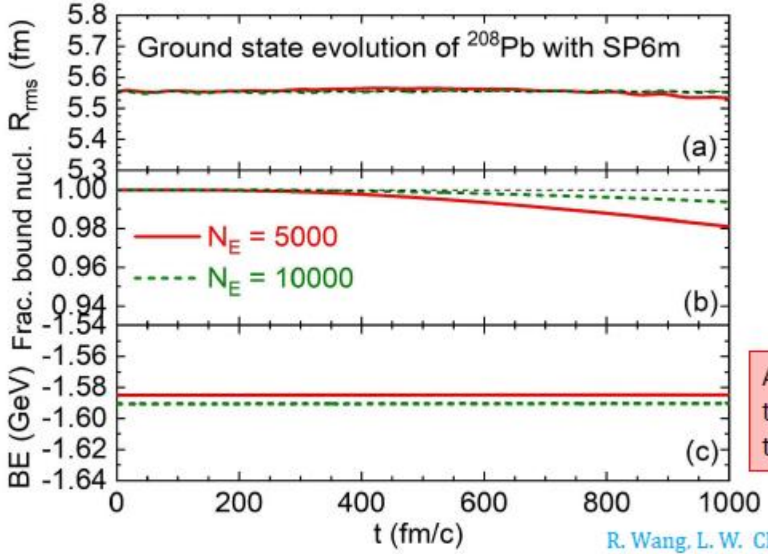

Free test nucleons are those whose form factor do not overlap with that of other test nucleons

$$\langle r^2 \rangle = N_{\rm nucl}^{-1} \int_{\rm bound} d^3r^2 \rho(r)$$

At 1000 fm/c, only about 2% of test nucleons evaporated from the nucleus for $N_E = 5000$ case

R. Wang, L. W. Chen, and Z. Zhang, PRC99, 044609 (2019)

Very stable ground state of the initialized nuclei!

The GPU parallel computing with large enough test particle number (up to ~100000 !)

王睿, LWC, 张振, PRC99, 044607 (2019)

(2) 随机碰撞方法

Physics Letters B 807 (2020) 135532

Contents lists available at ScienceDirect

Physics Letters B

www.elsevier.com/locate/physletb

ELSEVIER

Constraining the in-medium nucleon-nucleon cross section from the width of nuclear giant dipole resonance

Rui Wang[a,b], Zhen Zhang[c], Lie-Wen Chen[d], Che Ming Ko[e], Yu-Gang Ma[a,b]

基于格点Hamiltonian方法和随机碰撞方法，发展了完整的格点Boltzmann-Uehling-Uhlenbeck(LBUU)输运模型并成功用于描述原子核巨偶极共振宽度

王睿, 张振, LWC, C.M. Ko, and Y.G. Ma, PLB (2020)

frontiers in Physics

Invited Review

REVIEW
published: 06 October 2020
doi: 10.3389/fphy.2020.00330

Nuclear Collective Dynamics in Transport Model With the Lattice Hamiltonian Method

Rui Wang[1,2], Zhen Zhang[3], Lie-Wen Chen[4] and Yu-Gang Ma[1,2]*

王睿, 张振, LWC, and Y.G. Ma, Front. in Phys. (2020)

重离子碰撞: 微观输运模型-LBUU

(3) Skyrm赝势 – A Unified Energy Density Functional for HICs, Nuclear Structure and Neutron Stars

Skyrme pseudopotential

$$v_{Sk} = t_0^{(0)}(1 + x_0^{(0)}\hat{P}_\sigma) + \frac{1}{6}t_3^{(0)}(1 + x_3^{(0)}\hat{P}_\sigma)\rho^\alpha(\vec{R}) + \frac{1}{2}t_1^{(2)}(1 + x_1^{(2)}\hat{P}_\sigma)[\vec{k}'^2 + \vec{k}^2] + t_2^{(2)}(1 + x_2^{(2)}\hat{P}_\sigma)\vec{k}' \cdot \vec{k}$$

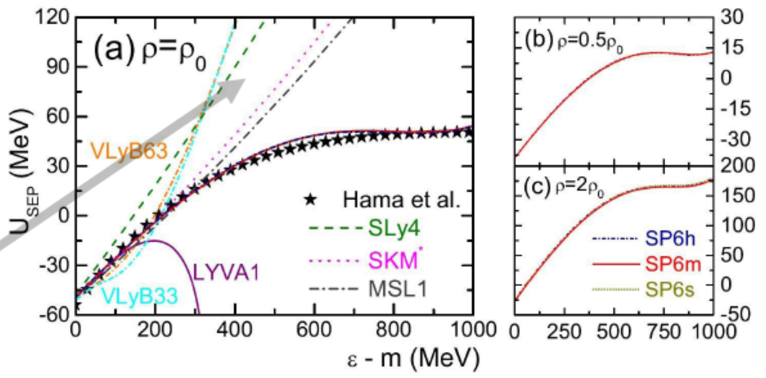

R. Wang, L.-W. Chen, and Y. Zhou, PRC98, 054618 (2018)

王睿, LWC, 周颖,
PRC98, 054618 (2018)

Can fit the experimental nucleon optical model potential up to ~1 GeV !

N3LO local nuclear energy density functional → Corresponding N3LO Skyrme pseudopotential

B.G. Carlsson et al PRC78,044326 (2008)

F. Raimondi et al PRC83,054311 (2011)

4^{th} and 6^{th} order of momentum

$$+\frac{1}{4}t_1^{(4)}(1 + x_1^{(4)}\hat{P}_\sigma)[(\vec{k}'^2 + \vec{k}^2)^2 + 4(\vec{k}' \cdot \vec{k})^2] + t_2^{(4)}(1 + x_2^{(4)}\hat{P}_\sigma)(\vec{k}' \cdot \vec{k})(\vec{k}'^2 + \vec{k}^2)$$

$$+\frac{1}{2}t_1^{(6)}(1 + x_1^{(6)}\hat{P}_\sigma)(\vec{k}'^2 + \vec{k}^2)^2[(\vec{k}'^2 + \vec{k}^2)^2 + 12(\vec{k}' \cdot \vec{k})^2]$$

$$+t_2^{(6)}(1 + x_2^{(6)}\hat{P}_\sigma)(\vec{k}' \cdot \vec{k})[3(\vec{k}'^2 + \vec{k}^2)^2 + 4(\vec{k}' \cdot \vec{k})^2]$$

plus spin-orbit and tensor terms
an overall $\delta(\vec{r}_1 - \vec{r}_2)$ is implicit

Suitable interactions for HICs at CEE/CSR/HIAF energies !
Also for nuclear structures and neutron stars !

重离子碰撞: 微观输运模型-LBUU

(4) 轻核自由度 – Dynamical treatment

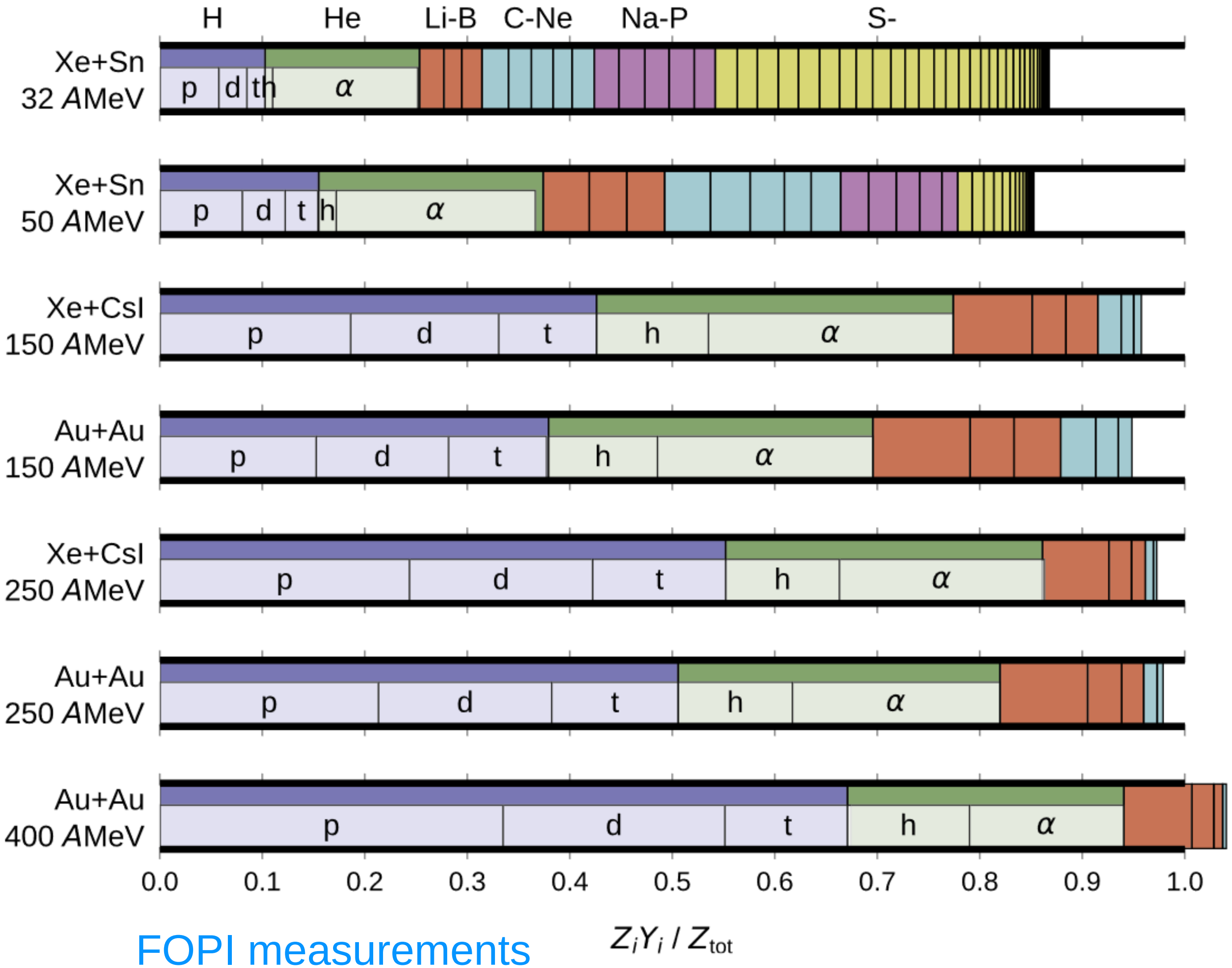

FOPI measurements

Light nuclei are important and account for a large portion of the measured final state charged particles

- Their production mechanism
- Their effects on nucleon/pion observables
- They may provide more efficient probes of nuclear equation of state
- Their in-medium properties in nuclear matter
- ……

One interesting feature is that more α are produced than helium-3 (h).

FOPI Collaboration, NPA 848, 366 (2010)

A. Ono, PNP 105, 139 (2019)

重离子碰撞: 微观输运模型-LBUU

(4) 轻核自由度 – Dynamical treatment

Light nuclei in Kinetic approach/LBUU

Kinetic equations are derived based on the closed time-path Green's function formulism

For example, in the deuteron case, the two-body Green's function G_2 satisfies an equation

$$G_2 = \mathscr{G}_2 + \frac{1}{4}\mathscr{G}_2 v G_2$$

The light nuclei are realized as poles of the many-body Green's function.

In the vicinity of the pole, we have

$$i\left\langle x \left| G_2^<(P,\Omega,R,T) \right| x' \right\rangle \sim \langle x|\phi(P,R,T)|\rangle\langle\phi(P,R,T)x'\rangle f_2(P,R,T) 2\pi\delta[\Omega - E(P,R,T)]$$

$$i\left\langle x \left| G_2^>(P,\Omega,R,T) \right| x' \right\rangle \sim \langle x|\phi(P,R,T)|\rangle\langle\phi(P,R,T)x'\rangle \left[1 + f_2(P,R,T)\right] 2\pi\delta[\Omega - E(P,R,T)]$$

P. Danielewicz and G. F. Bertsch, Nuclear Physics A533, 712-748 (1991)

Finally leads to equations of the occupation number f_τ of light nuclei

$$\left(\partial_t + \vec{\nabla}_p \epsilon_\tau \cdot \vec{\nabla}_r - \vec{\nabla}_r \epsilon_\tau \cdot \vec{\nabla}_p\right) f_\tau = \mathscr{K}_\tau^< \left[f_n, f_p, f_d, \cdots\right] (1 \pm f_\tau) - \mathscr{K}_\tau^> \left[f_n, f_p, f_d, \cdots\right] f_\tau, \quad \tau = n, p, d, t, h, \alpha$$

重离子碰撞: 微观输运模型-LBUU

(4) 轻核自由度 – Dynamical treatment

Light nuclei in Kinetic approach/LBUU

For example, the loss term of α-particle

$$K_{\alpha}^{>} f_{\alpha}=\frac{\mathcal{S}_{5'} f_{\alpha}}{2E_{\alpha}}\int\prod_{i=1'}^{5'}\frac{\mathrm{d}\vec{p}_i}{(2\pi\hbar)^3 2E_i}\frac{\mathrm{d}\vec{p}_N}{(2\pi\hbar)^3 2E_N}\overline{\left|\mathcal{M}_{N\alpha\to NNNNN}\right|^2} g_N f_N\prod_{i=1'}^{5'}(1\pm f_i)(2\pi)^4\delta^4\left(\sum_{i=1'}^{5'}p_i-p_N-p_\alpha\right)$$

$$+\frac{\mathcal{S}_{3'} f_{\alpha}}{2E_{\alpha}}\int\prod_{i=1'}^{3'}\frac{\mathrm{d}\vec{p}_i}{(2\pi\hbar)^3 2E_i}\frac{\mathrm{d}\vec{p}_N}{(2\pi\hbar)^3 2E_N}\overline{\left|\mathcal{M}_{N\alpha\to NNt}\right|^2} g_N f_N\prod_{i=1'}^{3'}(1\pm f_i)(2\pi)^4\delta^4\left(\sum_{i=1'}^{3'}p_i-p_N-p_\alpha\right)+t\to h$$

$$+\frac{\mathcal{S}_{2'} f_{\alpha}}{2E_{\alpha}}\int\prod_{i=1'}^{2'}\frac{\mathrm{d}\vec{p}_i}{(2\pi\hbar)^3 2E_i}\frac{\mathrm{d}\vec{p}_N}{(2\pi\hbar)^3 2E_N}\overline{\left|\mathcal{M}_{N\alpha\to dt}\right|^2} g_N f_N\prod_{i=1'}^{2'}(1\pm f_i)(2\pi)^4\delta^4\left(\sum_{i=1'}^{2'}p_i-p_N-p_\alpha\right)+t\to h$$

+ elastic part.

Light nuclei can be produced and dissociated through many-body scatterings (currently we have included the red ones)

- A = 2 $\pi NN\leftrightarrow\pi d$, $NNN\leftrightarrow Nd$
- A = 3 $\pi NNN\leftrightarrow\pi t(h)$, $\pi Nd\leftrightarrow\pi t(h)$, $NNNN\leftrightarrow Nt(h)$, $NNd\leftrightarrow Nt(h)$
- A = 4 $\pi NNNN\leftrightarrow\pi\alpha$, $\pi NNd\leftrightarrow\pi\alpha$, $\pi Nt(h)\leftrightarrow\pi\alpha$, $NNNNN\leftrightarrow N\alpha$, $NNNd\leftrightarrow N\alpha$, $NNt(h)\leftrightarrow N\alpha$, $dt(h)\leftrightarrow N\alpha$

- Many body **transition amplitudes** e.g., $\overline{\left|\mathcal{M}^2_{Npn\leftrightarrow Nd}\right|^2}$
- The medium effect of light nuclei – **Mott effect**

R. Wang et al., Phys.Rev.C 108 (2023) 3, L031601

R. Wang(王睿), Y.-G. Ma, L.-W. Chen, C. M. Ko, K.-J. Sun(孙开佳), Z. Zhang (张振), PRC108, L031601 (2023)

重离子碰撞: 微观输运模型-LBUU

(4) 轻核自由度 – Dynamical treatment

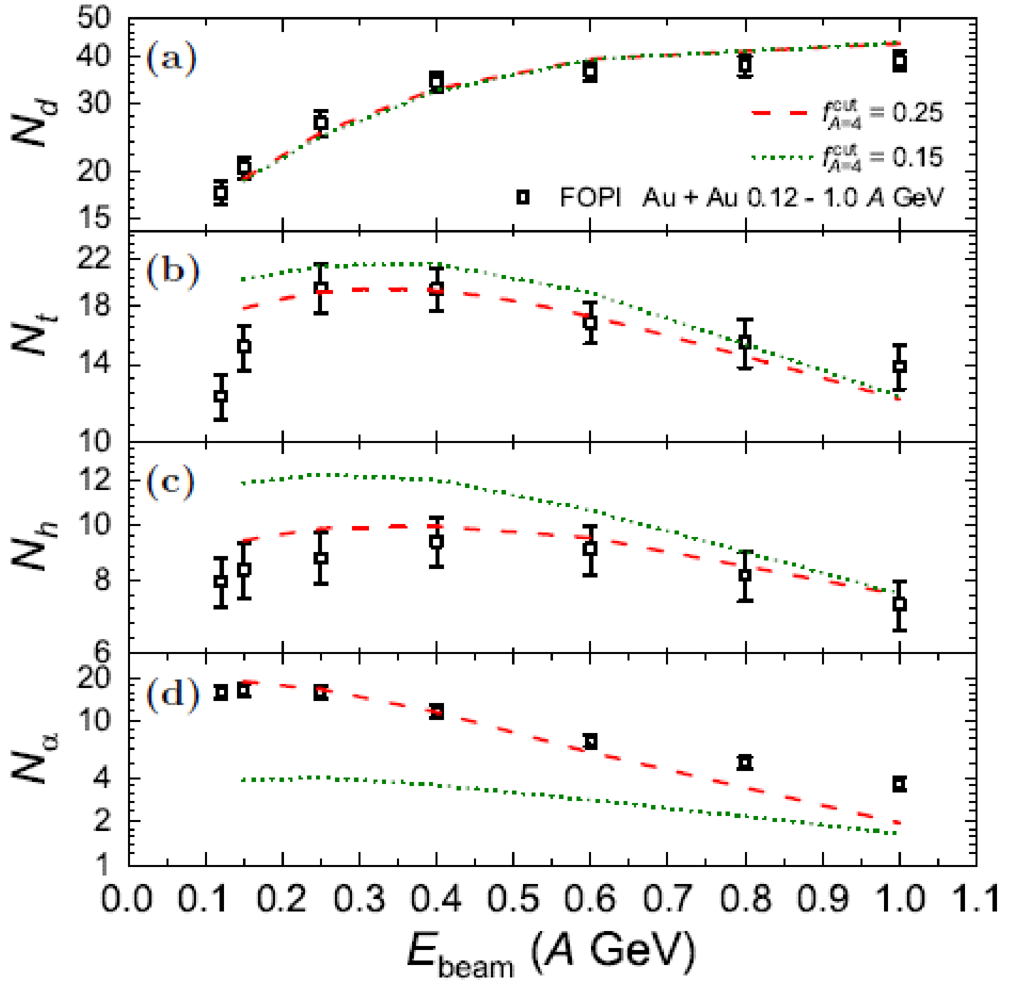


PHYSICAL REVIEW C **108**, L031601 (2023)

Letter

Kinetic approach of light-nuclei production in intermediate-energy heavy-ion collisions

Rui Wang[1,2,*] Yu-Gang Ma[1,3,†] Lie-Wen Chen[4,‡] Che Ming Ko[5,§] Kai-Jia Sun[1,3,∥] and Zhen Zhang[6,¶]

R. Wang(王睿), Y.-G. Ma, L.-W. Chen, C. M. Ko, K.-J. Sun(孙开佳), Z. Zhang (张振), PRC108, L031601 (2023)

格点BUU输运模型：基于动力学包含d, t, ^{3}He, ^{4}He等轻核自由度，同时考虑轻核的Mott效应，成功解释FOPI实验数据！

Light nuclei in Kinetic approach at RHIC:

K.-J. Sun(孙开佳), R. Wang(王睿), C. M. Ko, Y.-G. Ma, C. Shen (沈纯), Nature Comm. 15, 1074 (2024) [arXiv:2106.12742, 2207.12532]

重离子碰撞: 微观输运模型-LBUU

Skyrm赝势 – for HICs up to 1.5 AGeV (even higher) and Neutron Stars

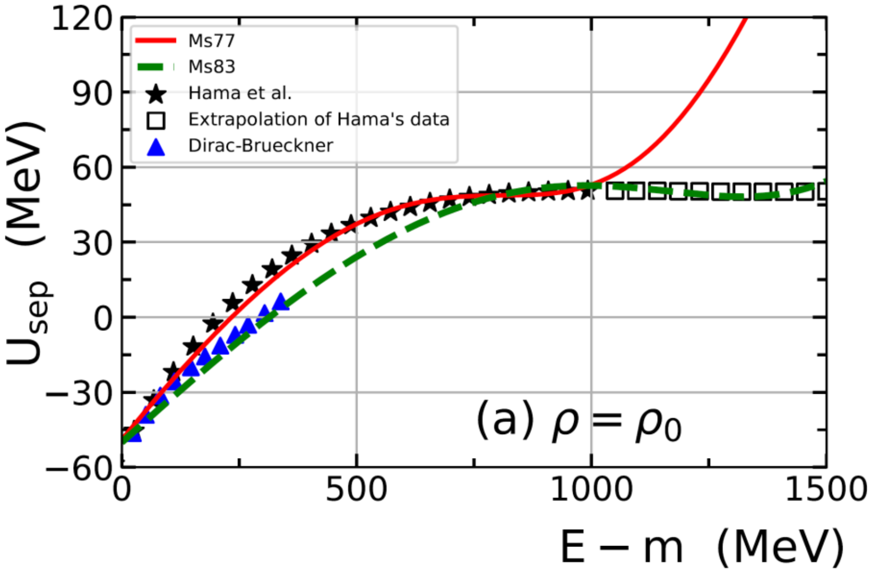

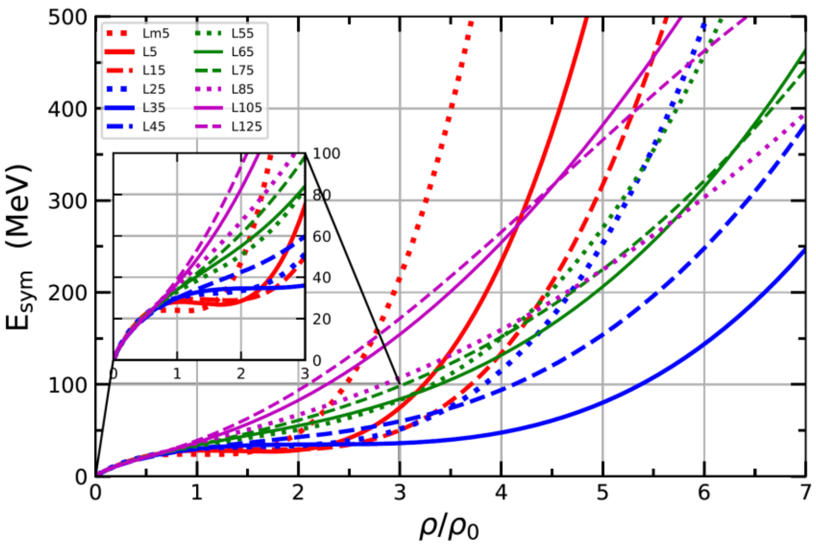

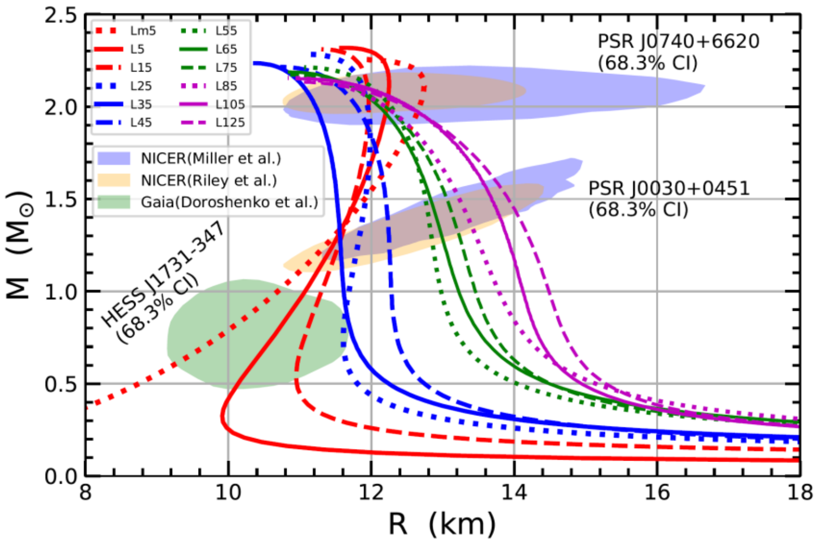

S.P. Wang(王斯沛), R. Wang(王睿), J.T. Ye(叶俊廷), LWC, PRC109, 054623 (2024)

A series of Skyrme pseudopotentials:

- Up to 1.5 AGeV (even higher)
- Various behaviors of High Density Esym
- Various Mass-Relation relation of Neutron Star
- Properties of Finite Nuclei
- Extended to Baryon Octets
- Relativistic Covariant

微观输运模型为通过中高能重离子碰撞来探索致密QCD物质的性质提供了重要的理论工具！

核物质对称能：实验探针

Promising Probes of the $E_{sym}(\rho)$
(an incomplete list !)

At sub-saturation densities (亚饱和密度行为)

- Sizes of n-skins of unstable nuclei from total reaction cross sections
- Proton-nucleus elastic scattering in inverse kinematics
- Parity violating electron scattering studies of the n-skin in ^{208}Pb
- n/p ratio of FAST, pre-equilibrium nucleons
- Isospin fractionation and isoscaling in nuclear multifragmentation
- Isospin diffusion/transport
- Neutron-proton differential flow
- Neutron-proton correlation functions at low relative momenta
- $t/^3He$ ratio
- Hard photon production
- Pigmy/Giant resonances
- Nucleon optical potential

Towards high densities reachable at CSR/Lanzhou, FAIR/GSI, RIKEN, GANIL and, FRIB/MSU (高密度行为)

- π^-/π^+ ratio, K^+/K^0 ratio?
- Neutron-proton differential transverse flow
- n/p ratio at mid-rapidity
- Nucleon elliptical flow at high transverse momenta
- n/p ratio of squeeze-out emission

B.A. Li, L.W. Chen, C.M. Ko
Phys. Rep. 464, 113(2008)
Citations: 1236+

放射性束流装置

可以产生极端丰中子的放射性核，为约束对称能提供了重要的实验基础

HIAF:
(2018-2025)
U:~0.8 AGeV

HIAF-U:
(2027-2032)
U:3-7 AGeV

BISOL:
Planning

上海交通大学 SHANGHAI JIAO TONG UNIVERSITY

核物质状态方程的特征参数

$$\boxed{E(\rho,\delta)=E_0(\rho)+E_{\mathrm{sym}}(\rho)\delta^2+E_{\mathrm{sym},4}(\rho)\delta^4+O(\delta^6)}\quad \boxed{\delta=(\rho_n-\rho_p)/\rho}\quad \boxed{\chi=\frac{\rho-\rho_0}{3\rho_0}}$$

$$E_0(\rho)=E_0(\rho_0)+\frac{K_0}{2!}\chi^2+\frac{J_0}{3!}\chi^3+\frac{I_0}{4!}\chi^4+O(\chi^5)\quad E_{\mathrm{sym}}(\rho)=E_{\mathrm{sym}}(\rho_0)+L\chi+\frac{K_{\mathrm{sym}}}{2!}\chi^2+\frac{J_{\mathrm{sym}}}{3!}\chi^3+\frac{I_{\mathrm{sym}}}{4!}\chi^4+O(\chi^5)$$

Order of the characteristic parameters according to the expansion with χ and δ:

Order-0: $E_0(\rho_0)$; Order-2: K_0, $E_{sym}(\rho_0)$;

Order-3: J_0, L; Order-4: I_0, K_{sym}, $E_{sym,4}(\rho_0)$

Order-0 → **$E_0(\rho_0)$ = -16±1 MeV**

Order-2 → **K_0 = 240±20 MeV, $E_{sym}(\rho_0)$ = 32.5±2.5 MeV**

Order-3 → **L = 55±25 MeV, J_0=???**

Order-4 → **I_0=???, K_{sym}=???, $E_{sym,4}(\rho_0)$ =???**

对称核物质

K_0: Incompressibility Coefficient

J_0: Skewness Coefficient

I_0: Kurtosis Coefficient

对称能

$E_{sym}(\rho_0)$: 饱和密度处对称能的大小

L : Slope parameter

K_{sym}: Curvature parameter

对称核物质的状态方程

(1) EOS of symmetric matter around the saturation density ρ_0

$$E_0(\rho) = E_0(\rho_0) + \frac{K_0}{2!}\chi^2 + \frac{J_0}{3!}\chi^3 + \mathcal{O}(\chi^4) \quad \chi = \frac{\rho - \rho_0}{3\rho_0}$$

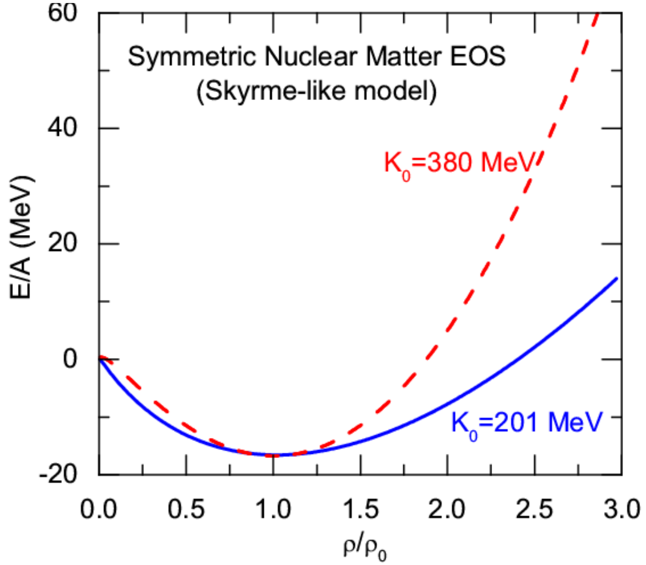

Incompressibility:

$$K_0 = 9\rho_0^2 \left(\frac{d^2E}{d\rho^2}\right)_{\rho_0}$$

Giant Monopole Resonance

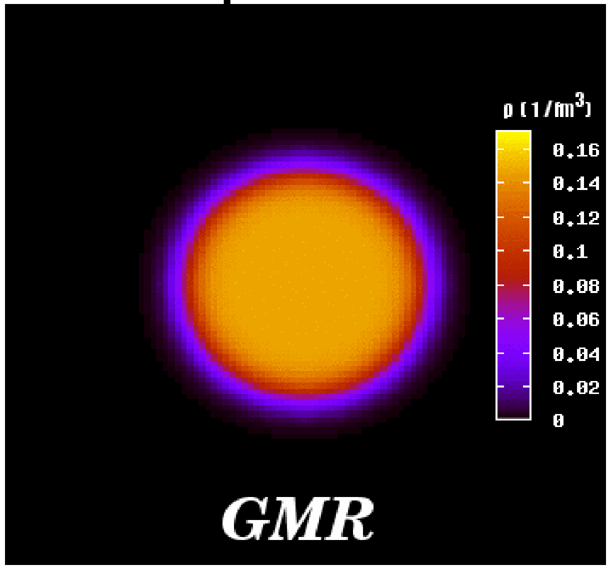

Frequency $f_{GMR} \propto \sqrt{K_0}$

K_0=231±5 MeV

Youngblood/Clark/Lui, PRL82, 691 (1999)

K0~230 MeV, Unified description for GMR of Pb and Sn, Z. Z. Li, Y. F. Niu, and G. Colò, PRL131, 082501(2023)

Recent results:

K_0=240±20 MeV **U. Garg and G. Colo, Prog. Part. Nucl. Phys. 101, 55(2018)**

U. Garg et al.
S. Shlomo et al.
G. Colo et al.
J. Piekarewicz et al.

Uncertainty of the extracted K_0 is mainly due to the uncertainty of *L* (slope parameter of the symmetry energy) and m^*_0 (isoscalar nucleon effective mass) (See, e.g., LWC/J.Z. Gu, JPG39,035104(2012))

对称核物质的状态方程

(2) EOS of symmetric matter for $1\rho_0 < \rho < 3\rho_0$ from K^+ production in HIC's

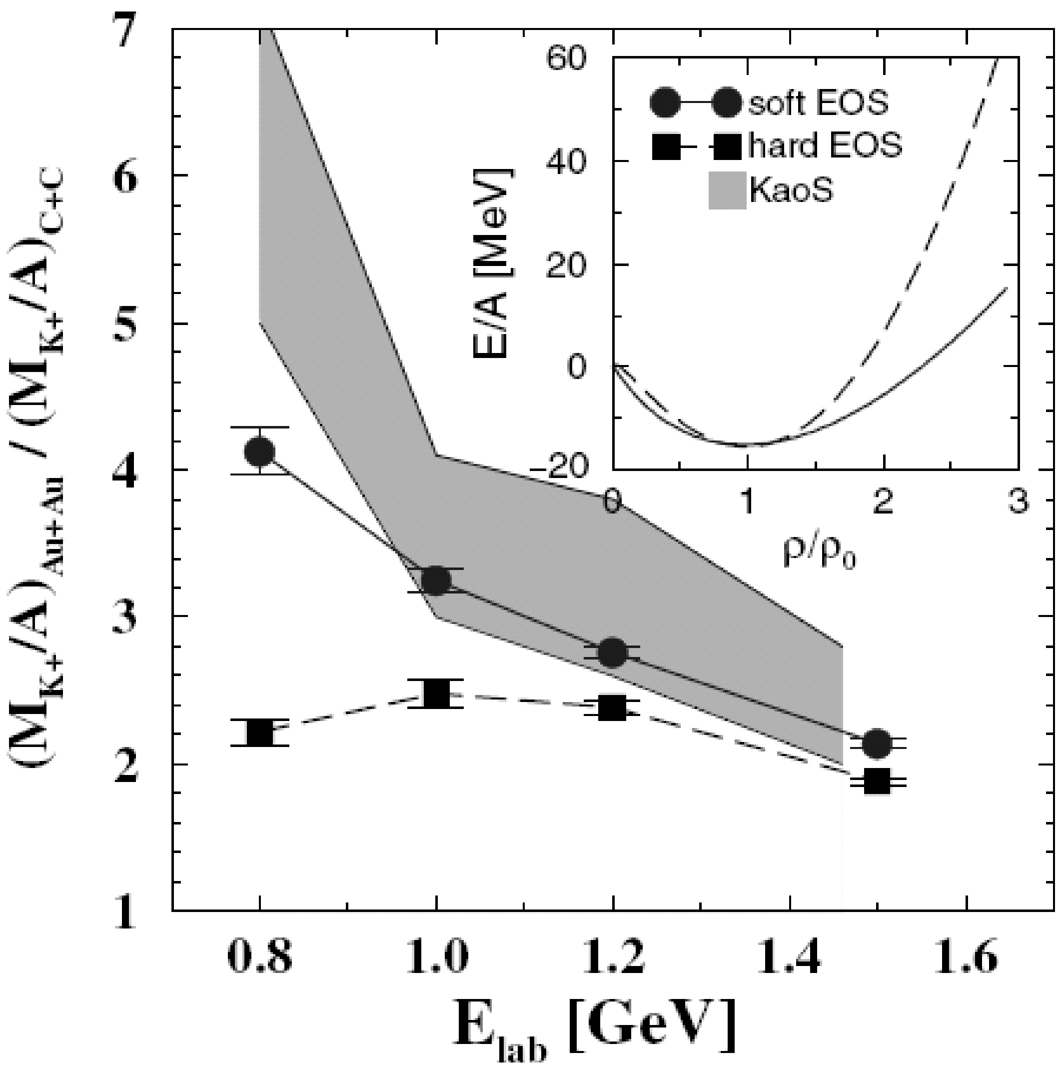

J. Aichelin and C.M. Ko, PRL55, (1985) 2661

C. Fuchs, Prog. Part. Nucl. Phys. 56, (2006) 1

C. Fuchs et al, PRL86, (2001) 1974

Transport calculations indicate that "results for the K^+ excitation function in Au + Au over C + C reactions as measured by the KaoS Collaboration strongly support the scenario with a **soft EOS**."

See also: C. Hartnack, H. Oeschler, and J. Aichelin, PRL96, 012302 (2006)

对称核物质的状态方程

(3) Present constraints on the EOS of symmetric nuclear matter for $2\rho_0 < \rho < 5\rho_0$ using flow data from BEVALAC, SIS/GSI and AGS

P. Danielewicz, R. Lacey and W.G. Lynch, Science 298, 1592 (2002)

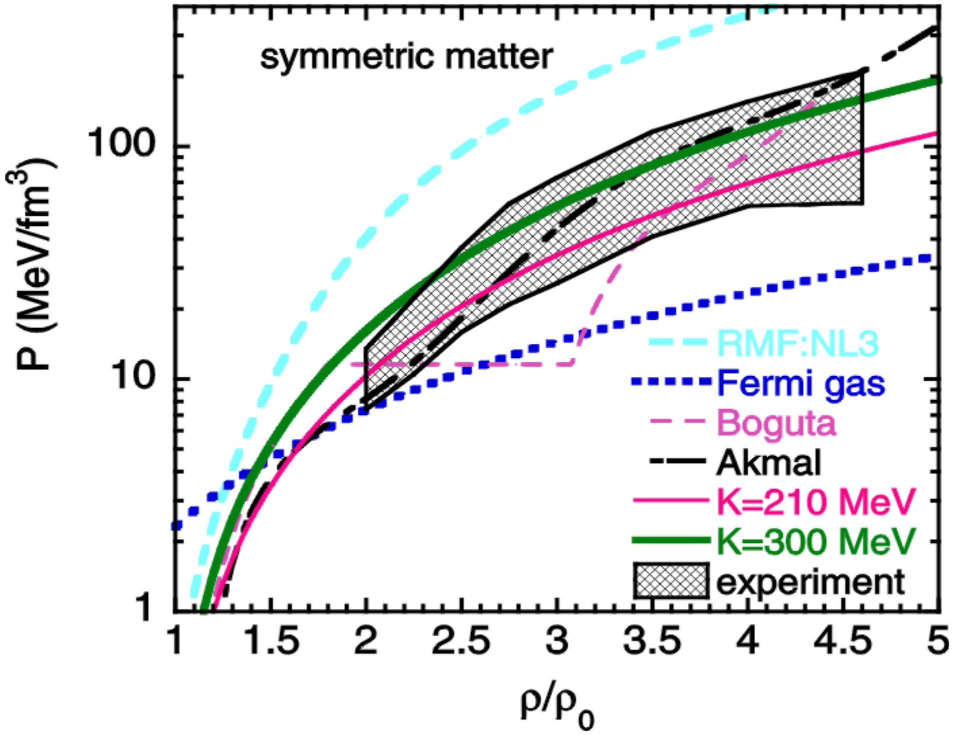

- Use constrained mean fields to predict the EOS for symmetric matter
  - Width of pressure domain reflects uncertainties in comparison and of assumed momentum dependence.

The highest pressure recorded under laboratory controlled conditions in nucleus-nucleus collisions

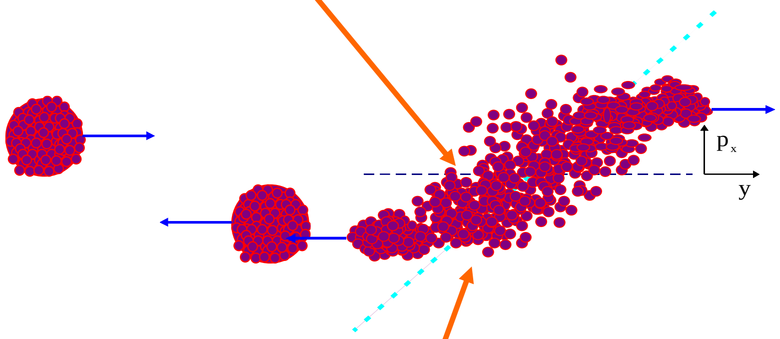

High density nuclear matter 2 to $5\rho_0$

$$\text{Pressure} \quad P(\rho) = \rho^2 \left(\frac{\partial E}{\partial \rho} \right)_s$$

对称核物质的状态方程

S. Huth et al., Nature 606, 276 (2022)

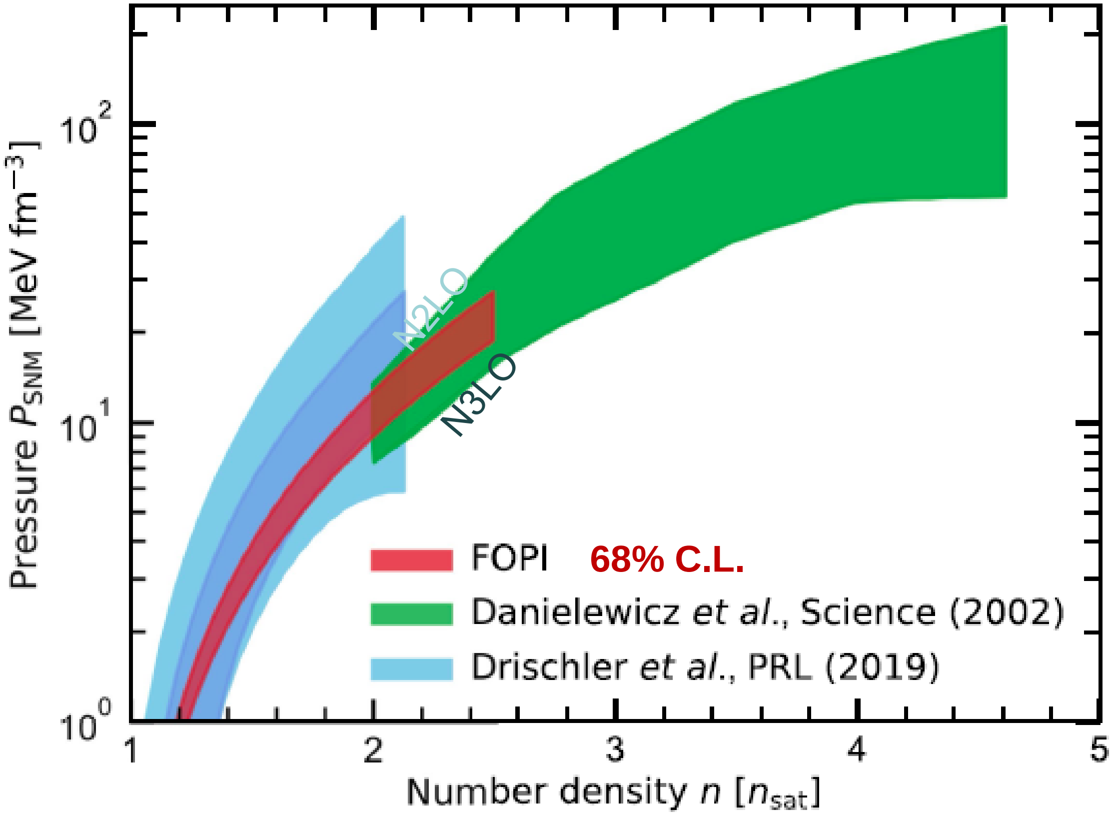

Incompressibility:

$$K_0 = 9\rho_0^2 \left(\frac{d^2E}{d\rho^2}\right)_{\rho_0}$$

- Around ρ_0: K_0=240±20 MeV from GMR [U. Garg and G. Colo, PPNP101, 55 (2018)]
- $1\rho_0 < \rho < 2.5\rho_0$ from elliptic flow data in HIC's from FOPI. [A. Le Fevre, NPA 945, 112 (2016)]
- $2\rho_0 < \rho < 5\rho_0$ using flow data from BEVALAC, SIS/GSI and AGS [P. Danielewicz et al., Science 298, 1592 (2002)]

The EOS of Symmetric NM(对称核物质) has been relatively well constrained!
(~Soft EOS of SNM at high densities)

核物质对称能：饱和密度附近

Current constraints (An incomplete list) on E_{sym} (ρ_0) and L from terrestrial experiments and astrophysical observations

Chen/Ko/Li, PRL94,032701 (2005) (isospin diffusion in HIC's, Citation: 481+)

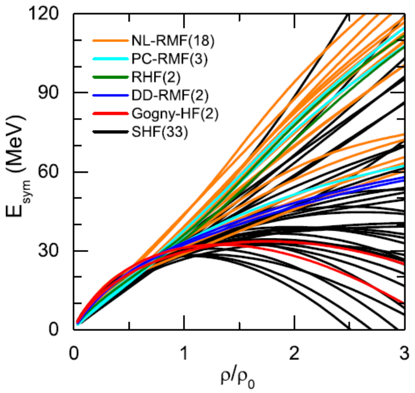

饱和密度处对称能的斜率

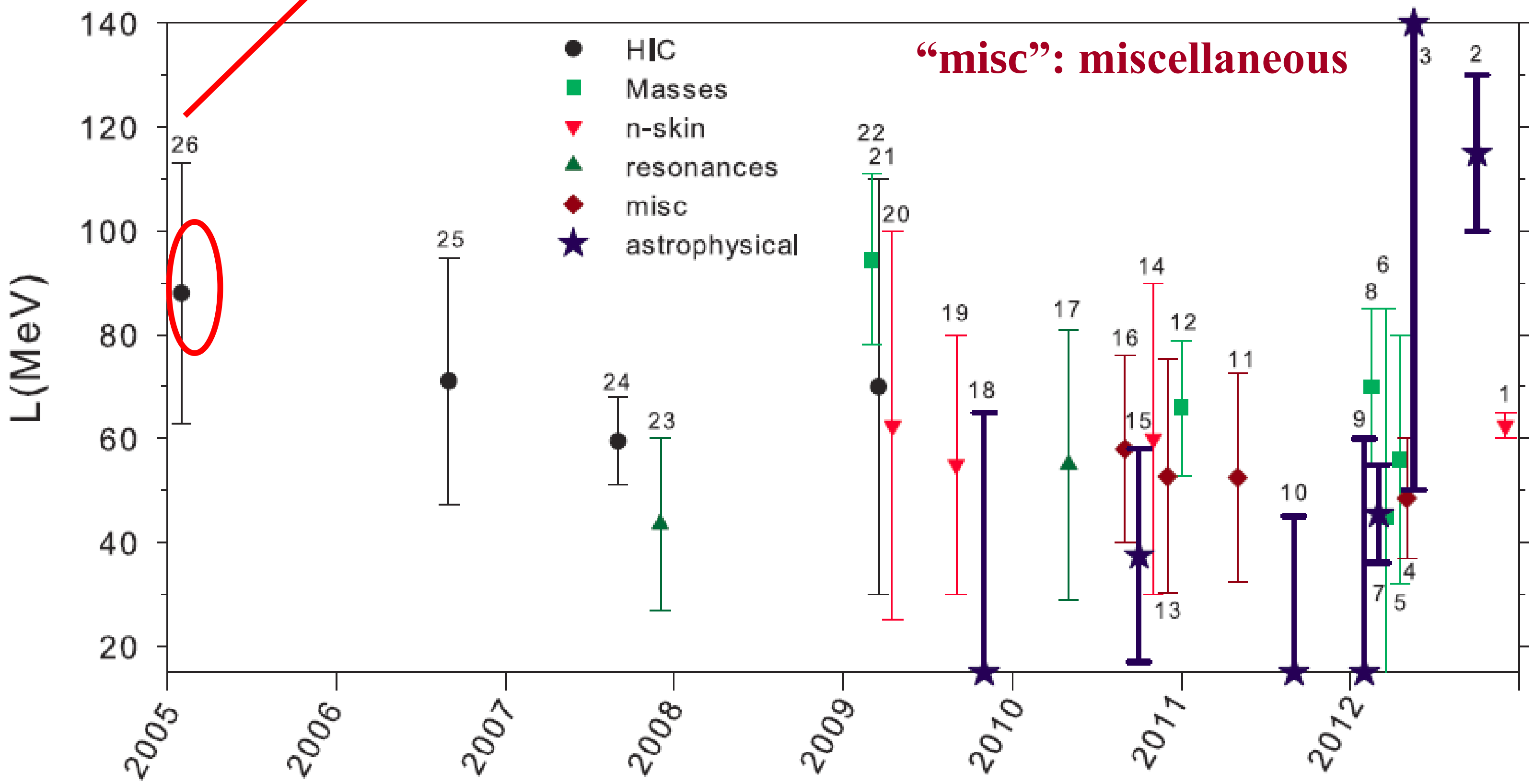

W.G. Newton et al., Journal of Physics: Conf. Series **420** (2013) 012145

核物质对称能：饱和密度附近

Current constraints (An incomplete list) on E_{sym} (ρ_0) and L from terrestrial experiments and astrophysical observations

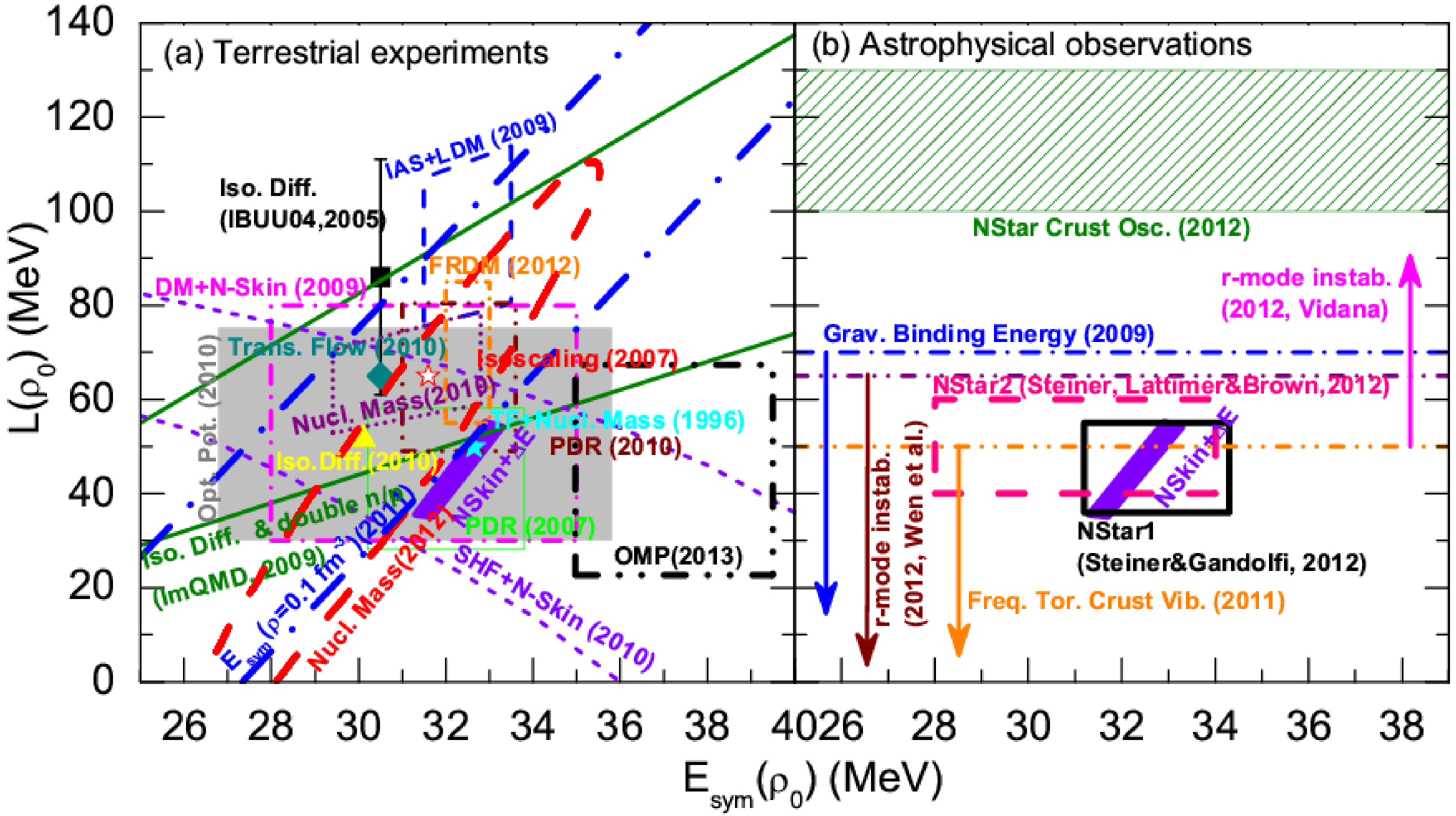

$E_{sym}(\rho_0)$ = 32.5±2.5 MeV, L = 55±25 MeV

L.W. Chen, Nucl. Phys. Rev. (原子核物理评论) 31, 273 (2014) [arXiv:1212.0284]

B.A. Li, L.W. Chen, F.J. Fattoyev, W.G. Newton, and C. Xu, J. Phys.: Conf. Ser. 413, 012021 (2013) [arXiv:1212.1178]

核物质对称能：饱和密度附近

Jim Lattimer and Andrew Steiner using 6 out of approximately 30 available constraints

饱和密度处对称能的斜率

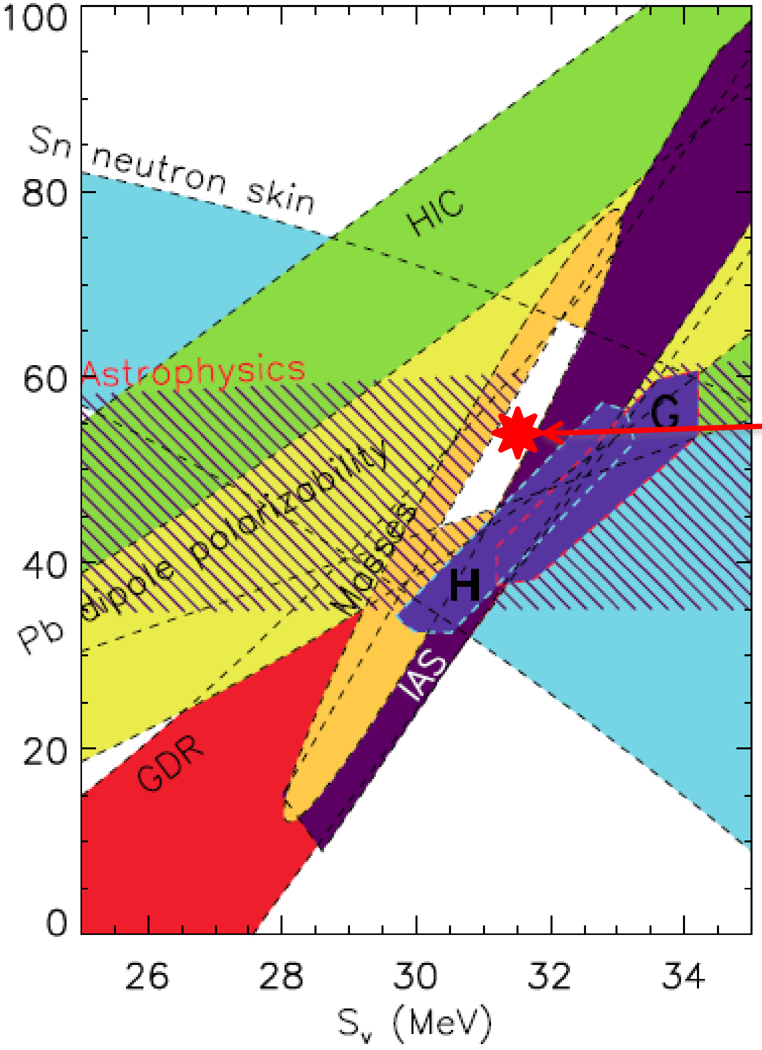

饱和密度处对称能的大小

J.M. Lattimer and A.W. Steiner, EPJA50, (2014) 40

The centroid is around S_v=31 MeV and L=50 MeV

核物质对称能：饱和密度附近

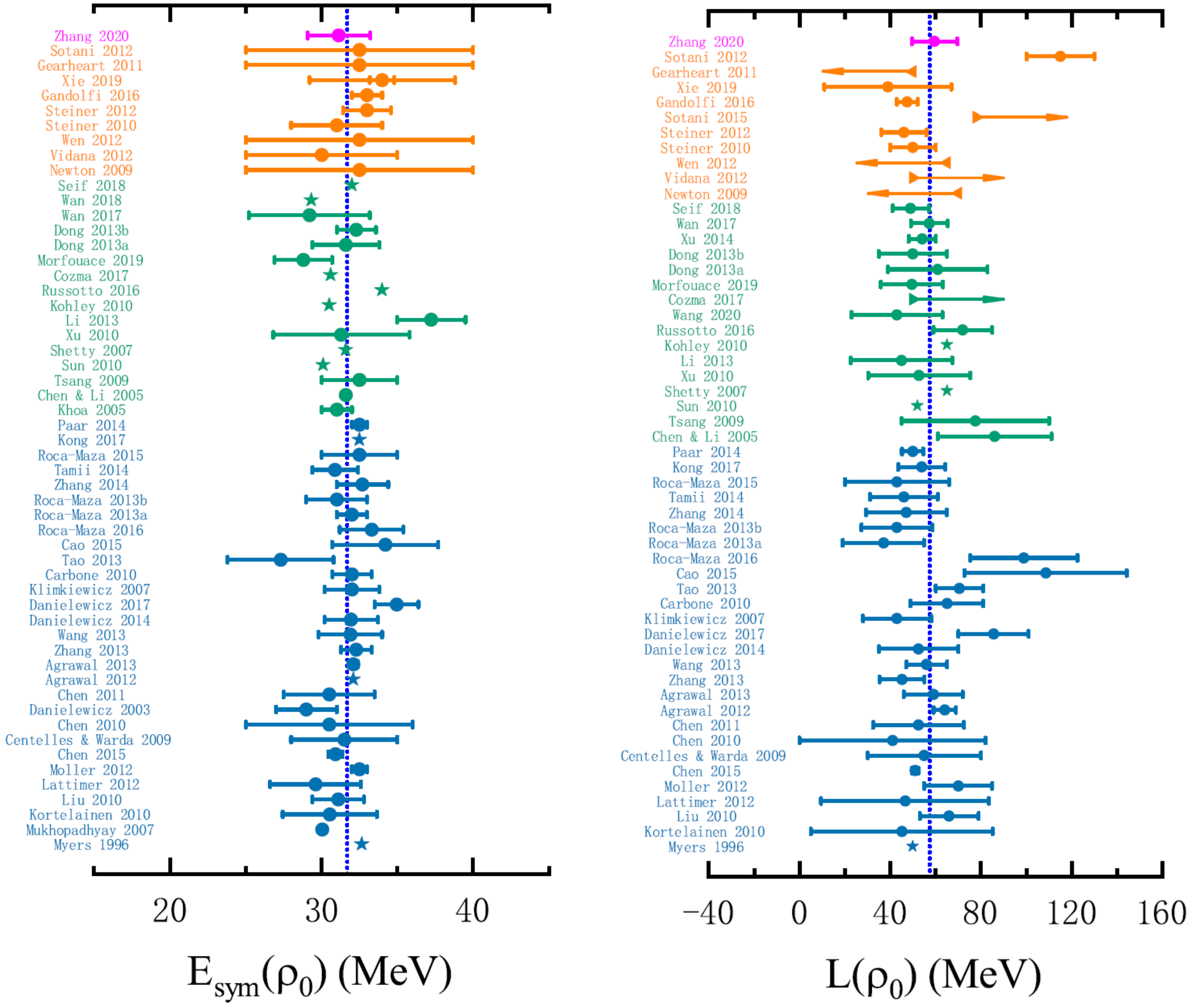

LWC et al., Invited Review/PPNP

58 analyses of terrestrial nuclear experiments and astrophysical observations

$$E_{sym}(\rho_0) = 31.7 \pm 3.1$$

$$L = 57.5 \pm 24.5 \text{ MeV}$$

Similar conclusion has been obtained in:

B. A. Li and X. Han, Phys. Lett. B727, 276 (2013);
M. Oertel, M. Hempel, T. Klahn, and S. Typel, Rev. Mod. Phys. 89, 015007 (2017).

Assuming all the constraints are equally reliable !!!

Very recent PREX-II/CREX data suggest stiff/soft Esym around saturation density, and strong tension is observed!

核物质对称能：亚饱和密度行为

Z. Zhang (张振)/LWC, PRC92, 031301(R) (2015)

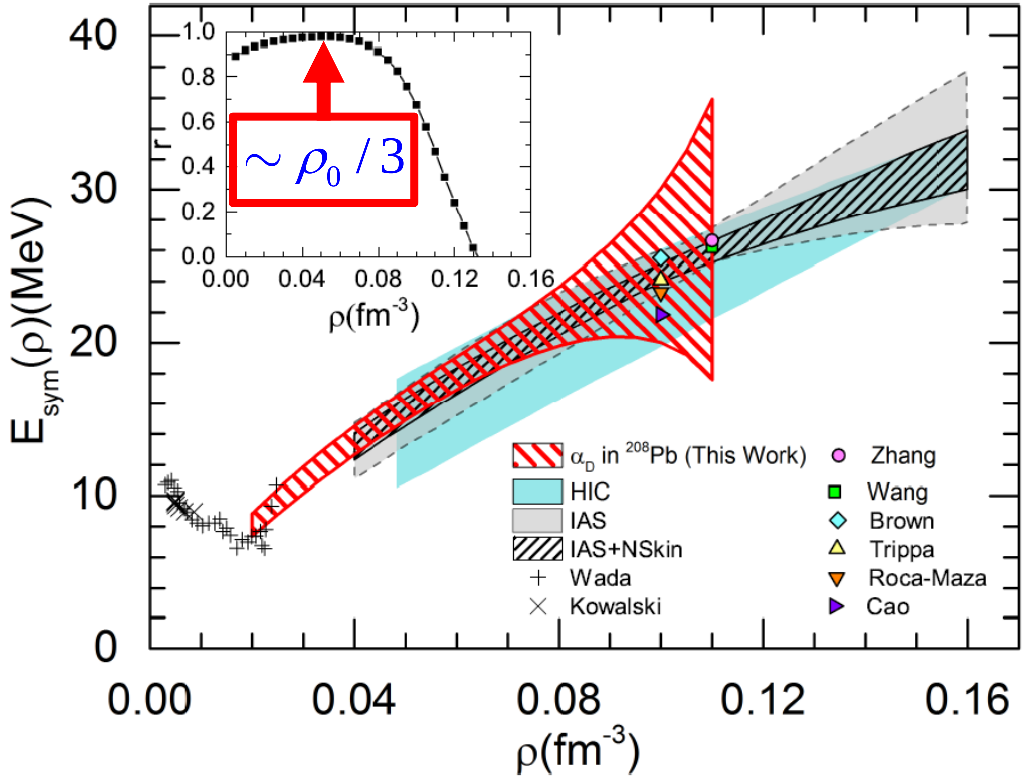

$\bullet 1/\alpha_D(A=208) \propto E_{sym}(\rho_{A=45}),\ \rho_{A=45} \approx 1/3\rho_0$

- HIC: Sn+Sn
  M.B. Tsang *et al.*, Phys. Rev. Lett.**102**, 122701(2009)
- IAS and IAS+NSkin
  P. Danielewicz and J. Lee, Nucl. Phys. **A922**, 1 (2014)
- Zhang: Isotope binding energy difference
  Z. Zhang and L.W. Chen, Phys. Lett. **B726**, 234 (2013)
- Wang: Fermi energy difference
  N. Wang *et al.*, Phys. Rev. C **87**, 034327 (2013)
- Brown: Doubly magic nuclei
  B.A. Brown, Phys. Rev. Lett. **11**, 232502 (2013)
- Trippa: Giant dipole resonance
  L. Trippa *et al.*, Phys. Rev. C **77**
- Roca-Maza: Giant quadrupole resonance
  X. Roca-Maza *et al.*, Phys. Rev. C **87**, 034301 (2013)
- Cao: Pygmy dipole resonance
  L.G. Cao and Z.Y. Ma, Chin. Phys. Lett. **25**, 1625 (2008)

Wada and Kowalski: experimental results of the symmetry energies at densities below 0.2ρ_0 and temperatures in the range 3 ~11 MeV from the analysis of cluster formation in heavy ion collisions.

Wada et al., Phys. Rev. C85, (2012) 064618; Kowlski et al., Phys. Rev. C75, (2007) 014601. Natowitz et al., Phys. Rev. Lett. 104, (2010) 202501.

对亚饱和密度区核物质对称能的认识已比较精确！

核物质对称能：亚饱和密度行为

Clustering effects on Esym within NL-RMF for n, p, t, h, α matter

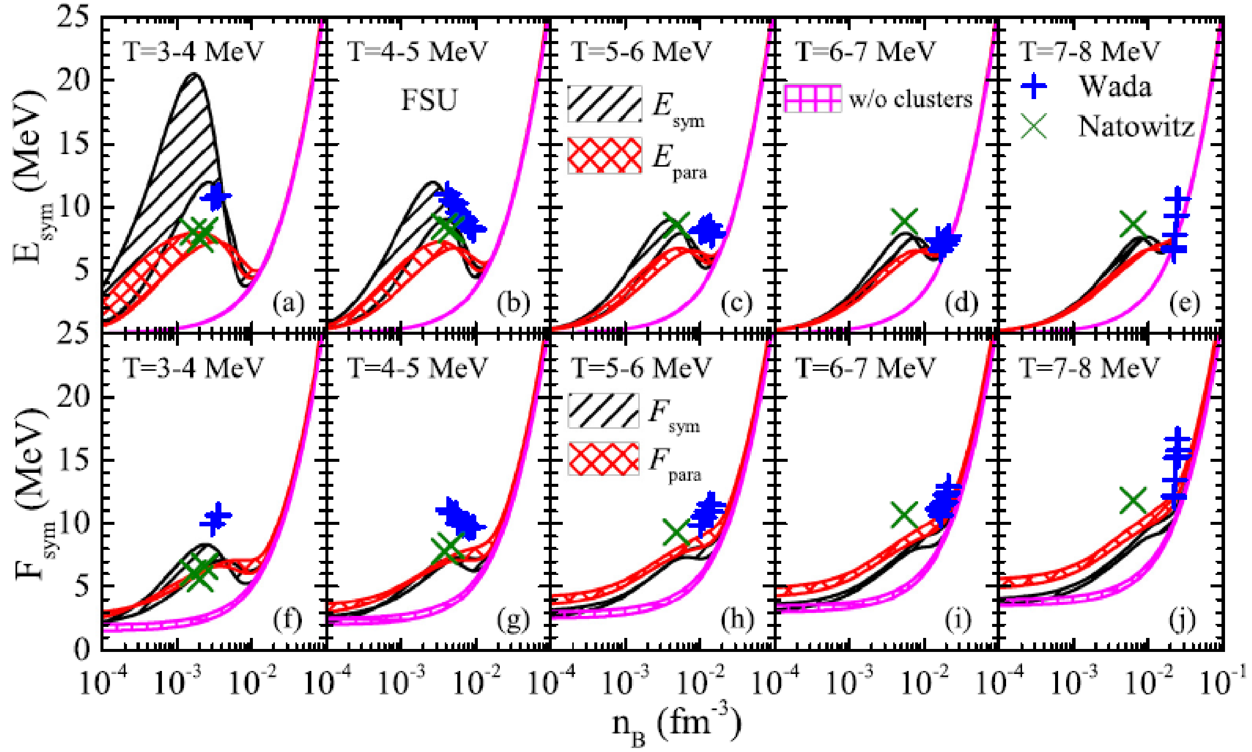

Zhao-Wen Zhang (张肇文) and LWC, PRC95, 064330 (2017)

Alpha BEC effects on Esym within NL-RMF for cold npα matter

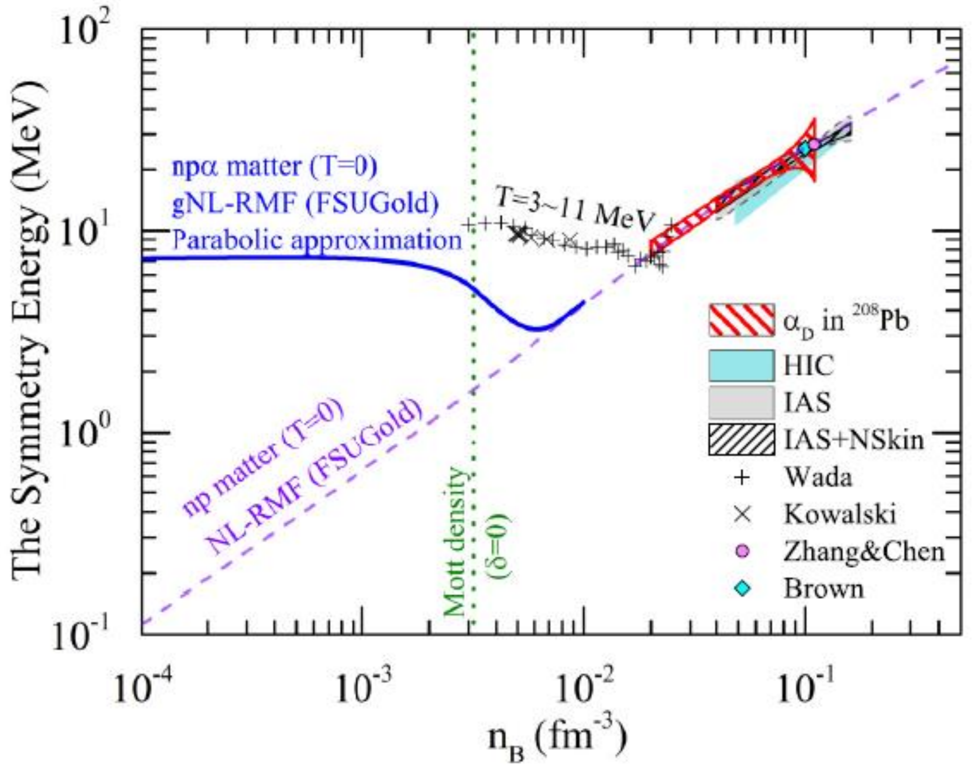

Zhao-Wen Zhang (张肇文) and LWC, PRC100, 054304 (2019)

See also: S. Typel, G. Röpke, T. Klähn, D. Blaschke, and H. H. Wolter, Phys. Rev. C 81, 015803 (2010).

核物质对称能：超饱和密度行为

A Soft or Stiff Esym at supra-saturation densities ???

pion ratio (FOPI): ImIQMD, Feng/Jin, PLB683, 140(2010)

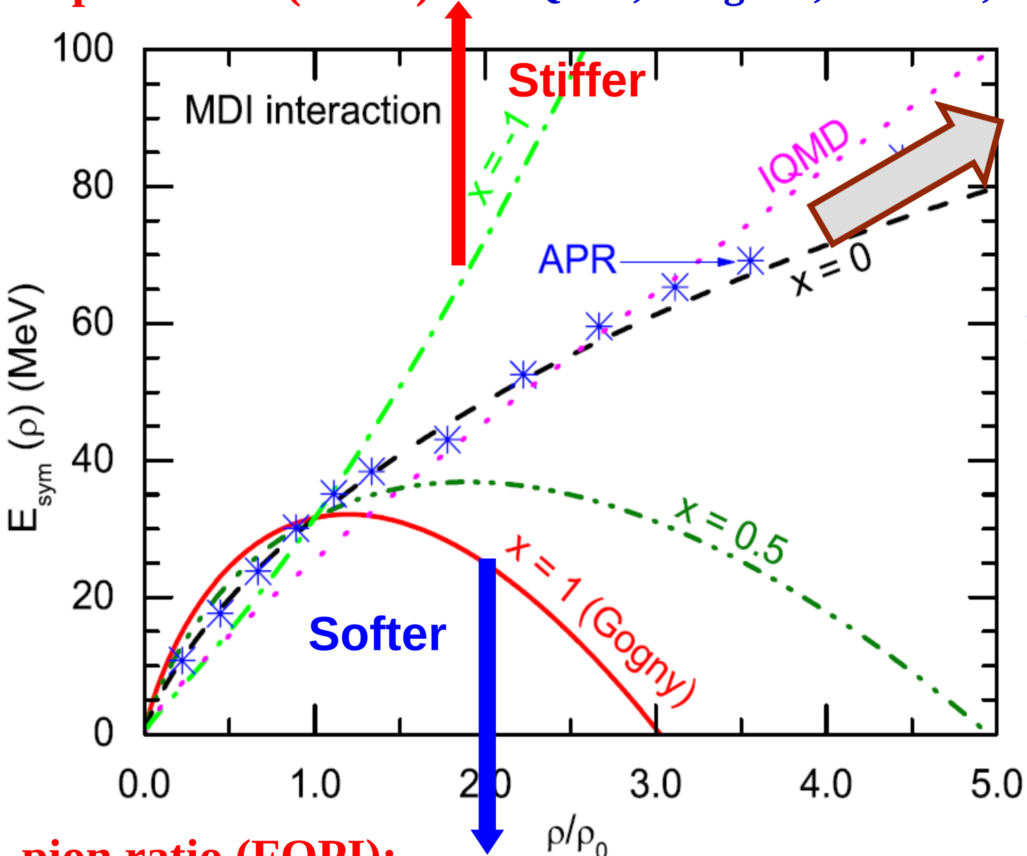

pion ratio (FOPI):
IBUU04, Xiao/Li/Chen/Yong/Zhang, PRL102,062502(2009)
ImIBLE, Xie/Su/Zhu/Zhang, PLB718,1510(2013)

n/p v2 (FOPI): $\boxed{(\rho/\rho_0)^\gamma \text{ with } \gamma = 0.9 \pm 0.4}$
Russotto/Trauntmann/Li et al., PLB697, 471(2011) (UrQMD)
PRC94, 034608 (2016) $\boxed{\gamma = 0.72 \pm 0.19}$

Cozma/Trauntmann/Li et al., PRC88, 044912 (2013) (Tubingen QMD - MDI)

对超饱和密度区核物质对称能的认识还很不清楚！

$E_{sym}(2\rho_0)$

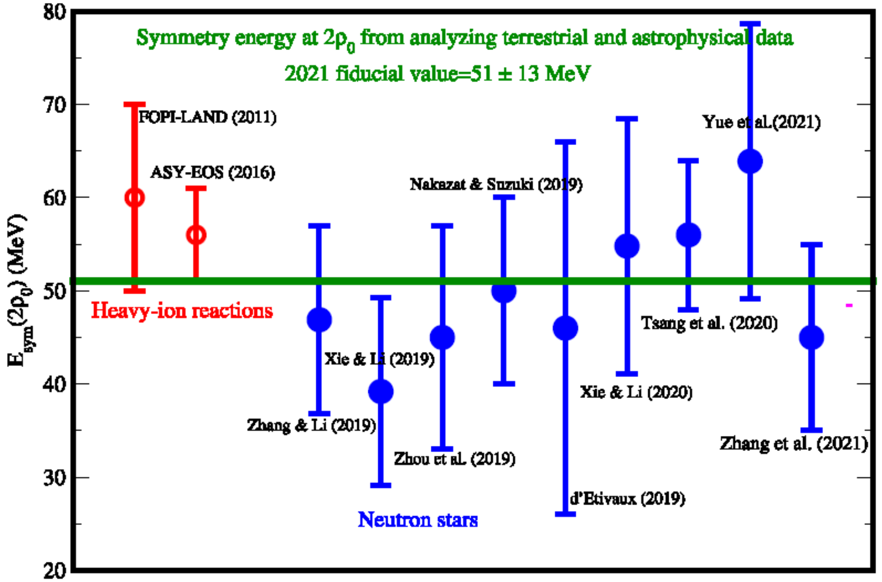

B.A.Li, B.J. Cai, W.J. Xie, and N.B. Zhang, Universe 7, 187 (2021)

SHANGHAI JIAO TONG UNIVERSITY

核物质对称能：现状

- There are MANY constraints on E_{sym} (ρ_0) and L, and the world average values are:

$$E_{sym}(\rho_0) = 31.7 \pm 3.1 \text{ MeV}$$
$$L = 57.5 \pm 24.5 \text{ MeV}$$

Very recent PREX-II/CREX makes the situation elusive !!! (See later)

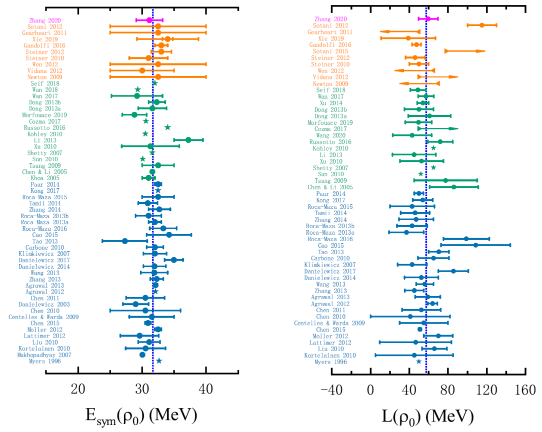

- The symmetry energy at subsaturation densities have been relatively well-constrained

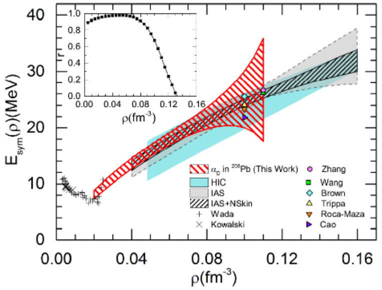

Z. Zhang(张振)/LWC, PLB726, 234 (2013); PRC92, 031301(R)(2015)

- Based on the GW multimessenger measurements, the high density Esym cannot be too stiff or too soft but still with large uncertainty!!! (See later)

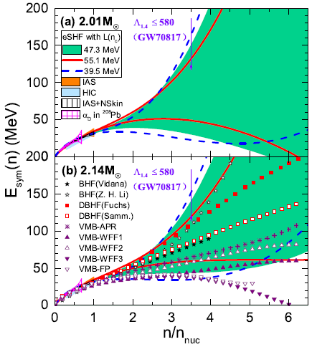

Y. Zhou (周颖), LWC, ApJ886, 52(2019) [arXiv:1907.12284]

Chinese@NuSYM15 (Krakow, Poland)

NuSYM16 (Tsinghua, Beijing, China)

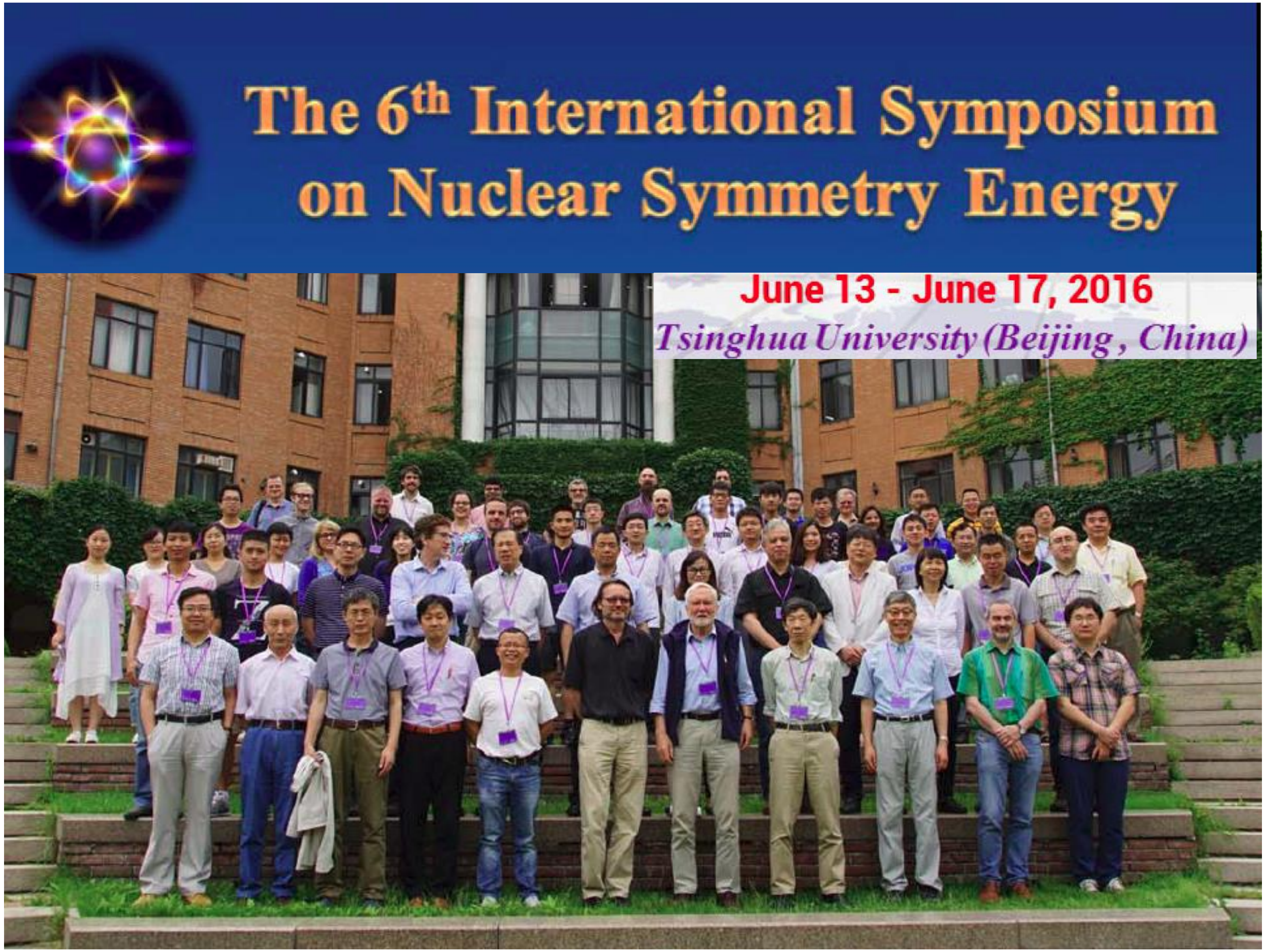

NuSYM17 (GANIL, Caen, France)

Quark matter symmetry energy

Strange Quark Matter (SQM):

SQM is made purely of deconfined *u*, *d*, and *s* quark matter (with some leptons), and might be the true ground state of QCD matter and absolutely stable (Bodmer–Witten–Terazawa hypothesis)

Isospin asymmetric quark matter:

Similar to the case of nuclear matter, the EOS of cold (**T=0)** quark matter consisting of **u**, **d** and **s** quarks, defined by its binding energy per baryon, can be expanded in isospin asymmetry δ as

$$E(n_B, \delta, n_s) = E_0(n_B, n_s) + E_{\text{sym}}(n_B, n_s)\delta^2 + \mathcal{O}(\delta^4)$$

Isospin asymmetry in ud quark matter:

$$\delta = -n_3/n_B = 3\frac{n_d - n_u}{n_d + n_u}$$

n_3: isospin density ($= n_u - n_d$); n_B: baryon density (u and d quarks)

n: udd p: uud

Pure neutron matter: $\delta = 3\frac{n_d - n_u}{n_d + n_u} = 1 \Longleftrightarrow \delta = \frac{\rho_n - \rho_p}{\rho_n + \rho_p} = 1$

Quark matter symmetry energy

Quark matter symmetry energy can be expressed as

$$E_{\mathrm{sym}}(n_B, n_s) = \frac{1}{2!}\frac{\partial^2 E(n_B,\delta,n_s)}{\partial\delta^2}\bigg|_{\delta=0}$$

Usually the high order expansion terms is very small, then we can use the parabolic approximation:

$$E(n_B,\delta,n_s) \simeq E_0(n_B,n_s) + E_{\mathrm{sym}}(n_B,n_s)\delta^2$$

$$E_{\mathrm{sym}}(n_B,n_s) \simeq \frac{1}{9}[\boxed{E(n_B,\delta=3,n_s)} - \boxed{E(n_B,\delta=0,n_s)}]$$

$n_u = 0$ *or* $nd = 0$

$n_u = n_d$

Quark Matter EOS: Theoretical Approaches

The quark matter EOS cannot be measured experimentally, its determination thus depends on theoretical approaches

- **Ab initio calculations?**

Lattice QCD: The regime of finite baryon density is still inaccessible by Monte Carlo because of the Fermion sign problem (Barbour et al. NPB, 1986)

Perturbative QCD: works only at extremely high baryon densities which are far beyond the HIC and Compact Stars (Freedman & Mclerran 1977, 1978; Fraga et al. 2001, 2002; Fraga & Romatschke 2005; Fraga 2006; Kurkela et al. 2010)

- **QCD-inspired effective phenomenological models**

The MIT bag model
The Nambu–Jona-Lasinio (NJL) model
The Dyson–Schwinger approach
The confined-density-dependent-mass (CDDM) model
The quasi-particle model
The holographical approach

……

Quark Stars: A first try for QM Esym

Very heavy pulsars:

PSR J0740+6620 (**Cromartie et al., Nature Astronomy 4, 74(2020)**): $2.14^{+0.10}_{-0.09} M_\odot$
PSR J0348+0432 (**Antoniadis et al., Science 340, 6131(2013)**): $2.01 \pm 0.04 M_\odot$

- **$2M_\odot$ pulsars seem to rule out conventional Quark Star (QS) models (whose EOS's are soft due to asymptotic freedom of QCD for quarks at extremely high density and the addition of s quarks), although some other models of pulsar-like stars with quark matter can still describe the large mass pulsar** (Alford & Reddy 2003; Baldo et al. 2003; Ruster & Rischke 2004; Alford et al. 2005, 2007; Klahn et al. 2007; Ippolito et al. 2008; Lai & Xu 2011; Weissenborn et al. 2011; de Avellar et al. 2011; Bonanno & Sedrakian 2012, ……).
- **All these models seem to indicate that to obtain a large mass (about $2M_\odot$) pulsar-like star with quark matter, the interaction between quarks should be very strong, which is remarkably consistent with the finding that quarks and gluons form a strongly interacting system in high energy HICs (sQGP).**
- **Significant isospin asymmetry is expected in QS, how about the quark matter Esym effects on properties of QS???**

Confined-isopsin-density-dependent-mass (CIDDM) model

In CIDDM model: P.C. Chu (初鹏程) & Chen, ApJ780, 135 (2014)

$$m_q = m_{q0} + m_I + m_{iso}$$
$$= m_{q0} + \frac{D}{{n_B}^{1/3}} - \boxed{\tau_q \delta D_I n_B^{\alpha} e^{-\beta n_B}}$$

Isospin dependent in-medium interactions

$$\tau_q = \begin{cases} 1 & u\ quark \\ -1 & d\ quark \\ 0 & s\ quark \end{cases}$$

$$\delta = 3\frac{n_d - n_u}{n_d + n_u} = \frac{n_n - n_p}{n_n + n_p}$$

α and β should be positive so that we can get

$$\lim_{n_B \to 0} m_I = \infty$$

$$\lim_{n_B \to \infty} m_I = 0$$

Some basic properties (very phenomenological)

- **Quark confinement**
- **Asymptotic freedom**
- **Chiral symmetry restored at high density**

Confined-isopsin-density-dependent-mass (CIDDM) model

The symmetry energy of different sets of parameters of CIDDM and relativistic mean field model with interaction NLρδ.

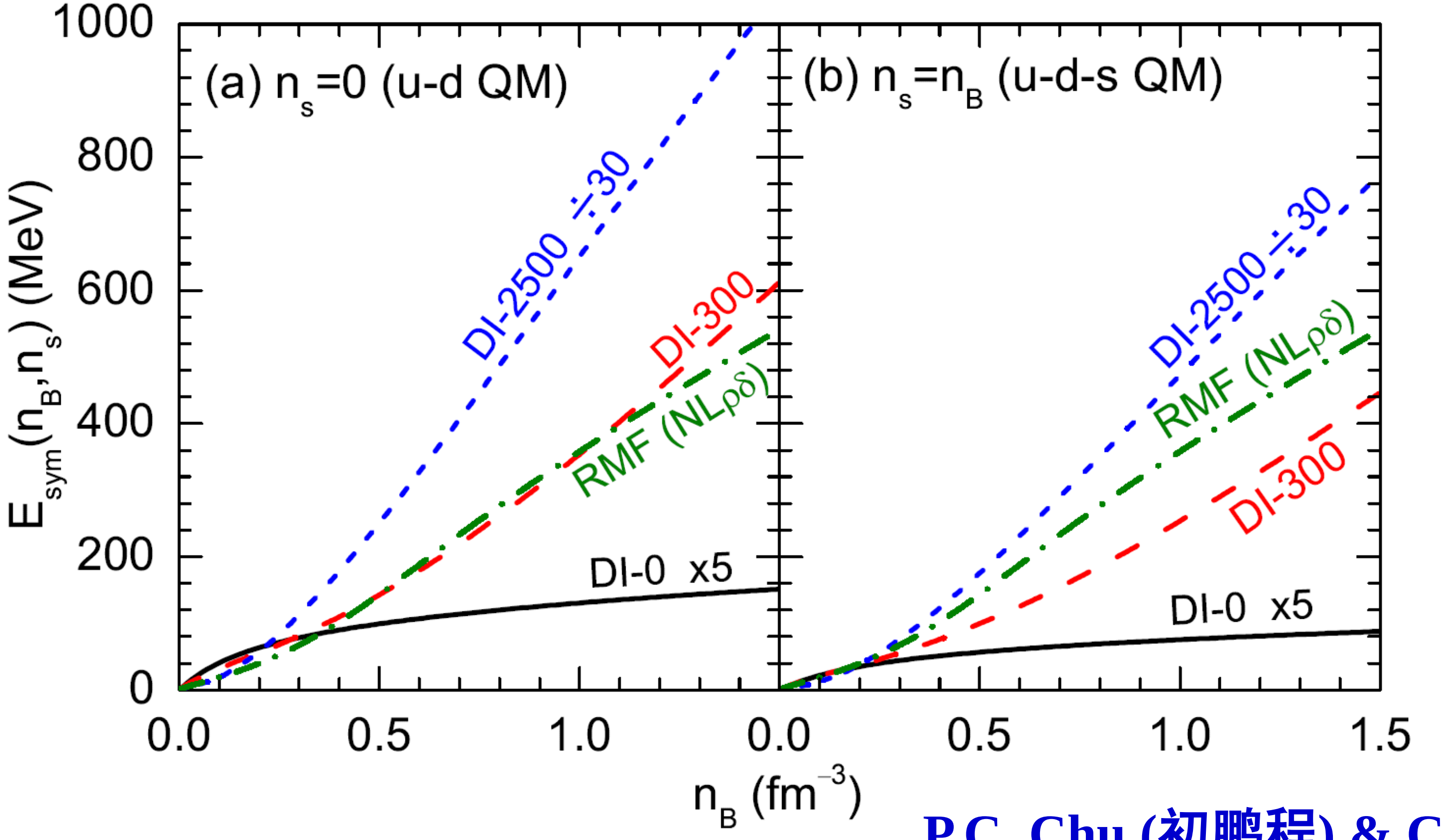

P.C. Chu (初鹏程) & Chen, ApJ780, 135 (2014)

Varying DI can significantly change the QM Esym!

Confined-isopsin-density-dependent-mass (CIDDM) model

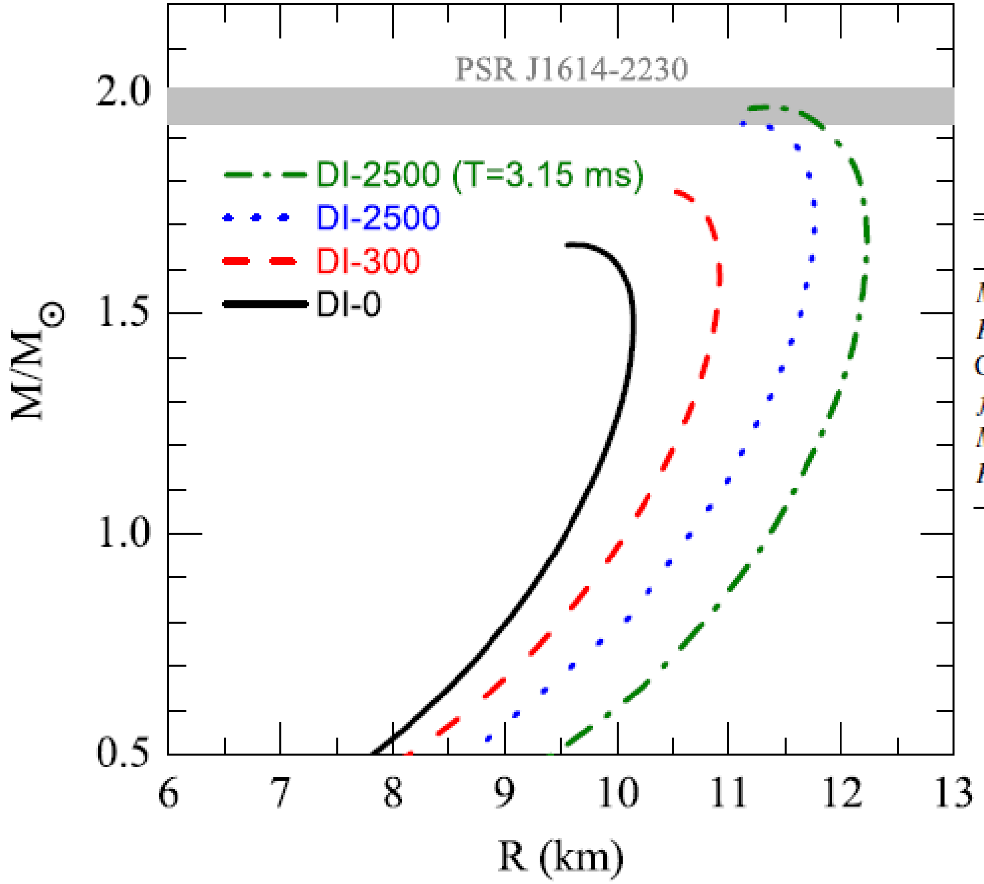

P.C. Chu (初鹏程) & Chen, ApJ780, 135 (2014)

Properties of Quark Stars in the CIDDM Model with DI-0, DI-300, and DI-2500

	DI-0	DI-300	DI-2500
$M/M_\odot$ (static)	1.65	1.78	1.93
R(km)(static)	9.60	10.40	11.12
Central density(fm^{-3})	1.31	1.11	1.06
$f_{\max}$ (Hz)	1680	1547	1458
$M/M_\odot$(at $f_{\max}$)	1.78	2.12	2.43
R(km)(equator at $f_{\max}$)	9.93	11.6	14.2

Rotating QS:
http://www.gravity.phys.uwm.edu/rns/

- **Varying QM Esym can significantly change the maximum mass of QS**
- **DI-2500 (huge QM Esym) can obtain 2$M_\odot$ QS (z=1/3)**

Confined-isopsin-density-dependent-mass (CIDDM) model

- The quark mass scaling parameter z is phenomenological in the CDDM model, and in principle it should be determined by non-perturbative QCD calculations.

$$m_q = m_{q0} + m_I + m_{iso}$$
$$= m_{q0} + \frac{D}{{n_B}^{1/3}} - \tau_q \delta D_I n_B^{\alpha} e^{-\beta n_B}$$

z=1/3

- In the original CDDM model, z=1 was assumed on the basis of the bag model argument (Fowler et al. 1981)

- A quark mass scaling parameter of z = 1/3 was derived on the basis of the in-medium chiral condensates and linear confinement (Peng et al. 1999)

- As pointed out by Li A. et al. (Li et al. 2010), however, the derivation in Peng et al. (1999) is still not well justified since only the first-order approximation of in-medium chiral condensates was considered and higher orders of the approximation could nontrivially complicate the quark mass scaling parameter.

So what will happen if the parameter z can be varied freely?

Confined-isopsin-density-dependent-mass (CIDDM) model

P.C. Chu (初鹏程) & Chen, ApJ780, 135 (2014)

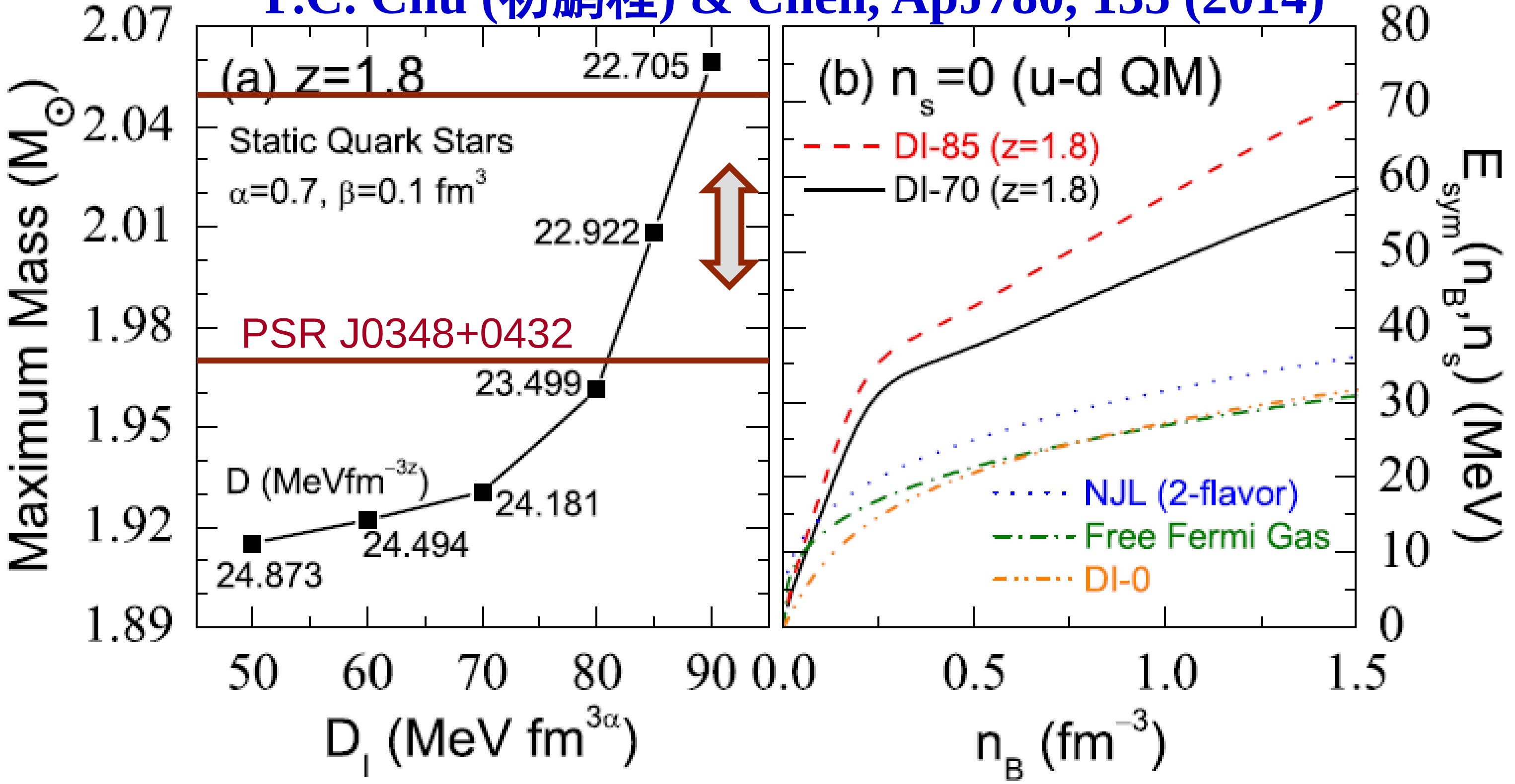

- For fixed values of the parameters *D* and *DI*, varying the scaling parameter *z* can significantly change the maximum mass of QS's and we find that *z* = 1.8 generally gives rise to the largest QS maximum mass.
- If the recently discovered large mass pulsar PSR J0348+0432 with a mass of 2.01+/-0.04 Msun is a quark star, then we have: Esym (QM) ~ 2 Esym of free quark gas or normal QM in NJL model

Isopsin dependent Confining Quark Matter (ICQM) model

P.C. Chu (初鹏程) & Chen, PRD 96, 083019 (2017)

$$\mathcal{H} = \sum_i (\alpha_i \cdot p_i + \beta_i M_i) + \sum_{i<j} \frac{\lambda(i)\lambda(j)}{4} V_{ij}$$

$$M_i = m_i + m_i^* \mathrm{sech}\left(\nu_i \frac{n_B}{n_0}\right) - \tau_i \delta D_I n_B^\alpha e^{-\beta n_B}$$

$$V_{ij} = \frac{4\pi}{9} \frac{1}{\ln(1 + [(\mathbf{k}_i - \mathbf{k}_j)^2 + D^{-2}]/\Lambda^2)} \times \frac{1}{(\mathbf{k}_i - \mathbf{k}_j)^2 + D^{-2}},$$

$$(D^{-1})^2 = \frac{2\alpha_0}{\pi} \sum_{i=u,d,s} k_i^f \sqrt{(k_i^f)^2 + M_i^2}$$

Some basic properties (very phenomenological)

- **Quark (de)confinement**
- **Asymptotic freedom**
- **Chiral symmetry restored at high density**

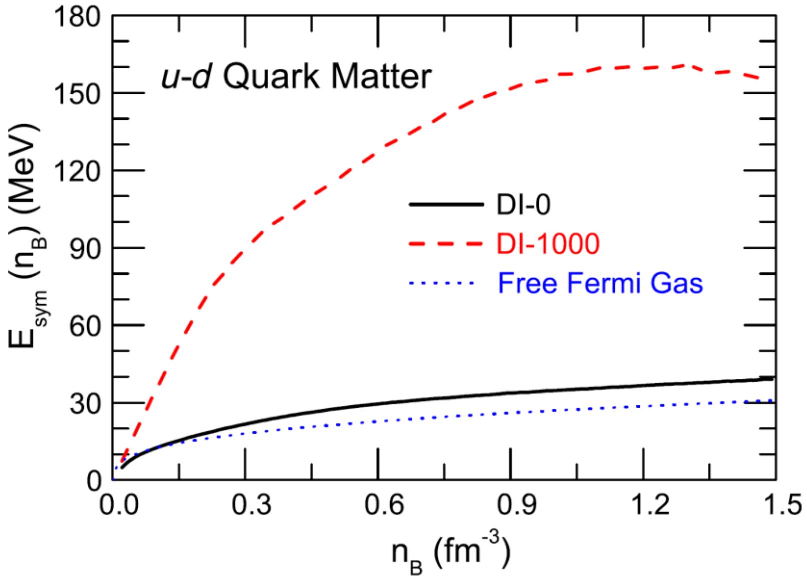

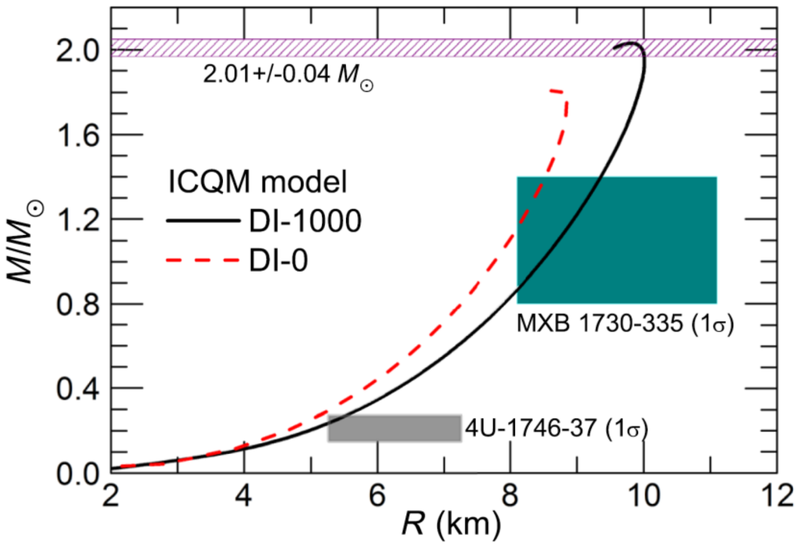

目录

- □ 致密QCD物质
- □ 致密QCD物质的状态方程：
  - ■ 对称能：核物质和夸克物质的状态方程
  - ■ 中子皮：Pb/Ca中子半径之谜
  - ■ 引力波：对称能的高密行为
- □ 致密QCD物质的相变：
  - ■ QCD相图：概述
  - ■ 重离子碰撞：粒子产生的并合模型
  - ■ 致密星：中子星、超新星、双星并合
- □ 总结和展望

原子核的中子皮

M. Thiel et al., JPG (2019)

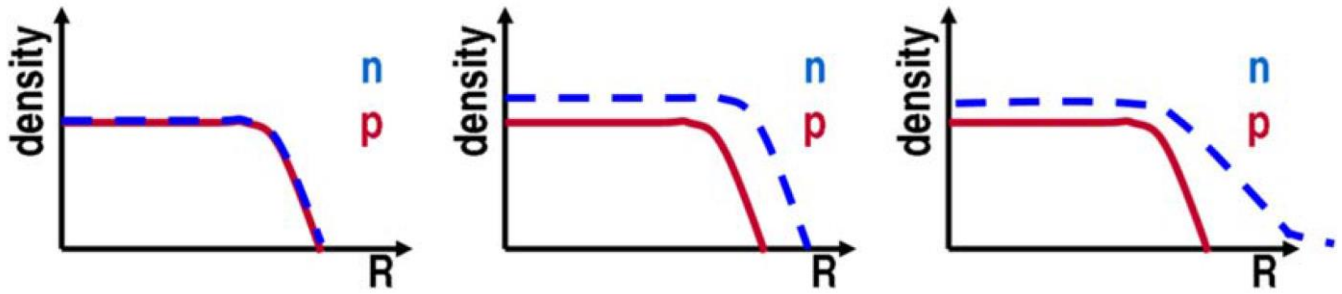

Figure 1. Schematic representation of charge and neutron density distributions. *Left:* Symmetric nuclear matter ($N = Z$) where $c_n \cong c_p$ and $a_n \cong a_p$. *Middle:* Asymmetric nuclear matter ($N \gg Z$) having a neutron skin: $c_n > c_p$ and $a_n \cong a_p$. *Right:* Asymmetric nuclear matter ($N \gg Z$) with a halo-type structure: $c_n > c_p$ and $a_n > a_p$.

Neutron skin thickness

$$R_{\text{skin}} = R_n - R_p$$

R_n : (point) neutron rms radius

R_p : (point) proton rms radius

$$\boxed{\rho(r) = \frac{\rho_o}{[1 + \exp(r - a)/c]}}$$

中子皮是对称能的黄金探针:

B.A. Brown, PRL (2000) (Citations: 751+)
R.J. Furnstahl, NPA (2002) (Citations: 396+)
LWC/Ko/Li, PRC (2005) (Citations: 280+)
M. Centelles et al., PRL102, 122502 (2009) (Citations: 455+)
LWC/Ko/Li/Xu, PRC82, 024321 (2010) (Citations: 286+)
Zhang(张振)/LWC, PLB726, 234 (2013) (Citations: 182+)

原子核的中子皮

实验上通过弹性散射测量形状因子来获取半径和分布信息

Form Factor (EM, Weak,…)

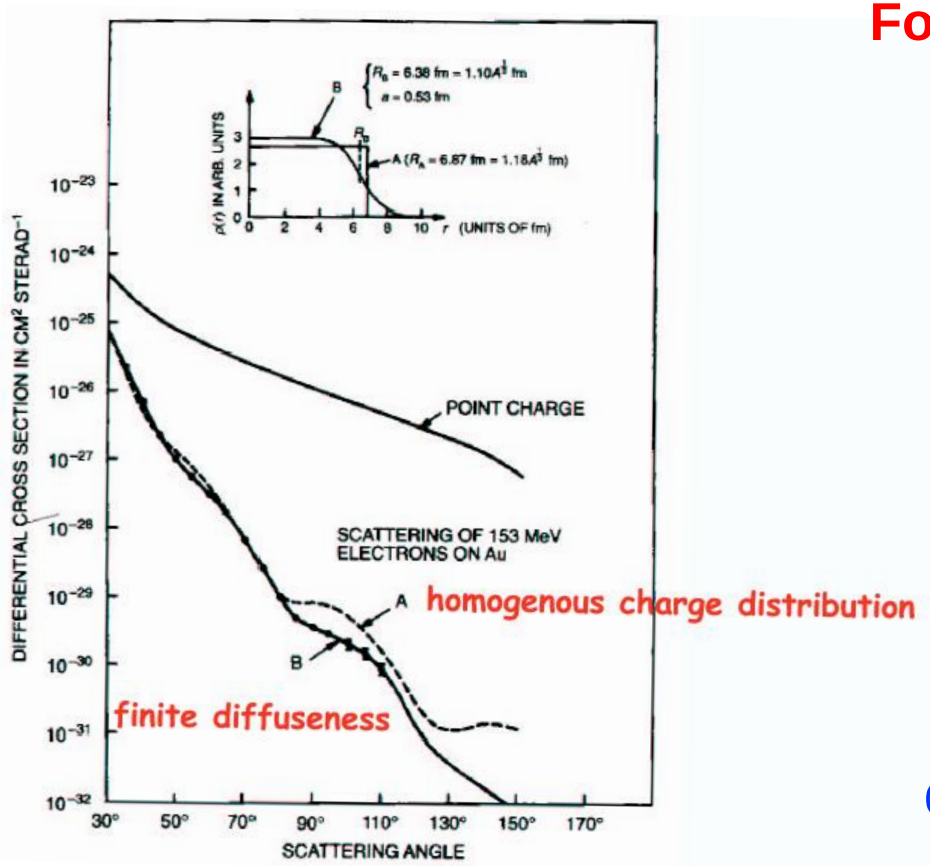

$$\frac{d\sigma}{d\Omega} = \left(\frac{d\sigma}{d\Omega}\right)_{\mathrm{Ru}} \left|F(\vec{q})\right|^2$$

$$F(\vec{q}) = \int e^{-i\vec{q}\cdot\vec{r}} \rho(\vec{r}) d\vec{r}$$

$$\langle r^2 \rangle = -6 \frac{\partial F(q^2)}{\partial q^2}\bigg|_{q=0}$$

$$\rho_c(\vec{r}) = \frac{Ze}{(2\pi)^3} \int e^{i\vec{q}\cdot\vec{r}} F(\vec{q}) d\vec{q}$$

Charge rms radius of ^{208}Pb:

$R_{ch} = 5.5012(13)\mathrm{fm}$

(with high precision: ~ 0.02 %)

Weak charge rms radius of ^{208}Pb:

? ? ? ~1%

Calculated and experimental densities

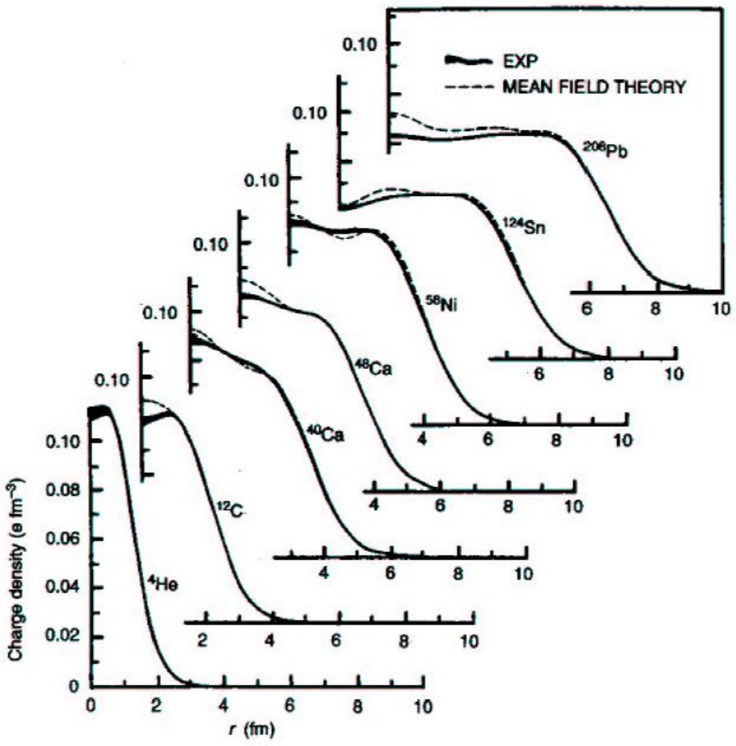

^{208}Pb Radius EXperiment: PREX

$Q_p^{(W)} = 0.0713$

$Q_n^{(W)} = -0.9888$

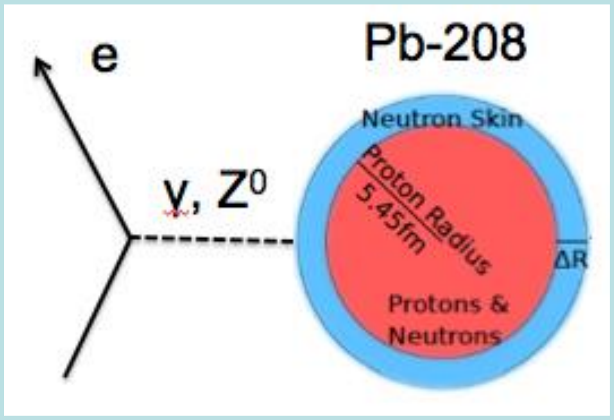

PREX@JLab

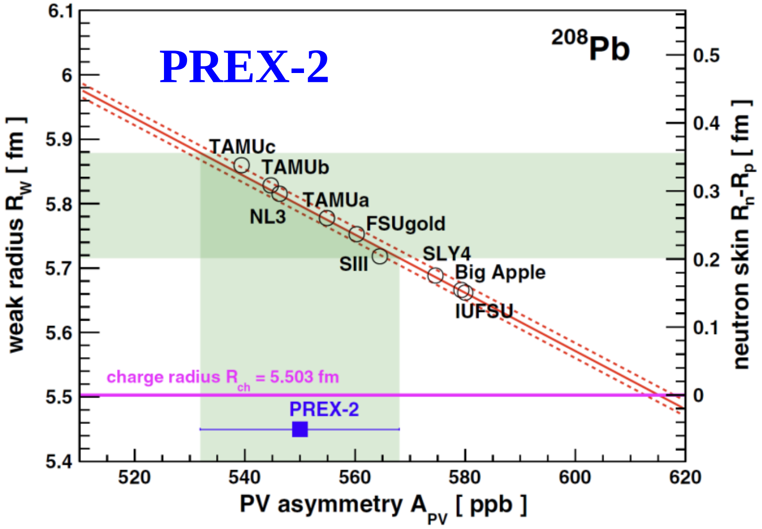

Adhikari et al., PRL126, 172502 (2021)

- **Parity-violating asymmetry** in longitudinally polarized elastic electron scattering :

$$A_{\rm PV} = \frac{\sigma_R - \sigma_L}{\sigma_R + \sigma_L} \approx \frac{G_F Q^2 |Q_W|}{4\sqrt{2}\pi\alpha Z} \frac{F_W(Q^2)}{F_{\rm ch}(Q^2)}$$

T.W. Donnelly et al., NPA503, 589 (1989); C.J. Horowitz et al., PRC63, 025501 (2001).

- **Free from most strong interaction uncertainties.**
- PREX-2 results ($\langle Q^2 \rangle = 0.00616$ GeV^2) :

$$A_{\rm PV}^{\rm meas} = 550 \pm 16(\text{ stat }) \pm 8(\text{ syst })\text{ppb}$$
$$F_W(\langle Q^2 \rangle) = 0.368 \pm 0.013(\text{exp}) \pm 0.001(\text{ theo })$$

^{208}Pb Parameter	Value
Weak radius (R_W)	5.800 ± 0.075 fm
Interior weak density (ρ_W^0)	-0.0796 ± 0.0038 fm^{-3}
Interior baryon density (ρ_b^0)	0.1480 ± 0.0038 fm^{-3}
Neutron skin ($R_n - R_p$)	0.283 ± 0.071 fm

^{208}Pb中子皮: PREX-2

Reed et al., PRL126, 172503 (2021)

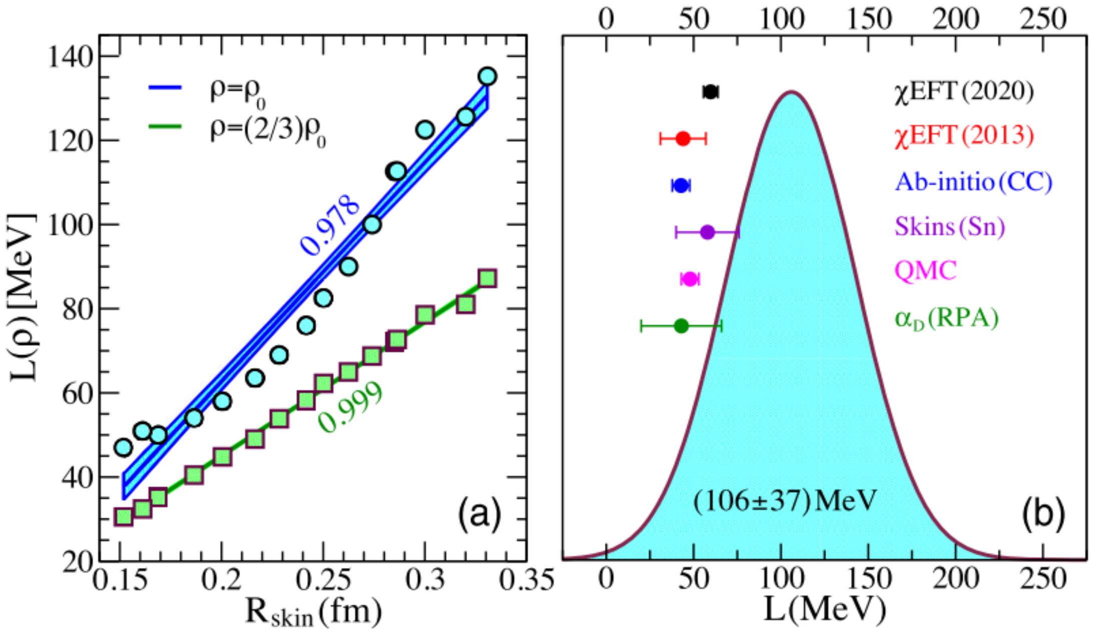

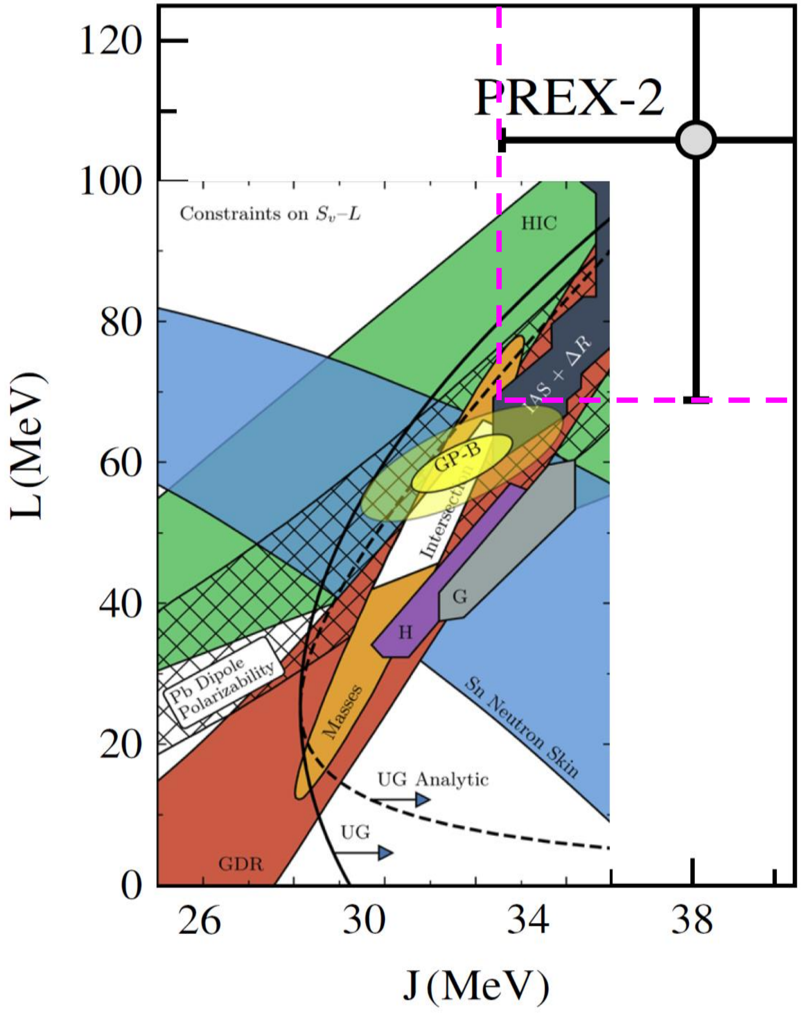

◆ **Superstiff symmetry energy from relativistic EDF analysis:**

$$J = (38.1 \pm 4.7)\ \text{MeV},$$

$$L = (106 \pm 37)\ \text{MeV},$$

◆ **Challenge our understanding of the symmetry energy.**

^{208}Pb中子皮: PREX-2

Reed et al., PRL126, 172503 (2021)

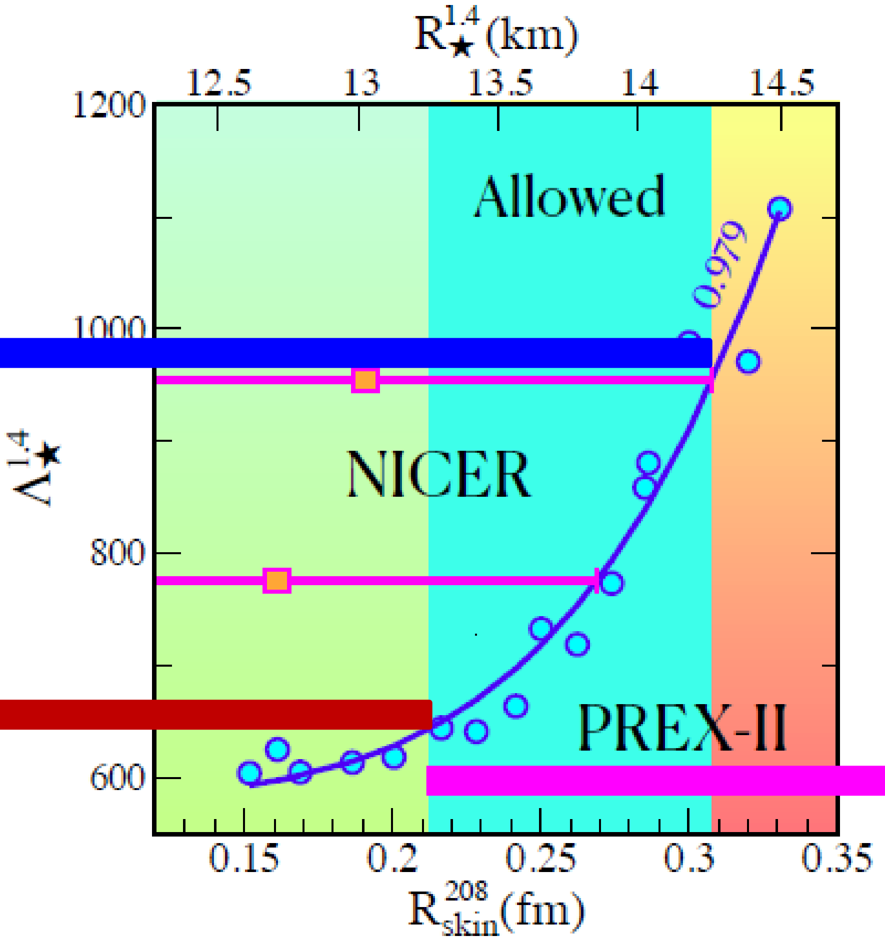

NICER

$\Lambda_{1.4}$ > 640 !!!

$R_n - R_p = 0.283 \pm 0.071$ fm

PREX-II: Rskin = [0.212, 0.354] fm for Pb208

RMF: $\Lambda_{1.4}$ is inconsistent with GW170817: $\Lambda_{1.4}$ <580 !!!

δ meson may help !

Fan Li (李帆)/Cai/Zhou/Jiang/LWC, ApJ 929, 183 (2022)

^{208}Pb中子皮: PREX-2

Implications of Rskin from PREX-II in the multimessenger era

Tong-Gang Yue (岳侗钢), LWC, Z. Zhang (张振), and Y. Zhou (周颖), PRReseach 4, L022054(2022)

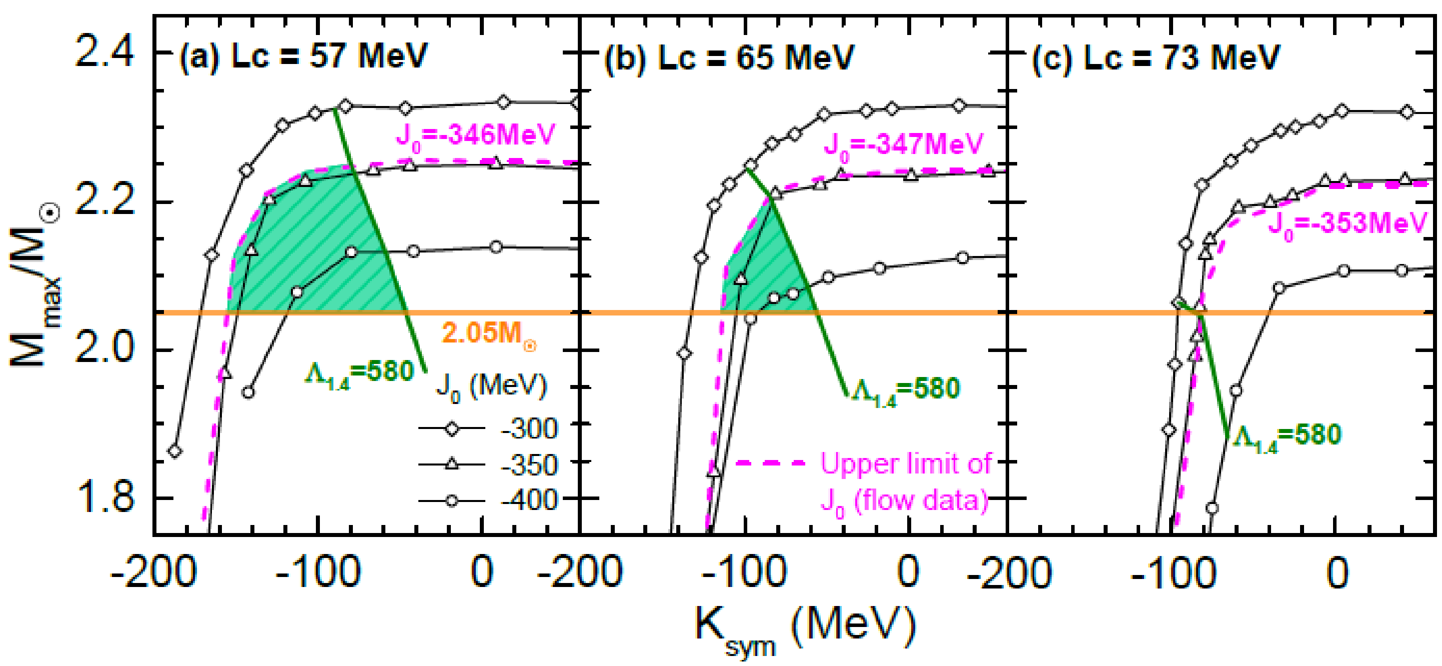

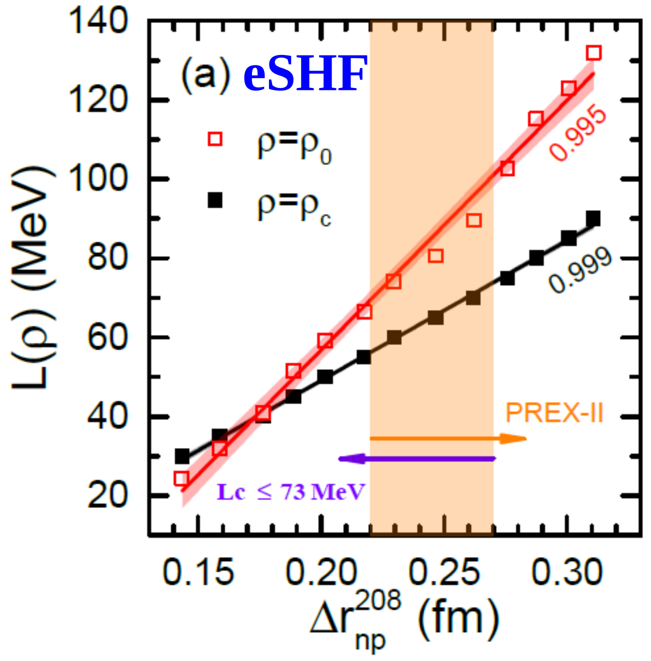

eSHF: Lc cannot be too big!!! Lc < 73 MeV and then set an upper limit on Rskin: <0.27 fm for Pb208

eSHF provides a single unified framework to simultaneously describe the finite nuclei (Eb, Rc, GMR, Nskin-PREX-II) + Flow data in HIC+NStar (e.g., NICER)+GW170817

$E_{sym}(\rho_0)$ =34.5±1.5 MeV and L=85.5±22.2 MeV

Very stiff Esym!

^{48}Ca Radius EXperiment: CREX

CREX, PRL129, 042501 (2022)

PHYSICAL REVIEW LETTERS **129,** 042501 (2022)

Editors' Suggestion

Precision Determination of the Neutral Weak Form Factor of ^{48}Ca

- Model-independent determination of charge-weak form factor difference:

$$\Delta F_{CW}^{48}(q) = 0.0277 \pm 0.0055, \quad q = 0.8733\ \mathrm{fm}^{-1},\ \mathrm{CREX}$$

$$\Delta F_{CW}^{208}(q) = 0.041 \pm 0.013,\ q = 0.3977\ \mathrm{fm}^{-1},\ \mathrm{PREX}$$

- Extracted neutron skin of Ca48

Quantity	Value ± (exp) ± (model) (fm)
$R_W - R_{ch}$	0.159 ± 0.026 ± 0.023
$R_n - R_p$	0.121 ± 0.026 ± 0.024

- **Strong tension between CREX and PREX-2 results?**

Too small Nskin of ^{48}Ca or too large Nskin of ^{208}Pb

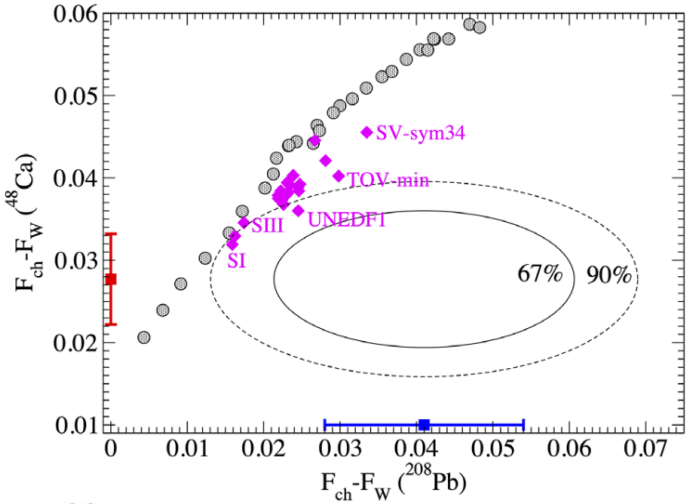

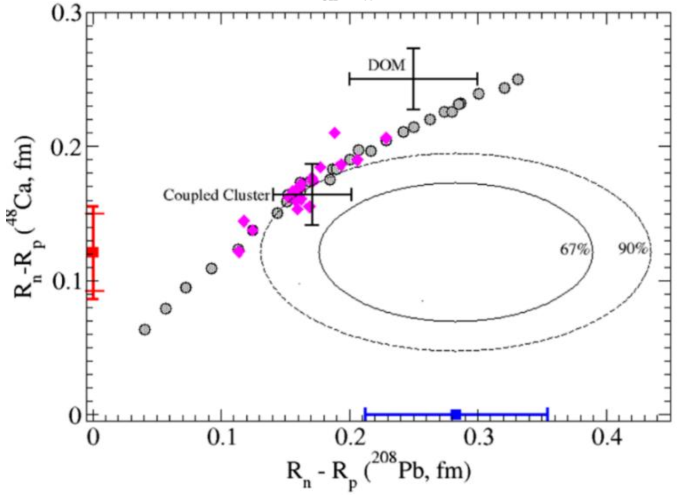

Challenging modern nuclear EDF theory!

"PREX-CREX Puzzle (Pb/Ca中子半径之谜)"

PREX and CREX: A Bayesian analysis

Zhang(张振)/Chen, PRC108, 024317 (2023) [arXiv: 2207.03328]

SHF
base data of nuclei

TABLE II. Experimental data and adopted errors used in the Bayesian analysis. The second line shows the globally adopted error for each observable. That error is multiplied for each observable by a further integer weight factor given in the parenthesis next to the data value.

Nuclei	E_B	r_c	R_d	σ	$\Delta\epsilon_{ls}$
	(1 MeV)	(0.02 fm)	(0.04 fm)	(0.04 fm)	(20%)
^{16}O	−127.620(4)	2.701(2)	2.777(2)	0.839(2)	6.30(3)
					6.10(3)
^{40}Ca	−342.051(3)	3.478(1)	3.845(1)	0.978(1)	
^{48}Ca	−415.990(1)	3.479(2)	3.964(1)	0.881(1)	
^{56}Ni	−483.990(5)	3.750(9)			
^{68}Ni	−590.430(1)				
^{100}Sn	−825.800(2)				
^{132}Sn	−1102.900(1)				1.35(1)
					1.65(1)
^{208}Pb	−1636.446(1)	5.504(1)	6.776(1)	0.913(1)	1.32(1)
					0.90(1)
					1.77(2)

Note. $\Delta\epsilon_{ls}$ data are for ^{16}O($1p_p$, $1p_n$), ^{132}Sn($2p_p$, $2d_n$), and ^{208}Pb($2d_p$, $3p_n$, $2f_n$), respectively.

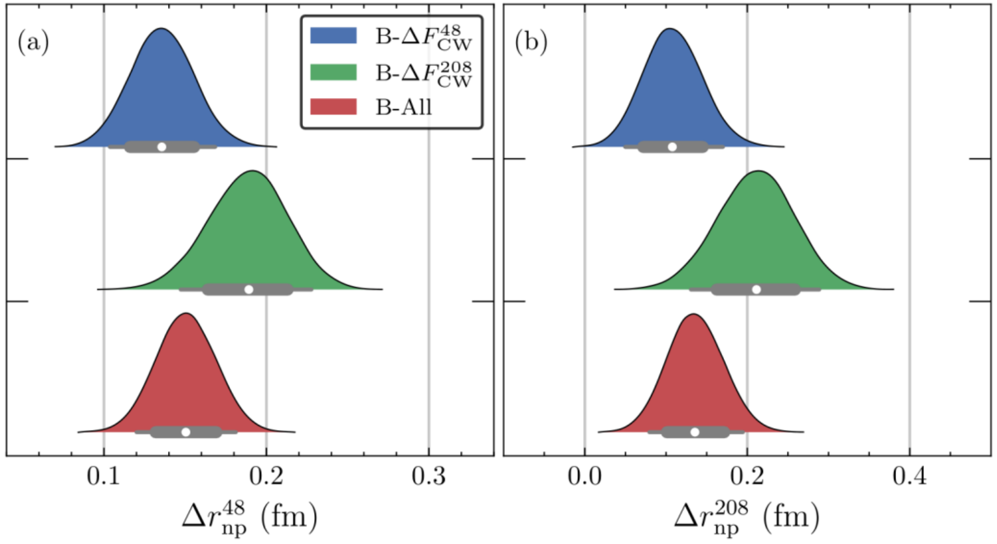

$0.150^{+0.019(0.031)}_{-0.019(0.030)}$ fm

$0.136^{+0.036(0.059)}_{-0.035(0.056)}$ fm

$$L(2\rho_0/3) = 34.1^{+10.1(16.8)}_{-9.2(14.8)}\ \text{MeV}$$

$$E_{\rm sym}(\rho_0) = 29.1^{+2.1(3.6)}_{-1.8(2.7)}\ \text{MeV}$$

$$L = 17.1^{+23.8(39.3)}_{-22.3(36.0)}\ \text{MeV}$$

Also n-p Fermi energy difference of ^{16}O, ^{40,48}Ca, ^{56}Ni, ^{132}Sn, ^{208}Pb and GMR of ^{208}Pb

- CREX and PREX are compatible in 90% C.L.
- PREX is less effective to constrain Esym due to its lower precision compared to CREX
- Combining CREX+PREX favor mildly soft Esym around saturation density!

中子皮 vs 自旋-轨道相互作用

LWC/Ko/Li/Xu, PRC82, 024321 (2010) (Citations: 282+)

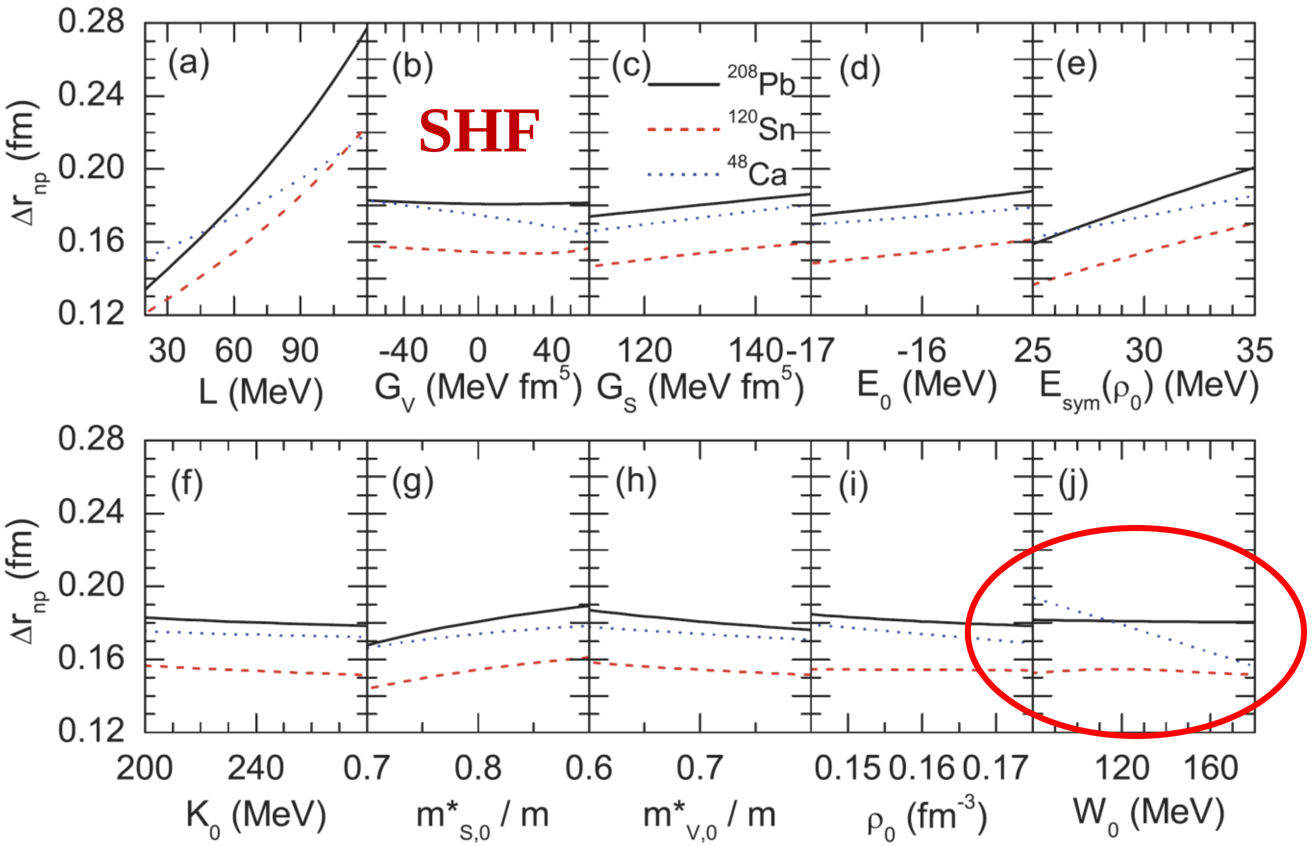

Horowitz/Piekarewitz, PRC86, 045503 (2012)

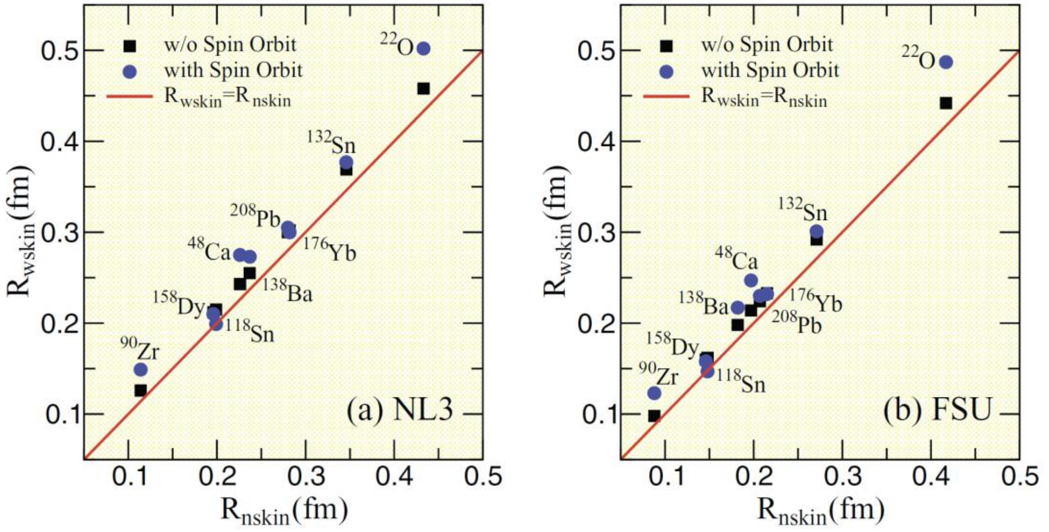

FIG. 2. (Color online) Electroweak skin (R_{wk}-R_{ch}) with and without spin-orbit corrections as a function of neutron skin (R_n-R_p) for the various neutron-rich nuclei considered in this work. Predictions are made using both the (a) NL3 and (b) FSU interactions.

- ☐ **The Nskin of Ca48 is sensitive to spin-orbit coupling W0 in the standard SHF!**
- ☐ **Spin-orbit coupling makes significant contribution to Rwk-Rch**

CREX/PREX: Strong Isovector Spin-Orbit Interaction

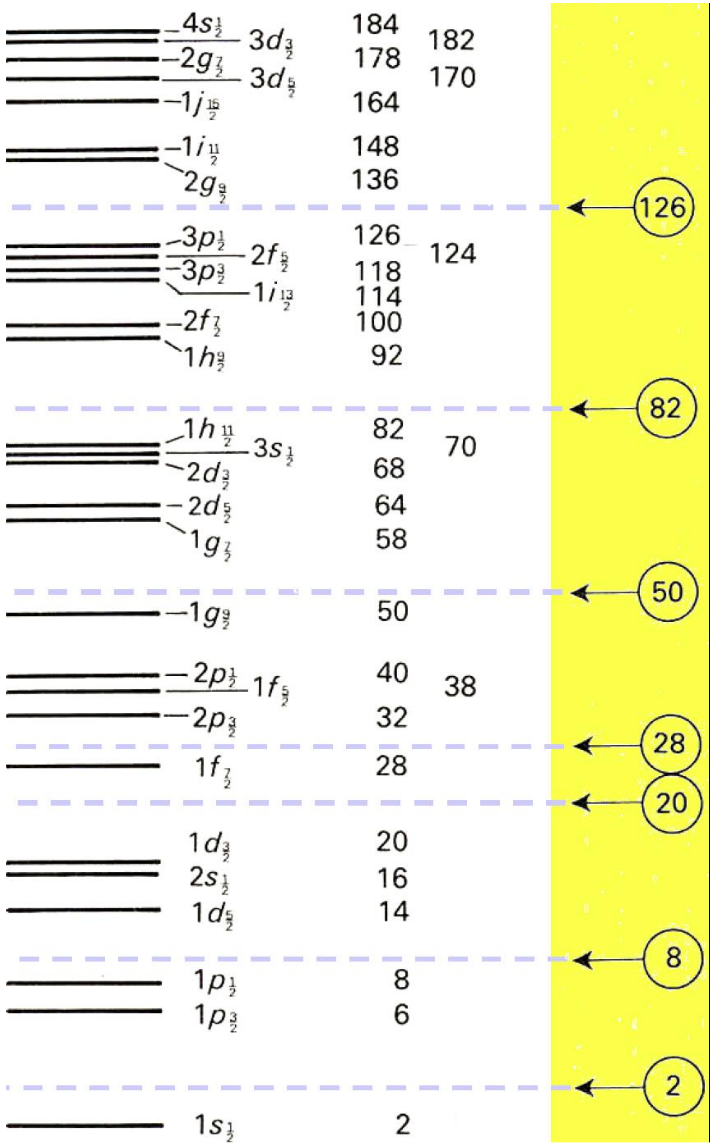

Ca48 and Pb208 have different **shell** and **surface** structures – Both are related to **Spin-Orbit** interaction

原子核幻数(Magic Numbers):

Strong Spin-Orbit

(l•s) Interaction

$$V(r) \rightarrow V(r) + W(r) L \bullet S$$

$$W(r) = -|V_{LS}| \left(\frac{\hbar}{m_\pi c} \right)^2 \frac{1}{r} \frac{dV(r)}{dr}$$

Mayer and Jensen (1949)

Nobel Prize, 1963 (Also Wigner)

Relativistic effects (Duerr, PR103, 469(1956))

中子和质子的自旋-轨道相互作用强度差不多吗?

CREX/PREX: Strong Isovector Spin-Orbit Interaction

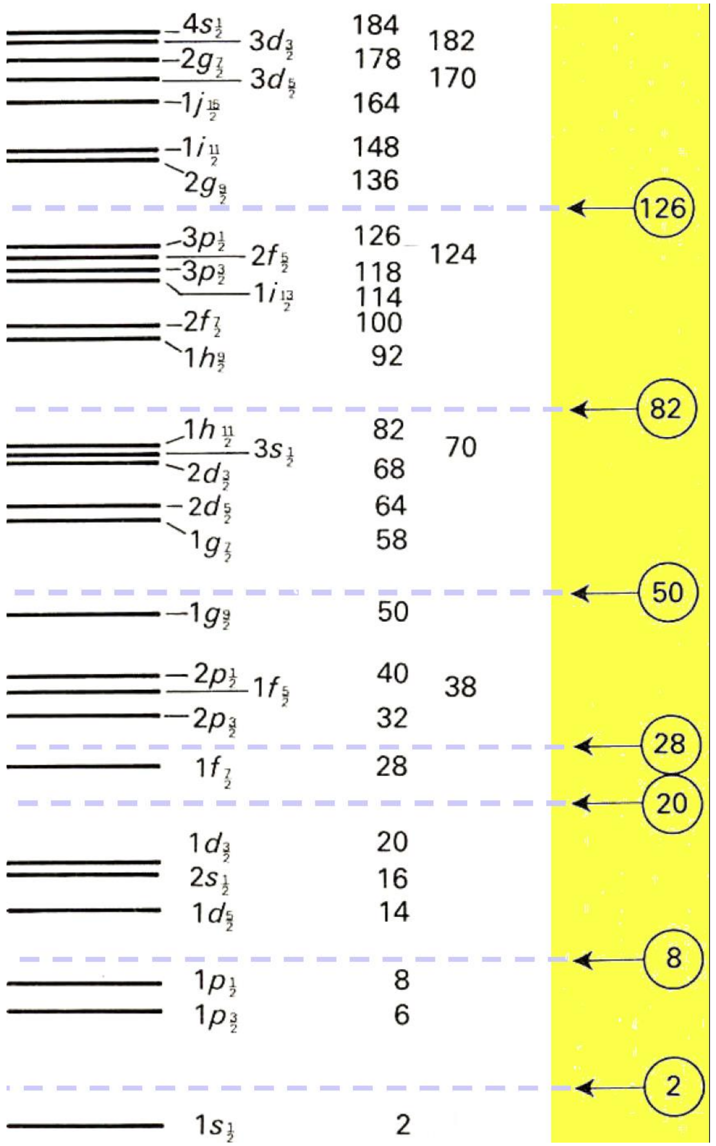

Total Hamiltonian Density from Spin-Orbit Interaction (also Tensor force):

$$-\frac{b_{\mathrm{IS}}}{2}\rho\nabla\cdot\boldsymbol{J}-\frac{b_{\mathrm{IV}}}{2}(\rho_n-\rho_p)\nabla\cdot(\boldsymbol{J}_n-\boldsymbol{J}_p)+\frac{1}{4}(\alpha_T+\beta_T)\boldsymbol{J}^2+\frac{1}{4}(\alpha_T-\beta_T)(\boldsymbol{J}_n-\boldsymbol{J}_p)^2$$

Spin-Orbit density:

$$\boxed{\begin{aligned} J_q(r) &= \frac{1}{4\pi r^3}\sum_i v_i^2\,(2j_i+1) \\ &\times\left[j_i\,(j_i+1)-l_i\,(l_i+1)-\frac{3}{4}\right]R_i^2(r)\end{aligned}}$$

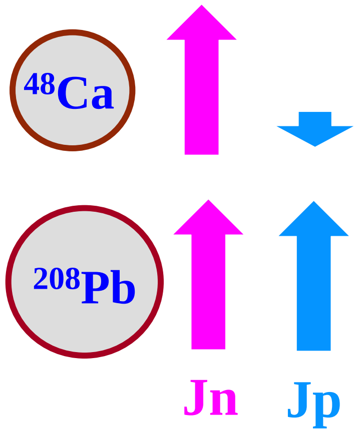

Jq ~ 0 for spin-saturated nuclei: Both $j_>$ =l+1/2 and $j_>$ =l-1/2 are occupied

Ca40: Jn ≈ 0, Jp ≈ 0
Ca48: Jp ≈ 0, Jn >> 0 due to the 8 1f7/2 neutrons of unpaired l•s partner
Pb208: Jn ≈ Jp >> 0 due to 14 1i13/2 neutrons and 12 1h11/2 protons

So Jn - Jp >> 0 for Ca48 while Jn - Jp ≈ 0 for Pb208:
Therefore, the isovector spin-orbit coupling b_{IV} is expected to have significant effect on Ca48 while essentially no influence on Pb208!

CREX/PREX: Strong Isovector Spin-Orbit Interaction

Tong-Gang Yue(岳侗钢)/Zhen Zhang(张振)/CLW, arXiv:2406.03844

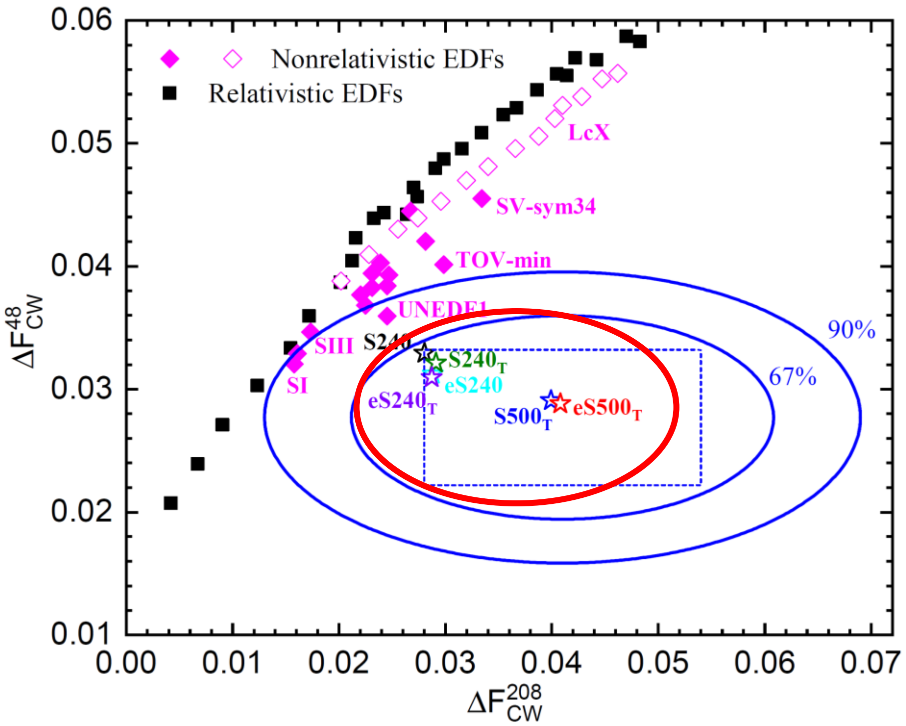

	S240	eS240	$S240_T$	$eS240_T$	$S500_T$	$eS500_T$
ρ_0	0.16359	0.15580	0.16498	0.15442	0.16342	0.15089
E_0	-16.147	-16.170	-16.220	-16.190	-16.288	-15.957
$\bar{m}_{s,0}$	0.982	0.939	0.993	0.865	1.022	0.921
$\bar{m}_{v,0}$	0.816	0.898	0.883	0.765	0.602	0.662
S	34.08	34.45	35.19	34.06	39.03	36.96
L	46.6	60.5	52.7	57.4	99.7	80.6
$K_{\rm sym}$	-207.4	-87.3	-190.4	-133.1	-101.1	-189.5
$\Delta F^{208}_{\rm CW}$	0.0280	0.0288	0.0291	0.0287	0.0400	0.0408
$\Delta F^{48}_{\rm CW}$	0.0329	0.0312	0.0321	0.0310	0.0291	0.0288
$\Delta r^{208}_{\rm np}$	0.189	0.195	0.194	0.195	0.263	0.273
$\Delta r^{48}_{\rm np}$	0.139	0.090	0.128	0.099	0.100	0.105
$\alpha^{208}_{\rm D}$	19.35	20.15	19.51	20.20	22.77	22.98
$\alpha^{48}_{\rm D}$	2.29	2.29	2.29	2.23	2.68	2.85

The isovector spin-orbit coupling b_{IV} should be larger than ~ 240 MeV fm^5 to fit CREX/PREX data (b_{IV} ~60 MeV fm^5 in conventional non-relativistic EDFs. Note: b_{IS} ~120 MeV fm^5)

中子和质子具有很不一样的自旋-轨道相互作用强度！

(b_{IV}~ 240 MeV fm^5 versus b_{IS} ~120 MeV fm^5)

- S500T and eS500T overpredict the measured electric dipole polarizability alphaD at RCNP
- S240/eS240/S240T/eS240T:
  Nskin(Pb208) ~ 0.19 fm, Nskin(Ca48) ~ 0.12 fm
  $E_{sym}(\rho_0)$ ~ 34 MeV, L ~ 55 MeV
  (Nicely agree with World Average Values!)

CREX/PREX: Strong Isovector Spin-Orbit Interaction

Tong-Gang Yue(岳侗钢)/Zhen Zhang(张振)/CLW, arXiv:2406.03844

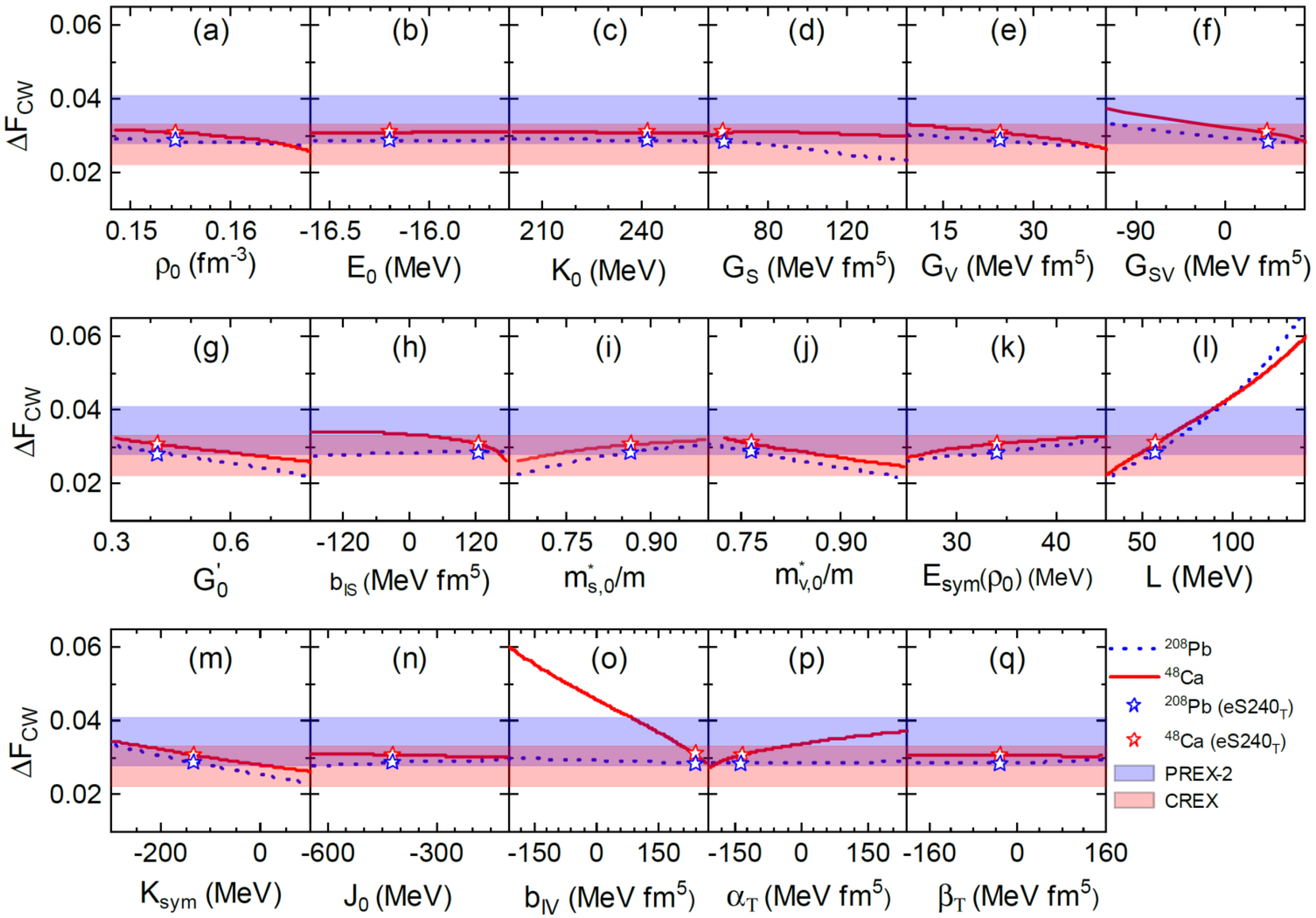

- The ΔFcw of both Pb208 and Ca48 is sensitive to L
- The isovector spin-orbit coupling b_{IV} has significant effect on Ca48 while essentially no influence on Pb208!

CREX/PREX: Strong Isovector Spin-Orbit Interaction

Tong-Gang Yue(岳侗钢)/Zhen Zhang(张振)/CLW, arXiv:2406.03844

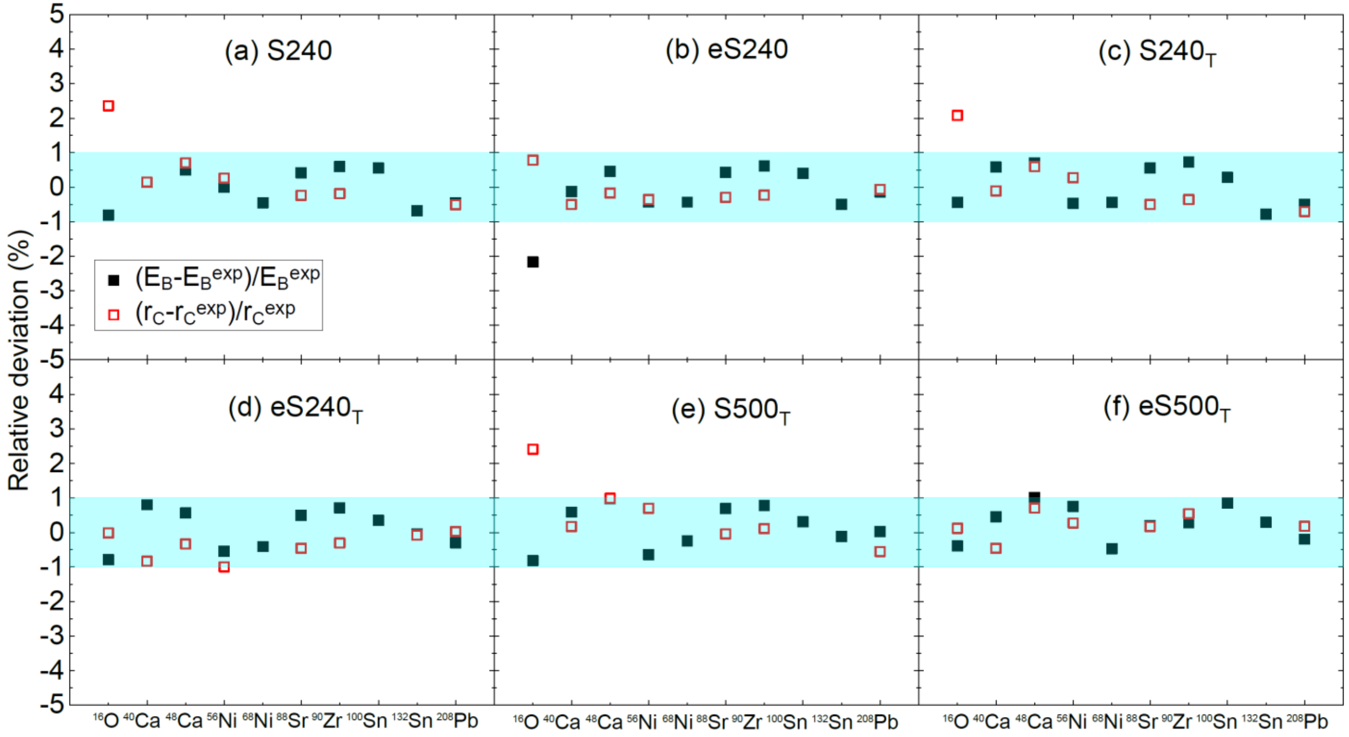

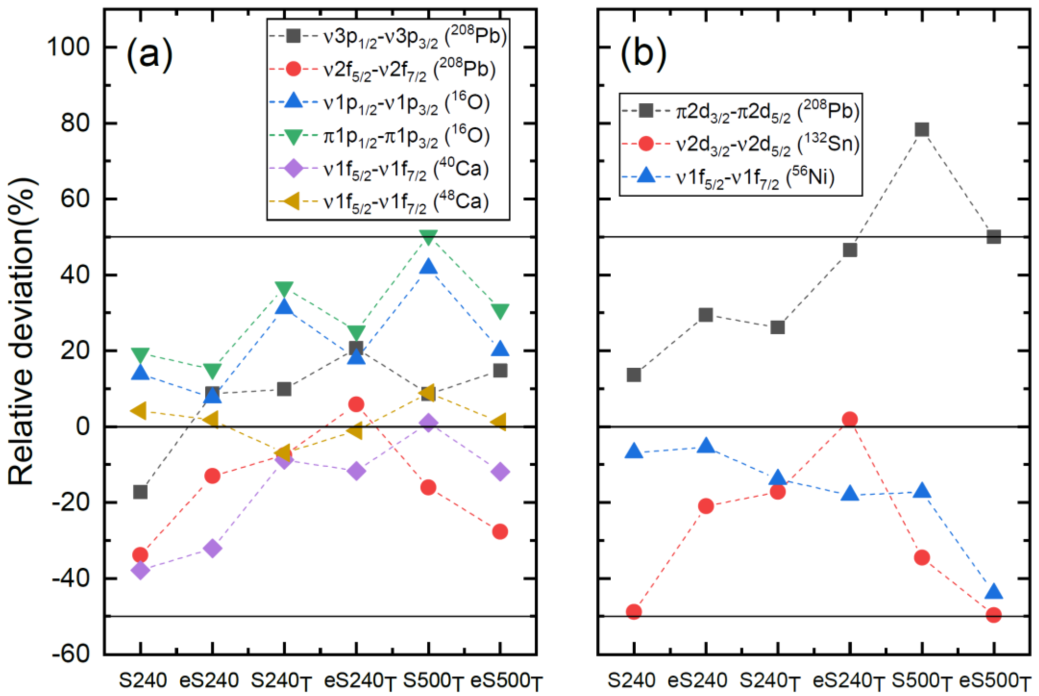

The new EDFs with strong isovector spin-orbit interaction can well describe the nuclear global properties!

CREX/PREX: Strong Isovector Spin-Orbit Interaction

Tong-Gang Yue(岳侗钢)/Zhen Zhang(张振)/CLW, arXiv:2406.03844

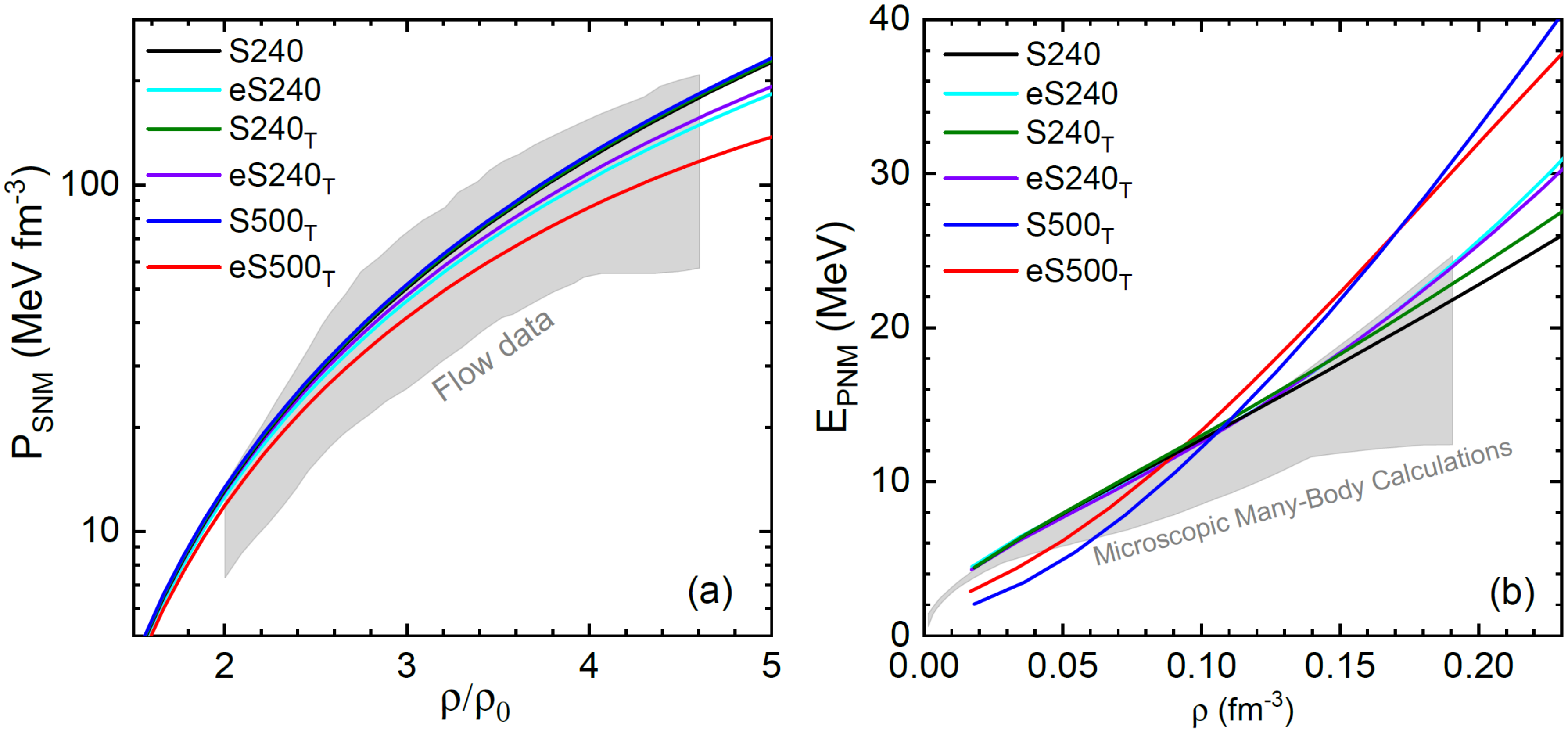

The new EDFs with strong isovector spin-orbit interaction can well describe the empirical EOS of SNM and PNM! (but S500T and eS500T predict too stiff PNM EOS)

CREX/PREX: Strong Isovector Spin-Orbit Interaction

Tong-Gang Yue(岳侗钢)/Zhen Zhang(张振)/CLW, arXiv:2406.03844

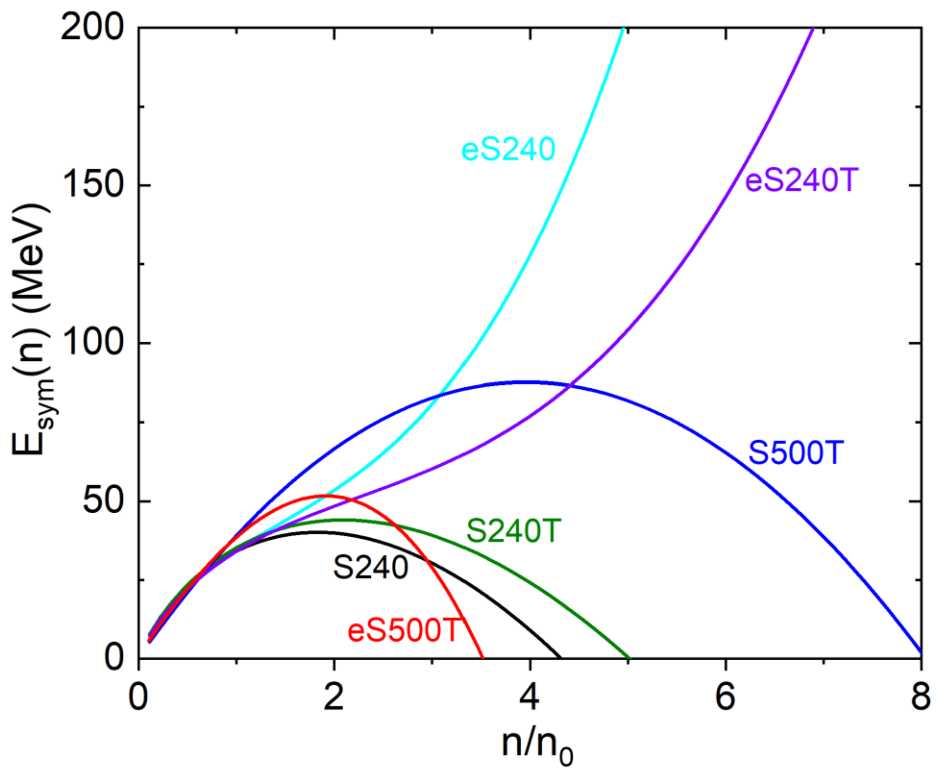

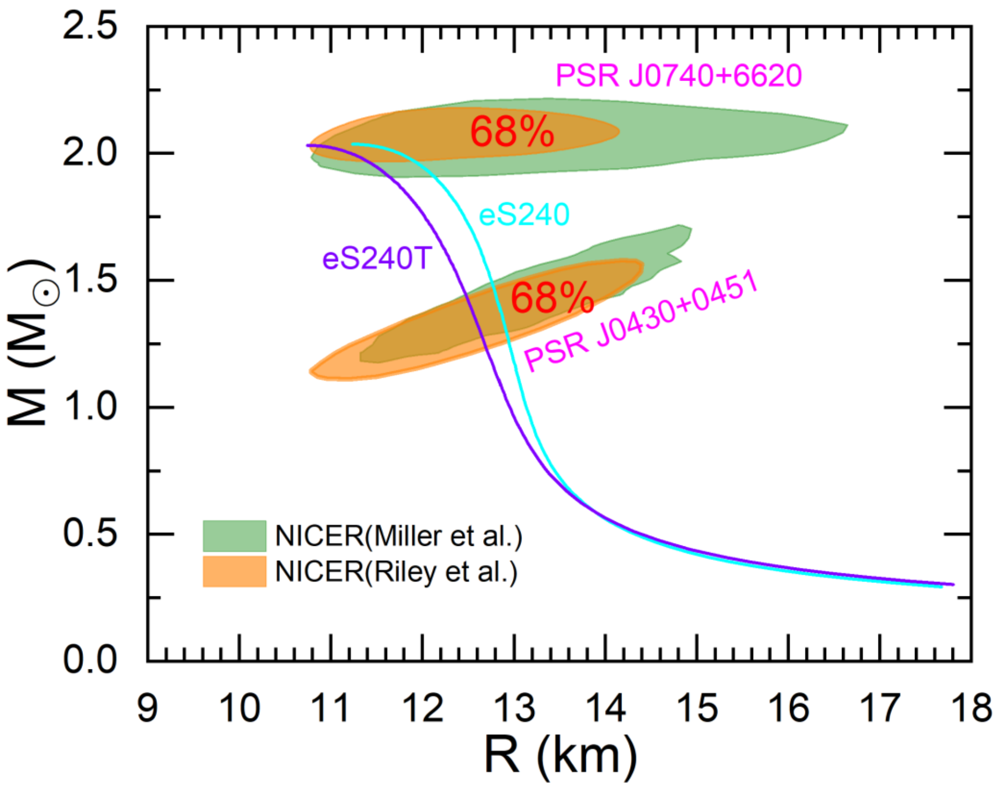

eS240T - $\Lambda_{1.4}$ =378; eS240 - $\Lambda_{1.4}$ = 463

GW170817 (LIGO/Virgo): 70< $\Lambda_{1.4}$ < 580 (Assuming NS)

eS240T和eS240能同时符合天文学观测数据!

强同位旋矢量自旋-轨道相互作用将对极端丰中子原子核的性质及其动力学产生深刻影响!

CREX/PREX: Strong Isovector Spin-Orbit Interaction

Some implications

- Such a strong isovector spin-orbit interaction is expected to have significant impacts on essentially all properties of neutron-rich nuclei: The location of neutron-drip line, shell evolution in exotic nuclei, the new magic number, the properties of superheavy nuclei, …

- Future PVES for some stable nuclei (MREX/MESA):
  Pb208, Ni60,…: Not sensitive to the isovector Spin-Orbit interactions (Esym);
  Ca48, Zr90,…: Sensitive to the isovector Spin-Orbit interactions (isovector spin-orbit coupling b_{IV})

目录

- □ 致密QCD物质
- □ 致密QCD物质的状态方程:
  - ■ 对称能：核物质和夸克物质的状态方程
  - ■ 中子皮：Pb/Ca中子半径之谜
  - ■ 引力波：对称能的高密行为
- □ 致密QCD物质的相变：
  - ■ QCD相图：概述
  - ■ 重离子碰撞：粒子产生的并合模型
  - ■ 致密星：中子星、超新星、双星并合
- □总结和展望

引力波

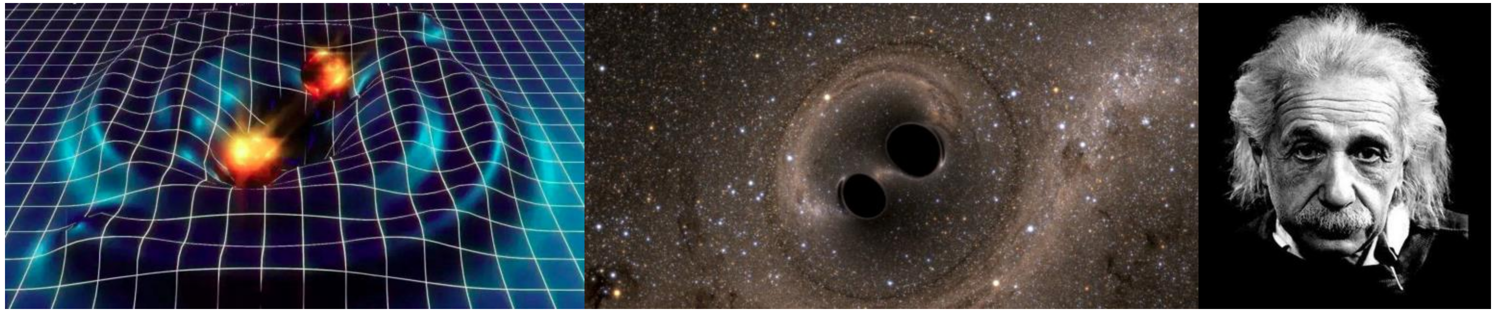

Einstein, A (June 1916). "Näherungsweise Integration der Feldgleichungen der Gravitation". Sitzungsberichte der Königlich Preussischen Akademie der Wissenschaften Berlin. part 1: 688–696

多信使时代: 引力波事件GW170817

PRL **119**, 161101 (2017) Selected for a Viewpoint in *Physics* PHYSICAL REVIEW LETTERS week ending 20 OCTOBER 2017

arXiv:1710.05832

GW170817: Observation of Gravitational Waves from a Binary Neutron Star Inspiral

B. P. Abbott *et al.**
(LIGO Scientific Collaboration and Virgo Collaboration)

Citations： 8152+

- On August 17, 2017, the merger of two neutron stars was observed with gravitational waves (GW) by the LIGO and Virgo detectors.
- The Fermi and Integral spacecrafts independently detected a short gamma ray burst.
- Extensive follow up observations detected this event at X-ray, ultra-violet, visible, infrared, and radio wavelengths.
- No ultra-high-energy gamma-rays and no neutrino candidates consistent with the source were found in follow-up searches. These observations support the hypothesis that GW170817 was produced by the merger of two neutron stars in NGC 4993 followed by a short gamma-ray burst (GRB 170817A) and a kilonova/macronova powered by the radioactive decay of *r*-process nuclei synthesized in the ejecta

开创了中子星观测的多信使时代！

LIGO/Virgo/KAGRA: 中子星并合引力波事件：2~20个/年！(A. Colombo et al., ApJ937, 79 (2022))

中子星的潮汐极化率Λ

Tidal Deformability (Polarizability)
(oscillation response coefficient λ)

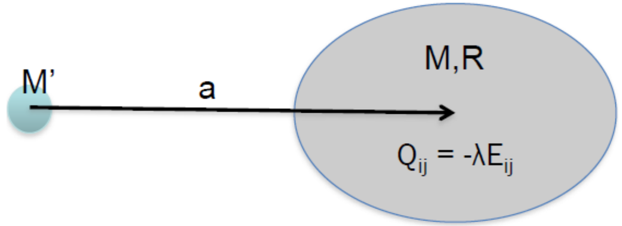

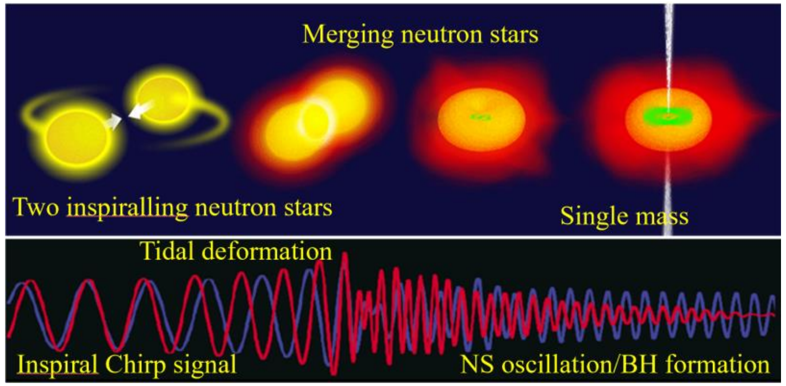

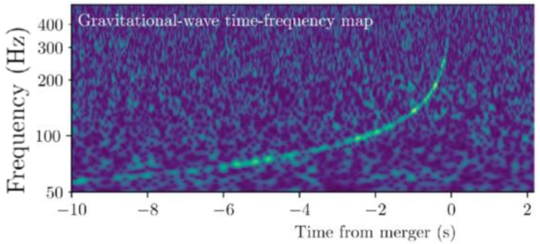

$$Q_{ij} = \lambda \varepsilon_{ij}$$

Q_{ij}: Quadrupole moment

ε_{ij}: Tidal field of companion

$$\boxed{\lambda = \frac{2}{3} k_2 R^5}$$

k_2: Love number
R: Radius
M: Mass

Dimensionless Tidal Deformability

$$\Lambda = \frac{2}{3} k_2 (R/M)^5$$

É.É. Flanagan and T. Hinderer, Phys. Rev. D 77, 021502(R) (2008)

中子星的潮汐极化率Λ

EOS +

$$\frac{dy}{dr} = -\frac{1}{r}[y^2 + yF(p,\varepsilon) + r^2 Q(p,\varepsilon)]$$

$$\frac{dp}{dr} = -\frac{(\varepsilon + p)(m + 4\pi r^3 p)}{r(r-2m)}$$

$$\frac{dm}{dr} = 4\pi r^2 \varepsilon$$

⇒

M

R

$y_R \equiv y(R)$

⇓

$$k_2 = \frac{1}{20}\left(\frac{R_s}{R}\right)^5 \left(1-\frac{R_s}{R}\right)^2 \left[2 - y_R + (y_R - 1)\frac{R_s}{R}\right] \left\{\frac{R_s}{R}\left(6 - 3y_R + \frac{3R_s}{2R}(5y_R - 8)\right)\right.$$
$$+\frac{1}{4}\left(\frac{R_s}{R}\right)^3 \left[26 - 22y_R + \frac{R_s}{R}(3y_R - 2) + \left(\frac{R_s}{R}\right)^2 (y_R + 1)\right]$$
$$\left. +3\left(1-\frac{R_s}{R}\right)^2 \left[2 - y_R + (y_R - 1)\frac{R_s}{R}\right] \ln\left(1 - \frac{R_s}{R}\right)\right\}^{-1}$$

$$F(r) = \frac{r - 4\pi r^3[\mathcal{E}(r) - P(r)]}{r - 2M(r)},$$

$$Q(r) = \frac{4\pi r\left[5\mathcal{E}(r) + 9P(r) + \frac{\mathcal{E}(r)+P(r)}{c_s^2} - \frac{6}{4\pi r^2}\right]}{r - 2M(r)} - 4\left\{\frac{M(r) + 4\pi r^3 P(r)}{r[r - 2M(r)]}\right\}^2.$$

⇓

$$\lambda = \frac{2}{3} k_2 R^5$$

中子星物质的状态方程

Our assumptions

- **Core of the neutron stars consist of infinite β-equilibrium npeμ matter with charge neutrality. Its EOS is determined by the Nuclear Energy Density Functionals**

- **The inner crust** $2.46\times10^{-4}\,\mathrm{fm}^{-3} = n_{\mathrm{out}} < n < n_t$

$$P = a + b\epsilon^{4/3}$$

n_t is determined self-consistently by using dynamical method

(J Xu(徐骏)/LWC/Li/Ma, ApJ697,1549(2009))

$$a = \frac{P_{\mathrm{out}}\epsilon_{\mathrm{t}}^{4/3} - P_{\mathrm{t}}\epsilon_{\mathrm{out}}^{4/3}}{\epsilon_{\mathrm{t}}^{4/3} - \epsilon_{\mathrm{out}}^{4/3}} \qquad b = \frac{P_{\mathrm{t}} - P_{\mathrm{out}}}{\epsilon_{\mathrm{t}}^{4/3} - \epsilon_{\mathrm{out}}^{4/3}}$$

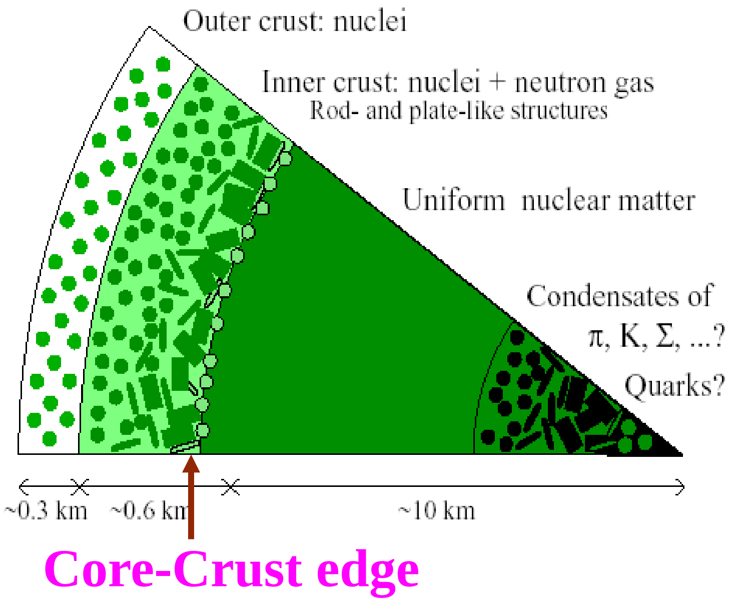

- **The outer crust**

$6.93\times10^{-13}\,\mathrm{fm}^{-3} < n < n_{\mathrm{out}}$ **(EOS of BPS)**

$4.73\times10^{-15}\,\mathrm{fm}^{-3} < n < 6.93\times10^{-13}\,\mathrm{fm}^{-3}$ **(EOS of Feynman-Metropolis-Teller)**

天文学观测：大质量中子星和Λ

PRL 119, 161101 (2017) Selected for a Viewpoint in *Physics* PHYSICAL REVIEW LETTERS week ending 20 OCTOBER 2017

GW170817: Observation of Gravitational Waves from a Binary Neutron Star Inspiral

B. P. Abbott *et al.*[*]
(LIGO Scientific Collaboration and Virgo Collaboration)

PRL121, 161101 (2018) (Citations： 2003+)

GW170817: Measurements of neutron star radii and equation of state

The LIGO Scientific Collaboration and The Virgo Collaboration
(compiled 30 May 2018)

GW170817 (LIGO/Virgo):
$70 < \Lambda_{1.4} < 580$ (Assuming NS)

A Massive Pulsar in a Compact Relativistic Binary
John Antoniadis *et al.*
Science **340**, (2013);
DOI: 10.1126/science.1233232

Science AAAS

Methods: We report on radio-timing observations of the pulsar J0348+0432 and phase-resolved optical spectroscopy of its white-dwarf companion, which is in a 2.46-hour orbit. We used these to derive the component masses and orbital parameters, infer the system's motion, and constrain its age.

Results: We find that the white dwarf has a mass of $0.172 \pm 0.003\ M_\odot$, which, combined with orbital velocity measurements, yields a pulsar mass of $2.01 \pm 0.04\ M_\odot$. Additionally, over a span of 2 years, we observed a significant decrease in the orbital period, $\dot{P}_b^{obs} = -8.6 \pm 1.4\ \mu s\ year^{-1}$ in our radio-timing data.

Observed heaviest Nstar (before 2019):

PSR J0348+0432

2.01 ± 0.04 solar mass ($M_\odot$)

状态方程: 有限核, 重离子碰撞, 中子星质量, 潮汐极化率

Y. Zhou(周颖)/LWC/Z. Zhang(张振), PRD99, 121301(R) (2019) [arXiv:1901.11364]

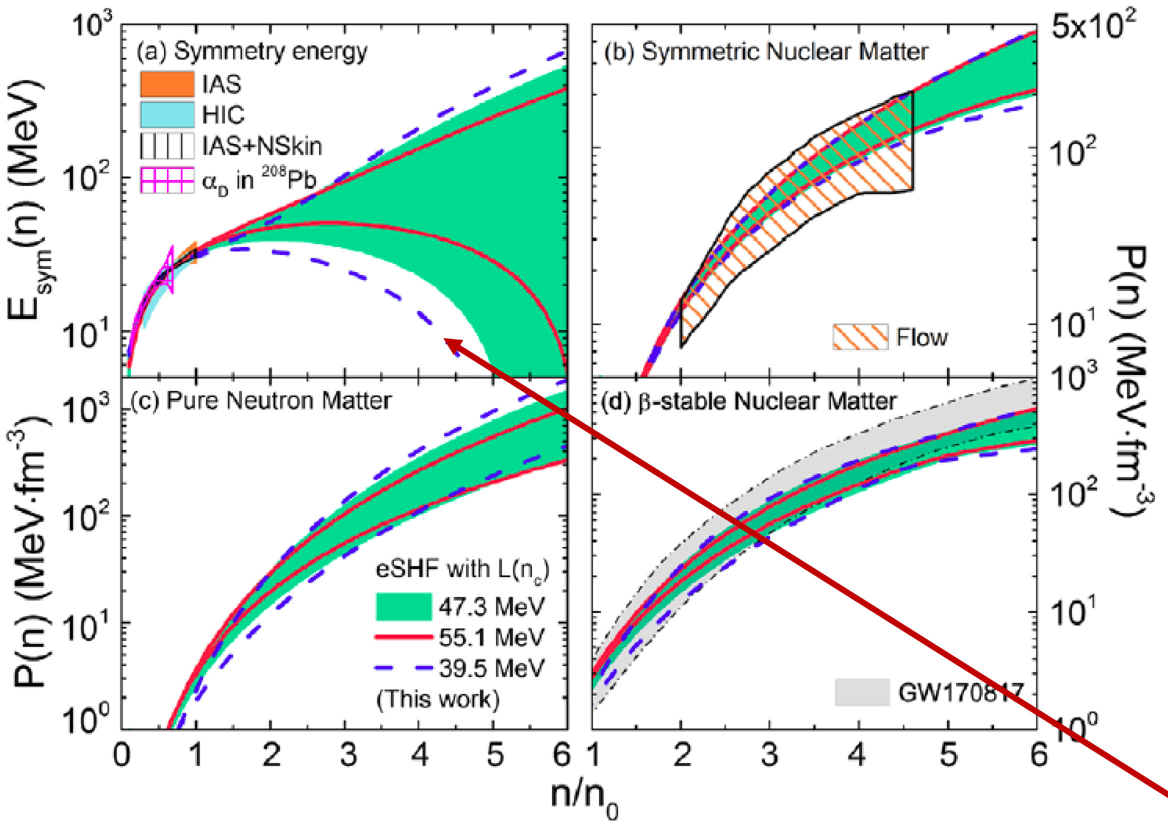

$L(\rho_c)$=47.3+/-7.8 MeV using α_D of ^{208}Pb (Z. Zhang(张振)/LWC, PRC90, 064317(2014))

Consistent with LIGO/Virgo constraints (see, e.g., D. Radice et al., ApJL852, L29(2018) but more stringent due to nuclear data added

$L(\rho_c)$=47.3 MeV:
J0:[-464,-342] MeV,
K_{sym}:[-175,-36] MeV
$E_{sym}(2\rho_0)$:[39.4, 54.5] MeV

基于同一个密度泛函extended Skyrme-Hartree-Fock(eSHF)，同时分析：有限核, 重离子碰撞, 中子星质量, 潮汐极化率

对称能高密行为仍然具有很大的不确定性，高密处甚至可能为负！

大质量中子星：M~2M$_\odot$

nature astronomy LETTERS
https://doi.org/10.1038/s41550-019-0880-2

2020

Relativistic Shapiro delay measurements of an extremely massive millisecond pulsar

H. T. Cromartie[1*], E. Fonseca[2], S. M. Ransom[3], P. B. Demorest[4], Z. Arzoumanian[5], H. Blumer[6,7], P. R. Brook[6,7], M. E. DeCesar[8], T. Dolch[9], J. A. Ellis[10], R. D. Ferdman[11], E. C. Ferrara[12,13], N. Garver-Daniels[6,7], P. A. Gentile[6,7], M. L. Jones[6,7], M. T. Lam[6,7], D. R. Lorimer[6,7], R. S. Lynch[14], M. A. McLaughlin[6,7], C. Ng[15,16], D. J. Nice[8], T. T. Pennucci[17], R. Spiewak[18], I. H. Stairs[15], K. Stovall[4], J. K. Swiggum[19] and W. W. Zhu[20]

edge-on) binary pulsar systems. By combining data from the North American Nanohertz Observatory for Gravitational Waves (NANOGrav) 12.5-yr data set with recent orbital-phase-specific observations using the Green Bank Telescope, we have measured the mass of the MSP J0740+6620 to be $\boxed{2.14^{+0.10}_{-0.09}}$ M$_\odot$ (68.3% credibility interval; the 95.4% credibility interval is $2.14^{+0.20}_{-0.18}$ $M_\odot$). It is highly likely to be the most massive neutron star yet observed, and serves as a strong constraint on the neutron star interior EoS.

The Astrophysical Journal Letters, 915:L12 (15pp), 2021 July 1 https://doi.org/10.3847/2041-8213/ac03b8

2021

Refined Mass and Geometric Measurements of the High-mass PSR J0740+6620

E. Fonseca[1,2,3,4], H. T. Cromartie[5,37], T. T. Pennucci[6,7], P. S. Ray[8], A. Yu. Kirichenko[9,10], S. M. Ransom[6], P. B. Demorest[11], I. H. Stairs[12], Z. Arzoumanian[13], L. Guillemot[14,15], A. Parthasarathy[16], M. Kerr[8], I. Cognard[14,15], P. T. Baker[17], H. Blumer[3,4], P. R. Brook[3,4], M. DeCesar[18], T. Dolch[19,20], F. A. Dong[12], E. C. Ferrara[21,22,23], W. Fiore[3,4], N. Garver-Daniels[3,4], D. C. Good[12], R. Jennings[24], M. L. Jones[25], V. M. Kaspi[1,2], M. T. Lam[26,27], D. R. Lorimer[3,4], J. Luo[28], A. McEwen[25], J. W. McKee[28], M. A. McLaughlin[3,4], N. McMann[29], B. W. Meyers[12], A. Naidu[30], C. Ng[31], D. J. Nice[32], N. Pol[29], H. A. Radovan[33], B. Shapiro-Albert[3,4], C. M. Tan[1,2]

ABSTRACT

We report results from continued timing observations of PSR J0740+6620, a high-mass, 2.8-ms radio pulsar in orbit with a likely ultra-cool white dwarf companion. Our data set consists of combined pulse arrival-time measurements made with the 100-m Green Bank Telescope and the Canadian Hydrogen Intensity Mapping Experiment telescope. We explore the significance of timing-based phenomena arising from general-relativistic dynamics and variations in pulse dispersion. When using various statistical methods, we find that combining ~ 1.5 years of additional, high-cadence timing data with previous measurements confirms and improves upon previous estimates of relativistic effects within the PSR J0740+6620 system, with the pulsar mass $\boxed{m_p = 2.08^{+0.07}_{-0.07}\ M_\odot}$ (68.3% credibility) determined by the relativistic Shapiro time delay. For the first time, we measure secular variation in the orbital period and argue that this effect arises from apparent acceleration due to significant transverse motion. After incorporating contributions from Galactic differential rotation and off-plane acceleration in the Galactic potential, we obtain a model-dependent distance of $d = 1.14^{+0.17}_{-0.15}$ kpc (68.3% credibility). This improved distance confirms the ultra-cool nature of the white dwarf companion determined from recent optical observations. We discuss the prospects for future observations with next-generation facilities, which will likely improve the precision on m_p for J0740+6620 by an order of magnitude within the next few years.

$$\boxed{2.08^{+0.07}_{-0.07} M_\odot \text{ for PSR J0740+6620}}$$

Heaviest Nstar observed so far with precise mass from radio-timing observation

大质量中子星排除“超软”高密对称能

Y. Zhou (周颖), L.W. Chen*, ApJ886, 52(2019) [arXiv:1907.12284]

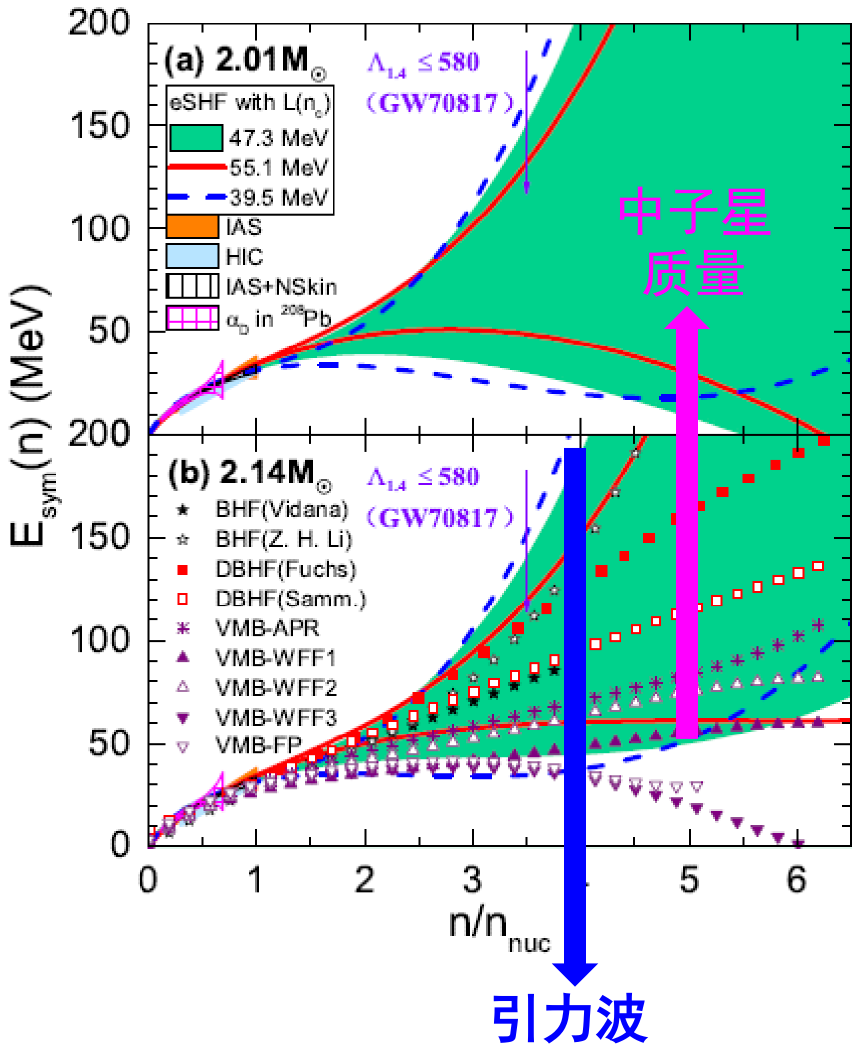

$$\frac{\hbar^2 k_F^2}{3m_s^*}(1+F_0') = \left.\frac{\partial^2 \mathcal{E}(\rho,\rho_1,s_0,s_1)}{\partial(\rho_1)^2}\right|_{\rho_1=s_0=s_1=0}$$

$$E_{\rm sym}(\rho) = \frac{\hbar^2 k_F^2}{6m_s^*}(1+F_0')$$

Z. Zhang(张振)/LWC, PRC94, 064326 (2016)

The Landau stability conditions,

$$F_l > -(2l+1),$$
$$F_l' > -(2l+1),$$
$$G_l > -(2l+1),$$
$$G_l' > -(2l+1),$$

$$\boxed{\mu_e = \mu_n - \mu_p = 4\delta E_{\rm sym}(\rho)}$$

Negative Esym leads to isospin instability: Pure Neutron Matter will appear

排除了“超软”的高密对称能，意味着中子星内部不存在纯中子物质！

目录

- 致密QCD物质
- 致密QCD物质的状态方程:
  - 对称能：核物质和夸克物质的状态方程
  - 中子皮：Pb/Ca中子半径之谜
  - 引力波：对称能的高密行为
- 致密QCD物质的相变：
  - QCD相图：概述
  - 重离子碰撞：粒子产生的并合模型
  - 致密星：中子星、超新星、双星并合
- 总结和展望

QCD相图

V.E. Fortov, Extreme States of Matter – on Earth and in the Cosmos, Springer-Verlag, 2011

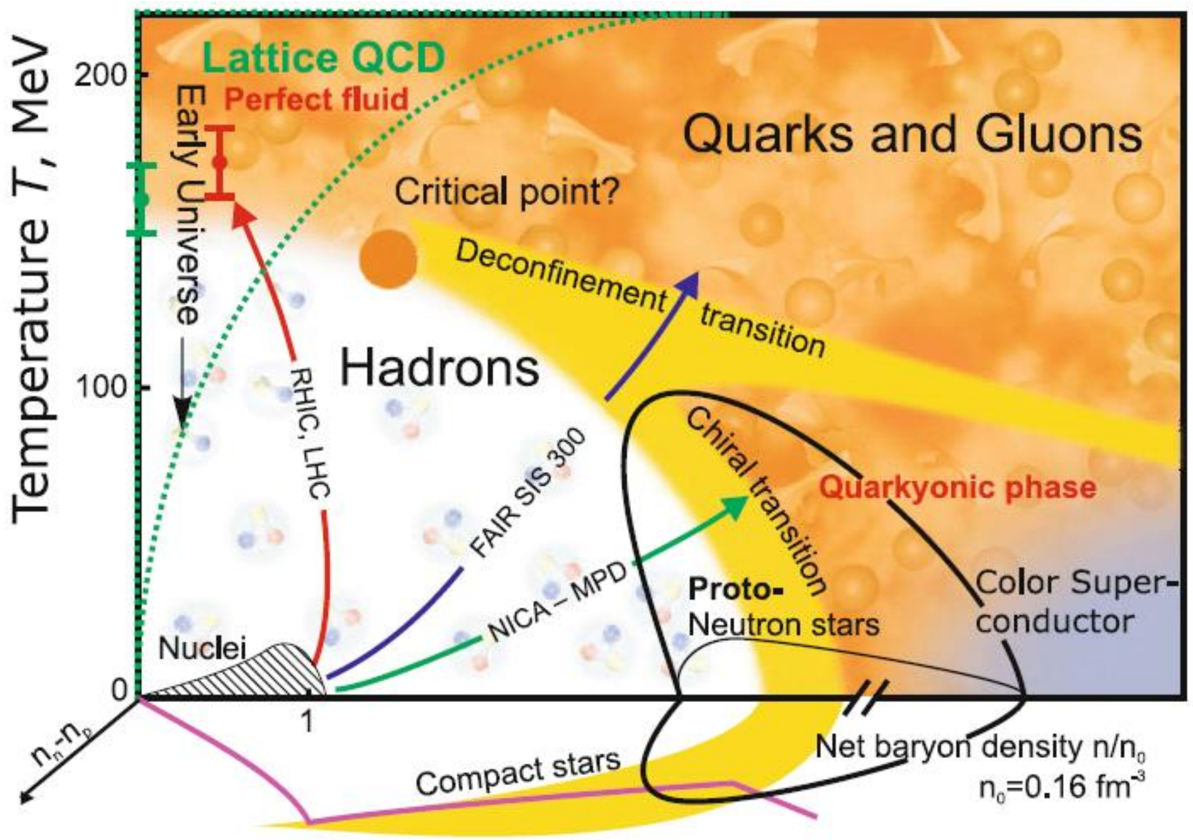

退禁闭相变?

液气相变?

手征相变?

水的液气相变:量热曲线(Caloric Curve)

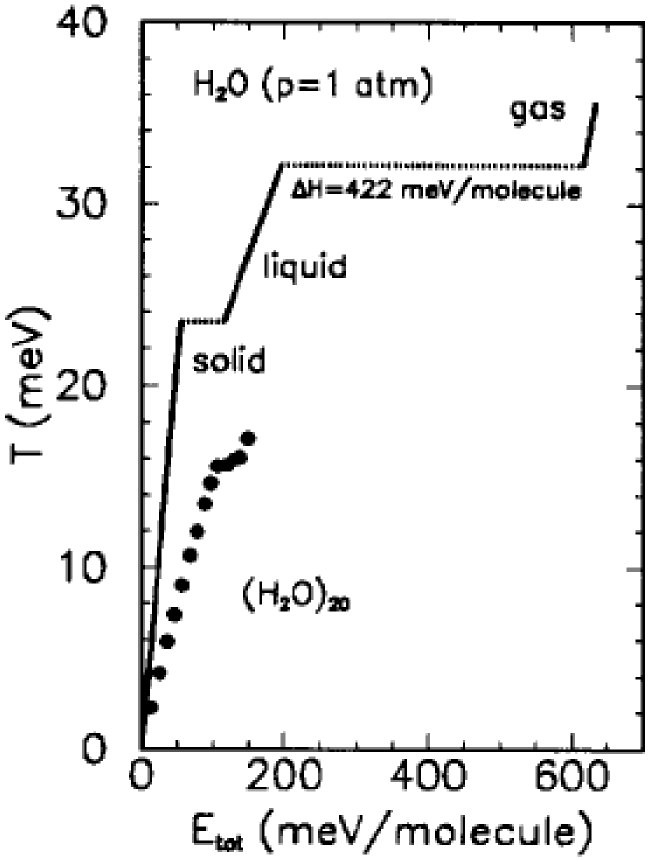

Pergamon
Prog. Part. Nucl. Phys., Vol. 39, pp. 443–501, 1997

0146-6410/97 $32.00 + 0.00
S0146-6410(97)00048-3

The Search for the Liquid–Gas Phase Transition in Nuclei

J. POCHODZALLA

Max-Planck Institut für Kernphysik, Saupfercheckweg 1, 69177 Heidelberg, Germany

Caloric curve !

Fig. 1. *Caloric curve of bulk water at atmospheric pressure (line) and of a water clusters consisting of 20 H_2O molecules predicted [Wales and Ohmine, 1993] by molecular dynamics calculations (dots).*

核物质的液气相变

核力短程排斥，长程吸引，与Van der Waals力相似，人们期望核物质存在液气相变

E. Epelbaum et al., RMP, 2009 (arXiv:0811.1338v1)

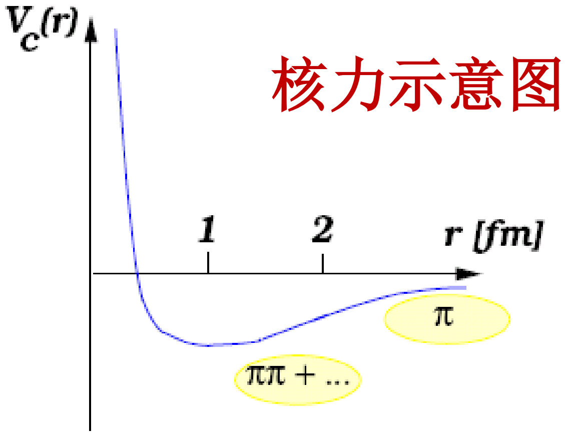

FIG. 1 Schematic plot of the central nucleon-nucleon potential. The longest range contribution is the one-pion-exchange, the intermediate range attraction is described by two-pion exchanges and other shorter ranged contributions. At even shorter distances, the NN interaction is strongly repulsive.

加热核物质：重离子碰撞

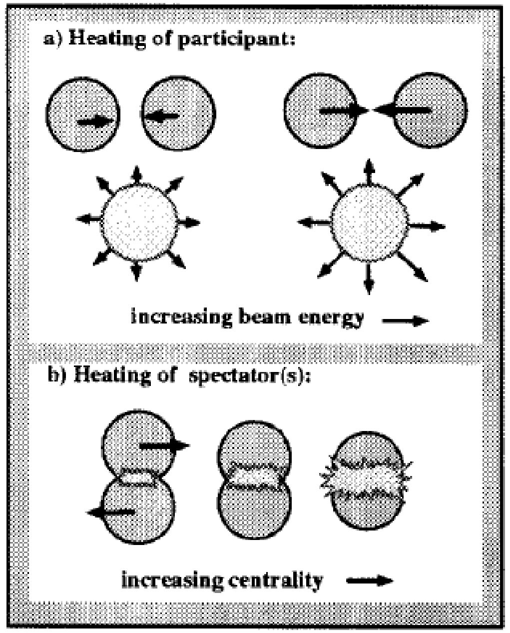

Fig. 2. *Pictorial view of the two different ways to produce boiling nuclei.*

核的量热曲线–I

ALADIN Data

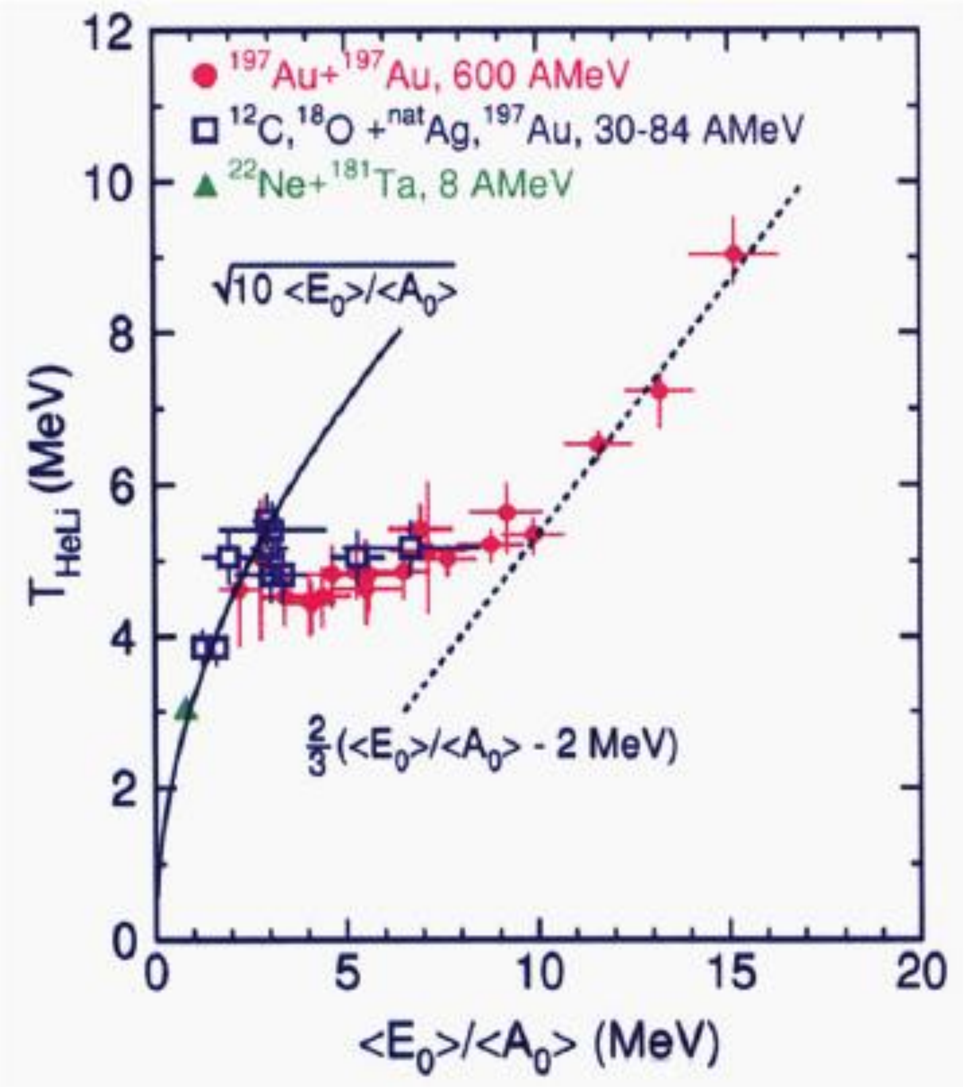

VOLUME 75, NUMBER 6 PHYSICAL REVIEW LETTERS 7 AUGUST 1995

Probing the Nuclear Liquid-Gas Phase Transition

J. Pochodzalla,[1] T. Möhlenkamp,[2] T. Rubehn,[1] A. Schüttauf,[3] A. Wörner,[1] E. Zude,[1] M. Begemann-Blaich,[1] Th. Blaich,[4] H. Emling,[1] A. Ferrero,[5,*] C. Gross,[1] G. Immé,[6] I. Iori,[5] G. J. Kunde,[1,†] W. D. Kunze,[1] V. Lindenstruth,[1,‡] U. Lynen,[1] A. Moroni,[5] W. F. J. Müller,[1] B. Ocker,[3] G. Raciti,[6] H. Sann,[1] C. Schwarz,[1] W. Seidel,[2] V. Serfling,[3] J. Stroth,[1] W. Trautmann,[1] A. Trzcinski,[7] A. Tucholski,[7] G. Verde,[5] and B. Zwieglinski[7]

[1]*Gesellschaft für Schwerionenforschung, 64220 Darmstadt, Germany*
[2]*Forschungszentrum Rossendorf, 01314 Dresden, Germany*
[3]*Institut für Kernphysik, Universität Frankfurt, 60486 Frankfurt, Germany*
[4]*Institut für Kernchemie, Universität Mainz, 55099 Mainz, Germany*
[5]*Dipartimento di Fisica, Universitá di Milano and INFN, 20133 Milano, Italy*
[6]*Dipartimento di Fisica dell' Universitáand INFN, 95129 Catania, Italy*
[7]*Soltan Institute for Nuclear Studies, 00 681 Warsaw, Hoza 69, Poland*

(Received 31 January 1995)

Fragment distributions resulting from Au + Au collisions at an incident energy of $E/A = 600$ MeV are studied. From the measured fragment and neutron distributions the mass and the excitation energy of the decaying prefragments were determined. A temperature scale was derived from observed yield ratios of He and Li isotopes. The relation between this isotope temperature and the excitation energy of the system exhibits a behavior which is expected for a phase transition. The nuclear vapor regime takes over at an excitation energy of 10 MeV per nucleon, a temperature of 5 MeV, and may be characterized by a density of 0.15–0.3 normal nuclear density.

ratios of He and Li isotopes. The relation between this isotope temperature and the excitation energy of the system exhibits a behavior which is expected for a phase transition. The nuclear vapor regime takes

核的量热曲线−II

INDRA Data

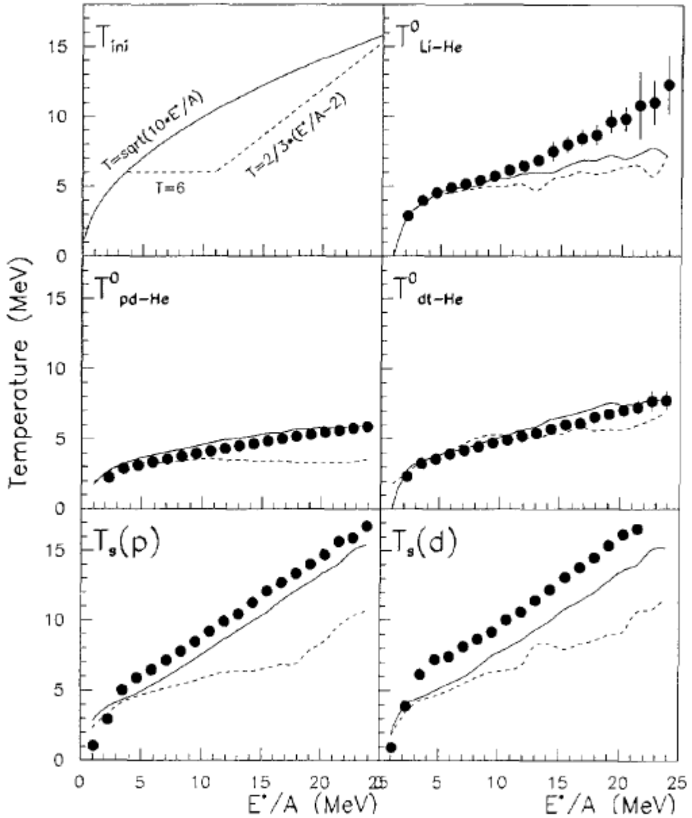

Fig. 2. Top left panel: correlation between initial temperature T_{ini} and excitation energy per nucleon E^*/A assumed in statistical decay calculations. Other panels: dependence of the apparent temperature on E^*/A. Dots: experimental data. Solid lines: Fermi gas with level density parameter $A/10$. Dashed lines: liquid-gas phase transition. From top to bottom: apparent temperatures from double isotope ratios ^{6}Li, ^{7}Li − ^{3}He, α, p, d − ^{3}He, α and d, t − ^{3}He, α, and slope parameters from proton and deuteron kinetic energy spectra.

ELSEVIER
2 January 1997
PHYSICS LETTERS B
Physics Letters B 390 (1997) 41–48

Surveying the nuclear caloric curve ★

Y.-G. Ma [a,1], A. Siwek [a,2], J. Péter [a], F. Gulminelli [a], R. Dayras [b], L. Nalpas [b], B. Tamain [a], E. Vient [a], G. Auger [c], Ch.O. Bacri [d], J. Benlliure [c], E. Bisquer [e], B. Borderie [d], R. Bougault [a], R. Brou [a], J.L. Charvet [b], A. Chbihi [c], J. Colin [a], D. Cussol [a], E. De Filippo [b], A. Demeyer [e], D. Doré [d], D. Durand [a], P. Ecomard [c], P. Eudes [f], E. Gerlic [e], D. Gourio [f], D. Guinet [e], R. Laforest [a], P. Lautesse [e], J.L. Laville [f], L. Lebreton [e], J.F. Lecolley [a], A. Le Fèvre [c], T. Lefort [a], R. Legrain [b], O. Lopez [a], M. Louvel [a], J. Łukasik [d], N. Marie [c], V. Métivier [f], A. Ouatizerga [d], M. Parlog [d], E. Plagnol [d], A. Rahmani [f], T. Reposeur [f], M.F. Rivet [d], E. Rosato [a], F. Saint-Laurent [c], M. Squalli [d], J.C. Steckmeyer [a], M. Stern [e], L. Tassan-Got [d], C. Volant [b], J.P. Wieleczko [c]

Abstract

The 4π array INDRA was used to detect nearly all charged products emitted in Ar + Ni collisions between 52 and 95 MeV/u. The charge, mass and excitation energy E^* of the quasi-projectiles have been reconstructed event by event. Excitation energies up to 25 MeV per nucleon are reached. Apparent temperatures obtained from several double isotopic yield ratios Tr^0 show different dependences upon E^*. $T^0_{^6\mathrm{Li}/^7\mathrm{Li}-^3\mathrm{He}\alpha}$ yields the highest values, as well as the high energy slopes Ts of the kinetic energy spectra. Two statistical models, sequential evaporation and gas in complete equilibrium, taking into account side feeding and discrete excited states population, show that the data can be explained by a steady increase of the initial temperature with excitation energy without evidence for a liquid-gas phase transition.

Too small finite system???

For a review, see, e.g.,

S. Das Gupta, A. Z. Mekjian, and M. B. Tsang,
Adv. Nucl. Phys., (2001); nucl-th/0009033

核的液气相变:高能质子轰击金核

VOLUME 88, NUMBER 2 PHYSICAL REVIEW LETTERS 14 JANUARY 2002

Event-by-Event Analysis of Proton-Induced Nuclear Multifragmentation: Determination of the Phase Transition Universality Class in a System with Extreme Finite-Size Constraints

M. Kleine Berkenbusch, W. Bauer,* K. Dillman, and S. Pratt
National Superconducting Cyclotron Laboratory and Department of Physics and Astronomy, Michigan State University,

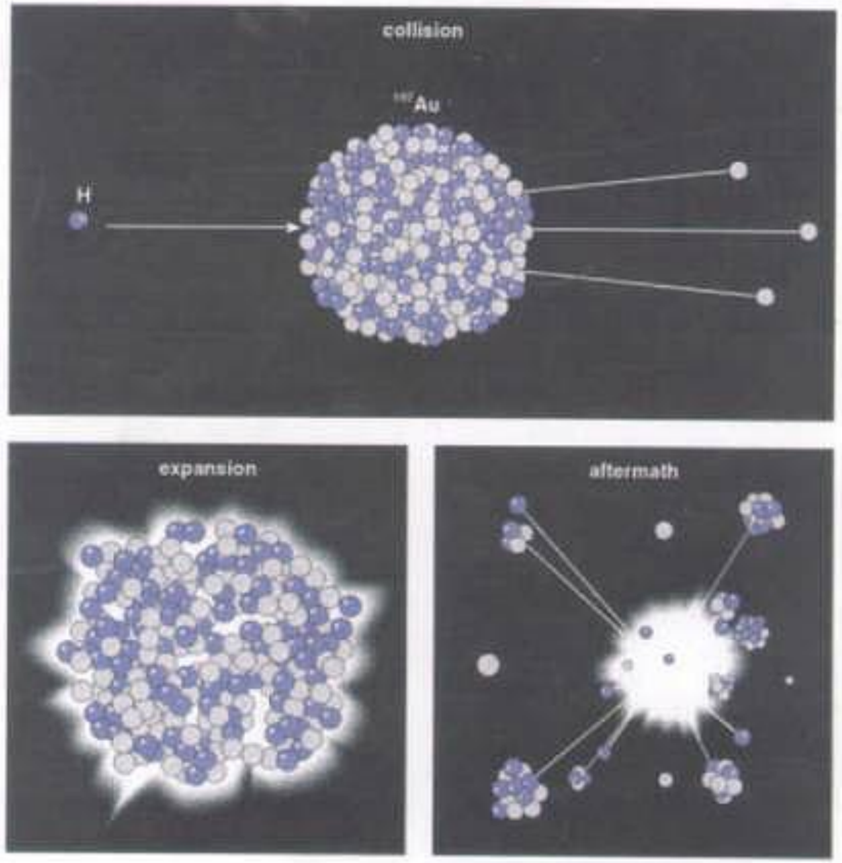

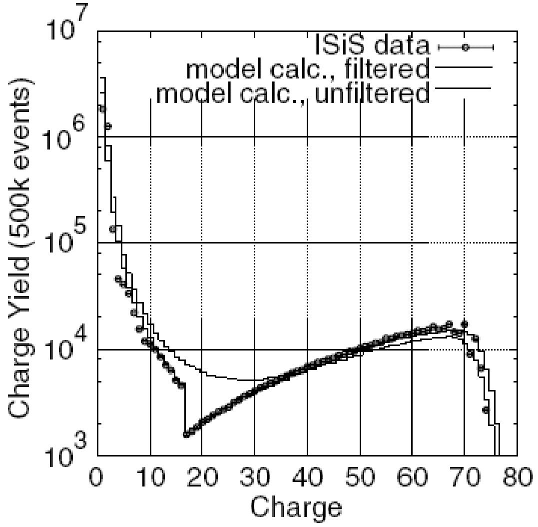

FIG. 1. Inclusive charge yield spectra for the reaction p + Au at 10.2 GeV. The round plot symbols represent the ISiS dat. The dotted histogram is the result of the corresponding percolation model calculation. The thick histogram represents the output of the calculation, filtered through the detector acceptance corrections.

A percolation model of nuclear fragmentation is used to interpret 10.2 GeV/c p + ^{197}Au multifragmentation data. Emphasis is put on finding signatures of a continuous nuclear matter phase transition in finite nuclear systems. Based on model calculations, corrections accounting for physical constraints of the fragment detection and sequential decay processes are derived. Strong circumstantial evidence for a continuous phase transition is found, and the values of two critical exponents, $\sigma = 0.5 \pm 0.1$ and $\tau = 2.35 \pm 0.05$, are extracted from the data. A critical temperature of $T_c = 8.3 \pm 0.2$ MeV is found.

核物质的液气相变:同位旋相关性

J. Xu(徐俊), LWC, B.A. Li, H.R. Ma, PRC77, 014302(2008)

同位旋非对称度
δ ＝(N-Z)/A

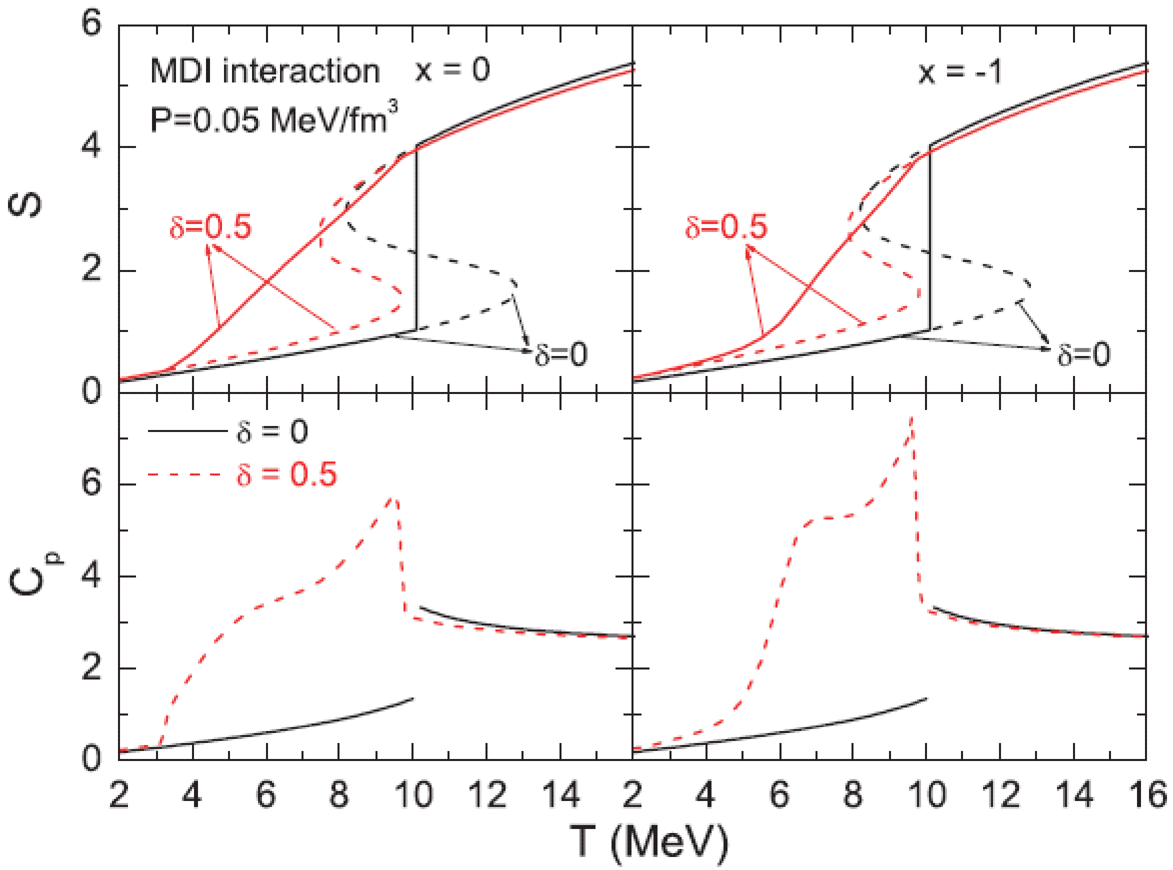

- 核物质相变过程：重子数守恒和同位旋守恒
- 同位旋效应：对称核物质 - 一级相变；非对称核物质 - 二级相变

相对论重离子碰撞：QCD相变–恢复真空破缺的对称性

相对论重离子碰撞实验 - 探索新的物质形态:夸克胶子等离子体

Workshop on BeV/n collisions of heavy ions –how and why? Bear Mountain, 1974

T D Lee emphasized, whether the vacuum is a medium whose properties one could change; "we should investigate, "he pointed out, "... phenomena by ***distributing high energy or high nucleon density over a relatively large volume***."If in this way one could ***restore broken symmetries of the vacuum***, then it might be possible to ***create abnormal dense states of nuclear matter***.

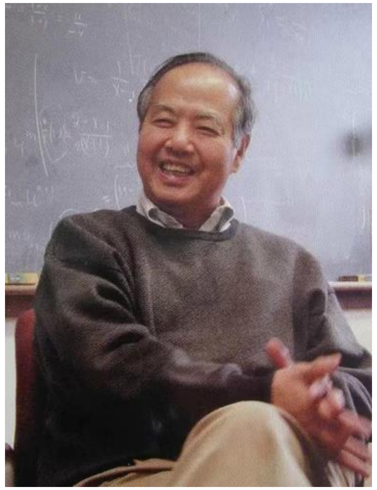

Tsung Dao Lee
(1926 - 2024)

Reviews of Modern Physics, Vol. 47, No. 2, April 1975

Abnormal nuclear states and vacuum excitation*†

T. D. Lee

Physics Department, Columbia University, New York, New York 10027

We examine the theoretical possibility that at high densities there may exist a new type of nuclear state in which the nucleon mass is either zero or nearly zero. The related phenomenon of vacuum excitation is also discussed.

dimensions. In order to study the question of "vacuum," we must turn to a different direction; we should investigate some "bulk" phenomena by distributing high energy over a relatively large volume. *The fact that this direction has never been explored should*, by itself, *serve as an incentive for doing such experiments*. As we have discussed, there are possibilities that abnormal states may be created, in which the nucleon mass may be very different from its normal value. It is conceivable that inside the volume of the abnormal state, some of the symmetry properties may become changed, or even that the usual roles of strong and weak interactions may become altered. If indeed the properties of the "vacuum" can be transformed, we may eventually be led to some even more striking consequences than those that have been discussed in this lecture.

Bavalac / LBL (1 GeV/u)
SIS / GSI (1 GeV/u)
AGS / BNL (10 GeV/u)
SPS / CERN (100 GeV/u)
RHIC / BNL
LHC / CERN

深切缅怀李政道先生

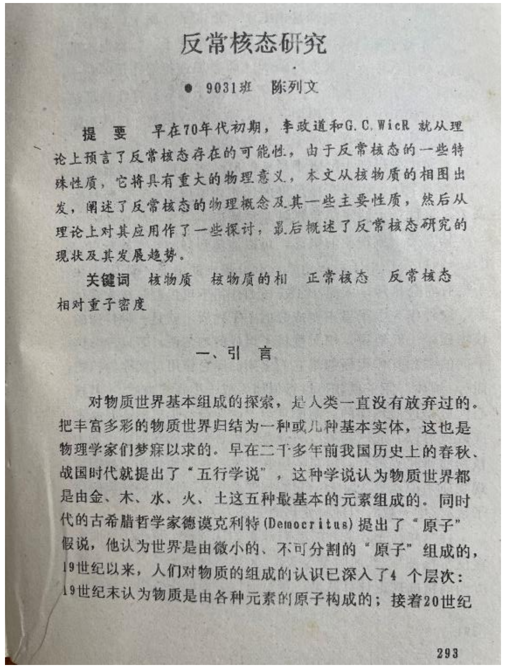

反常核态研究

● 9031班 陈列文

提 要 早在70年代初期，李政道和G. C. WicR 就从理论上预言了反常核态存在的可能性，由于反常核态的一些特殊性质，它将具有重大的物理意义，本文从核物质的相图出发，阐述了反常核态的物理概念及其一些主要性质，然后从理论上对其应用作了一些探讨，最后概述了反常核态研究的现状及其发展趋势。

关键词 核物质 核物质的相 正常核态 反常核态 相对重子密度

一、引 言

对物质世界基本组成的探索，是人类一直没有放弃过的。把丰富多彩的物质世界归结为一种或几种基本实体，这也是物理学家们梦寐以求的。早在二千多年前我国历史上的春秋、战国时代就提出了"五行学说"，这种学说认为物质世界都是由金、木、水、火、土这五种最基本的元素组成的。同时代的古希腊哲学家德谟克利特(Democritus)提出了"原子"假说，他认为世界是由微小的、不可分割的"原子"组成的，19世纪以来，人们对物质的组成的认识已深入了4 个层次：19世纪末认为物质是由各种元素的原子构成的；接着20世纪

293

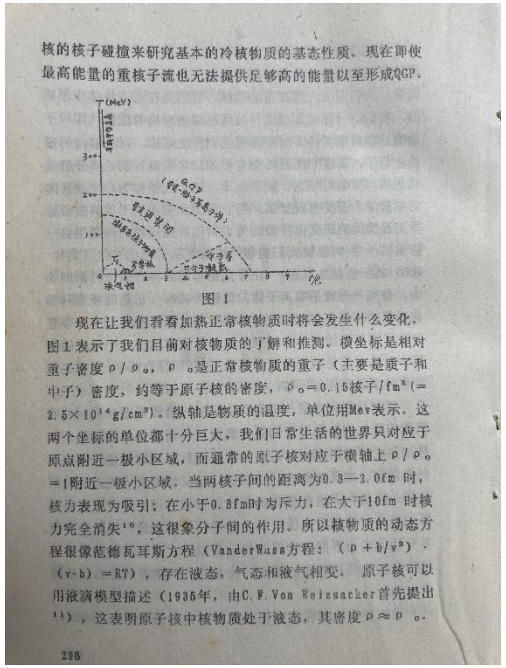

核的核子碰撞来研究基本的冷核物质的基态性质。现在即使最高能量的重核子流也无法提供足够高的能量以至形成QGP。

图 1

现在让我们看看加热正常核物质时将会发生什么变化。图1表示了我们目前对核物质的了解和推测。横坐标是相对重子密度ρ/ρ₀，ρ₀是正常核物质的重子（主要是质子和中子）密度，约等于原子核的密度，ρ₀=0.15核子/fm³(=2.5×10¹⁴g/cm³)。纵轴是物质的温度，单位用Mev表示。这两个坐标的单位都十分巨大，我们日常生活的世界只对应于原点附近一极小区域，而通常的原子核对应于横轴上ρ/ρ₀=1附近一极小区域。当两核子间的距离为0.8—2.0fm 时，核力表现为吸引；在小于0.8fm时为斥力，在大于10fm 时核力完全消失¹⁰，这很象分子间的作用。所以核物质的动态方程很像范德瓦耳斯方程（VanderWaas方程：（ρ+b/v²）·（v-b）=RT），存在液态，气态和液气相变。原子核可以用液滴模型描述（1935年，由C. F. Von Weizsacker首先提出¹¹），这表明原子核中核物质处于液态，其密度ρ≈ρ₀。

298

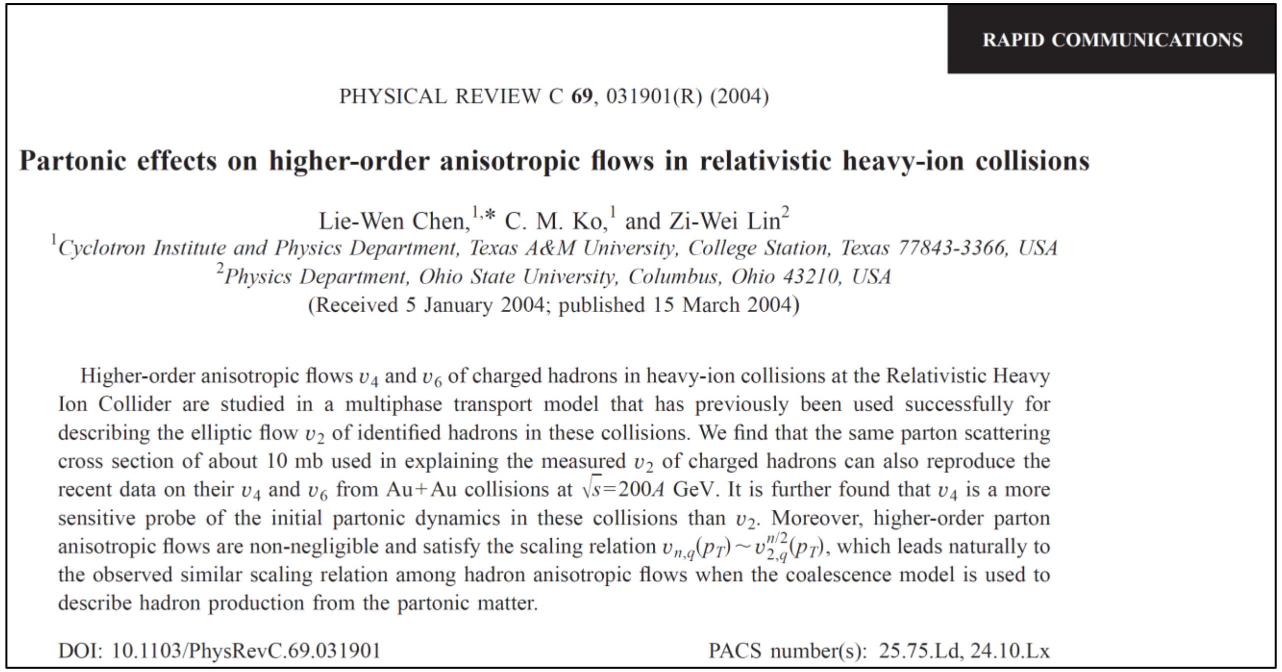

RAPID COMMUNICATIONS

PHYSICAL REVIEW C **69**, 031901(R) (2004)

Partonic effects on higher-order anisotropic flows in relativistic heavy-ion collisions

Lie-Wen Chen,[1,*] C. M. Ko,[1] and Zi-Wei Lin[2]
[1]*Cyclotron Institute and Physics Department, Texas A&M University, College Station, Texas 77843-3366, USA*
[2]*Physics Department, Ohio State University, Columbus, Ohio 43210, USA*
(Received 5 January 2004; published 15 March 2004)

Higher-order anisotropic flows v_4 and v_6 of charged hadrons in heavy-ion collisions at the Relativistic Heavy Ion Collider are studied in a multiphase transport model that has previously been used successfully for describing the elliptic flow v_2 of identified hadrons in these collisions. We find that the same parton scattering cross section of about 10 mb used in explaining the measured v_2 of charged hadrons can also reproduce the recent data on their v_4 and v_6 from Au+Au collisions at $\sqrt{s}=200A$ GeV. It is further found that v_4 is a more sensitive probe of the initial partonic dynamics in these collisions than v_2. Moreover, higher-order parton anisotropic flows are non-negligible and satisfy the scaling relation $v_{n,q}(p_T) \sim v_{2,q}^{n/2}(p_T)$, which leads naturally to the observed similar scaling relation among hadron anisotropic flows when the coalescence model is used to describe hadron production from the partonic matter.

DOI: 10.1103/PhysRevC.69.031901 PACS number(s): 25.75.Ld, 24.10.Lx

陈列文的本科毕业论文
(1994.6，湘潭)

陈列文的第一篇RHIC物理的学术论文
(2004.3，美国德州)

深切缅怀李政道先生

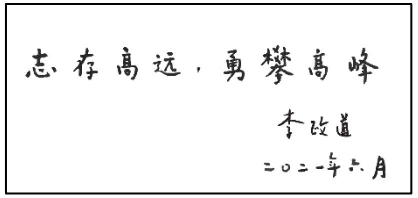

李政道先生莅临上海交通大学
(2009.5，物理楼610会议室)

“李政道物理班”招生宣讲
(2021.5.15，菁菁堂)

“李政道物理班”开班仪式
(2021.9.11，李政道图书馆)

小爆炸(Little Bang)

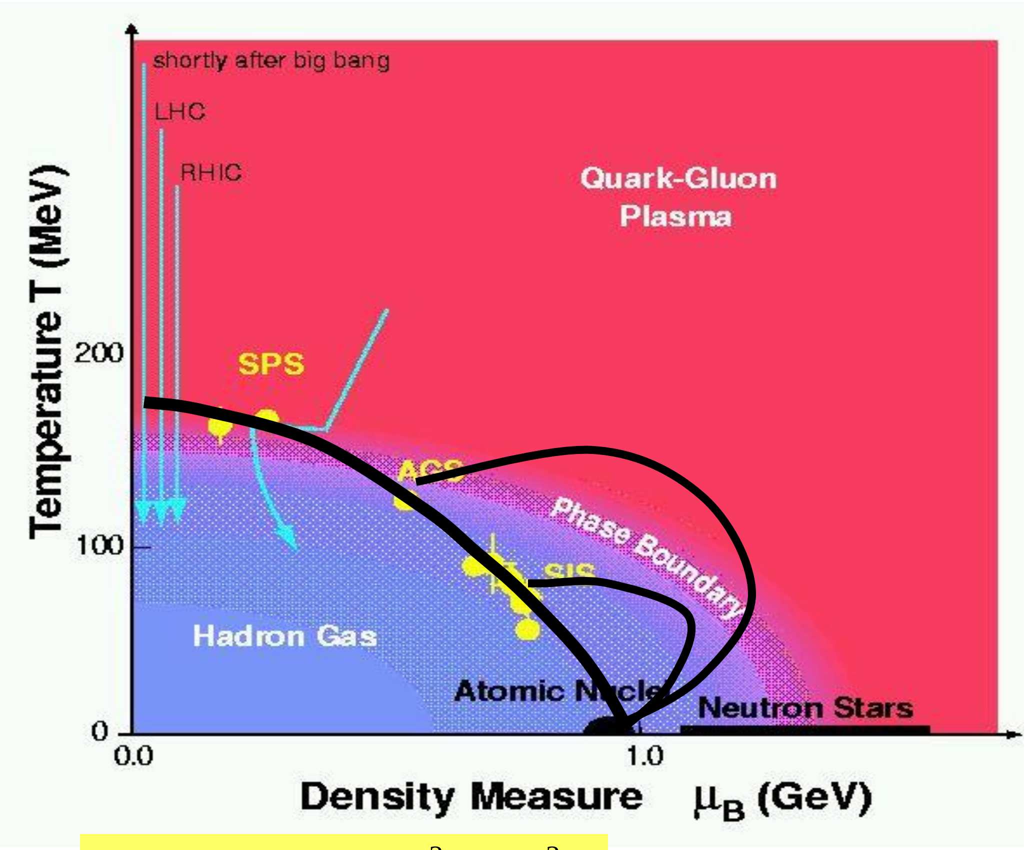

$$s_{NN} = (p_A + p_B)^2 = E_{CMS}^2$$

From high μ_B regime to high T regime

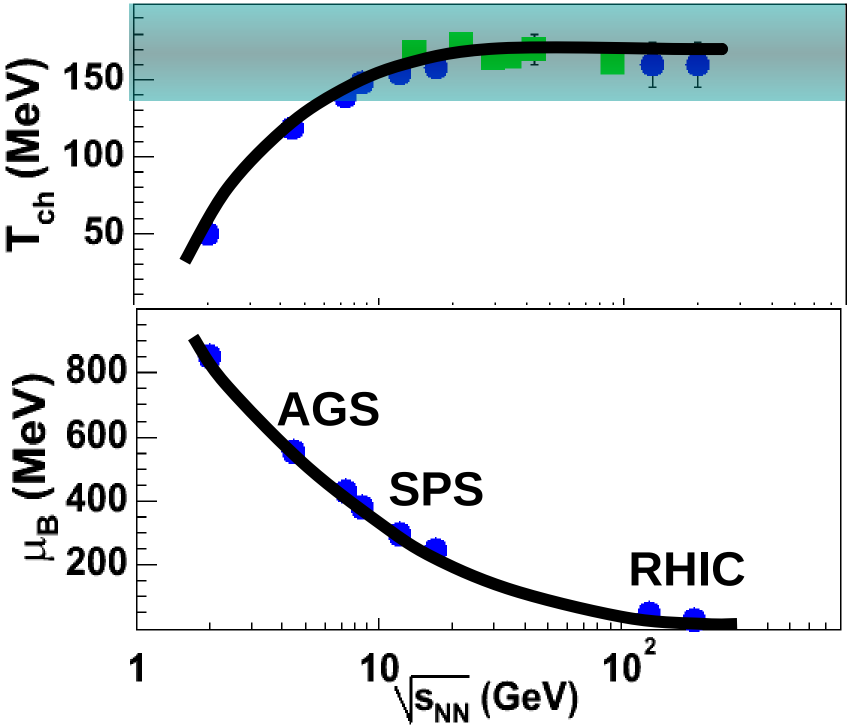

We do not observe hadronic systems with T> 170 MeV

(Hadronic Matter “melting point” - Hagedorn Temperature)

小爆炸的不同阶段

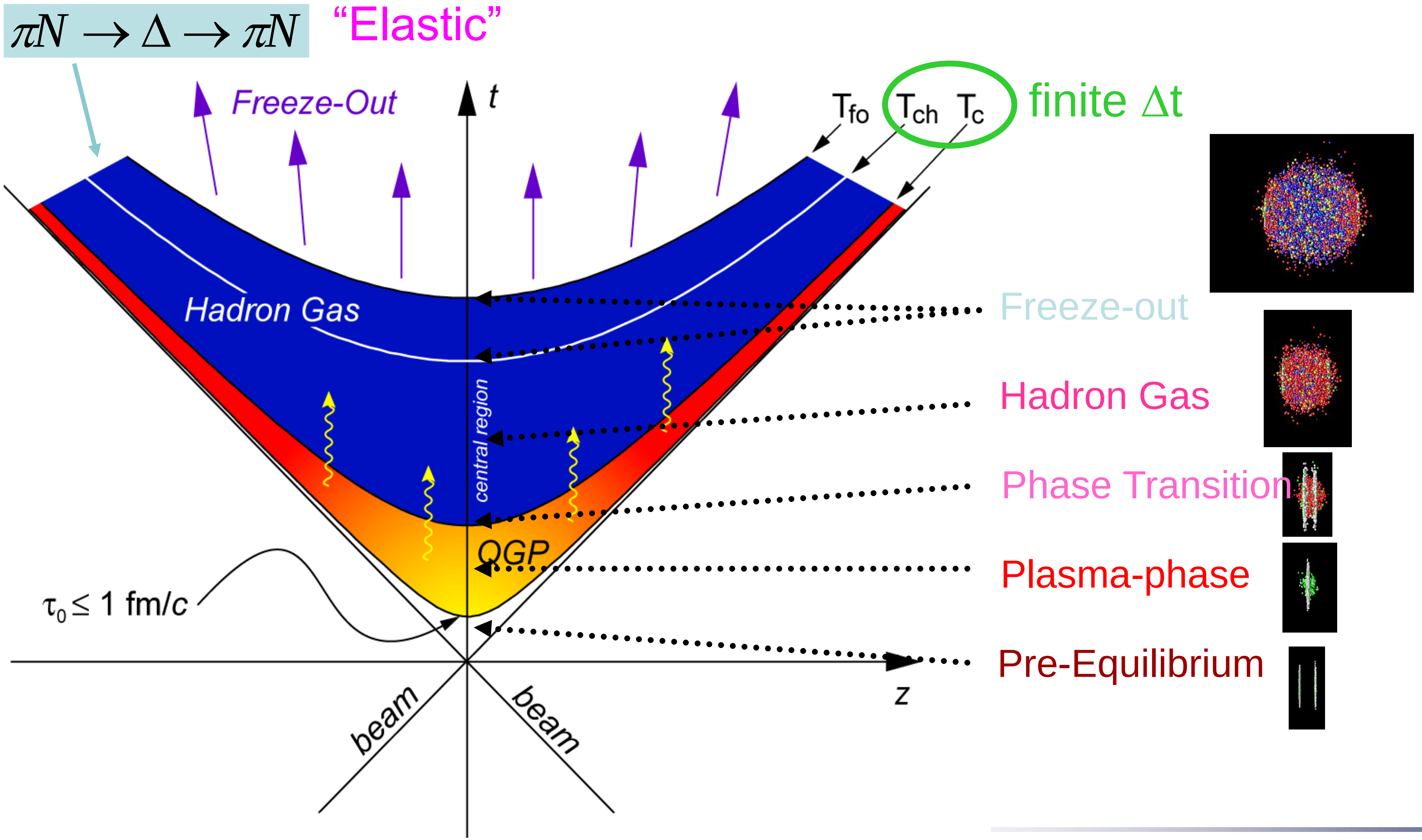
$\pi N \to \Delta \to \pi N$
"Elastic"
Freeze-Out
t
T_{fo} T_{ch} T_c
finite Δt
Hadron Gas
central region
QGP
$\tau_0 \leq 1$ fm/c
z
beam
beam
Freeze-out
Hadron Gas
Phase Transition
Plasma-phase
Pre-Equilibrium

QGP相变

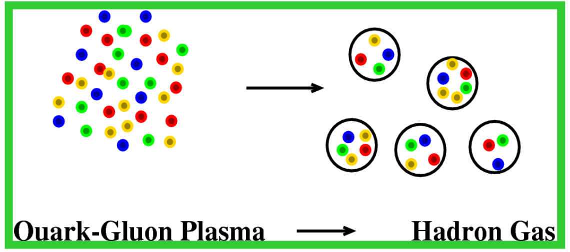

Free massless gas

$$\frac{E}{V} = \frac{g}{(2\pi)^3}\int_0^\infty d^3p\, p\, f(p) = g_{tot}\frac{\pi}{30}T^4$$

$$g_{tot} = g_g + \tfrac{7}{8}(g_q + g_{\bar{q}})$$

$$g_g = 16\ ,\ \ g_q = g_{\bar{q}} = N_c N_s N_f$$

Bag Model (cosm. cost.)

$$P_H = -\frac{\partial E_H}{\partial V} = -B + \frac{C}{4\pi R^4}$$

$$P = 0 \Leftrightarrow R_H$$

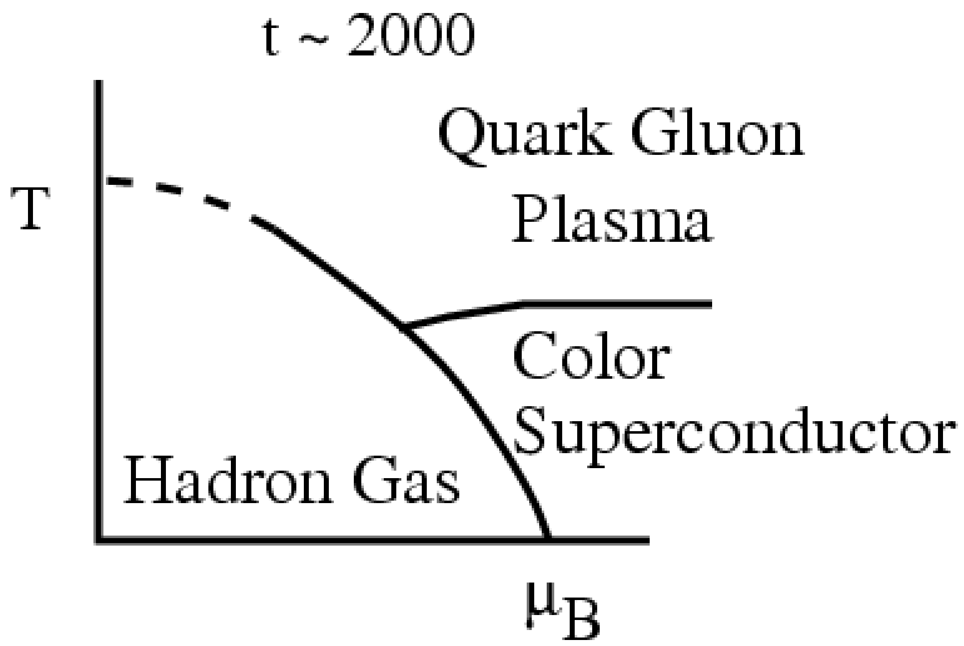

Pressure exceeds the Bag pressure -> quark liberation

$$T_c = \left(\frac{90}{37\pi^2}\right)^{1/4} B^{1/4}$$

$B^{1/4}$ ~ 210 MeV

-> T_c ~ 145 MeV

Extension to finite μ_B , μ_I

相变形式

相变的阶数

Phase transition of order n-th means the n-th derivative of the free energy F is discontinous

$$\varepsilon = \frac{F + T\frac{\partial F}{\partial T}}{V}$$

一阶 **Mixed phase**

$$C_V = \frac{\partial^2 F}{\partial T^2}$$

二阶 **Critical behavior**

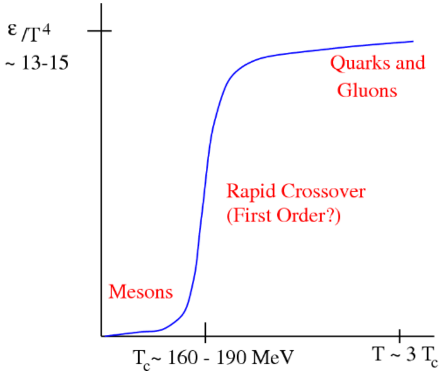

Cross over

Not a mixed phase, but a continous modification of the matter between the two phases

QCD Phase Diagram

A selection of representations of the QCD phase diagram in the (μ_B, T) plane

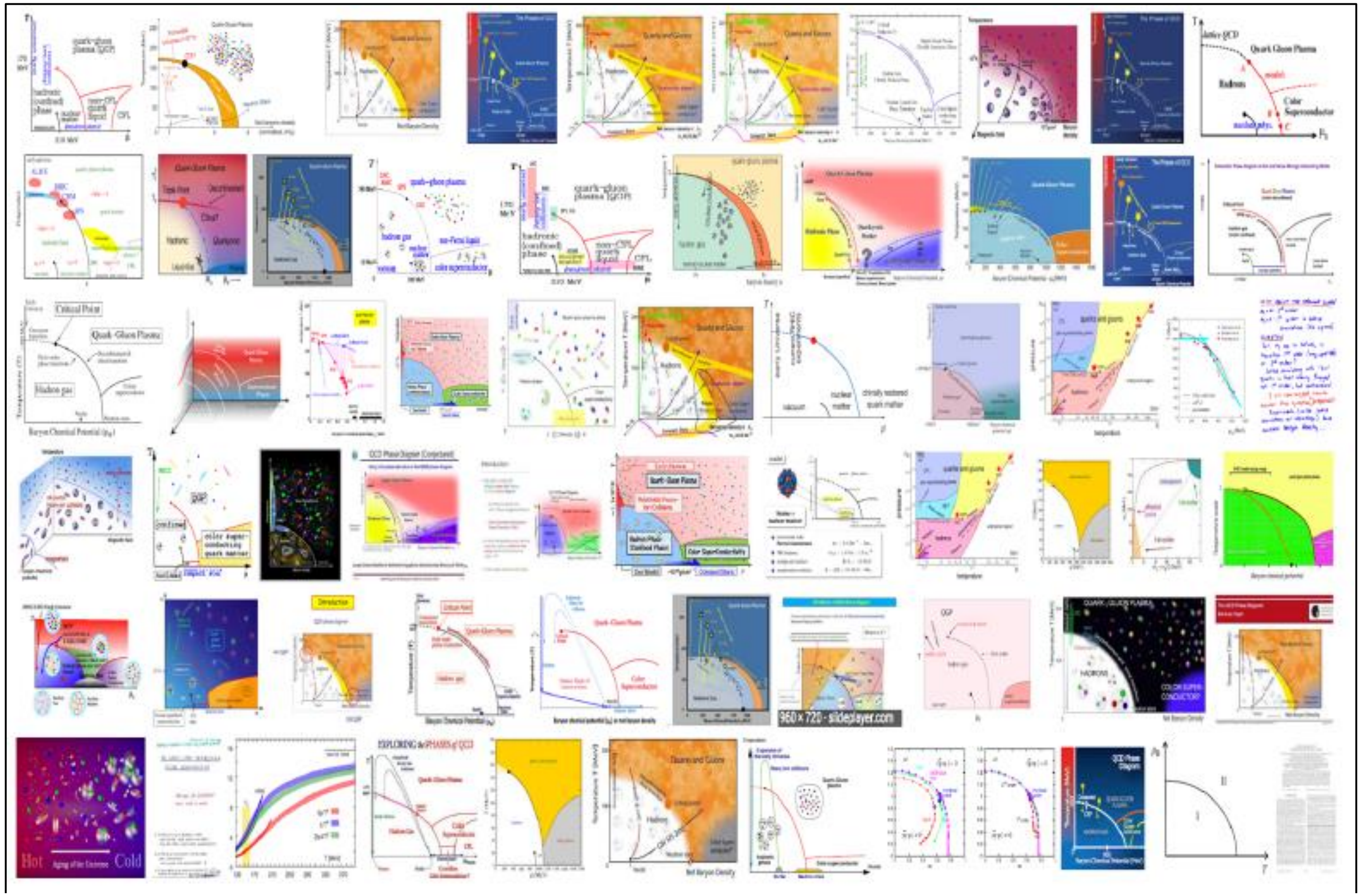

Holy Grail of Nuclear Physics

"All science is either physics or stamp collecting." --- Ernest Rutherford

"The Way Forward – Closing Remarks at Quark Matter 2017", W.A. Zajc, [arXiv:1707.01993]

CEP from Lattice and effective field theories

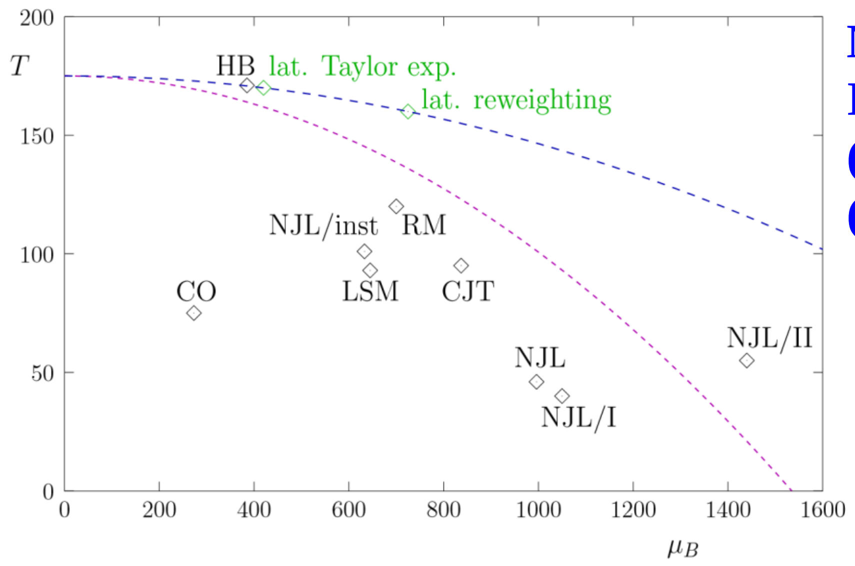

M.A. Stephanov, IJMPA20, 4387 (2005)
(Theory Review)

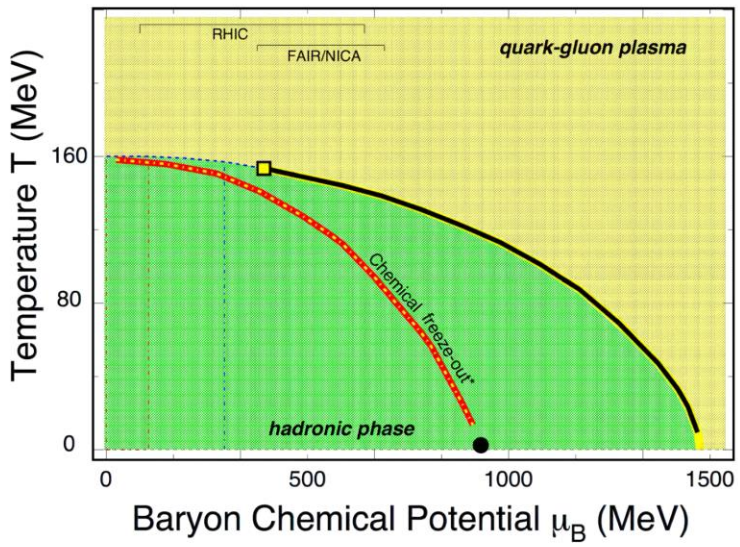

X.F. Luo and N. Xu, NST28, 112 (2017)
(Exp. Review)

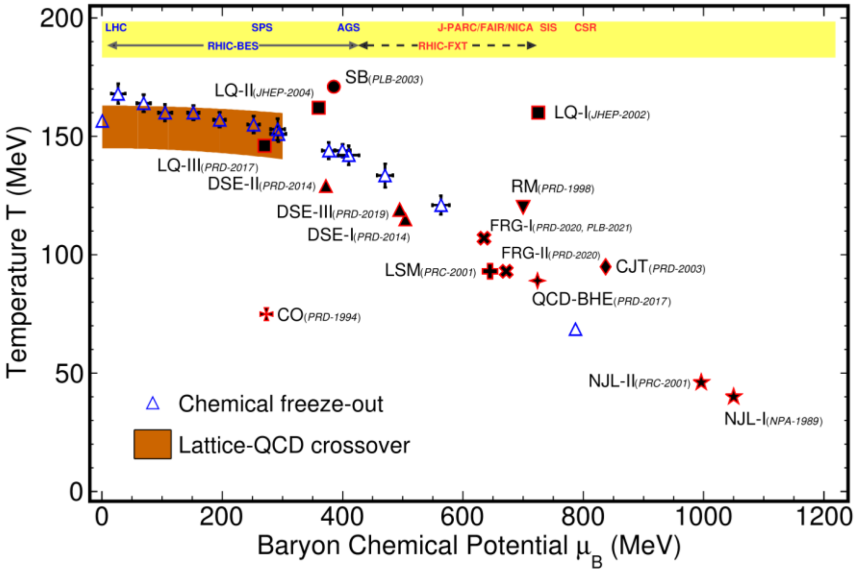

A. Pandav, D. Mallick, B. Mohanty, PPNP125, 103960 (2022)
(Exp. Review)

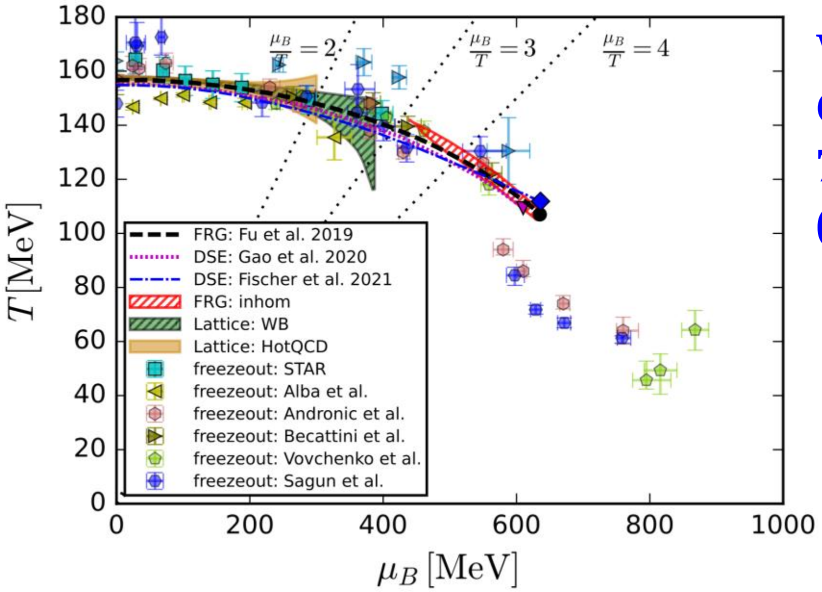

W. J. Fu, Com. Theor. Phys. 74, 097304 (2022)
(Theory Review)

QCD Phase Diagram

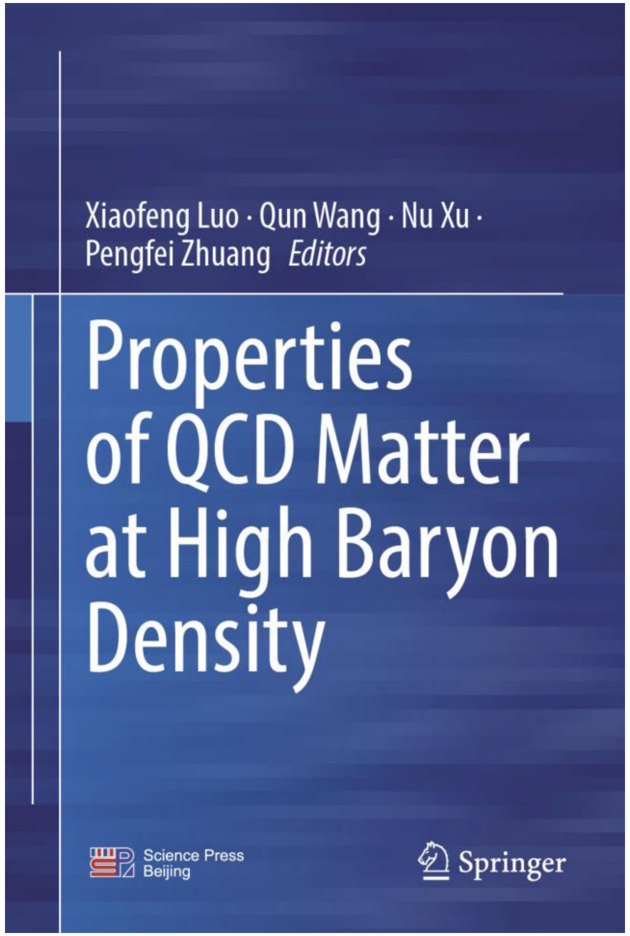

ISBN 978-981-19-4440-6 ISBN 978-981-19-4441-3 (eBook)
https://doi.org/10.1007/978-981-19-4441-3

Jointly published with Science Press
The print edition is not for sale in China mainland. Customers from China mainland please order the print book from: Science Press.

Contents

目录

- □ 致密QCD物质
- □ 致密QCD物质的状态方程:
  - ■ 对称能：核物质和夸克物质的状态方程
  - ■ 中子皮：Pb/Ca中子半径之谜
  - ■ 引力波：对称能的高密行为
- □ 致密QCD物质的相变：
  - ■ QCD相图：概述
  - ■ 重离子碰撞：粒子产生的并合模型
  - ■ 致密星：中子星、超新星、双星并合
- □总结和展望

Basic idea

Baryon density fluctuation vs light nuclei production

Baryon density fluctuation
is closely related to
the correlation between nucleons.

The correlation between nucleons
determines
the production of light nuclei

Baryon density fluctuation in vicinity
of first-order phase transition/CEP
could be deciphered from
the production of light nuclei

Cluster Production: Coalescence?

Coalescence model provides a useful approach to describe light cluster production in HIC

- **Coalescence model** provides a useful tool to describe light nuclei production in HIC
- **Coalescence model** also provides a useful tool to describe hadron production from partonic matter (hadronization)
- ……

Butler, Pearson, Sato, Yazaki, Gyulassy, Frankel, Remler, Dove, Scheibl, Heinz, Schnedermann, Mattiello, Nagle, Polleri, …
Biro, Zimanyi, Levai, Csizmadia, Hwa, Yang, Ko, Lin , Greco, Chen, Fries, Muller, Nonaka, Bass, Voloshin, Molnar, Xie, Shao, …

Parton coalescence mechanism at RHIC

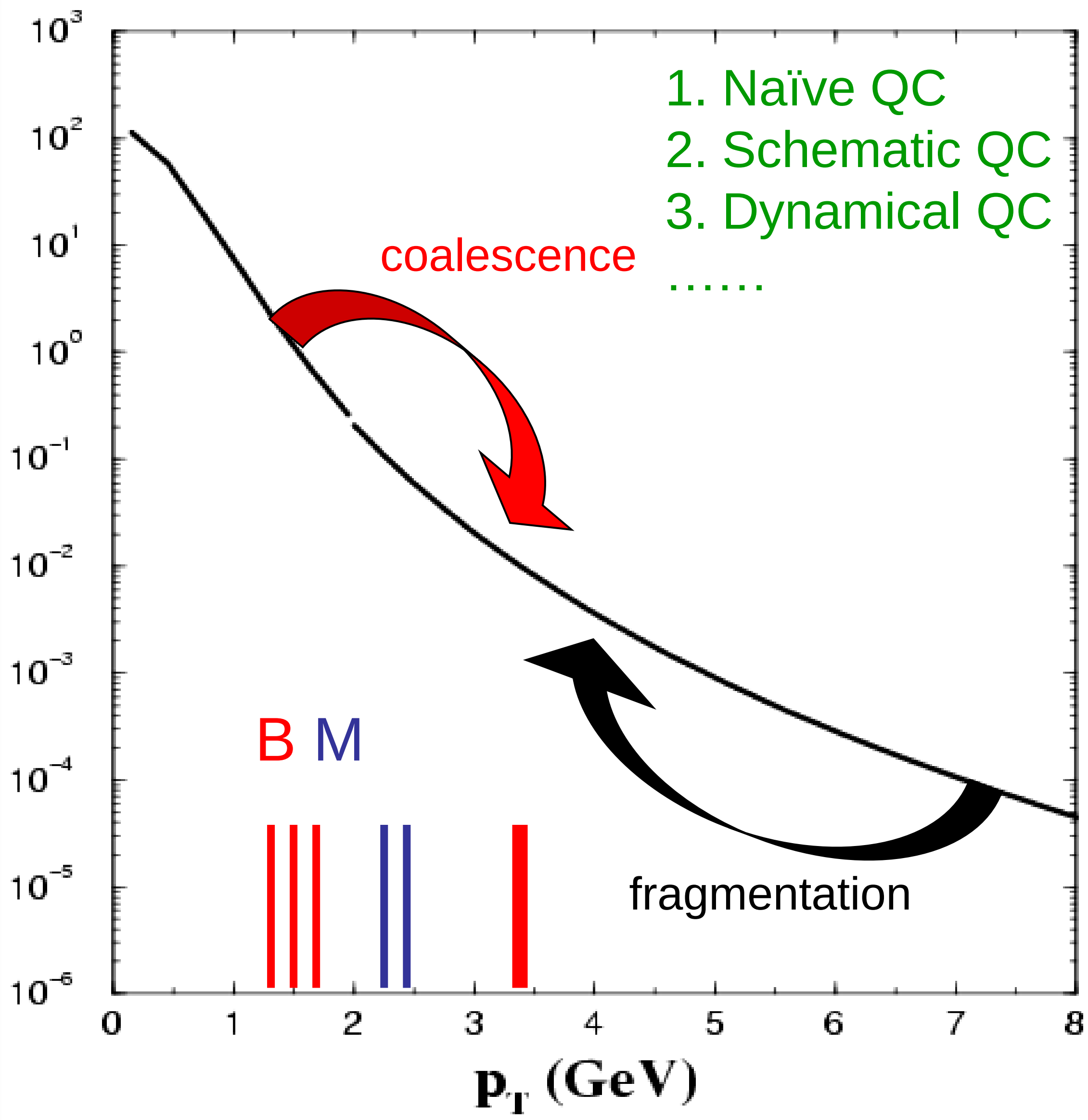

Lin/Ko
PRL89, 202302 (2002);

S.A. Voloshin,
NPA715, 379(2003);

Greco/Ko/Levai,
PRL90, 202302 (2003);

Fries/Muller/Nonaka/Bass
PRL90, 202303 (2003);

Hwa/Yang
PRC67, 034902 (2003);
064902 (2003);

Molnar/Voloshin
PRL91, 092301 (2003)

$$B(p_T) \Leftarrow 3q(p_T/3)$$

$$M(p_T) \Leftarrow 2q(p_T/2)$$

上海交通大學 SHANGHAI JIAO TONG UNIVERSITY

Deuteron production in HIC

The correlation between neutron and proton with small relative momentum and deuteron formation both appear due to the final state interaction (S. Mrowczynsky, PLB248 (1990), P. Danielewicz et al., PLB274 (1992))

The n-p pair in a scattering state with small relative momentum and deuteron (n-p pair in a bound state) should provide the same space-time information about the size of an emission source

Using stiff symmetry energy will produce more deuterons than using soft symmetry energy?

Similarly to the n-p correlation function (HBT), deuteron yield in HIC's induced by neutron-rich nuclei is also a sensitive probe of the nuclear symmetry energy!!!

n-p HBT: Chen/Greco/Ko/Li, PRL90, 162701(2003); PRC68, 014605 (2003)

Deuteron: Chen/Ko/Li, PRC68, 017601 (2003); NPA729, 809 (2003)

Analytical Coalescence Formula

Analytical coalescence formula: COAL-SH (ShangHai)

COAL-Ex
(ExHIC Collaboration)
S. Cho et al.,
PRL106, 212001 (2011)
PRC84, 064910 (2011)

$$N_c = g_{\rm rel} g_{\rm size} g_c M^{3/2} \left[\prod_{i=1}^{A} \frac{N_i}{m_i^{3/2}} \right] \times \prod_{i=1}^{A-1} \frac{(4\pi/\omega)^{3/2}}{Vx(1+x^2)} \left(\frac{x^2}{1+x^2} \right)^{l_i} G(l_i, x).$$

K. J. Sun(孙开佳)/LWC, PRC95, 044905 (2017)
(Open source on github:
https://github.com/kaijiasun/ExoticCoalescence)

$$x^2 = \frac{2T_{\rm eff}}{w} \qquad G(l,x) = \sum_{k=0}^{l} \frac{l!}{k!(l-k)!} \frac{1}{(2k+1)x^{2k}}$$

$$g_{\rm rel} \approx 1, g_{\rm size} \approx 1, l_i = 0$$

COAL-SH:
COAL-Ex +
Longitudinal dimension
+ rel. corrections
+ finite size corrections
K. J. Sun(孙开佳)/LWC,
PRC95, 044905 (2017)

$$N_{\rm d} = g_{\rm d} \frac{(m_n+m_p)^{3/2}}{m_p^{3/2} m_n^{3/2}} \frac{N_p N_n}{V} \frac{(4\pi/\omega_{\rm d})^{3/2}}{x_{\rm d}(1+x_{\rm d}^2)},$$

$$N_{^3{\rm H}} = g_{^3{\rm H}} \frac{(2m_n+m_p)^{3/2}}{m_p^{3/2} m_n^3} \frac{N_p N_n^2}{V^2} \frac{(4\pi/\omega_{^3{\rm H}})^3}{x_{^3{\rm H}}^2(1+x_{^3{\rm H}}^2)^2},$$

$$w_d = 8.1 \text{ MeV}$$
$$w_{^3{\rm H}} = 13.4 \text{ MeV}$$
$$x_d \gg 1, x_{^3{\rm H}} \gg 1$$

$$N_{\rm d} = \frac{3}{2^{1/2}} \left(\frac{2\pi}{m_0 T_{\rm eff}} \right)^{3/2} \frac{N_p N_n}{V},$$

$$N_{^3{\rm H}} = \frac{3^{3/2}}{4} \left(\frac{2\pi}{m_0 T_{\rm eff}} \right)^{3} \frac{N_p N_n^2}{V^2}.$$

$$m_n = m_p = m_0$$

Cluster Yields w/o density fluctuation

$$N_{\mathrm{d}} = \frac{3}{2^{1/2}}\left(\frac{2\pi}{m_0 T_{\mathrm{eff}}}\right)^{3/2}\frac{N_p N_n}{V},$$
$$N_{^3\mathrm{H}} = \frac{3^{3/2}}{4}\left(\frac{2\pi}{m_0 T_{\mathrm{eff}}}\right)^{3}\frac{N_p N_n^2}{V^2}.$$

The above equations are consistent with conventional thermal model:

$$N^{\mathrm{th}} = \frac{gV}{(2\pi)^3}4\pi T m^2 K_2\left(\frac{m}{T}\right)\mathrm{e}^{\frac{\mu}{T}}$$

$$T = T_{\mathrm{eff}}$$

$$N_p^{\mathrm{th}} = \frac{g_p V}{(2\pi)^3}(2\pi m_0 T)^{\frac{3}{2}}\mathrm{e}^{\frac{\mu_p - m_0}{T}},$$
$$N_d^{\mathrm{th}} = \frac{g_d V}{(2\pi)^3}(4\pi m_0 T)^{\frac{3}{2}}\mathrm{e}^{\frac{2\mu_p - 2m_0}{T}},$$
$$N_{^3\mathrm{He}}^{\mathrm{th}} = \frac{g_{^3\mathrm{He}} V}{(2\pi)^3}(6\pi m_0 T)^{\frac{3}{2}}\mathrm{e}^{\frac{3\mu_p - 3m_0}{T}},$$

K_2 is the modified Bessel function

$$K_\nu(x) \to \sqrt{\frac{\pi}{2x}}e^{-x}\left(1 + \frac{4\nu^2 - 1}{8x} + \mathcal{O}\left(\frac{1}{x^2}\right)\right)$$

K. J. Sun(孙开佳), LWC, C.M. Ko, and Z. Xu, PLB774, 103 (2017) [arXiv:1702.07620 (2017)]

SHANGHAI JIAO TONG UNIVERSITY 上海交通大学

Cluster Yields with density fluctuation

Density fluctuation over space:

Neutron: $\rho_n(\mathbf{x}) = \frac{1}{V}\int \rho_n(\mathbf{x})d^3\mathbf{x} + \delta\rho_n(\mathbf{x}) = \langle\rho_n\rangle + \delta\rho_n(\mathbf{x})$ $\quad \langle\delta\rho_n\rangle = 0$

Proton: $\rho_p(\mathbf{x}) = \frac{1}{V}\int \rho_p(\mathbf{x})d^3\mathbf{x} + \delta\rho_p(\mathbf{x}) = \langle\rho_p\rangle + \delta\rho_p(\mathbf{x})$ $\quad \langle\delta\rho_p\rangle = 0$

$$N_d \approx \frac{3}{2^{1/2}}\left(\frac{2\pi}{mT}\right)^{3/2}\int d^3\mathbf{x}\,\rho_n(\mathbf{x})\rho_p(\mathbf{x})$$

$$\boxed{N_d \approx \frac{3}{2^{1/2}}\left(\frac{2\pi}{mT}\right)^{3/2} N_p\langle\rho_n\rangle(1+C_{np})}$$

d yield ~ Cnp

$$N_{^3H} \approx \frac{3^{3/2}}{4}\left(\frac{2\pi}{mT}\right)^{3}\int d^3\mathbf{x}\,\rho_n^2(\mathbf{x})\rho_p(\mathbf{x})$$

$$\boxed{N_{^3H} \approx \frac{3^{3/2}}{4}\left(\frac{2\pi}{mT}\right)^{3} N_p\langle\rho_n\rangle^2(1+\Delta\rho_n+2C_{np})}$$

^{3}H yield ~ the relative den. Fluc. +Cnp!

n and p density correlation function: $C_{np} = \langle\delta\rho_n\delta\rho_p\rangle/(\langle\rho_n\rangle\langle\rho_p\rangle)$

n relative density fluctuation: $\Delta\rho_n = \langle(\delta\rho_n)^2\rangle/\langle\rho_n\rangle^2$

Isospin relative density fluctuation: $\Delta\rho_I = \frac{\langle(\delta\rho_n - \delta\rho_p)^2\rangle}{(\langle\rho_n\rangle + \langle\rho_p\rangle)^2} = \frac{R_{np}^2\Delta\rho_p - 2R_{np}C_{np} + \Delta\rho_n}{(1+R_{np})^2}$

$R_{np} = N_p/N_n = \langle\rho_p\rangle/\langle\rho_n\rangle$

K. J. Sun(孙开佳), LWC, C.M. Ko, J. Pu(普洁), and Z. Xu, PLB781, 499(2018) [arXiv:1801.09382]

Cluster Yields with density fluctuation

K. J. Sun(孙开佳), LWC, C.M. Ko, J. Pu(普洁), and Z. Xu, PLB781, 499(2018) [arXiv:1801.09382]

$$\boxed{\begin{aligned} C_{np} &\approx g_{\text{p-d}} R_{np} V_{ph} \mathcal{O}_{\text{p-d}} - 1, \\ \Delta\rho_n &\approx g_{\text{p-d-t}} (1 + C_{np})^2 \mathcal{O}_{\text{p-d-t}} - 2C_{np} - 1 \end{aligned}}$$

$$g_{\text{p-d}} = \frac{2^{1/2}}{3(2\pi)^3}$$

$$g_{\text{p-d-t}} = 9/4 \times (4/3)^{3/2}$$

$$R_{np} = N_p/N_n = \langle\rho_p\rangle/\langle\rho_n\rangle \qquad N_p/N_n = (\pi^+/\pi^-)^{1/2}$$

$$\mathcal{O}_{\text{p-d}} = N_d/N_p^2 \qquad \mathcal{O}_{\text{p-d-t}} = N_p N_{^3H}/N_d^2$$

Assuming $C_{np} = \langle\delta\rho_n\delta\rho_p\rangle/(\langle\rho_n\rangle\langle\rho_p\rangle)$ **is much less than 1 leads to very simple relation:**

$$\boxed{\mathcal{O}_{\text{p-d-t}} \approx g(1 + \Delta n)}$$

$$\Delta n = \langle(\delta n)^2\rangle/\langle n\rangle^2$$

$$g = 4/9 \times (3/4)^{3/2} \approx 0.29.$$

Cluster Yields with density fluctuation correlation length

K. J. Sun(孙开佳), C.M. Ko, and F. Li(李峰), PLB816, 136258(2021) [arXiv:2008.0225]

$$C_2(x_1-x_2) \approx \lambda\langle\rho_n\rangle\langle\rho_p\rangle \frac{e^{-|x_1-x_2|/\xi}}{|x_1-x_2|^{1+\eta}} \quad \text{(singular part only)}$$

with $\boldsymbol{\xi}$ being the density − density correlation length

$$0 < \langle\delta N^2\rangle \sim \int dx C_2(x) \sim \lambda\xi^2 \to \lambda > 0$$

$$N_d = \frac{3}{\sqrt{2}}\left(\frac{2\pi}{mT}\right)^{\frac{3}{2}} N_p\langle\rho_n\rangle\left[1 + C_{np} + \frac{\lambda}{\sigma_d} G\left(\frac{\xi}{\sigma_d}\right)\right]$$

$$N_t = \frac{3^{3/2}}{4}\left(\frac{2\pi}{mT}\right)^3 N_p\langle\rho_n\rangle^2\left[1 + 2C_{np} + \Delta\rho_n + \frac{3\lambda}{\sigma_t} G\left(\frac{\xi}{\sigma_t}\right) + O(G^2)\right]$$

$$C_{\rm np} = \langle\delta\rho_{\rm n}(\mathbf{x})\delta\rho_{\rm p}(\mathbf{x})\rangle/(\langle\rho_{\rm n}\rangle\langle\rho_{\rm p}\rangle) \quad C_2(\mathbf{x}_1,\mathbf{x}_2) \approx \lambda\langle\rho_n\rangle\langle\rho_p\rangle \frac{e^{-|\mathbf{x}_1-\mathbf{x}_2|/\xi}}{|\mathbf{x}_1-\mathbf{x}_2|^{1+\eta}}$$

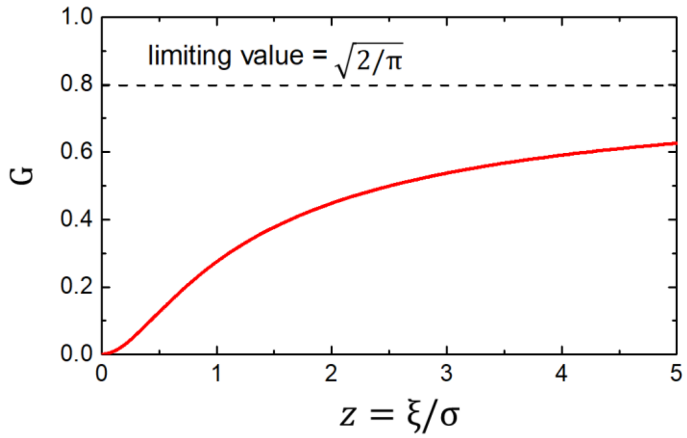

Pre-factors are thermal yields w/o density fluc./corr.

Ratio: $\boxed{\frac{N_t N_p}{N_d^2} \approx \frac{1}{2\sqrt{3}}\left[1 + \Delta\rho_n + \frac{\lambda}{\sigma} G\left(\frac{\xi}{\sigma}\right)\right]}$, $\frac{3\ pairs}{2\ pairs} \sim 1\ pair,\ \sigma \approx 2$ fm

Peak structure and CEP

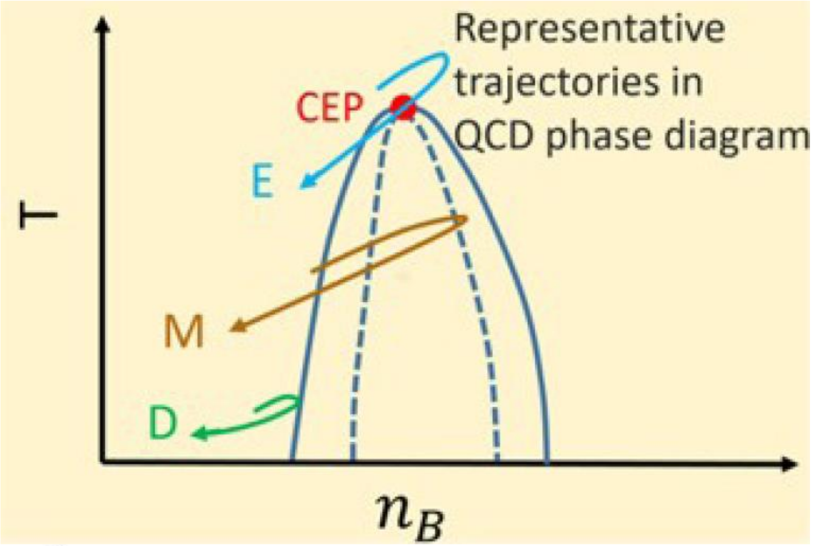

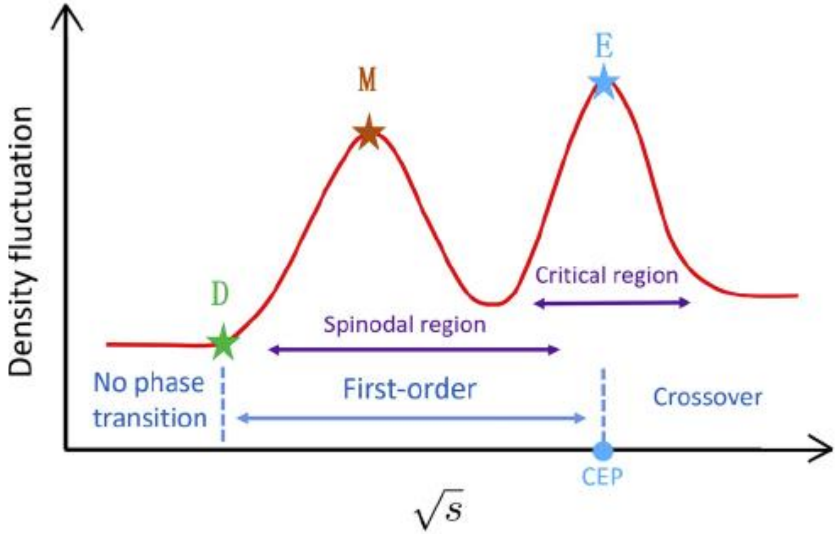

K. J. Sun(孙开佳), LWC, C.M. Ko, J. Pu(普洁), and Z. Xu, PLB781, 499(2018) [arXiv:1801.09382]

K. Huang, Intro. Stat. Phys (p.58)

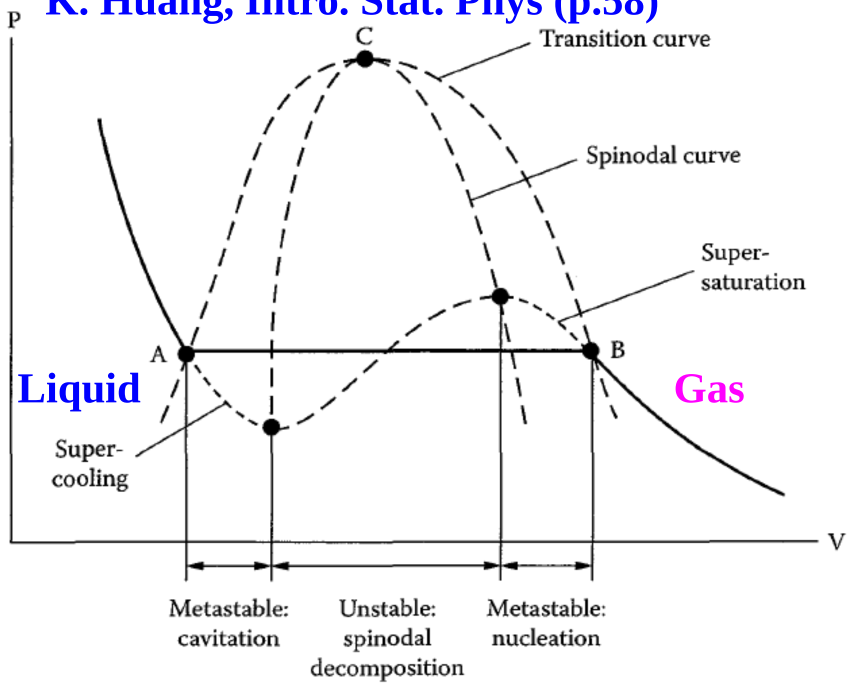

$$(\Delta M)^2 \propto N(V) \int d\mathbf{r}\, G(r) \propto N(V)\xi^2(t)$$

Fluc. Corr. Func. Corr. Length

Critical point: Largest density fluctuation (e.g., critical opalescence,《相变和临界现象》-于渌，郝柏林

First-order phase transition: Large density fluctuations due to spinodal instability (but take time to build)

Steinheimer/Randrup/Koch(12,14); Herold et al.(14); Li/Ko (16)

Circumstantial evidence of peak structure?

Yields dN/dy of p, d and ^{3}H at midrapidity, together with the yield ratio π^+/π^- measured in central Pb+Pb collisions at 20 AGeV ($0-7\%$ centrality, $\sqrt{s_{NN}}=6.3$ GeV), 30 AGeV ($0-7\%$ centrality, $\sqrt{s_{NN}}=7.6$ GeV), 40 AGeV ($0-7\%$ centrality, $\sqrt{s_{NN}}=8.8$ GeV), 80 AGeV ($0-7\%$ centrality, $\sqrt{s_{NN}}=12.3$ GeV), and 158 AGeV ($0-12\%$ centrality, $\sqrt{s_{NN}}=17.3$ GeV) by the NA49 Collaboration [31,41,42]. Also given are the chemical freeze-out temperature T_{ch} (GeV) and volume V_{ch} (fm^3), the derived yield ratios $\mathcal{O}_{p\text{-}d}$ and $\mathcal{O}_{p\text{-}d\text{-}t}$, and the extracted C_{np}, $\Delta\rho_n$ and $\Delta\rho_l$. In obtaining $\mathcal{O}_{p\text{-}d}$ and $\mathcal{O}_{p\text{-}d\text{-}t}$, the weak decay contributions to the yield of proton from hyperons are corrected by using results from the statistical model (see text for details).

$\sqrt{s_{NN}}$	p	d	^{3}H(10^{-3})	π^+/π^-	T_{ch}	V_{ch}	$\mathcal{O}_{p\text{-}d}(10^{-4})$	$\mathcal{O}_{p\text{-}d\text{-}t}$	C_{np}	$\Delta\rho_n$	$\Delta\rho_l$
6.3	46.1 ± 2.1	2.094 ± 0.168	$43.7(\pm6.4)$	0.86	0.131	1389	10.5 ± 0.11	0.444 ± 0.014	-0.636 ± 0.004	0.475 ± 0.007	0.556 ± 0.004
7.6	42.1 ± 2.0	1.379 ± 0.111	$22.3(\pm3.4)$	0.88	0.139	1212	8.78 ± 0.13	0.465 ± 0.019	-0.707 ± 0.004	0.551 ± 0.007	0.629 ± 0.004
8.8	41.3 ± 1.1	1.065 ± 0.086	$14.8(\pm2.6)$	0.90	0.144	1166	7.32 ± 0.20	0.500 ± 0.020	-0.749 ± 0.007	0.606 ± 0.045	0.677 ± 0.006
12.3	30.1 ± 1.0	0.543 ± 0.044	$4.49(\pm0.94)$	0.91	0.153	1231	7.70 ± 0.11	0.404 ± 0.034	-0.693 ± 0.004	0.518 ± 0.012	0.605 ± 0.006
17.3	23.9 ± 1.0	0.279 ± 0.023	$1.58(\pm0.31)$	0.93	0.159	1389	6.66 ± 0.01	0.415 ± 0.032	-0.681 ± 0.0004	0.507 ± 0.011	0.594 ± 0.006

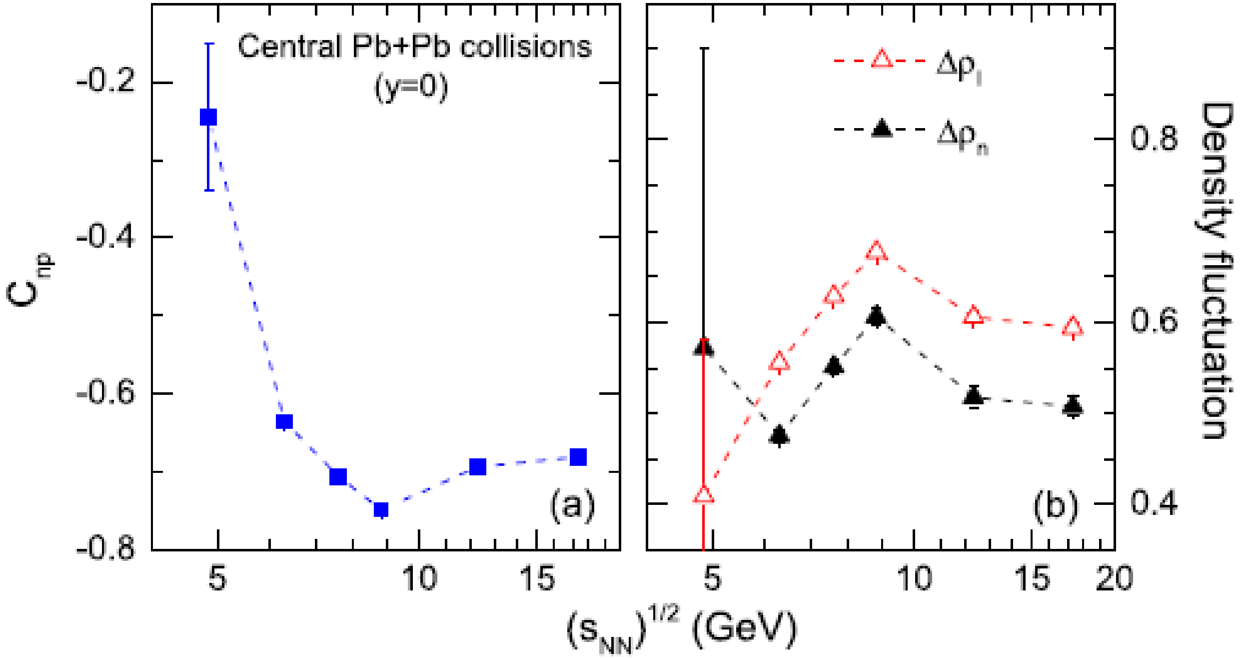

From NA49 Collaboration

T. Anticic et al. (NA49 Collaboration), Phys. Rev. C 94, 044906 (2016).

For $\Delta\rho_n$:

- A peak is observed at 8.8 GeV;
- There is another possible peak below 6.3 GeV

K. J. Sun(孙开佳), LWC, C.M. Ko, J. Pu(普洁), and Z. Xu, PLB781, 499(2018) [arXiv:1801.09382]

Energy dependence of tp/d^2

Dingwei Zhang(CCNU)for STAR Collaboration, QM2019

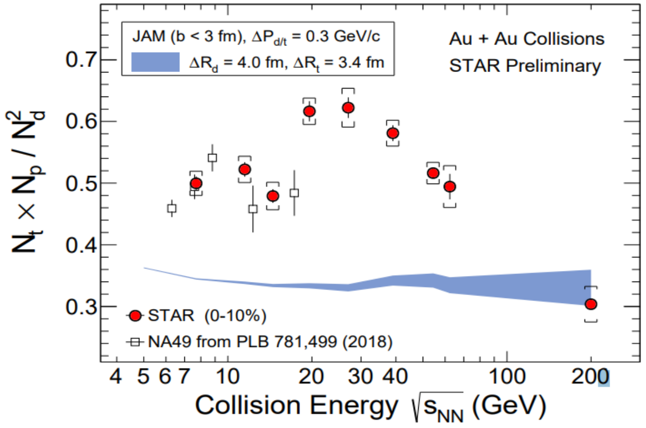

Model calculations without the inclusion of a first-order or second-order phase transition, e.g., JAM+COAL, AMPT+COAL, MUSIC+COAL, UrQMD+COAL, and SHM, all give flat energy dependence

W. Zhao et al., arXiv:2009. 06959(2020)
D. Zhang (STAR), arXiv:2002.10677(2020)
H. Liu et al., Phys. Lett. B805, 135452 (2020)
V.Vovchenko et al., arXiv:2004.04411(2020)
K. J. Sun and C. M. Ko, arXiv:2005.00182(2020)

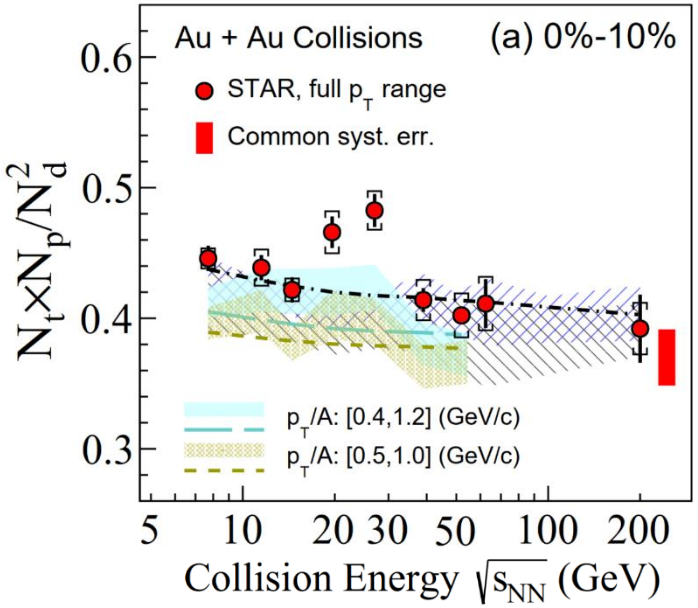

STAR: PRL130, 202301 (2023)

A clear peak has been observed around 20-30 Ge in STAR data!

Centrality dependence of tp/d^2 w/o 1st-order PT

This ratio increases in peripheral collisions due to the effects of finite nuclei sizes

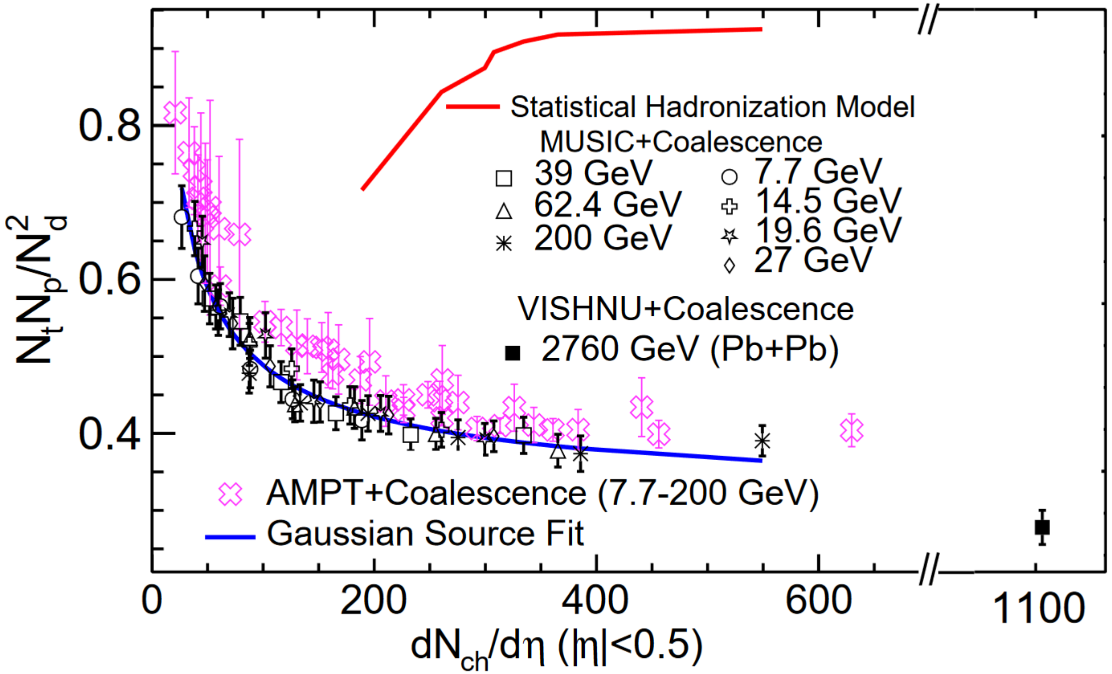

Gaussian source:

$$\frac{N_t N_p}{N_d^2} = \frac{4}{9}\left(\frac{1+\frac{2r_d^2}{3R^2}}{1+\frac{r_t^2}{2R^2}}\right)^3 = \frac{4}{9}\left(1+\frac{\frac{4}{3}r_d^2 - r_t^2}{2R^2+r_t^2}\right)^3$$

W.B. Zhao, K. J. Sun, C. M. Ko, and X. F. Luo, PLB820 (2021) 136571

S. Wu, K. Murase, S. Tang, and H. Song, arXiv:2205. 14302(2022)

1st-order PT effects on tp/d^2

The eNJL provides a flexible equation of state (EoS) . The critical temperature can be easily changed by varying the strength of the scalar-vector interaction without affecting the vacuum properties.

Lagrangian density for eNJL:

$$
\begin{aligned}
\mathcal{L} &= \bar{\psi}(i\gamma^\mu\partial_\mu - \hat{m})\psi + G_S \sum_{a=0}^{8}[(\bar{\psi}\lambda^a\psi)^2 + (\bar{\psi}i\gamma_5\lambda^a\psi)^2] \\
&- K\{[\det[\bar{\psi}(1+\gamma_5)\psi] + \det[\bar{\psi}(1-\gamma_5)\psi]\} \\
&+ \boxed{G_{SV}\left\{\sum_{a=1}^{3}[(\bar{\psi}\lambda^a\psi)^2 + (\bar{\psi}i\gamma_5\lambda^a\psi)^2]\right\} \times \left\{\sum_{a=1}^{3}[(\bar{\psi}\gamma^\mu\lambda^a\psi)^2 + (\bar{\psi}\gamma_5\gamma^\mu\lambda^a\psi)^2]\right\}}, \qquad (1)
\end{aligned}
$$

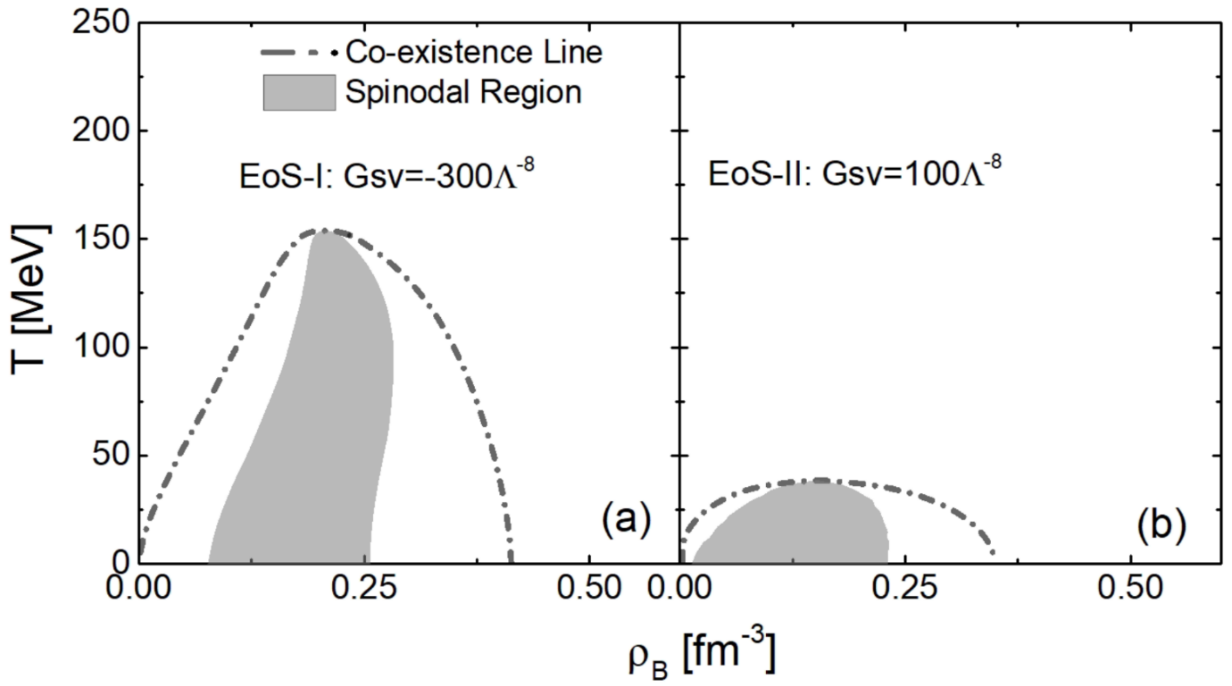

K. J. Sun(孙开佳), C. M. Ko, S. Cao, and F. Li(李峰), Phys. Rev. D 103, 014006 (2021)

1st-order PT effects on tp/d^2

Spinodal instability

$$\left(\frac{\partial p}{\partial \rho}\right)_T < 0$$

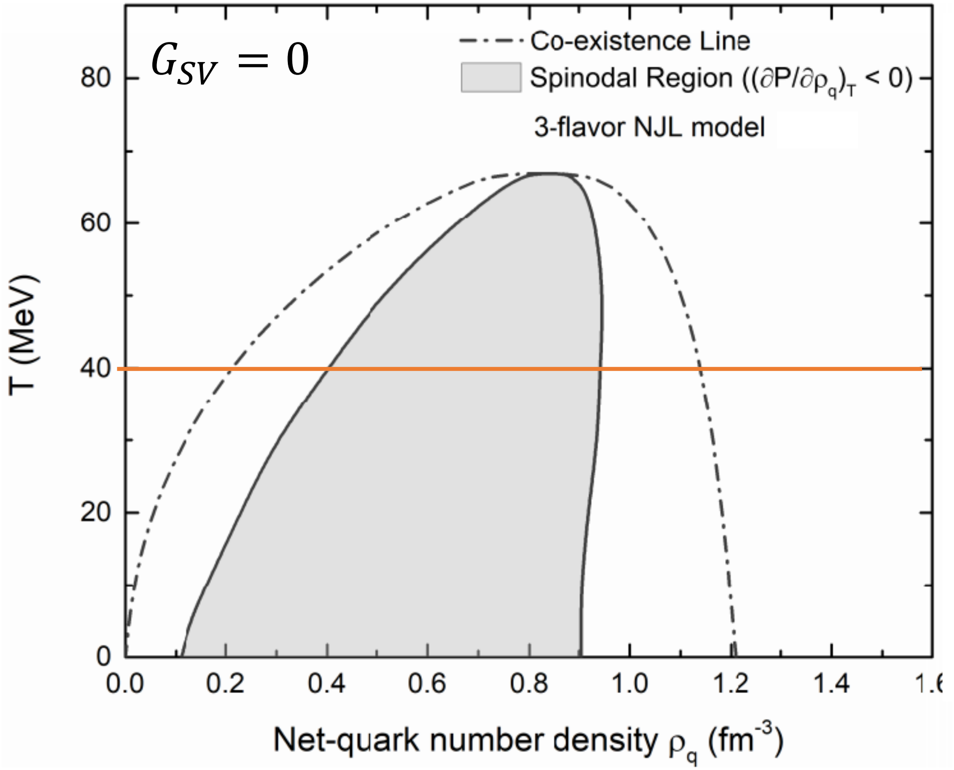

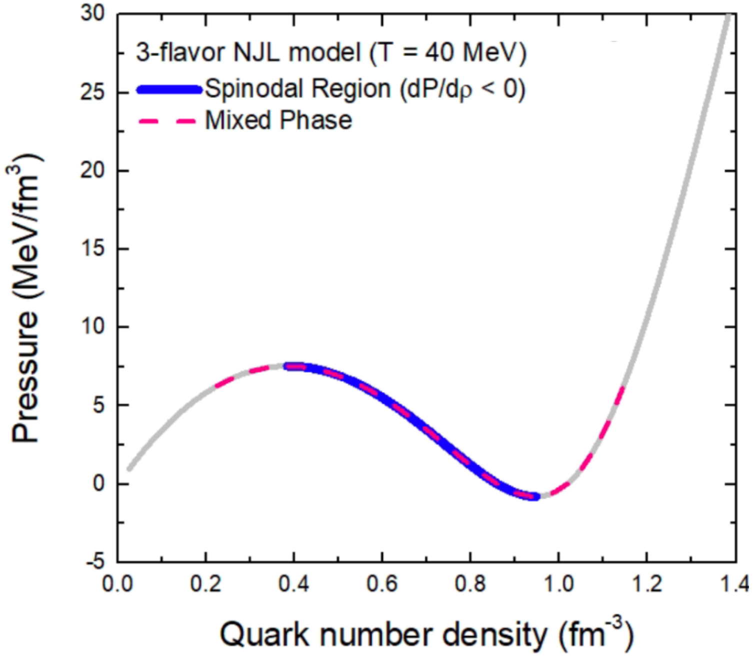

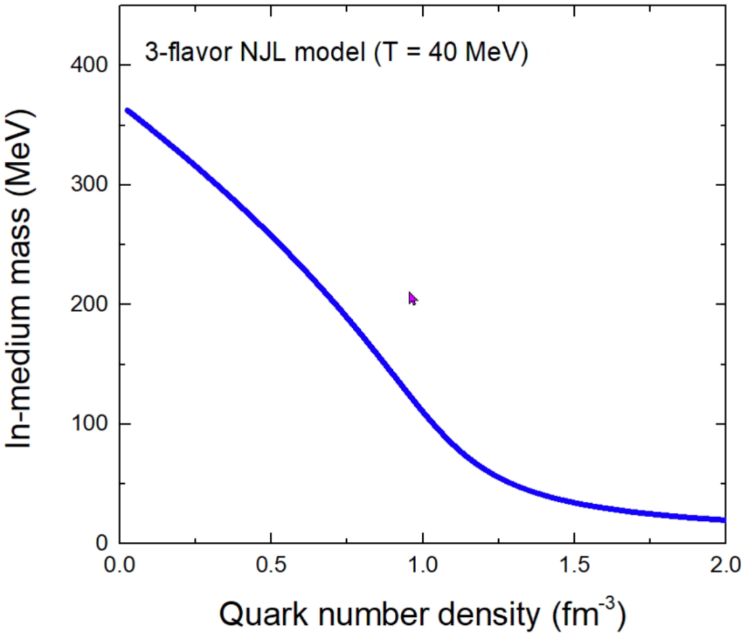

Spinodal instability **First-Order Chiral PT**

K. J. Sun(孙开佳), C. M. Ko, S. Cao, and F. Li(李峰), Phys. Rev. D 103, 014006 (2021)

First-order phase transition and baryon density fluctuation

Transport Model + NJL

With first-order phase transition

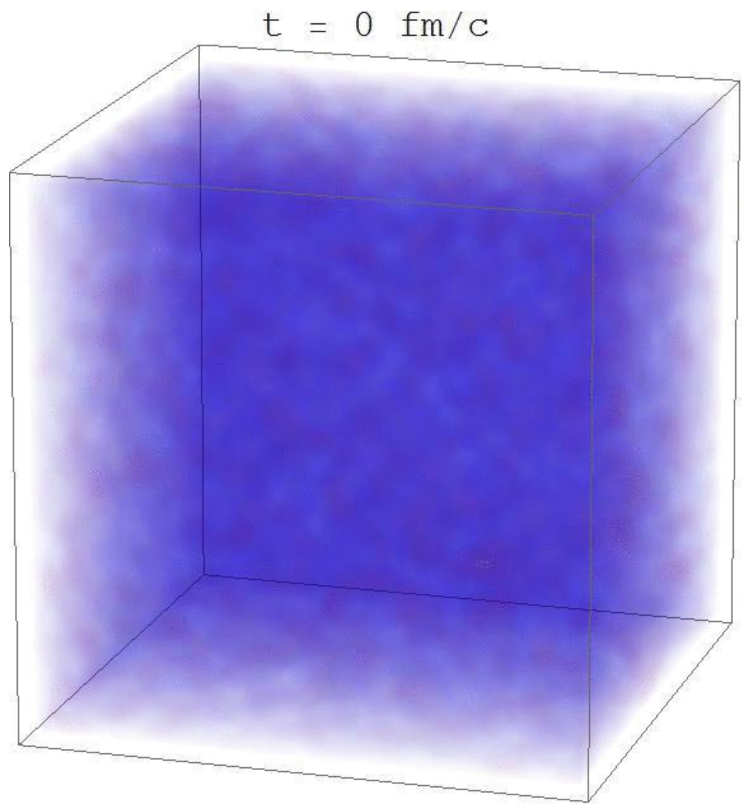

No first-order phase transition

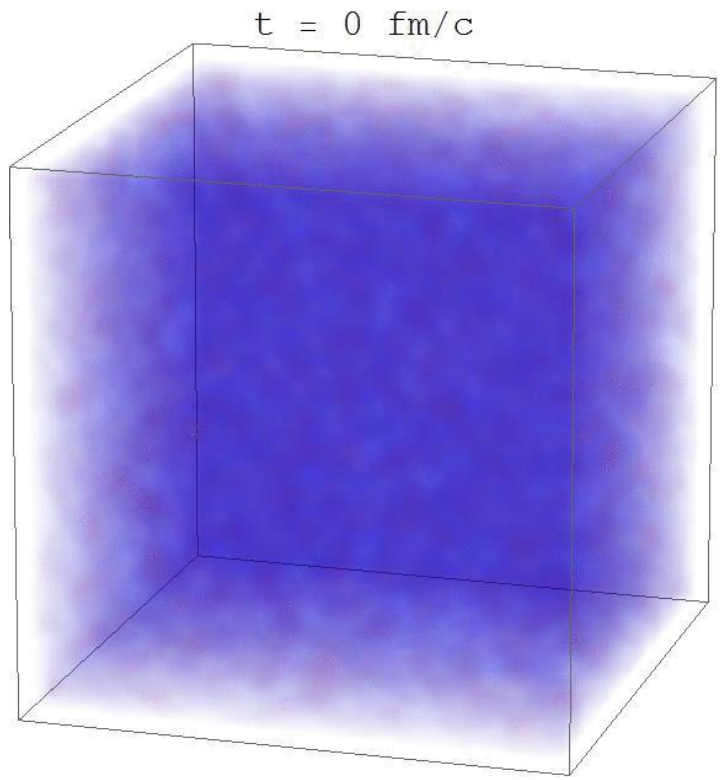

Taken from Feng Li(李峰)'s talk at Shanghai, 01/2017

F. Li(李峰) and C.M. Ko, Phys. Rev. C 93, 035205 (2016).

1st-order PT effects on tp/d^2

Dynamical Transport model

K. J. Sun(孙开佳), W. H. Zhou(周文豪), LWC, C. M. Ko, F. Li(李峰), and R. Wang(王睿), and J. Xu(徐骏), arXiv:2205.11010(2022)

Initialization

↓

Parton evolution
Mean field (eNJL) + scattering

Exhibits dynamical chiral phase transition

↓ *Hadronization: Quark coalescence*

ART(A Relativistic Transport model for hadrons)

↓ *Nucleon coalescence*

Light nuclei

1^{st}-order PT effects on tp/d^2

Trajectories in the phase diagram

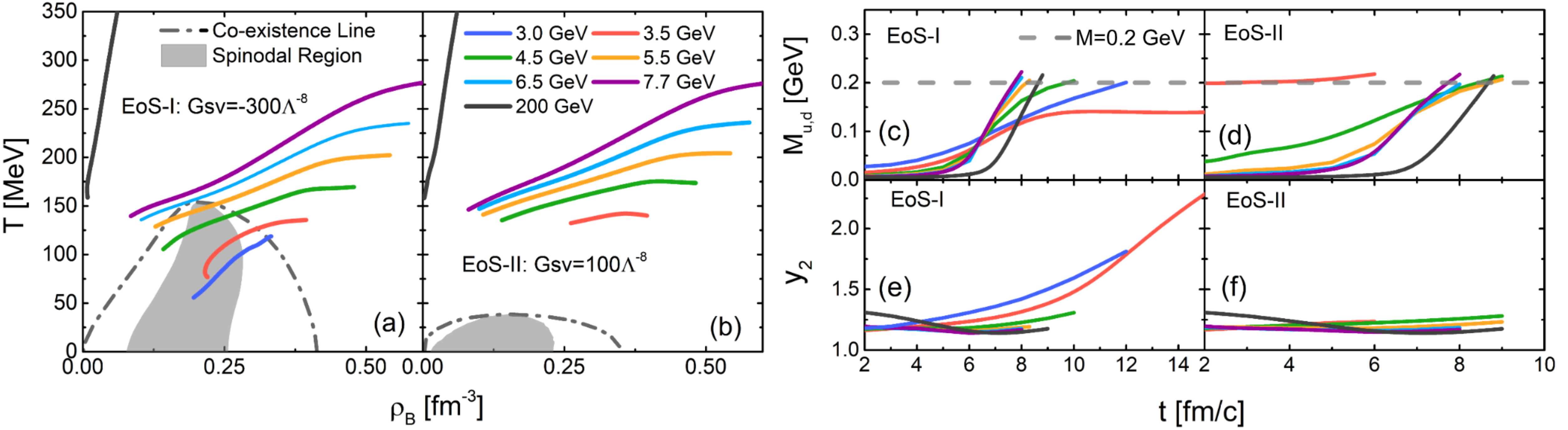

$$\overline{\rho^N} = \frac{\int d\mathbf{x}\rho^{(N+1)}(\mathbf{x})}{\int d\mathbf{x}\rho(\mathbf{x})} \qquad y_2 = \frac{[\int d\mathbf{x}\rho(\mathbf{x})][\int d\mathbf{x}\rho^{3}(\mathbf{x})]}{[\int d\mathbf{x}\rho^{2}(\mathbf{x})]^{2}}$$

K. J. Sun(孙开佳), W. H. Zhou(周文豪), LWC, C. M. Ko, F. Li(李峰), and R. Wang(王睿), and J. Xu(徐骏), arXiv:2205.11010(2022)

1st-order PT effects on tp/d^2

Survival of density fluctuation in expanding fireball

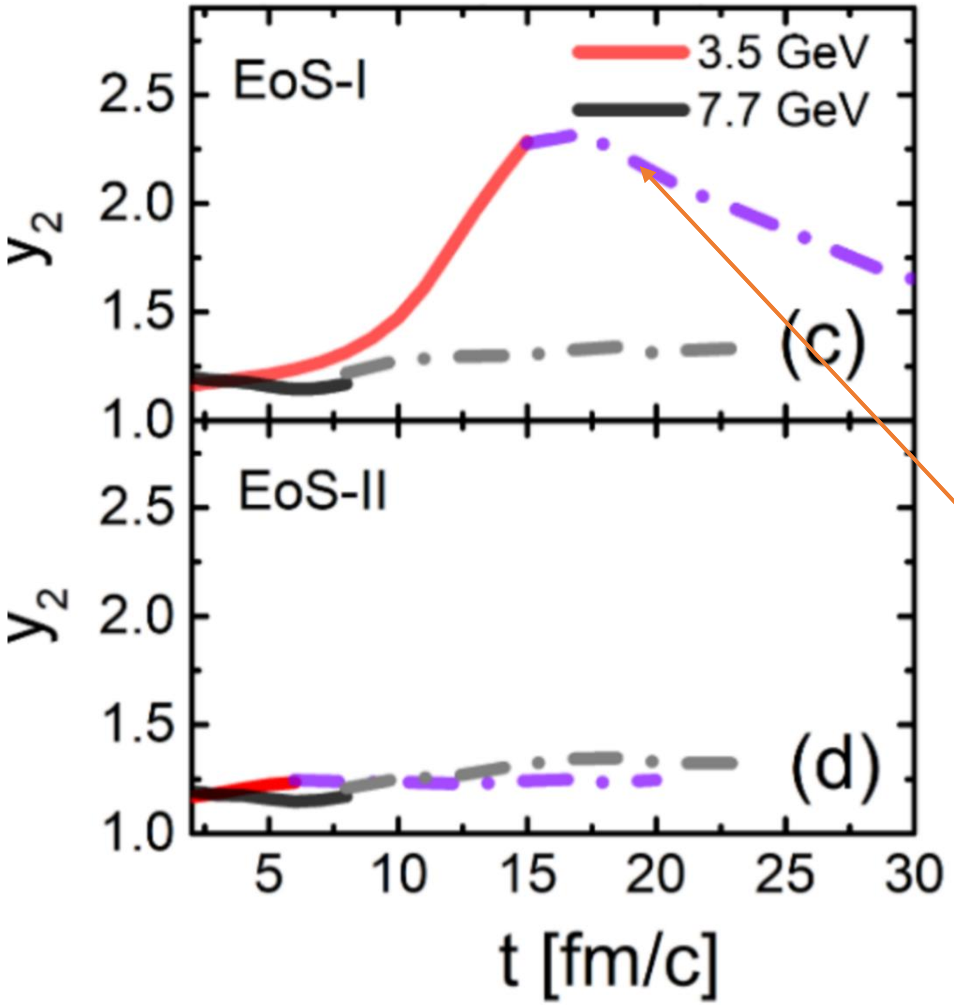

Density moment:

$$\overline{\rho^N} = \frac{\int d\mathbf{x}\rho^{(N+1)}(\mathbf{x})}{\int d\mathbf{x}\rho(\mathbf{x})}$$

$$y_2 = \frac{[\int d\mathbf{x}\rho(\mathbf{x})][\int d\mathbf{x}\rho^3(\mathbf{x})]}{[\int d\mathbf{x}\rho^2(\mathbf{x})]^2}$$

If the expansion is self-similar or scale invariant

$$\rho(\lambda(t)x, t) = \alpha(t)\rho(x, t_h)$$

then $y_2(t) = y_2(t_h)$, i.e., remains a constant

'Memory effects': Large density inhomogeneity survives to kinetic freezeout

Energy dependence of tp/d^2 with 1st-order PT

K. J. Sun(孙开佳), W. H. Zhou(周文豪), LWC, C. M. Ko, F. Li(李峰), and R. Wang(王睿), and J. Xu(徐骏), arXiv:2205.11010(2022)

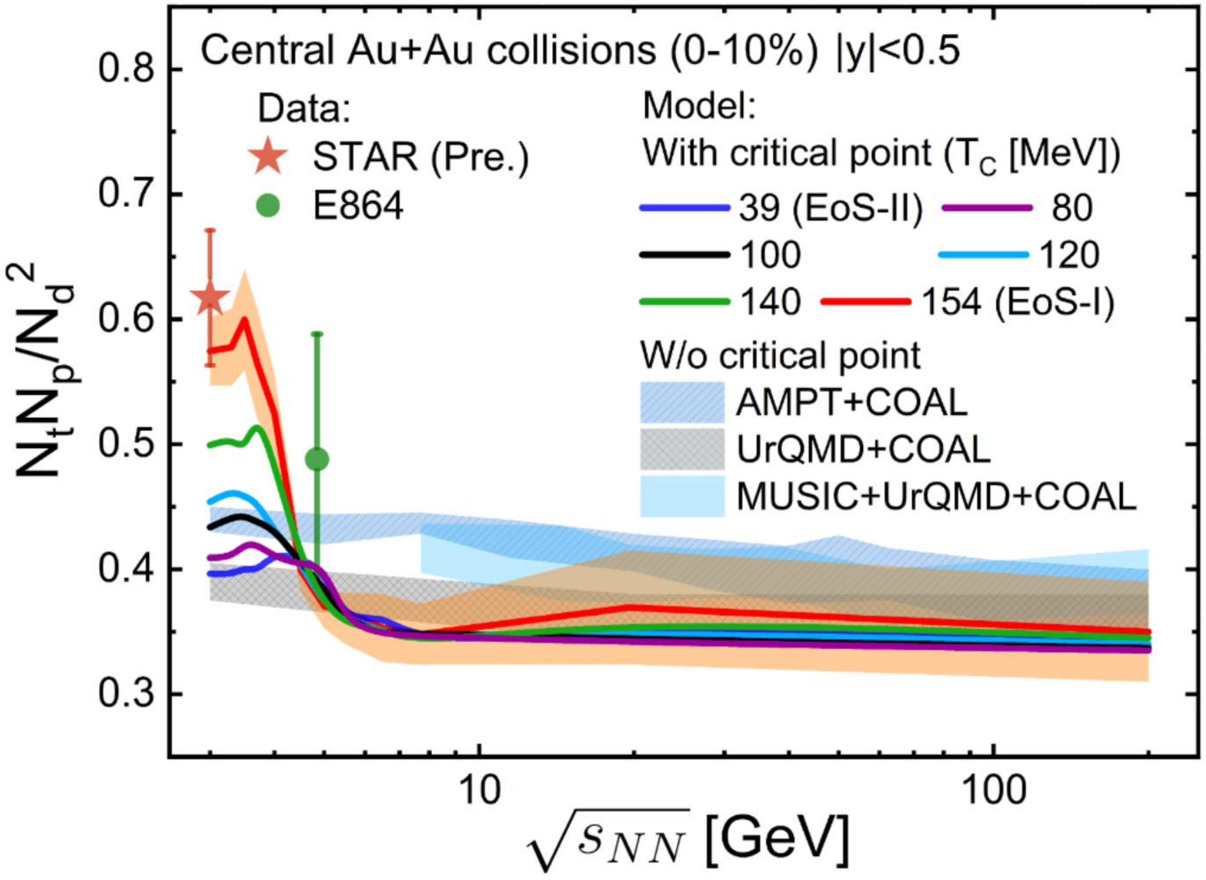

1. Without a first-order phase transition : The energy dependence of tp/d^2 is almost flat.
2. With a first-order phase transition: The spinodal instability induced enhancement of tp/d^2 during the first-order phase transition increases as increasing the critical temperature.

Data:
Hui Liu (STAR), QM2022
T. A. Armstrong et al. (E864), PRC 61, 064908 (2000).

Centrality dependence of tp/d^2 with 1st-order PT

K. J. Sun(孙开佳), W. H. Zhou(周文豪), LWC, C. M. Ko, F. Li(李峰), and R. Wang(王睿), and J. Xu(徐骏), arXiv:2205.11010(2022)

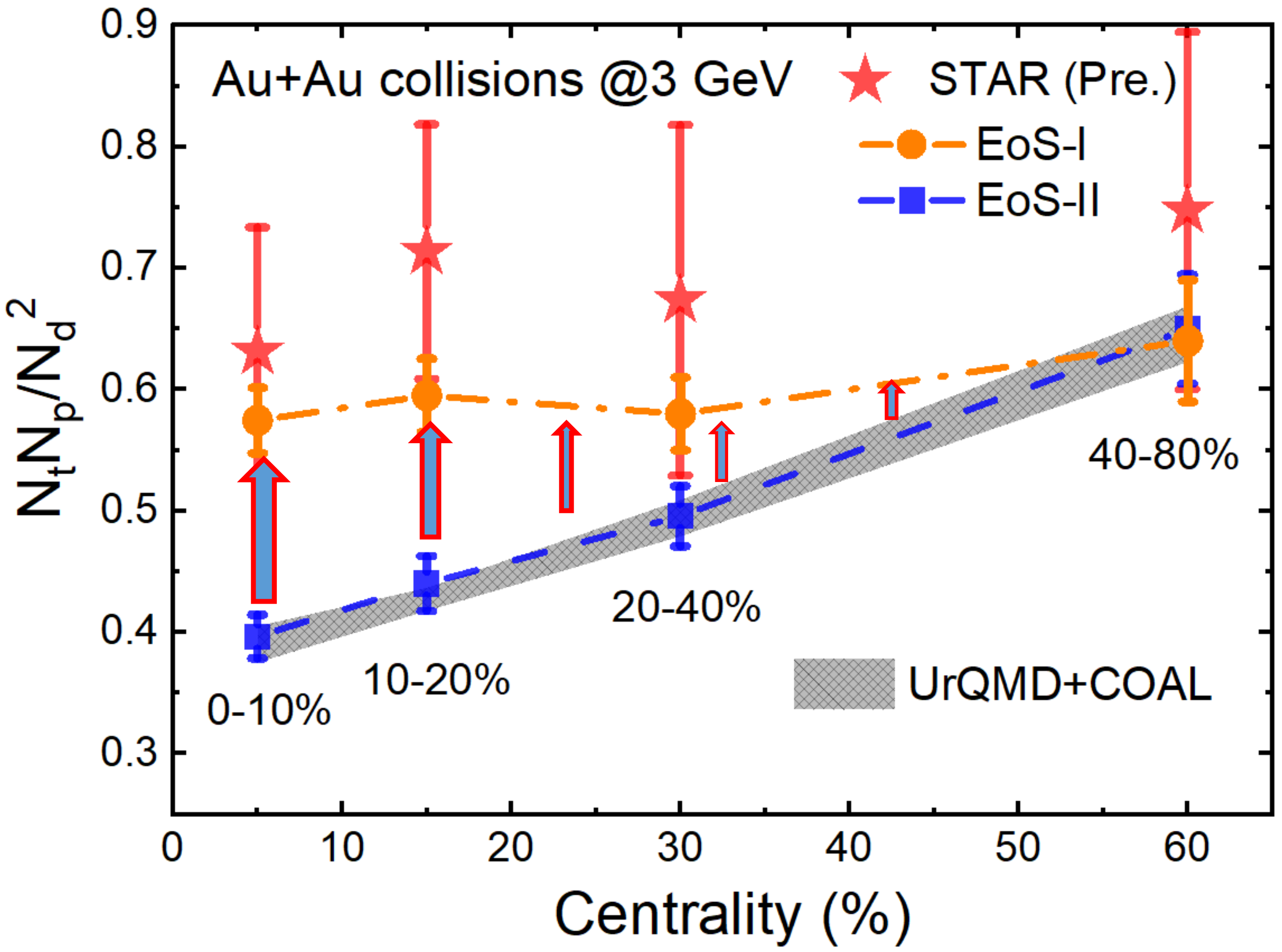

The spinodal enhancement of tp/d^2 subsides with increasing collision centrality because of smaller fireball lifetime in more peripheral collisions.

The slope with EoS-I is 5 times smaller

目录

- □ 致密QCD物质
- □ 致密QCD物质的状态方程：
  - ■ 对称能：核物质和夸克物质的状态方程
  - ■ 中子皮：Pb/Ca中子半径之谜
  - ■ 引力波：对称能的高密行为
- □ 致密QCD物质的相变：
  - ■ QCD相图：概述
  - ■ 重离子碰撞：粒子产生的并合模型
  - ■ 致密星：中子星、超新星、双星并合
- □ 总结和展望

NICER: 同时测量中子星的质量-半径

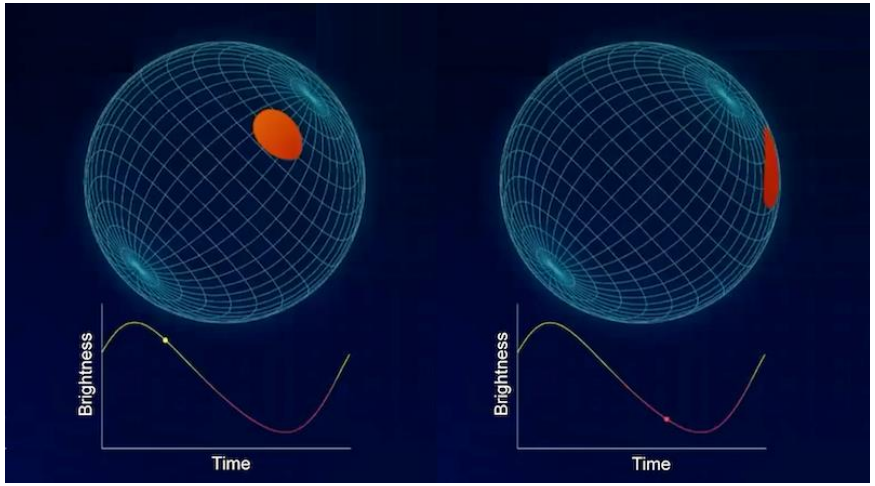

https://physics.aps.org/articles/v14/64

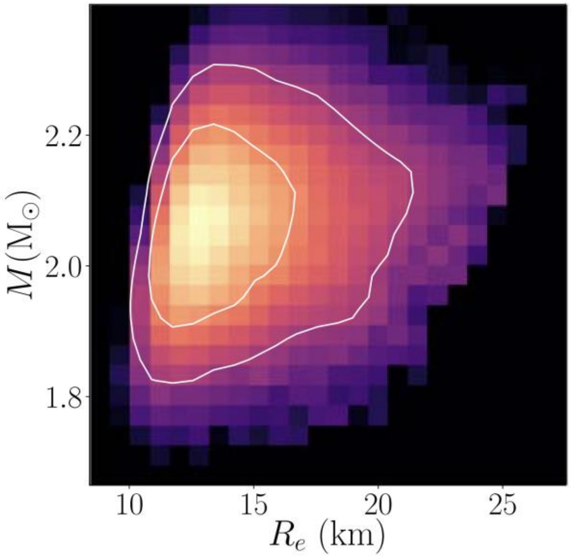

Miller et al., ApJL, 2021

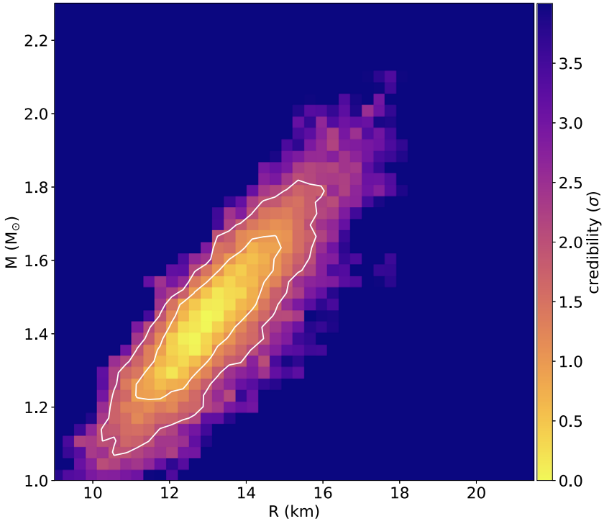

Miller et al., ApJL, 2019

NICER:
Neutron star Interior
Composition ExploreR
(中子星内部组成探测器/NASA)

Tracking the x-ray emission from "hot spots"

PSR J0740+6620 $M = 2.09^{+0.09}_{-0.09} M_\odot$ and $R = 13.7^{+2.6}_{-1.5}$ km

PSR J0030+0451 $M = 1.44^{+0.15}_{-0.14} M_\odot$ and $R = 13.02^{+1.24}_{-1.06}$ km

Posterior samples are publicly available!

脉冲星的本质

Pulsars: Neutron Stars? Quark Stars? Others?

F. Weber, PPNP54, 193 (2005)

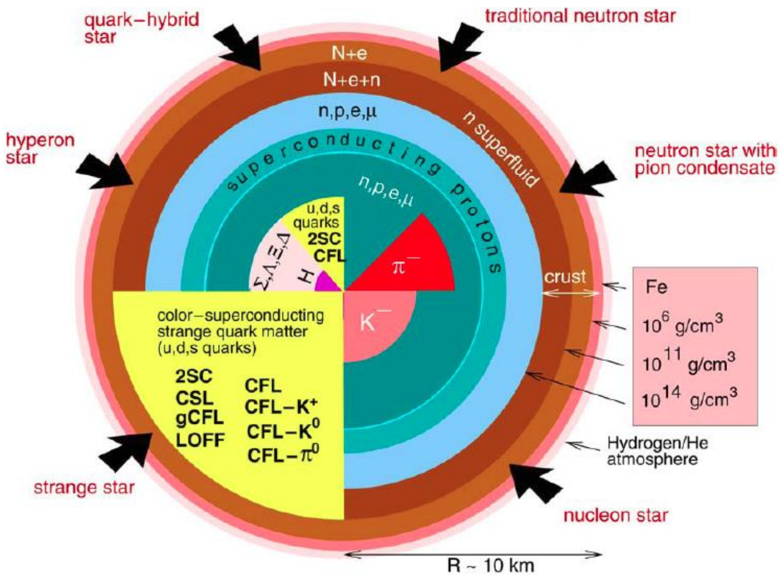

Mass: ~ 1.4 $M_\odot$, Radius: ~ 10 km

Extremely neutron-rich matter

Density at the center: ~ $6\rho_0$

Average density: ~ $2.5\rho_0$

Neutron Stars

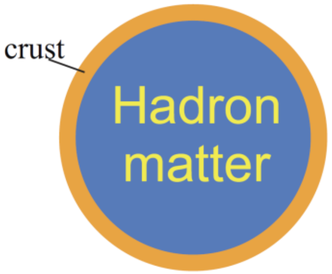

Hadron star:
quarks confined
gravity-bound

Hybrid/mixed star:
quarks de-con./con.
gravity-bound

Quark Stars

Quark star:
quarks de-confined
self-bound on surface

Strangeon Stars

Quark-cluster star:
quarks localized
self-bound on surface

R. X. Xu and Y.J Gao, arXiv:1601.05607

V.E. Fortov, Extreme States of Matter – on Earth and in the Cosmos, Springer-Verlag Berlin Heidelberg 2011

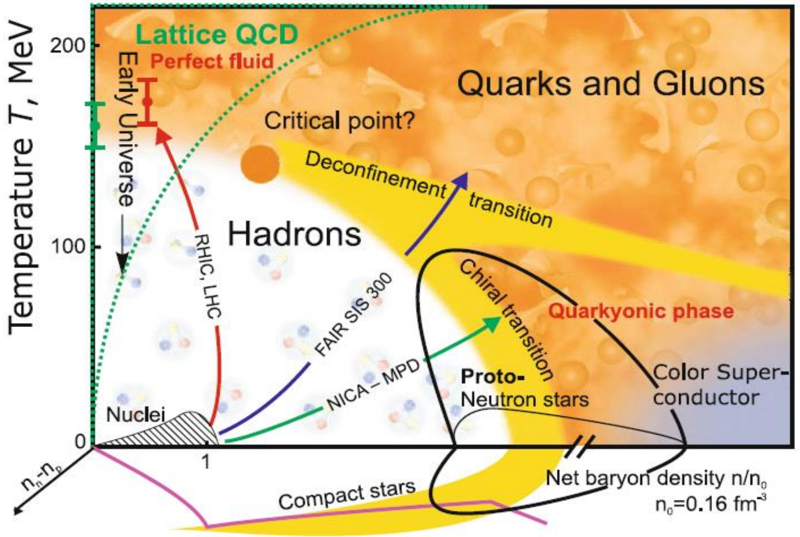

Bodmer-Witten-Terazawa Conjecture:

the deconfined strange quark matter could be the true ground state of QCD

脉冲星的本质:模型无关的贝叶斯推断？

Zheng Cao (曹政)/LWC,
arXiv:2308.16783

Sound speed extension to high density to match pQCD

$$c_s^2(n) = \frac{(n_{i+1} - n)\, c_{s,i}^2 + (n - n_i)\, c_{s,i+1}^2}{n_{i+1} - n_i}$$

$$\mu(n) = \mu_1 \exp\left[\int_{n_1}^{n} dn' \frac{c_s^2(n')}{n'}\right]$$

$$\varepsilon(n) = \varepsilon_1 + \int_{n_1}^{n} dn' \mu(n'),$$

$$p(n) = -\varepsilon(n) + \mu(n) n.$$

I. Tews et al., ApJ860, 149 (2018);
T. Gorda et al., PRL127, 162003(2021)
E. Annala et al., PRX12, 011058(2022)

Ingo Tews

pQCD $\sim 40 n_0$

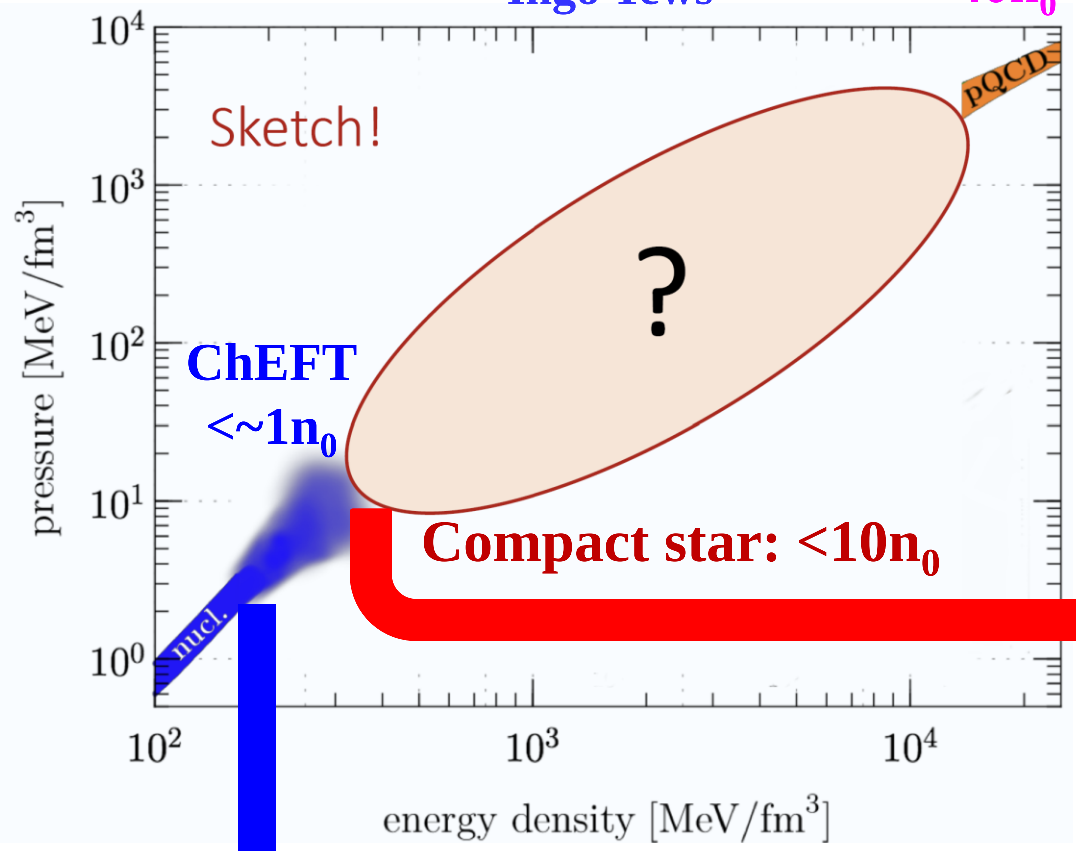

Quark stars (with sharp surface)
(it is self-bound and could contain uds, ud, even strangeons, and has a sharp surface – zero-pressure point at which the E/A < 930 MeV)

Neutron stars (with crust)
(its core could contain Hyperons, Condensates, Quark Matter, …)

脉冲星的本质:模型无关的贝叶斯推断？

$$p(\theta|\vec{d},\mathcal{H}) = \frac{\prod_i \mathcal{L}(d_i|\theta,\mathcal{H})\pi(\theta|\mathcal{H})}{\mathcal{Z}_{\mathcal{H}}(\vec{d})} \qquad \mathcal{Z}_{\mathcal{H}}(\vec{d}) \equiv \int \prod_i \mathcal{L}(d_i|\theta,\mathcal{H})\pi(\theta|\mathcal{H})d\theta \qquad \boxed{\mathcal{B}^{\rm NS}_{\rm QS} = \mathcal{Z}_{\rm NS}(\vec{d})/\mathcal{Z}_{\rm QS}(\vec{d})}$$

Zheng Cao (曹政)/LWC, arXiv:2308.16783

Bayesian analyses combining

- **ChEFT: n<1.1n_0**
- **pQCD: High Densities**
- **Nstar Mmax: ~2$M_\odot$**
- **Nstar MR: NICER**
- **GW: GW170817, GW190425**

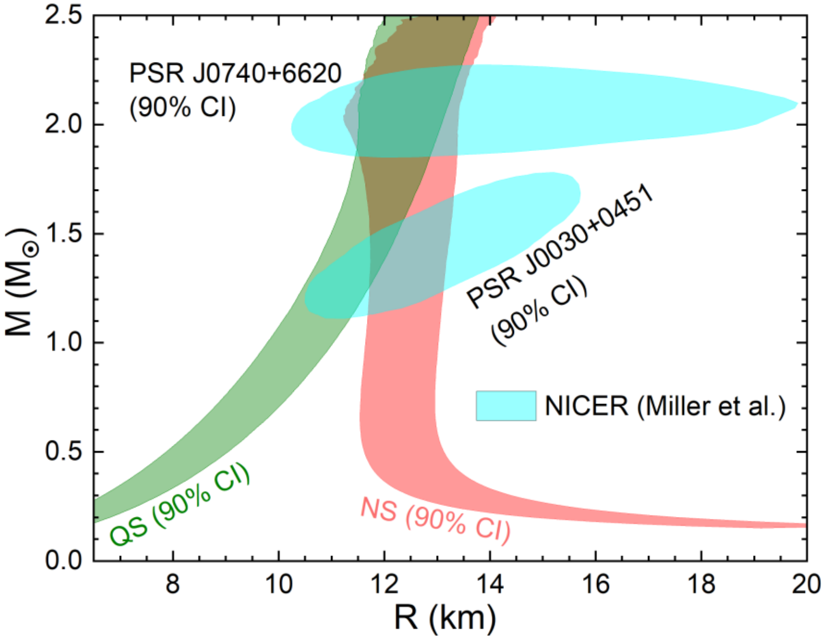

Bayes Factor

$\mathcal{B}^{H_1}_{H_0}$	Interpretation
> 100	Extreme evidence for H_1
30–100	Very strong evidence for H_1
10–30	Strong evidence for H_1
3–10	Moderate evidence for H_1
1–3	Anecdotal evidence for H_1
1	No evidence
1/3–1	Anecdotal evidence for H_0
1/10–1/3	Moderate evidence for H_0
1/30–1/10	Strong evidence for H_0
1/100–1/30	Very strong evidence for H_0
< 1/100	Extreme evidence for H_0

Lee/Wagenmakers, Bayesian Cognitive Modeling (Cambridge University Press, 2014).

$\boxed{\mathcal{B}^{\rm NS}_{\rm QS} = 11.5}$ **Mainly due to NICER M-R of PSR J0030+0451, and then GW170817!**

- **Bayesian analyses combining ChEFT + pQCD + Nstar Mmax + GW+ Nstar MR suggests that the NS hypothesis is strongly favored against QS hypothesis!**
- **Bodmer-Witten-Terazawa Conjecture is disfavored! Natural explanation on the fact that there is so far no definite evidence for the existence of strangelet-like exotic objects.**

状态方程: 模型无关的贝叶斯推断？

Zheng Cao (曹政)/LWC, arXiv:2308.16783

Bayesian analyses combining
- ChEFT: $n<1.1n_0$
- pQCD: High Densities
- Nstar Mmax: $\sim 2M_\odot$
- Nstar MR: NICER
- GW: GW170817, GW190425

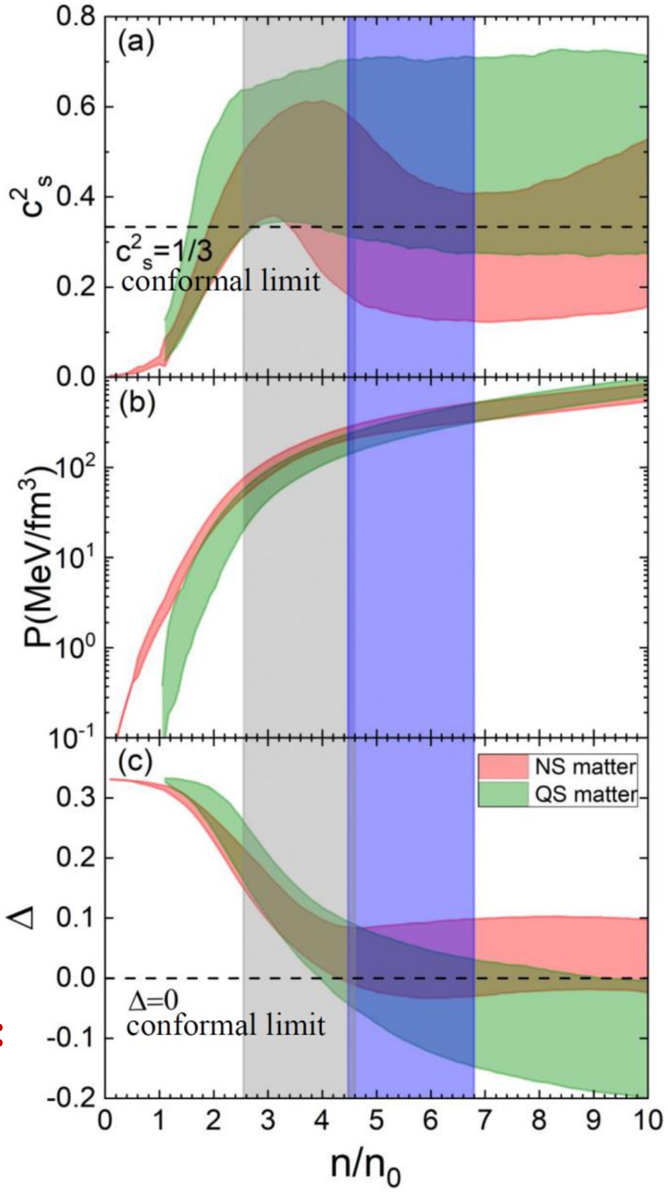

Trace anomaly:

$$\Delta = 1/3 - p/\epsilon$$

A new measure of conformality: Fujimoto/Fukushima/McLerran /Praszalowicz, PRL129, 252702 (2022)

Position of Maximum c_s^2 in Neutron Star Matter: $\sim 3.5n_0$

Central density inside Neutron Star at Maximum mass : $\sim 6n_0$

- A clear peak appeared in NS matter around 3-4 n_0, disappears in the QS case (Quarkyonic matter? McLerran/Reddy PRL (2019); Skymion matter? Y.L. Ma/Rho; Esym? N.B. Zhang/B.A. Li; …)
- Peak structure depends on pQCD, $\sim 2M_\odot$ and the input low density EOS (Crust/Surface)
- Dense matter approach to its conformal limit in the core of heavy NS, but NOT in QS, suggesting that QM may appear in the center of heavy NSs (see also Annala et al., Nature Phys. 16, 907 (2020); Fujimoto et al., PRL129, 252702 (2022); Marczenko et al., PRC 107, 025802 (2023); Annala et al., arXiv:2303.11356)

Quark Core in Massive NStars?

E. Annala et al., Nature Phys. 16, 907 (2020)

nature physics
LETTERS
https://doi.org/10.1038/s41567-020-0914-9
Check for updates

OPEN

Evidence for quark-matter cores in massive neutron stars

Eemeli Annala[1], Tyler Gorda[2], Aleksi Kurkela[3,4], Joonas Nättilä[5,6,7] and Aleksi Vuorinen[1]

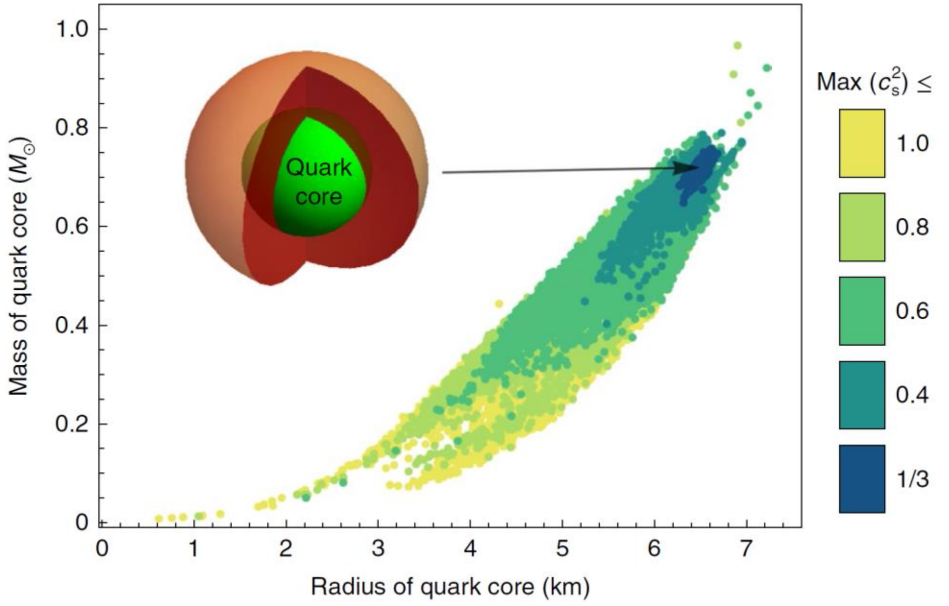

~570000 EOSs: M>1.97 Msun and 70<Λ1.4<580

PHYSICAL REVIEW D **80**, 066003 (2009)

Bound on the speed of sound from holography

Aleksey Cherman* and Thomas D. Cohen†
Center for Fundamental Physics, Department of Physics, University of Maryland, College Park, Maryland 20742-4111, USA

Abhinav Nellore‡
Joseph Henry Laboratories, Princeton University, Princeton, New Jersey 08544, USA
(Received 12 May 2009; published 3 September 2009)

We show that the squared speed of sound v_s^2 is bounded from above at high temperatures by the conformal value of 1/3 in a class of strongly coupled four-dimensional field theories, given some mild technical assumptions. This class consists of field theories that have gravity duals sourced by a single-scalar field. There are no known examples to date of field theories with gravity duals for which v_s^2 exceeds 1/3 in energetically favored configurations. We conjecture that $v_s^2 = 1/3$ represents an upper bound for a broad class of four-dimensional theories.

PRL **114**, 031103 (2015) PHYSICAL REVIEW LETTERS week ending 23 JANUARY 2015

Sound Velocity Bound and Neutron Stars

Paulo Bedaque
Department of Physics, University of Maryland, College Park, Maryland 20742, USA

Andrew W. Steiner
Institute for Nuclear Theory, University of Washington, Seattle, Washington 98195, USA;
Department of Physics and Astronomy, University of Tennessee, Knoxville, Tennessee 37996, USA;
and Physics Division, Oak Ridge National Laboratory, Oak Ridge, Tennessee 37831, USA
(Received 10 October 2014; published 21 January 2015)

It has been conjectured that the velocity of sound in any medium is smaller than the velocity of light in vacuum divided by $\sqrt{3}$. Simple arguments support this bound in nonrelativistic and/or weakly coupled theories. The bound has been demonstrated in several classes of strongly coupled theories with gravity duals and is saturated only in conformal theories. We point out that the existence of neutron stars with masses around two solar masses combined with the knowledge of the equation of state of hadronic matter at "low" densities is in strong tension with this bound.

Quark Core in Massive NStars?

ImMDI (improved isospin- and momentum-dependent interaction) + SU(3) NJL

$$\varepsilon_Q = -2N_c \sum_{i=u,d,s} \int_0^\Lambda \frac{d^3p}{(2\pi)^3} E_i (1 - f_i - \bar{f}_i) - \sum_{i=u,d,s} (\tilde{\mu}_i - \mu_i)\rho_i + G_S(\sigma_u^2 + \sigma_d^2 + \sigma_s^2) - 4K\sigma_u\sigma_d\sigma_s - G_V(\rho_u^2 + \rho_d^2 + \rho_s^2) + G_{IS}(\sigma_u - \sigma_d)^2 - G_{IV}(\rho_u - \rho_d)^2 - \varepsilon_0.$$

$$T^H = T^Q, \qquad P^H = P^Q,$$
$$\mu_B = \mu_B^H = \mu_B^Q, \qquad \mu_c = \mu_c^H = \mu_c^Q.$$

$$\mu_i = \mu_B b_i - \mu_c q_i, \qquad P^H = P^Q,$$
$$\rho_B = (1-Y)(\rho_n + \rho_p) + \frac{Y}{3}(\rho_u + \rho_d + \rho_s),$$
$$0 = (1-Y)\rho_p + \frac{Y}{3}(2\rho_u - \rho_d - \rho_s) - \rho_e - \rho_\mu,$$

$$V_{ImMDI} = \frac{A_u \rho_n \rho_p}{\rho_0} + \frac{A_l}{2\rho_0}(\rho_n^2 + \rho_p^2) + \frac{B}{\sigma+1}\frac{\rho^{\sigma+1}}{\rho_0^\sigma} \times (1 - x\delta^2) + \frac{1}{\rho_0}\sum_{\tau,\tau'} C_{\tau,\tau'} \times \iint d^3\vec{p}\, d^3\vec{p}' \frac{f_\tau(\vec{r},\vec{p}) f_{\tau'}(\vec{r},\vec{p}')}{1 + (\vec{p} - \vec{p}')^2/\Lambda^2},$$

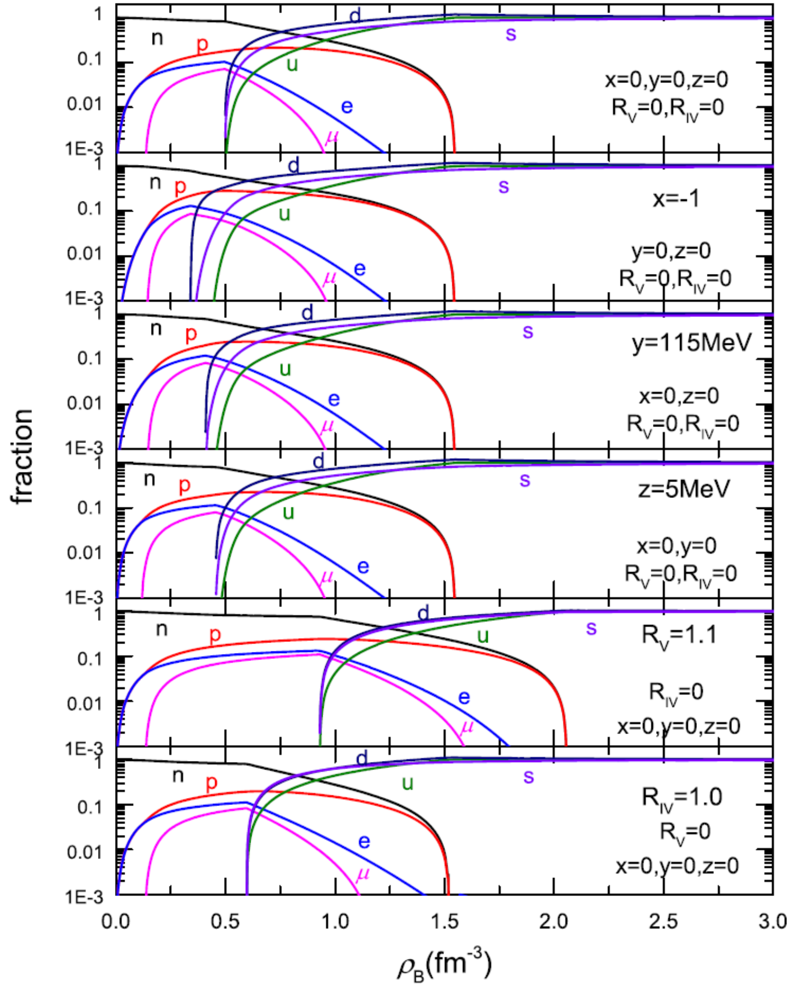

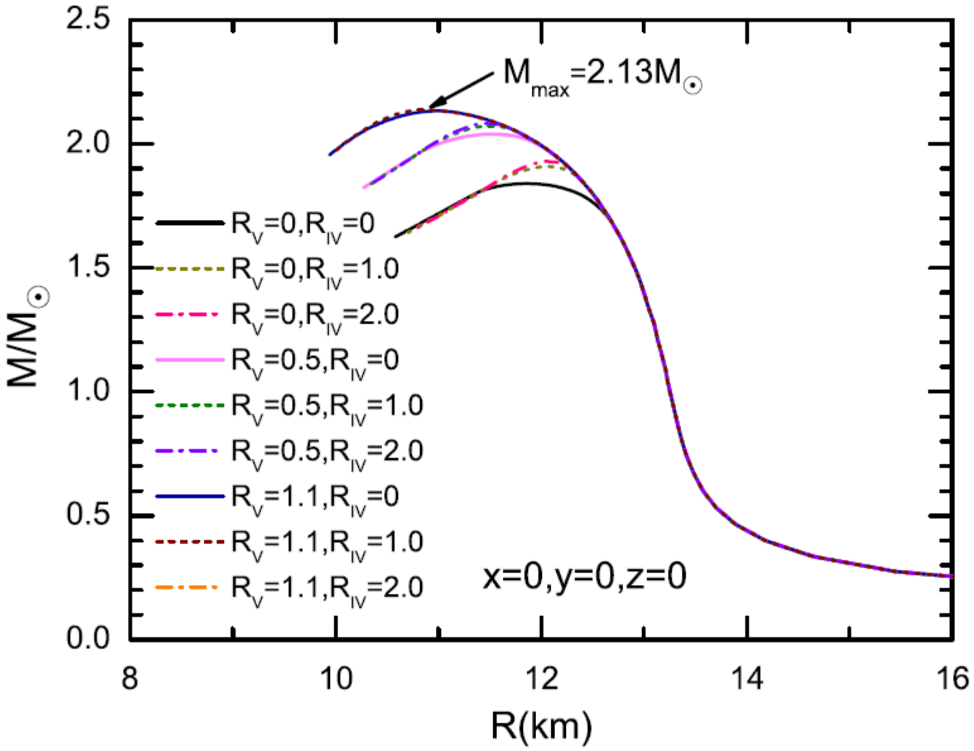

H. Liu, J. Xu(徐骏), and P.C. Chu(初鹏程), PRD 105, 043015 (2022)

Quark Core in Massive NStars?

ImMDI (improved isospin- and momentum-dependent interaction) + SU(3) NJL

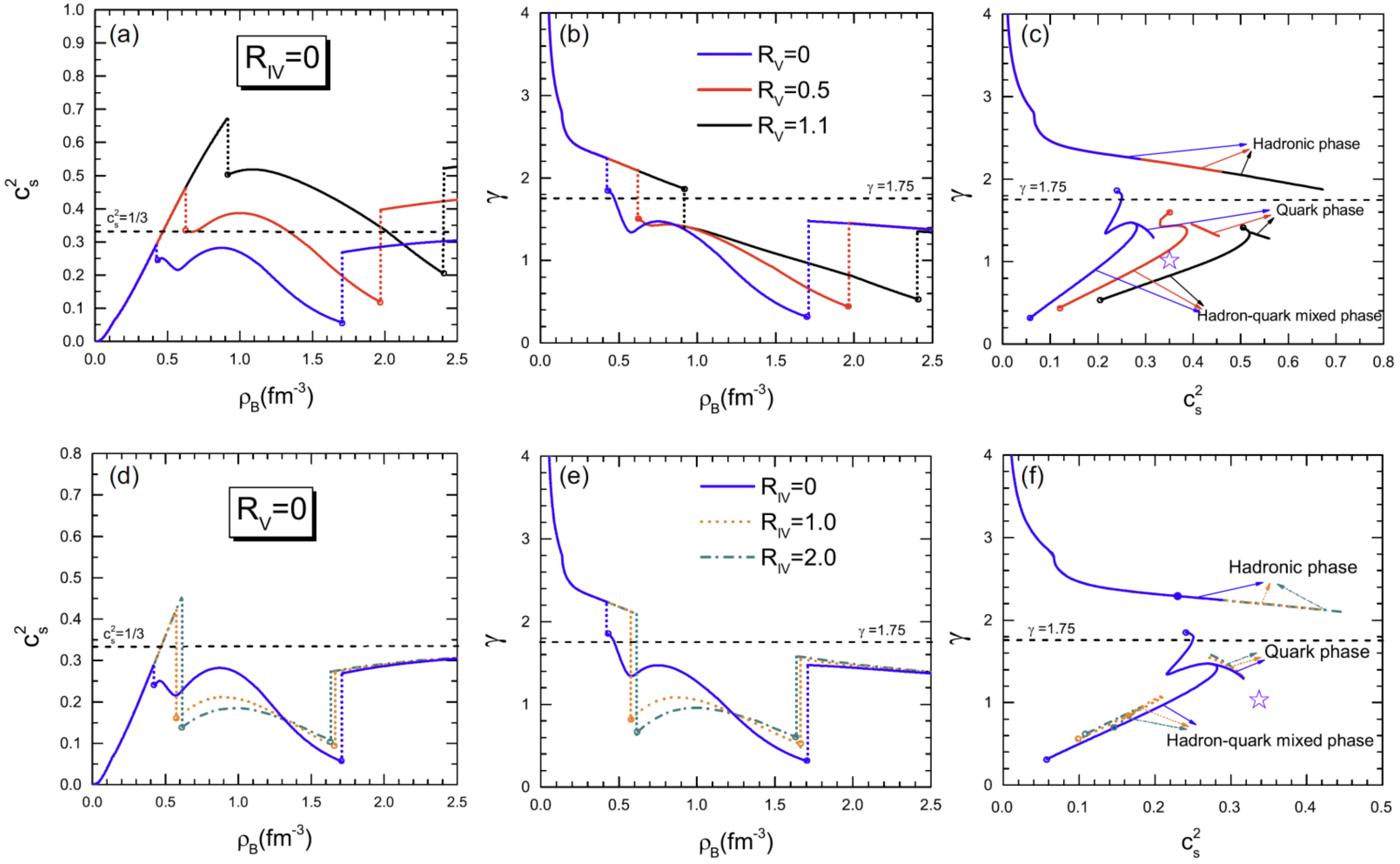

H. Liu, X.M. Zhang and P.C. Chu(初鹏程), PRD 107, 094032 (2023)

Quark Core in Massive NStars?

ImMDI (improved isospin- and momentum-dependent interaction) + SU(3) NJL

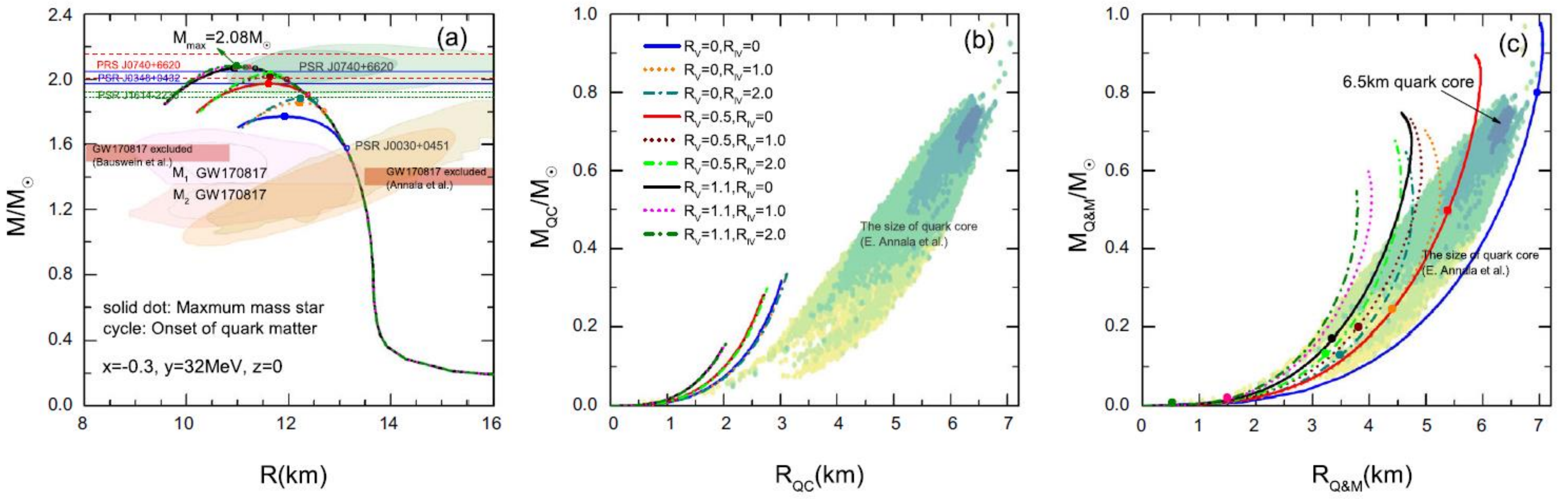

H. Liu, X.M. Zhang and P.C. Chu(初鹏程), PRD 107, 094032 (2023)

Quarkyonic Matter in Massive NStars?

PHYSICAL REVIEW LETTERS **122,** 122701 (2019)

Quarkyonic Matter and Neutron Stars

Larry McLerran and Sanjay Reddy
Institute for Nuclear Theory and Department of Physics, University of Washington, Seattle, Washington 98195, USA

(Received 30 December 2018; revised manuscript received 19 February 2019; published 26 March 2019)

We consider quarkyonic matter to naturally explain the observed properties of neutron stars. We argue that such matter might exist at densities close to that of nuclear matter, and at the onset, the pressure and the sound velocity in quarkyonic matter increase rapidly. In the limit of large number of quark colors N_c, this transition is characterized by a discontinuous change in pressure as a function of baryon number density. We make a simple model of quarkyonic matter and show that generically the sound velocity is a nonmonotonic function of density—it reaches a maximum at relatively low density, decreases, and then increases again to its asymptotic value of $1/\sqrt{3}$.

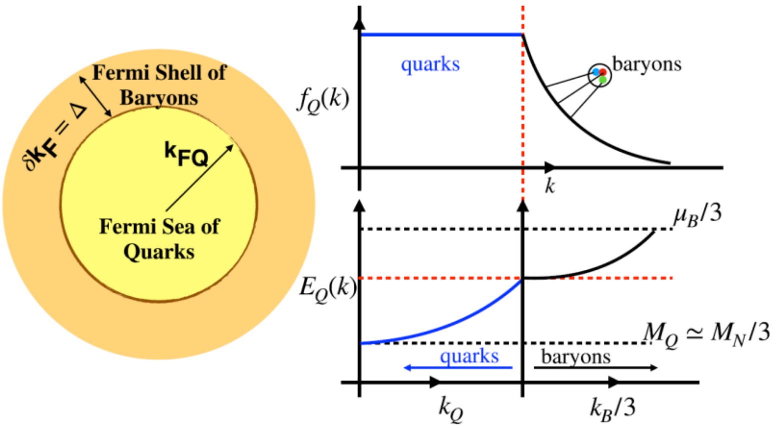

FIG. 1. The schematic shows the momentum distribution of quarks and baryons. The diffuse distribution of quarks in the right-hand upper graph indicates they are confined inside baryons that occupy momentum states with width $\delta k_F = \Delta$.

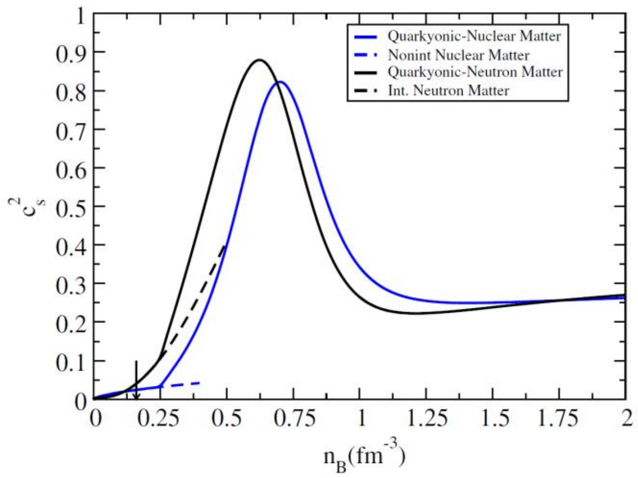

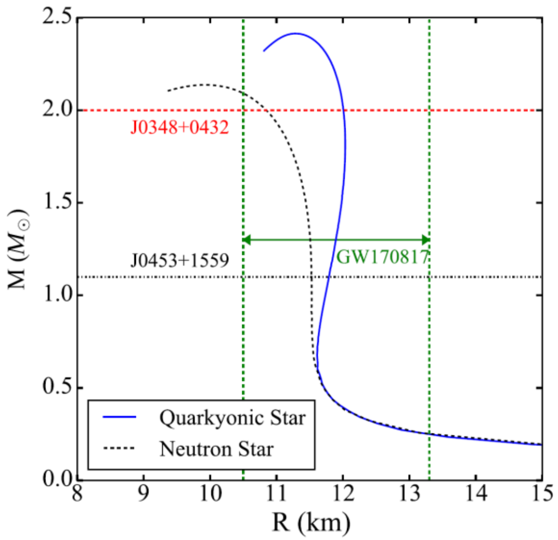

上海交通大學 SHANGHAI JIAO TONG UNIVERSITY

Topology Change in Dense Matter?


Brief Review

Modern Physics Letters A
Vol. 37, No. 3 (2022) 2230003 (22 pages)

DOI: 10.1142/S0217732322300038

World Scientific
www.worldscientific.com

Cusp in the symmetry energy, speed of sound in neutron stars and emergent pseudo-conformal symmetry

Hyun Kyu Lee
Department of Physics, Hanyang University, Seoul 133-791, Korea
hyunkyu@hanyang.ac.kr

Yong-Liang Ma
School of Fundamental Physics and Mathematical Sciences,
Hangzhou Institute for Advanced Study, UCAS, Hangzhou, 310024, China
International Center for Theoretical Physics Asia-Pacific, Beijing/Hanzhou, China
ylma@ucas.ac.cn

Won-Gi Paeng
A I Lab., Clunix, Seoul 07209, Korea
wgpaeng@clunix.com

Mannque Rho*
Université Paris-Saclay, Institut de Physique Théorique,
CNRS, CEA, 91191, Gif-sur-Yvette, France
mannque.rho@ipht.fr

H.K. Li, Y.L. Ma, W.G. Paeng and M. Rho, MPLA 37, 2230003 (2022)

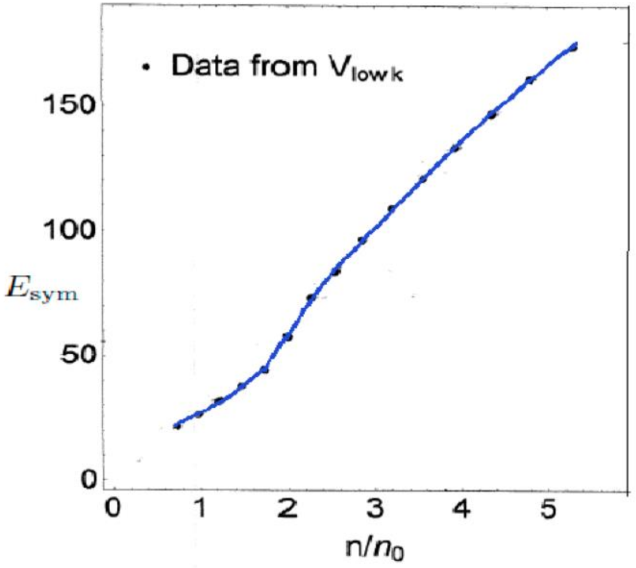

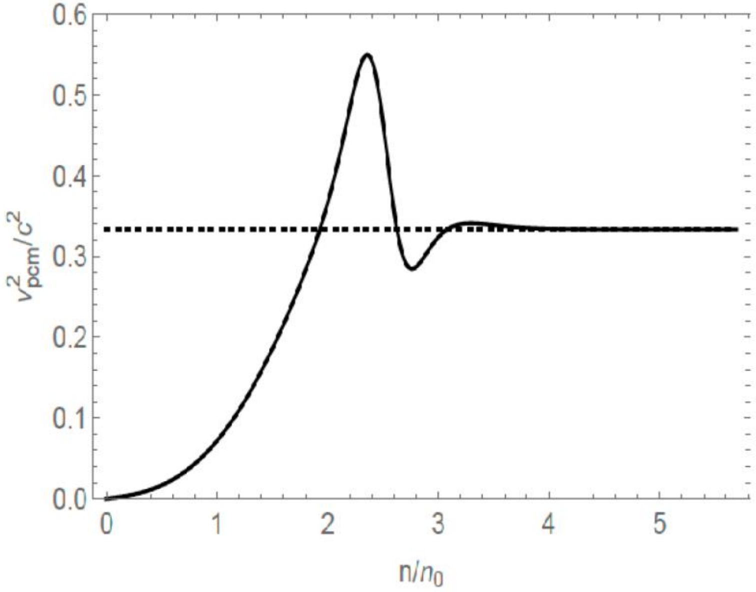

High Density Esym?

N.B. Zhang and B.A. Li, EPJA59, 86(2023)

S.P. Wang(王斯沛), R. Wang(王睿), J.T. Ye(叶俊廷), and LWC, PRC109, 054623(2024)

Eur. Phys. J. A (2023) 59:86
https://doi.org/10.1140/epja/s10050-023-01010-x
THE EUROPEAN PHYSICAL JOURNAL A
Check for updates
Regular Article - Theoretical Physics

Impact of symmetry energy on sound speed and spinodal decomposition in dense neutron-rich matter

Nai-Bo Zhang[1,a], Bao-An Li[2,b]
[1] School of Physics, Southeast University, Nanjing 211189, China
[2] Department of Physics and Astronomy, Texas A&M University-Commerce, Commerce, TX 75429, USA

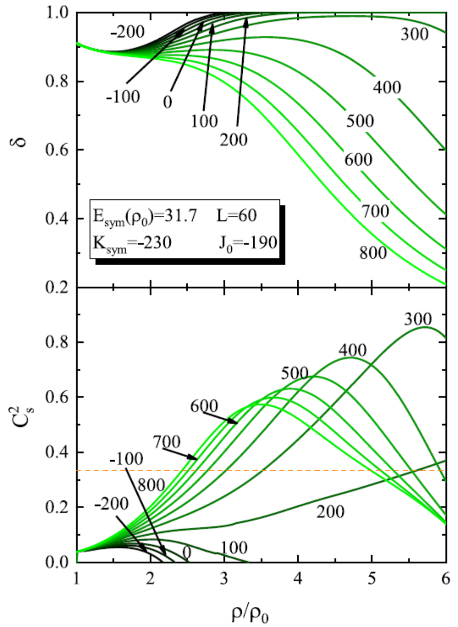

Fig. 6 The density profile of isospin asymmetry $\delta(\rho)$ (upper panel) and the corresponding sound speed squared $C_s^2(\rho)$ in unit of c^2 in neutron stars at β-equilibrium with J_{sym} varying between − 200 and 800 MeV but other parameters fixed at their currently known most probable values indicated. The orange dashed line corresponds to the conformal limit $C^2 < 1/3$.

PHYSICAL REVIEW C **109**, 054623 (2024)

Extended Skyrme effective interactions for transport models and neutron stars

Si-Pei Wang,[1] Rui Wang,[2] Jun-Ting Ye,[1] and Lie-Wen Chen[1,*]
[1] *School of Physics and Astronomy, Shanghai Key Laboratory for Particle Physics and Cosmology, and Key Laboratory for Particle Astrophysics and Cosmology (MOE), Shanghai Jiao Tong University, Shanghai 200240, China*
[2] *Istituto Nazionale di Fisica Nucleare (INFN), Sezione di Catania, I-95123 Catania, Italy*

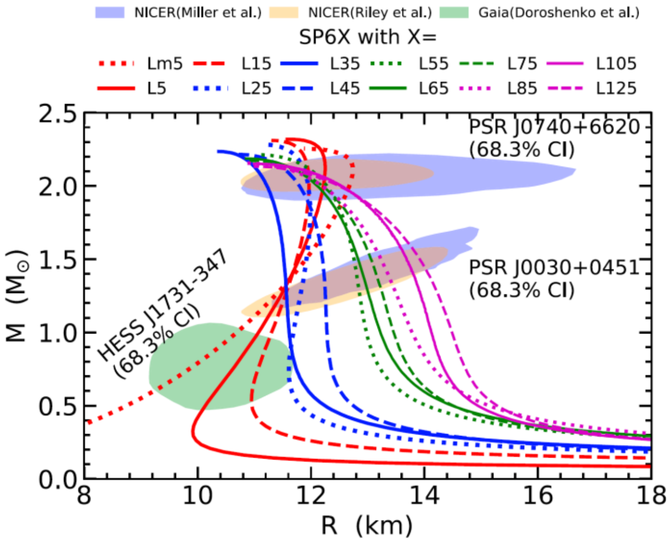

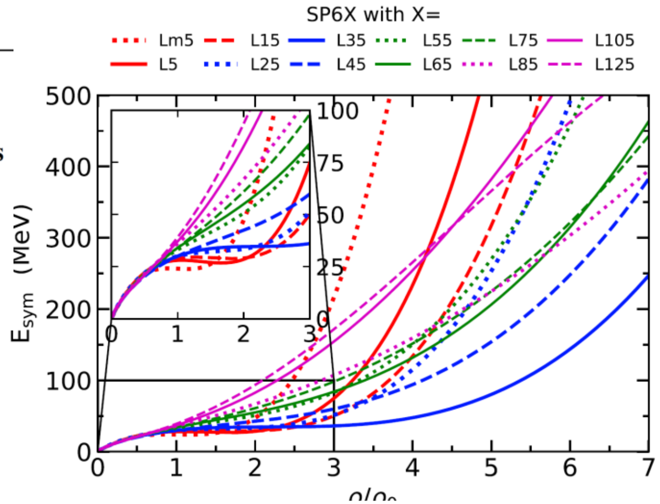

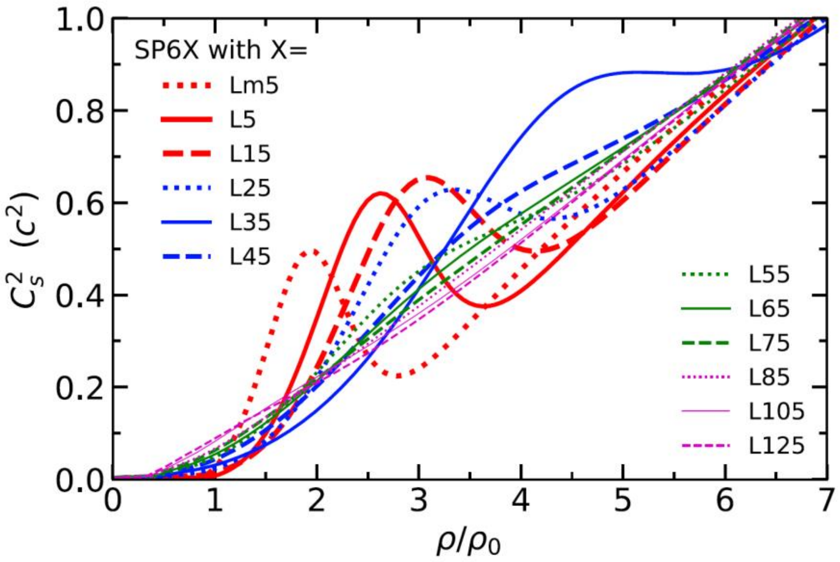

Hyperon Appearance in NStars?

J.T. Ye (叶俊廷) et al. (Preliminary Results)

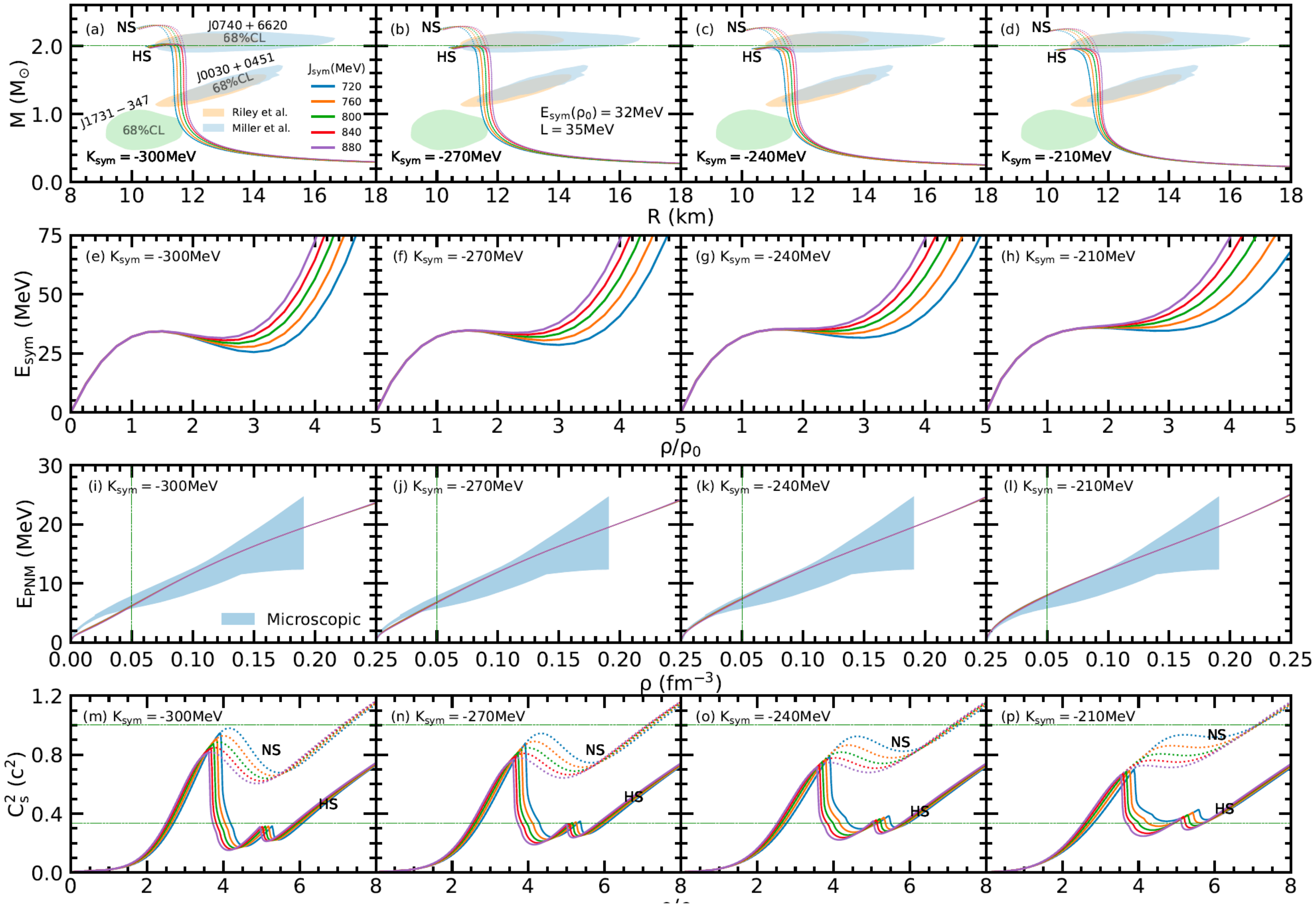

First-Order Hadron-Quark PT in CCSNe

S. Zha(查帅) et al. PRL125, 051102(2020)

Hadronic EOS: STOS H. Shen, H. Toki, K. Oyamatsu, and K. Sumiyoshi, Prog. Theor. Phys. 100, 1013 (1998).

Quark Matter EOS: MIT Bag Model

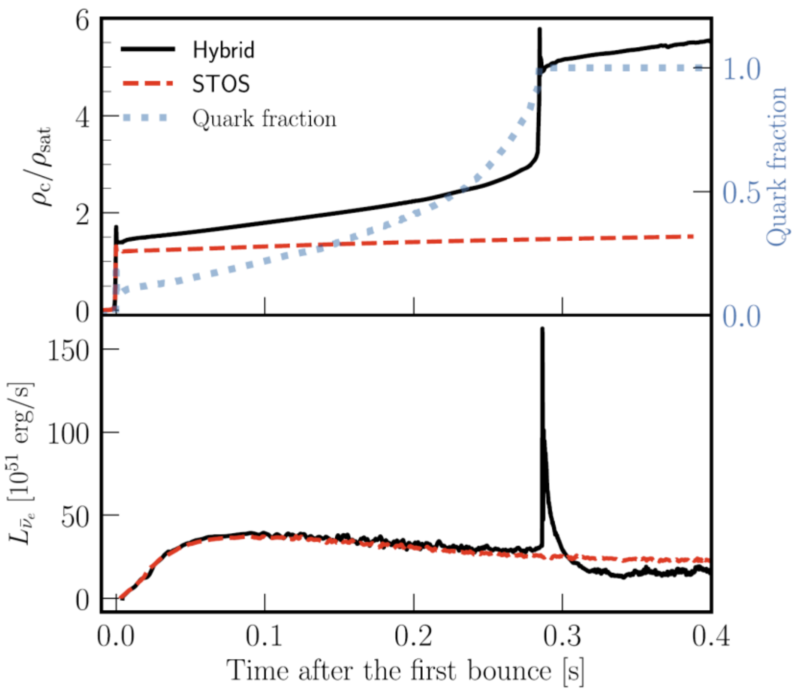

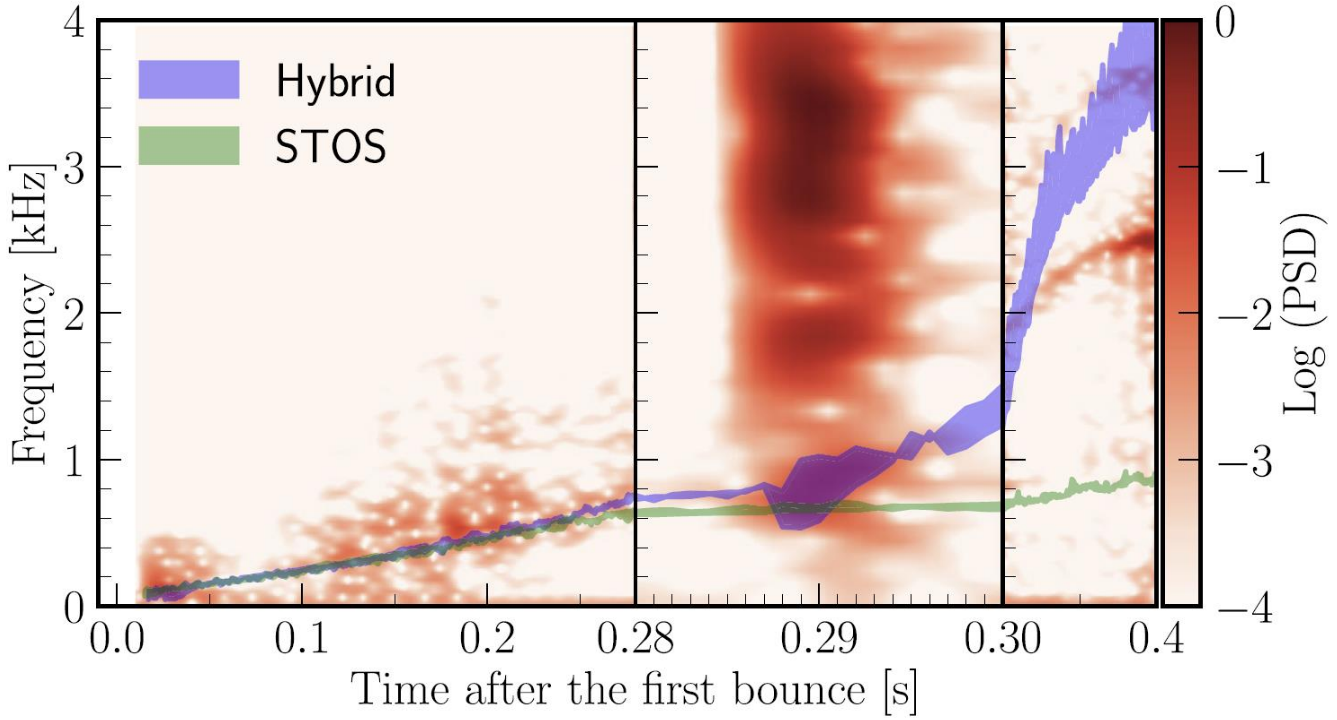

FOPT: Second neutrino burst

FOPT: Strong GW burst

Hadron-Quark PT in NStar Merger

Y. Fujimoto et al. PRL130, 091404(2023)

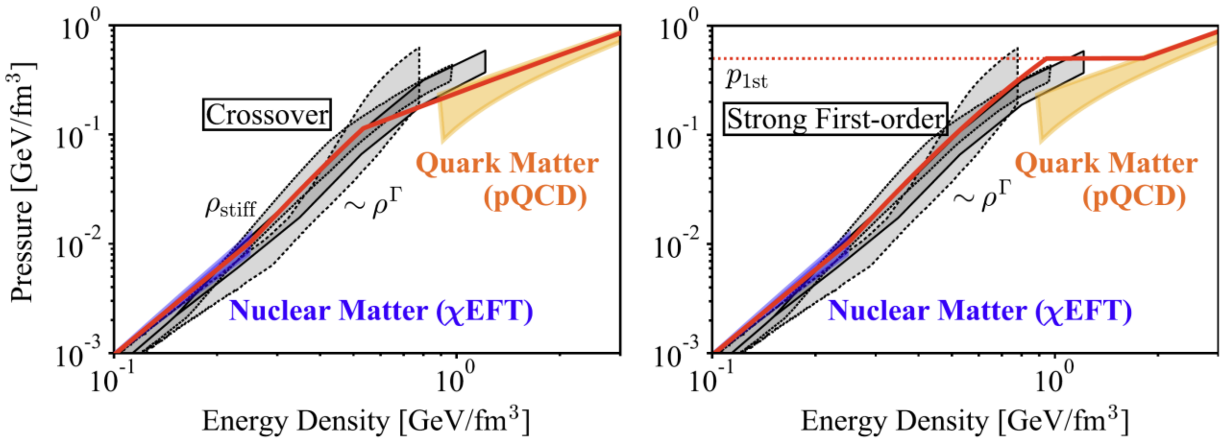

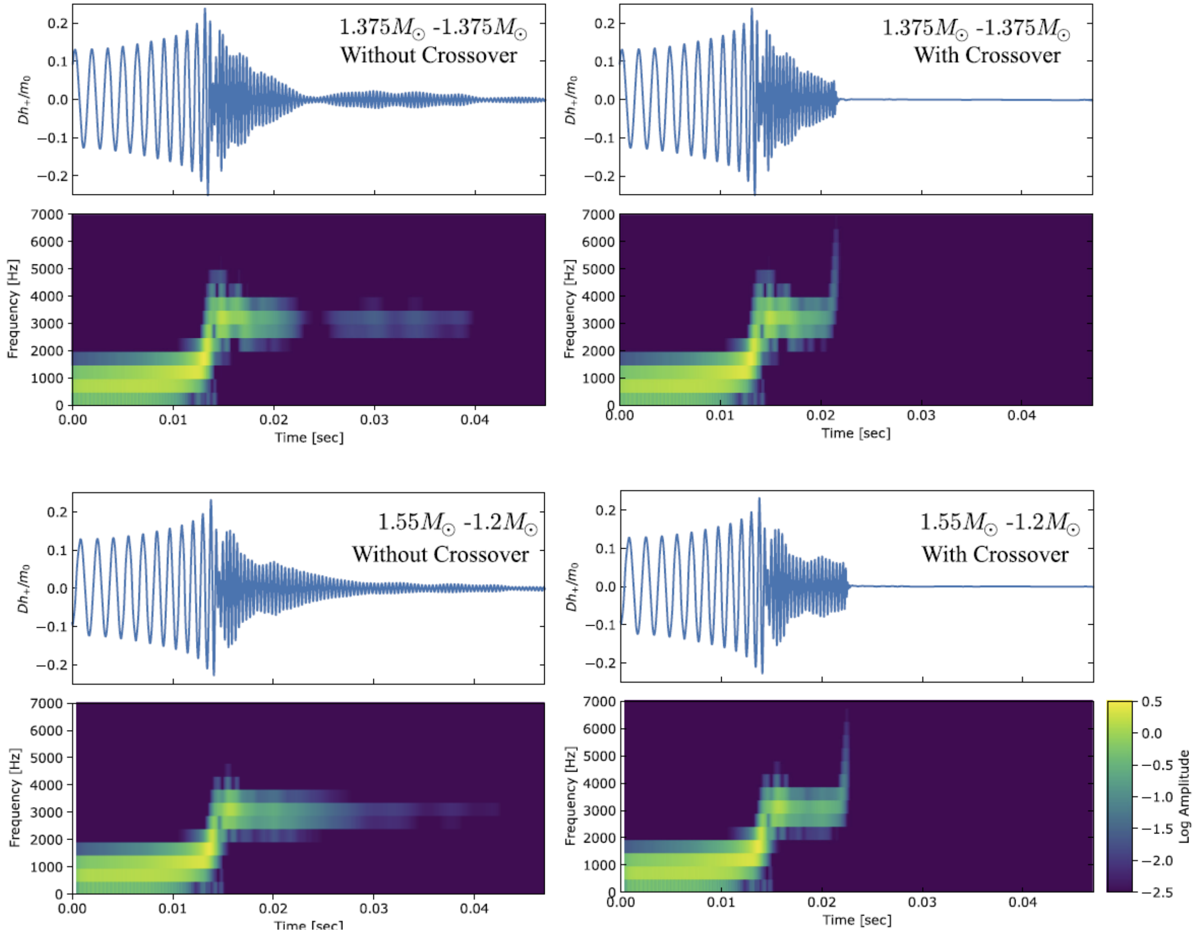

GW signal is very different between Crossover and FOPT!

目录

- 致密QCD物质
- 致密QCD物质的状态方程:
  - 对称能：核物质和夸克物质的状态方程
  - 中子皮：Pb/Ca中子半径之谜
  - 引力波：对称能的高密行为
- 致密QCD物质的相变：
  - QCD相图：概述
  - 重离子碰撞：粒子产生的并合模型
  - 致密星：中子星、超新星、双星并合
- 总结和展望

上海交通大學 SHANGHAI JIAO TONG UNIVERSITY

总结和展望

- 通过重离子碰撞，核结构(mass, neutron skin, GR/PG…), 以及核子光学势的研究，我们已经对**亚饱和密度**以及**饱和密度附近**核物质对称能有了比较好的认识：
  - ➢ 亚饱和密度区的核物质对称能 – 比较精确
  - ➢ 饱和密度附近的核物质对称能:

  World Average: $E_{sym}(\rho_0)$ =31.7±3.1 MeV and L=57.5±24.5 MeV

  更精确的约束需要更精确的实验数据和更可靠的理论方法!

- 决定对称能的**高密行为**依然是一个巨大的挑战, **丰中子核引起的重离子碰撞**(未来HIAF)的实验数据以及**中子星/引力波观测数据**将非常重要

- 致密QCD物质的相结构及相变行为依然扑朔迷离, **重离子碰撞的轻核产生**以及**超新星/中子星/双星并合引力波**等高质量的实验和天文观测数据将提供关键线索

上海交通大學
SHANGHAI JIAO TONG UNIVERSITY

谢 谢！
Thanks！